U.S. Department
of Commerce

Volume 119
Number 4
October 2021

Fishery Bulletin

Pacific Islands Fisheries
Science Center Library

Received on: May '22

U.S. Department of Commerce

Gina M. Raimondo
Secretary

National Oceanic and Atmospheric Administration

Richard W. Spinrad
Administrator

National Marine Fisheries Service

Janet Coit
Assistant Administrator
for Fisheries

Fishery Bulletin

Scientific Editor
José I. Castro
National Marine Fisheries Service, NOAA
263 13th Avenue South
Saint Petersburg, Florida 33701

Managing Editor
Kathryn Dennis
Scientific Publications Office
National Marine Fisheries Service, NOAA
1845 Wasp Boulevard, Building 176
Honolulu, Hawaii 96818

Associate Editor
Cara Mayo
Scientific Publications Office
National Marine Fisheries Service, NOAA
7600 Sand Point Way NE
Seattle, Washington 98115-0070

Editorial Board

Henry L. Bart Jr.	Tulane University, New Orleans, Louisiana
Matthew D. Campbell	National Marine Fisheries Service, Pascagoula, Mississippi
Shannon L. Cass-Calay	National Marine Fisheries Service, Miami, Florida
William B. Driggers III	National Marine Fisheries Service, Pascagoula, Mississippi
Gretchen L. Grammer	South Australian Research and Development Institute, Adelaide, Australia
Richard Langton	National Marine Fisheries Service, Walpole, Maine (retired)
Richard S. McBride	National Marine Fisheries Service, Woods Hole, Massachusetts
Richard L. Merrick	National Marine Fisheries Service, Falmouth, Massachusetts (retired)
Richard D. Methot	National Marine Fisheries Service, Seattle, Washington
Lisa J. Natanson	National Marine Fisheries Service, Narragansett, Rhode Island
Mark S. Peterson	University of Southern Mississippi, Ocean Springs, Mississippi
André E. Punt	University of Washington, Seattle, Washington
Joseph M. Quattro	University of South Carolina, Columbia, South Carolina
John F. Walter III	National Marine Fisheries Service, Miami, Florida
Bruce Wright	Aleutian Pribilof Island Association, Anchorage, Alaska

***Fishery Bulletin* website: https://spo.nmfs.noaa.gov/fb.htm**

Fishery Bulletin (ISSN 0090-0656) is published quarterly by the Scientific Publications Office, National Marine Fisheries Service, NOAA, 7600 Sand Point Way NE, Seattle, WA 98115-0070.

Although the contents of this publication have not been copyrighted and may be reprinted entirely, reference to source is appreciated.

The Secretary of Commerce has determined that the publication of this periodical is necessary according to law for the transaction of public business of this Department. Use of funds for printing of this periodical has been approved by the Director of the Office of Management and Budget.

For Sale by the Superintendent of Documents, U.S. Government Publishing Office, Washington, DC 20401. Subscription price per year: $32.00 domestic and $44.80 foreign. Cost per single issue: $19.00 domestic and $26.60 foreign. **See back for order form.**

Fishery Bulletin carries original research reports on investigations in fishery science, engineering, and economics. It began as the Bulletin of the United States Fish Commission in 1881; it became the Bulletin of the Bureau of Fisheries in 1904 and the *Fishery Bulletin* of the U.S. Fish and Wildlife Service in 1941. Separates were issued as documents through volume 46; the last document was no. 1103. Beginning with volume 47 in 1931 and continuing through volume 62 in 1963, each separate appeared as a numbered bulletin. A new system began in 1963, with volume 63, in which papers are bound together in a single issue. Beginning with volume 70, number 1, January 1972, *Fishery Bulletin* became a periodical, issued quarterly. In this form, it is available by subscription from the Superintendent of Documents, U.S. Government Publishing Office, Washington, DC 20401. It is also available free in limited numbers to libraries, research institutions, and state and federal agencies and in exchange for other scientific publications.

U.S. Department of Commerce
Seattle, Washington

Volume 119
Number 4
October 2021

Fishery Bulletin

Contents

Articles

201–215 **Stephanie A. Berkman, Trent M. Sutton, Franz J. Mueter, and Brian W. Elliott**

Effects of early-life stage and environmental factors on the freshwater and marine survival of Chinook salmon (*Oncorhynchus tshawytscha*) in rivers of Southeast Alaska

216–230 **Matthew D. Campbell, Ariane Huddleston, David Somerton, M. Elizabeth Clarke, Waldo Wakefield, Steve Murawski, Chris Taylor, Hanumant Singh, Yogesh Girdhar, and Mary Yoklavich**

Assessment of attraction and avoidance behaviors of fish in response to the proximity of transiting underwater vehicles

231–242 **W. David McElroy, Jessica Blaylock, Gary R. Shepherd, Christopher M. Legault, Paul C. Nitschke, and Katherine A. Sosebee**

Comparison of a bottom longline survey and a bottom trawl survey for 2 groundfish species in the Gulf of Maine to evaluate habitat-related availability of large fish

243–254 **Adam G. Fox, Nathaniel Q. Hancock, J. Andrew Marbury, Adam J. Kaeser, and Douglas L. Peterson**

Recruitment and survival of juvenile Gulf sturgeon (*Acipenser oxyrinchus desotoi*) in the Apalachicola River in Florida

Note

255–260 **Emily P. Bond and Michael C. James**

Postrelease movements of leatherback turtles (*Dermochelys coriacea*) following incidental capture in fishing gear in the Atlantic Ocean

The National Marine Fisheries Service (NMFS) does not approve, recommend, or endorse any proprietary product or proprietary material mentioned in this publication. No reference shall be made to NMFS, or to this publication furnished by NMFS, in any advertising or sales promotion that would indicate or imply that NMFS approves, recommends, or endorses any proprietary product or proprietary material mentioned herein or that has as its purpose an intent to cause directly or indirectly the advertised product to be used or purchased because of this NMFS publication.

The NMFS Scientific Publications Office is not responsible for the contents of the articles.

Articles

261–273 **Elise R. Koob, Scott P. Elzey, John W. Mandelman, and Michael P. Armstrong**

Age validation of the northern stock of black sea bass (*Centropristis striata*) in the Atlantic Ocean

274–293 **Leanne M. Poussard, Eric N. Powell, and Daniel R. Hennen**

Discriminating between high- and low-quality field depletion experiments through simulation analysis

294 **Acknowledgment of reviewers**

295–298 **Guidelines for authors**

National Marine Fisheries Service
NOAA

Fishery Bulletin
established in 1881

Spencer F. Baird
First U.S. Commissioner of Fisheries and founder of *Fishery Bulletin*

Effects of early-life stage and environmental factors on the freshwater and marine survival of Chinook salmon (*Oncorhynchus tshawytscha*) in rivers of Southeast Alaska

Stephanie A. Berkman (contact author)[1]
Trent M. Sutton[1]
Franz J. Mueter[2]
Brian W. Elliott[3]

Email address for contact author: stephberkman@gmail.com

[1] Fisheries Department
College of Fisheries and Ocean Sciences
University of Alaska Fairbanks
P.O. Box 757220
Fairbanks, Alaska 99775

[2] Fisheries Department
College of Fisheries and Ocean Sciences
University of Alaska Fairbanks
17101 Point Lena Loop Road
Juneau, Alaska 99801

[3] Division of Sport Fish
Alaska Department of Fish and Game
Mile 1 Haines Highway
Haines, Alaska 99827

Abstract—Highly variable recruitment and declines in productivity of Chinook salmon (*Oncorhynchus tshawytscha*) have created economic and cultural hardships throughout Alaska. Therefore, it is necessary to understand the factors influencing these declines. In this study, principal component analysis and regression were used to determine how biological and environmental factors have influenced freshwater survival, smolt production, and marine survival of Chinook salmon in the Chilkat River (brood years 1999–2009) and marine survival in the Stikine River (brood years 1998–2009). Smolt production in the Chilkat River was higher in years when parr had shorter average mid-eye fork lengths, river discharge was low in the fall (P=0.05), and river temperatures and discharge were high in early spring (P=0.03), indicating density-dependent growth in fresh water and the importance of river conditions to annual growth and abundance of this species. Marine survival of fish in the Stikine River was positively related to smolt length, indicating higher survival in years when smolts were larger (coefficient of multiple determination [R^2]=0.26). Greater marine survival of salmon in the Chilkat River occurred in years when smolt migrations ended later in the month of May, smolts were larger, and discharge was lower (R^2=0.5) than in other years. These results indicate the importance of the early marine period in determining year-class strength and highlight the variation in mechanisms that influence survival of stocks of Chinook salmon.

Manuscript submitted 2 October 2020.
Manuscript accepted 2 September 2021.
Fish. Bull. 119:201–215 (2021).
Online publication date: 22 October 2021.
doi: 10.7755/FB.119.4.1

The views and opinions expressed or implied in this article are those of the author (or authors) and do not necessarily reflect the position of the National Marine Fisheries Service, NOAA.

Survival of salmon species (*Oncorhynchus* spp.) of the Pacific Ocean varies with life stage. As a result, identifying critical periods of mortality that determine brood strength can lead to more specific analyses of biotic and abiotic factors that may affect stocks. Although life history strategies vary by species and stock, most salmon undergo single or multiple freshwater wintering periods before migrating to the marine environment (McCormick et al., 1998; Quinn, 2005). The freshwater overwinter and early marine entry periods are frequently recognized as critical periods and bottlenecks for survival in the life history of salmon species in the Pacific Ocean (Beamish and Mahnken, 2001).

In fresh water, parr must survive at least one winter period of freezing water temperatures, low river discharge, surface ice, and low productivity (Biro et al., 2004; Huusko et al., 2007). Results of previous research indicate that overwinter survival of juvenile salmonids is related to body size, with larger individuals having higher survival rates than smaller ones (Zabel and Achord, 2004). Larger, faster-growing individuals can better escape size-selective mortality (such as that resulting from predation), have a larger gape size (enabling the consumption of a greater diversity of prey that are larger and have higher energy), have greater lipid reserves, and have a lower relative metabolic rate, all of which help to sustain them during winter months (Houde, 1987; Sogard, 1997; Biro et al., 2004; Thompson and Beauchamp, 2014). Larger body sizes may also enable these individuals to secure higher quality winter habitats (Quinn and Peterson, 1996; Zabel and Achord, 2004).

Environmental conditions before, during, and after winter can also influence survival (Cunjak, 1988; Lawson et al., 2004). Low water temperatures (<0°C) reduce metabolic rates, reducing feeding efficiency, capability to avoid

predators, and ability to respond to shifting ice conditions (Brown et al., 2011). Stressors from environmental conditions can cause metabolic deficits that lead to starvation or increased predation due to forage-based, risk-taking behaviors (Cunjak, 1988; Biro et al., 2003). Reductions in river discharge during the fall, when fish are moving to overwintering sites, and during winter can limit habitat accessibility and availability, and higher river discharge generally increases suitable habitat and carrying capacity of fish, reducing competitive interactions among juveniles (Lawson et al., 2004; Huusko et al., 2007). However, events of extremely high winter discharge can flush parr from winter habitats, restrict areas for effective drift foraging, and cause ice-related events of fish mortality (Lawson et al., 2004; Huusko et al., 2007; Neuswanger et al., 2014). Increases in turbidity that result from high discharge can further reduce the foraging ability of parr by limiting visibility but can protect fish from visual predators as well (Lawson et al., 2004; Neuswanger et al., 2014).

Following winter, parr undergo behavioral and physical changes, known as smoltification, and become adapted to living in a marine environment (Healey, 1991). Early marine entry is a critical period for juvenile salmon that can determine strength of brood years (BYs) (Beamish and Mahnken, 2001; Mueter et al., 2002a). Movements of salmon smolts from fresh to marine waters follows the evolutionary concept of risk and reward, the notion that it is energetically advantageous yet riskier to migrate to and feed in the ocean than it is to remain in resource-limited fresh waters (Jonsson and Jonsson, 1993; Quinn, 2005). Results of previous research on smolt migration indicate that large variability in marine survival may be due to migration timing and a match or mismatch between smolt arrival in the ocean and nearshore marine conditions, including food availability (Rikardsen et al., 2004; Hvidsten et al., 2009). Smolt body size and changes in river conditions, such as increases in temperature and river discharge, have been linked to the timing of smolt migration (Bohlin et al., 1993; Vega et al., 2017). Environmental changes, such as increases in water temperature, trigger migratory movements, but river discharge may augment migration as higher flows allow some passive transportation downstream (Bohlin et al., 1993; McCormick et al., 1998).

Correlations between body size, early marine growth, and survival have been observed in most species of salmon in the Pacific and Atlantic Oceans (Holtby et al., 1990; Koenings et al., 1993; Mortensen et al., 2000; Antonsson et al., 2010; Murphy et al., 2013). The critical size and critical period hypothesis is that, for Pacific salmon (*Oncorhynchus* spp.), the majority of natural mortality in marine environments occurs during 2 periods: 1) mortality of fish due to predation in the early marine period and 2) mortality of fish smaller than a critical size due to their inability to meet minimum metabolic requirements during their first year at sea (Beamish and Mahnken, 2001). Larger, faster-growing individuals are able to capture larger prey at an earlier age, resulting in improved metabolic efficiency and greater growth (Quinn, 2005). Fish typically have an optimal temperature range, within which metabolic rate is most efficient and growth is maximized (Wootton, 1998). Regional ocean conditions, including upwelling and advection, affect water temperatures and prey abundances and distributions; in turn, these conditions may benefit or hinder growth and survival (Cole, 2000; Mortensen et al., 2000; Mueter et al., 2002b). Body size of juveniles during the early marine period is more influential during years when mortality is high and marine survival is below average, indicating that having a large body size is more important when marine conditions are suboptimal for growth and survival (Holtby et al., 1990; Graham et al., 2019).

Although results of previous research indicate the importance of physical and environmental conditions to the survival of stocks of Pacific salmon in fresh water during the early marine period, the factors influencing variability in recruitment and survival can be unique to each stock and remain unknown for many stocks (Malick et al., 2009). Chinook salmon (*O. tshawytscha*) in Alaska support important and diverse subsistence, commercial, recreational, and personal use fisheries. In Southeast Alaska (SEAK), declines in abundance and catch of stocks of Chinook salmon, increased variability in productivity, and overfishing over the past 60 years have led to fishing restrictions, which have created cultural, social, and economic hardships for communities in this region (ADFG CSRT[1]). With impending threats, including climate change and mine development, it is imperative to understand the basic mechanisms affecting survival and recruitment of this species.

The objectives of this study were 1) to examine influences of biological (parr length) and local environmental (temperature and discharge) factors on freshwater overwinter survival and smolt production of Chinook salmon in the Chilkat River, in SEAK near Juneau; 2) to determine how biological factors, such as smolt body size and migration timing, and local environmental factors, including regional sea-surface temperatures (SSTs) and river discharge and temperatures, influenced marine survival of Chinook salmon in the Chilkat River; and 3) to determine how a biological factor, smolt body size, and local environmental factors, including regional SSTs and river discharge, influenced marine survival of Chinook salmon in the Stikine River, further southeast in SEAK. This research helps clarify the factors that influence freshwater overwinter and marine survival of Chinook salmon and will allow managers to develop more accurate and reliable catch forecasts.

Materials and methods

Study sites

The Chilkat and Stikine Rivers were selected for this study because they support important regional stocks

[1] ADFG CSRT (Alaska Department of Fish and Game Chinook Salmon Research Team). 2013. Chinook salmon stock assessment and research plan, 2013. Alaska Dep. Fish Game, Special Publ. 13–01, 56 p. [Available from website.]

of Chinook salmon and long-term data exists for both systems. These rivers are 2 of the 11 indicator systems selected by the Alaska Department of Fish and Game (ADFG) and Fisheries and Oceans Canada to be sampled and studied as part of in-depth stock assessments for Chinook salmon (ADFG CSRT[1]). This monitoring program was initiated because of statewide and regional stock declines for this species and the need for increased information for run forecasting (ADFG CSRT[1]).

The Chilkat River is a moderately sized, glacially fed river that originates at the Chilkat Glacier in British Columbia, Canada, and drains into Lynn Canal near Haines, Alaska (ADFG CSRT[1]; Elliott and Peterson[2]) (Fig. 1). This river supports the fifth-largest stock of Chinook salmon in SEAK, with an annual spawning run of about 4000 large (>660 mm in mid-eye fork length) fish (ADFG CSRT[1]). Adult Chinook salmon from the Chilkat River typically grow in the inside marine waters of northern SEAK (Elliott and Peterson[2]).

The Stikine River is a transboundary river originating in British Columbia and draining near Wrangell, Alaska. Chinook salmon in this system are jointly managed by the ADFG and Fisheries and Oceans Canada (Jaecks et al.[3]) (Fig. 1). The Stikine River supports the second-largest stock of Chinook salmon in SEAK, with an annual spawning run of about 22,000 large fish (Pahlke[4]; ADFG CSRT[1]). Adult Chinook salmon from the Stikine River primarily grow in the Gulf of Alaska and the Bering Sea (Pahlke et al.[5]).

Chinook salmon in both rivers have a stream-type life history, where juveniles reside in fresh water for 1 year before migrating downstream as age-2 smolts (Quinn, 2005; ADFG CSRT[1]). The age structure for returning adults was similar for Chinook salmon from the Stikine and Chilkat Rivers, with most adults returning to fresh water after 2–4 years in the marine environment (Chapell[6]). Sampling effort and design of surveys to estimate smolt abundance and adult return were similar for work in both rivers. However, surveys of freshwater juvenile Chinook salmon conducted in the fall and spring in the Chilkat River allowed assessment of additional freshwater processes (overwinter survival and smolt production); as a result, data from each river system were analyzed separately.

[2] Elliott, B. W., and R. L. Peterson. 2018. Production and harvest of Chilkat River Chinook and coho salmon, 2018–2019. Alaska Dep. Fish Game, Reg. Oper. Plan SF.1J.2018.10, 47 p.. [Available from website.]

[3] Jaecks, T., P. Richards, S. J. H. Power, P. Etherton, and I. Boyce. 2015. Estimation of smolt production and harvest of Stikine River Chinook salmon, 2015. Alaska Dep. Fish Game, Reg. Oper. Plan SF.1J.2015.04, 18 p. [Available from website.]

[4] Pahlke, K. A. 2010. Escapements of Chinook salmon in Southeast Alaska and transboundary rivers in 2008. Alaska Dep. Fish Game, Fish. Data Ser. 10-71, 38 p. [Available from website.]

[5] Pahlke, K. A., P. Richards, and P. Etherton. 2010. Production of Chinook salmon from the Stikine River, 1999–2002. Alaska Dep. Fish Game, Fish. Data Ser. 10-03, 16 p. [Available from website.]

[6] Chapell, R. S. 2013. Production, escapement, and juvenile tagging of Chilkat River Chinook salmon in 2010. Alaska Dep. Fish Game, Fish. Data Ser. 13-25, 48 p. [Available from website.]

Chilkat River

Biological data We estimated values for several biological attributes for Chinook salmon in the Chilkat River by using data from 2 efforts conducted by the ADFG: a tagging study in which coded-wire tags (CWTs) are attached to juveniles in both the fall and spring (we used data for the period 2000–2011) and a mark-recapture program that targeted adults (we used data for the period 2002–2016) (Elliott and Power[7]; Elliott and Peterson[2]). The biological factors estimated were marine survival, the rate of survival from freshwater emigration to return for spawning (BYs: 1999–2009); smolt abundance, the number of juvenile salmon in the spring; smolt mean mid-eye fork length (in millimeters); parr abundance, the number of juvenile salmon in the fall; parr mean mid-eye fork length (in millimeters); and overwinter survival, the survival rate of juvenile salmon from the fall to the spring.

The mark-recapture survey was executed by using a 2-event sampling scheme for a closed population. For the first sampling event, adult Chinook salmon were captured and marked between 10 June and 24 July of each survey year in the lower Chilkat River. For the second sampling event, adults were captured from August through mid-September in each survey year in the 3 principal spawning tributaries of the Chilkat River, the Kelsall, Tahini, and Klehini Rivers. Chinook salmon captured during sampling events were measured to the nearest 5-mm interval of mid-eye fork length, their sex was determined, scales were sampled, and the fish were inspected for the presence or absence of an adipose fin (small fin located between the dorsal and caudal fins). Fish that did not have an adipose fin were processed and scanned with a CWT detector (Elliott and Power[7]).

Data from both sampling events were tabulated, and Petersen estimators were used to estimate abundance, given that all assumptions of the model were met during sampling (Seber, 1982). Size, age, and sex selectivity in sampling data were evaluated by using Kolomogorov–Smirnov tests. If selectivity was present in data from either the first or second sampling event, a stratified Petersen model was used to eliminate variability in capture probability (Elliott and Power[7]). Adult abundance was estimated by using results from both the mark-recapture and CWT surveys. Marked adult fish from the Chilkat River were primarily recovered in seasonal troll, SEAK sport, drift gill-net, or purse seine fisheries during annual surveys conducted by the ADFG, which aims to sample 20% of the catch of Chinook salmon in SEAK (Elliott and Peterson[2]). Marine survival was calculated by using the estimated values for smolt and adult abundance associated with each BY.

The CWT survey of juvenile Chinook salmon was initiated in 2000 to estimate parr and smolt abundance, smolt emigration, and marine catch of the stock in the Chilkat

[7] Elliott, B. W., and S. J. H. Power. 2015. Chilkat River Chinook salmon escapement studies in 2015. Alaska Dep. Fish Game, Reg. Oper. Plan SF.1J.2015.13, 31 p. [Available from website.]

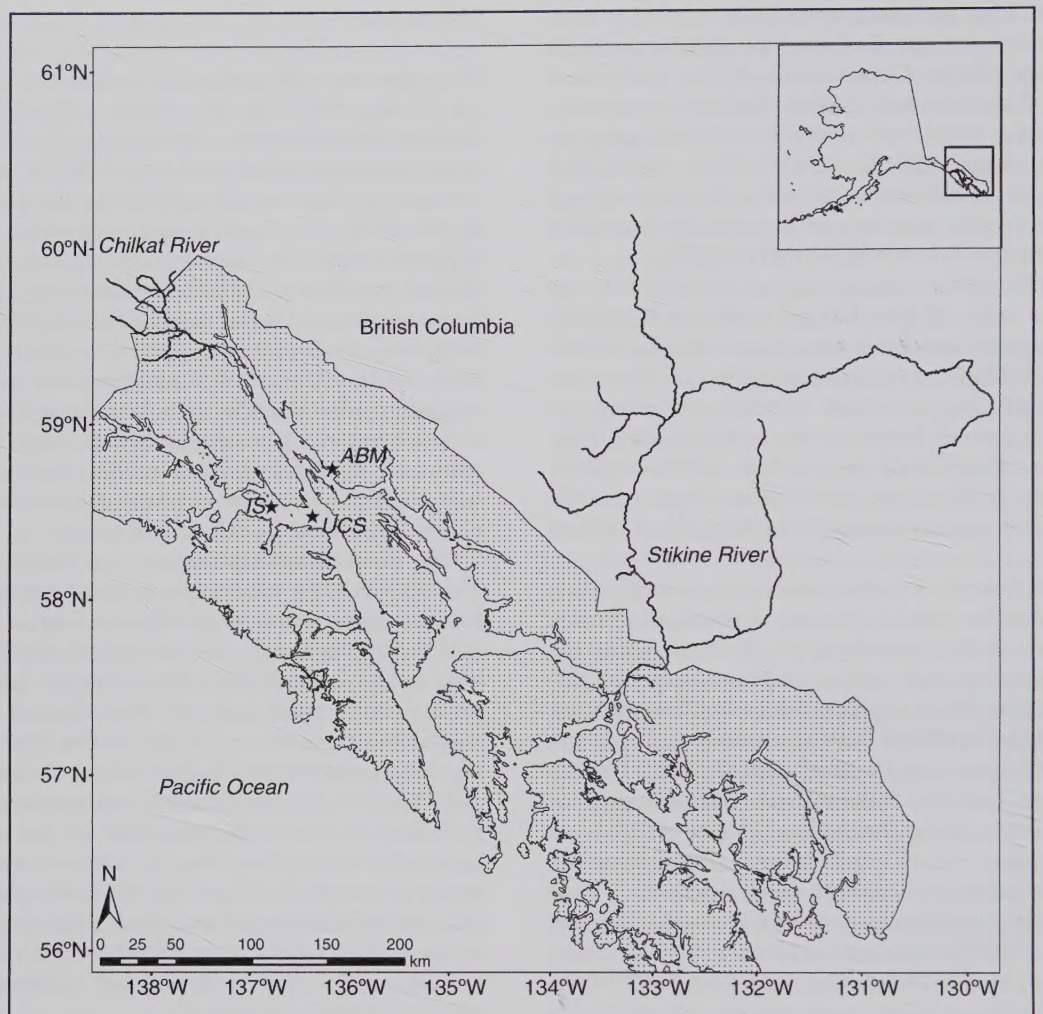

Figure 1

Map of the Chilkat and Stikine Rivers in Southeast Alaska and in British Columbia, Canada. The influence of environmental and biological factors on marine survival, freshwater overwinter survival, and smolt production of Chinook salmon (*Oncorhynchus tshawytscha*) from these rivers was examined. Chinook salmon sampled from the Chilkat River were from the brood years 1999–2009 and those sampled from the Stikine River were from the brood years 1998–2009. The stars indicate the 3 locations where sea-surface temperatures were collected monthly from May through August during 1997–2015: Auke Bay Monitor (ABM), Upper Chatam Strait (UCS), and Icy Strait (IS).

River (Chapell[6]). The tagging of juveniles occurred from mid-September through October for parr and from April through May for smolts. The fall sampling period began in September at upriver locations and moved downstream as the season progressed, ending at the lower portion of the main stem of the Chilkat River. Spring sampling started in April and was conducted entirely on the lower portion of the main stem of the Chilkat River. In both sampling periods, juvenile Chinook salmon were captured each day by using 100 Gee minnow traps (Cuba Specialty Manufacturing[8], Fillmore, NY) baited with disinfected salmon roe (Chapell[6]). The ADFG fit a statistical model to CWT data from both sampling events to estimate parr abundance, smolt abundance, and overwinter survival (Elliott and Peterson[2]). Estimates of total annual abundance of smolts were used to represent freshwater smolt production.

Data from the spring sampling of the CWT program in the Chilkat River were used to create indices of smolt migration timing. The number of minnow traps and catches of Chinook salmon were used to calculate the daily catch per unit of effort over the spring sampling period (early April–late May) for each reach of the river (Elliott and Peterson[2]). The daily catch per unit of effort in the lower Chilkat River was used as a proxy for the total number of fish migrating to the ocean each day. To capture differences in annual migration timing, the ordinal date

[8] Mention of trade names or commercial companies is for identification purposes only and does not imply endorsement by the National Marine Fisheries Service, NOAA.

when 95% of smolts had been captured was used to define the end of the outmigration period. This index was used in this study rather than an estimate of the start or median migration date because smolt sampling began after the start of migration in some years, making accurate estimation of passage dates difficult. In addition, this index was assumed to be resistant to the biases associated with minnow trap catch data, indicating that daily variability in catch can be based on location, not on the actual number of fish outmigrating on a given day. This is because the index used in our study is based on a consistent decline in daily number of fish caught over the course of the migration period rather than on the number of fish caught on any single day. (He and Lodge, 1990).

Physical data: overwinter survival To determine the local factors influencing overwinter survival of Chinook salmon in the Chilkat River, environmental data for BYs during the fall and spring freshwater periods were examined. River discharge data were not available for the Chilkat River during 2000–2010 (BYs 1999–2009); therefore, the combined standardized mean monthly discharge from the Taku, Stikine, and Antler Rivers during 1998–2015 for fall (September–November) and spring (March–April) was used as a proxy for river discharge in SEAK. These rivers were chosen because they were the only glacial systems in the region with data for the entire study period. These rivers represent a range of drainage sizes, with mean annual discharges during 2014–2016 of 4 m^3/s for the Antler River, 401 m^3/s for the Taku River, and 1660 m^3/s for the Stikine River. Discharge data were obtained from the U. S. Geological Survey (USGS) National Water Information System (available from website, accessed February 2017) as follows: Taku River near Juneau (USGS gauging station no. 15041200), Stikine River near Wrangell (USGS gauging station no. 15024800), and Antler River near Auke Bay, Alaska (USGS gauging station no. 15055500). Although river discharge during winter may also affect overwinter survival (Lawson et al., 2004), the USGS rated discharge measurements from ice-covered rivers as poor, and rivers in SEAK are typically ice covered from December through early March (B. Elliott, personal commun.).

Long-term monthly temperature data were not available for the Chilkat River; however, air temperature data were available for a NOAA station close to the Chilkat River in Klukwan, Alaska (Haines 40 NW [station ID: USC00503504]; Global Summary of the Month data set based on the Global Historical Climatology Network daily data set available from website, accessed February 2017). Because stream temperatures are strongly correlated with air temperature above freezing (0°C), daily air temperatures from the Haines 40 NW station for September–November (fall) and March–April (spring) were used as proxies for stream water temperatures (Mohseni and Stefan, 1999). Although the relationship between air and water temperatures may be different for glacially fed streams, the air temperature indices used in these analyses likely captured the annual variation in water temperatures.

Physical data: marine survival To analyze how regional environmental factors that occur during the early marine period correlate to marine survival of Chinook salmon in the Chilkat River, SSTs from inshore marine waters of SEAK (in degrees Celsius) were collected by NOAA during the Southeast Alaska Coastal Monitoring survey in 1997–2015 (Orsi and Fergusson[9]). Sea-surface temperature was sampled monthly from May through August by using a conductivity, temperature, and depth sonde at a depth of 3 m at 3 different locations (Orsi and Fergusson[9]). These sampling locations represented inshore (Auke Bay Monitor) and strait (Upper Chatham Strait and Icy Strait) growing habitats (Orsi and Fergusson[9]) (Fig. 1). Because Chinook salmon in SEAK migrate to the marine environment from April through late May, an index of marine entry SSTs was developed by averaging the SSTs for all stations during June and July (Orsi and Fergusson[9]; Elliott and Peterson[2]). This index was lagged by 2 years (BY+2 years) to reflect conditions during ocean entry.

River conditions during smolt outmigration were also used in the analysis of marine survival. Average river temperature and river discharge at the time of outmigration (April–May) can affect run timing and early ocean conditions experienced by smolts. River temperature data were collected by the ADFG during smolt sampling of the CWT program for the period 2001–2011 (Elliott and Peterson[2]). Daily temperatures were averaged for each year to develop a variable for overall spring river water temperature. Using the previously described proxy for river discharge in SEAK, a spring migration period discharge index was developed by averaging monthly mean discharge (SEAK index on standardized scale) for April–May, the primary migration period for smolt Chinook salmon.

Data analysis The influence of biological and environmental factors on overwinter survival and smolt production of Chinook salmon in the Chilkat River was determined through principal component analysis and principal component regression. During preliminary examination of the data, the Pearson product-moment correlation coefficient (r) was used to make pairwise comparisons between explanatory variables. Results indicate significant positive correlation between parr length and fall discharge and early spring temperature and discharge (Table 1). Because of small sample sizes (n=11), 5 explanatory variables and multicollinearity between variables were most appropriate for principal component analysis and principal component regression. The environmental explanatory variables were lagged to represent conditions experienced by fish during their first fall prior to wintering in fresh water (BY+1) and during the following spring during outmigration (BY+2). Parr length, fall and spring discharge, and fall and spring air temperature were included in the analysis and new linear combinations of the standardized

[9] Orsi, J. A., and E. A. Fergusson. 2016. Annual survey of juvenile salmon, ecologically-related species, and biophysical factors in the marine waters of southeastern Alaska, May–August 2015. North Pac. Anadromous Fish Comm. Doc., 71 p. [Available from website.]

Table 1

Mean estimates of and Pearson product-moment correlation coefficients (r) from pairwise comparisons of explanatory variables used in analyses of freshwater survival and production (smolt abundance) and marine survival of Chinook salmon (*Oncorhynchus tshawytscha*) in the Chilkat River (with data for brood years 1999–2009) and in analyses of marine survival of Chinook salmon in the Stikine River (with data for brood years 1998–2009) in Southeast Alaska. Variables include mean parr mid-eye fork length, mean river discharge and air temperature in the fall (September–November), mean river discharge and air temperature in early spring (March–April), mean smolt length, migration timing, sea-surface temperature (SST), and mean river discharge and water temperature in the spring (April–May). A standardized index, based on monthly mean discharge averaged across rivers in Southeast Alaska for the primary migration period of smolts (April–May), was used for discharge in the Chilkat River. Data for river water temperature were not available for the Chilkat River. An asterisk (*) indicates a significant correlation between variables ($P<0.05$). SD=standard deviation.

	Estimate		r			
Variable	Mean	SD	Parr length	Fall discharge	Spring discharge	Fall temperature
Chilkat River: freshwater survival and production						
Parr length (mm)	68.85	2.67	–			
Fall discharge (index)	−0.06	0.76	0.71*	–		
Spring discharge (index)	−0.04	1.05	0.00	0.25	–	
Fall temperature (°C)	3.16	0.74	0.09	0.39	0.29	–
Spring temperature (°C)	−0.83	1.73	−0.54	−0.08	0.66*	0.11

	Estimate		r			
Variable	Mean	SD	Migration timing	SST	Smolt length	Spring discharge
Chilkat River: marine survival						
Migration timing (ordinal date)	136.09	4.16	–			
SST (°C)	12.03	0.79	−0.05	–		
Smolt length (mm)	73.42	3.37	0.73*	−0.10	–	
Spring discharge (index)	−0.02	1.03	−0.69*	0.53	−0.56	–
Spring temperature (°C)	4.34	0.76	0.44	−0.18	0.30	−0.32

	Estimate		r		
Variable	Mean	SD	SST	Smolt length	Spring discharge
Stikine River: marine survival					
SST (°C)	73.58	3.03	–		
Smolt length (mm)	12.07	0.77	−0.18	–	
Spring discharge (m^3/s)	40,499	11,381	−0.35	0.44	–

variables (mean: 0; standard deviation: 1) were created by using principal component analysis with varimax rotation (Jackson, 2005).

The number of rotated components (RCs) that contained interpretable information were chosen through a visual assessment of a scree plot. Principal component regression models were fit to test for significant relationships between response variables (log-transformed overwinter survival and smolt production) and RCs. In addition, to uncover potential density dependence during the pre-smolt freshwater period, a simple linear regression was fit to describe the relationship between parr abundance and parr length.

Principal component analysis in combination with principal component regression was used to estimate effects of biological and environmental factors on marine survival of Chinook salmon in the Chilkat River because of the low sample size, high number of explanatory variables, and multicollinearity. Results of pairwise comparisons of explanatory variables made by using the r indicate significant correlation between the timing of the end of the smolt migration and smolt length (positive) and late spring discharge (negative) (Table 1). For these analyses, log-transformed marine survival was used as the response variable, and principal component (PC) variables that combine spring river temperature and discharge, summer SST, ordinal date at the end of smolt outmigration, and smolt length were included as explanatory variables. Environmental and run timing variables were lagged (BY+2)

to represent conditions and run timing experienced by a given BY. All statistical analyses were conducted in R, vers. 3.6.3 (R Core Team, 2020).

Stikine River

Biological data Marine survival, smolt abundance, and smolt fork length (in millimeters) of Chinook salmon returning to the Stikine River (BYs 1998–2009) were estimated with data collected by the ADFG, Fisheries and Oceans Canada, and Tahltan First Nation during the mark-recapture survey of adult Chinook salmon (we used data for the period 2001–2016) and during the CWT survey conducted in spring (we used data for the period 2000–2011) (Pahlke et al.[5]; Jaecks et al.[3]; Jaecks[10]). Data from the mark-recapture program were used to estimate in-river abundance of large Chinook salmon in the Stikine River, and those estimates, in turn, were used to calculate marine survival. The mark-recapture experiment was completed in 2 phases. During the first phase, Chinook salmon were captured during May–July with drift gill nets on the lower Stikine River; during the second phase, fish were captured from June through August with the same gear on the spawning grounds upriver (Jaecks et al.[11]). Captured Chinook salmon were measured for mid-eye fork length, externally examined to determine sex, sampled for scales, marked, and then released. Fish in both phases with missing adipose fins were processed similar to such Chinook salmon caught in the Chilkat River. The estimated abundance parameter was tabulated by using Chapman's modification of the Petersen estimator, as long as all assumptions were met (Seber, 1982). When assumptions were violated, a variety of stratification and modeling techniques were used on data to correct for bias as much as possible (Jaecks et al.[11]).

Data from the CWT study of juvenile Chinook salmon were used to estimate the number of smolts emigrating from the Stikine River. This study was designed as a modified Petersen 2-event mark-recapture effort, where the tagging of juveniles (>50 mm in fork length) in the spring was the first sampling event and the mark-recapture of adults (described previously) was the second sampling event. Juvenile Chinook salmon were sampled annually in mid-April in the lower reaches (U.S. side) of the Stikine River (Jaecks et al.[3]). Salmon were caught by using beach seines that were 18 by 2 m or 24 by 2 m (depending on the crew), all with 63.5-cm mesh, and by using Gee minnow traps baited with disinfected salmon roe. Smolt abundance was estimated, by using adult mark-recapture data, for the 5 years it takes for each brood of smolts to return to the river. The fraction of the population that had been originally marked was estimated each year. If those estimates were similar for all years, data were pooled and Chapman's modification of Petersen's estimator was used. If the estimates for the fraction of the population that had been marked were not consistent, the estimates were averaged over the years (Jaecks et al.[3]). Marked adult fish from the Stikine River were primarily recovered in marine, troll, and drift gill-net fisheries (Pahlke et al.[5]).

Physical data To assess the relationship between marine survival and regional environmental conditions during the early marine period for Chinook salmon from the Stikine River, SST and river discharge were included in the model. Sea-surface temperature, as described previously, was similarly used to represent conditions of the inshore marine waters of SEAK (in degrees Celsius) upon ocean entry of Chinook salmon (June–July). To represent river conditions during outmigration, data for monthly mean river discharge in the Stikine River was averaged for April–May (USGS gauging station no. 15024800). Data on river water temperatures were not available for the Stikine River and, therefore, not included in the model.

Data analysis For Chinook salmon in the Stikine River, multiple and simple linear regression analyses were used to test for significant relationships between log-transformed marine survival and spring discharge, summer SST, and smolt length. Environmental variables were lagged (BY+2) to represent experienced conditions of a given BY. The statistical approach used to examine factors for fish in the Stikine River was more simplistic than that used in analyses conducted for fish in the Chilkat River because there were fewer explanatory variables (n=3) and no correlation between those variables according to a pairwise comparison (Table 1). Results of the preliminary exploration of variables included in the analyses for salmon in the Stikine River indicate the presence of a possible outlier; therefore, robust linear regression analyses were used as implemented in the function lmRob of the robust package (vers. 0.5-0.0; Wang et al., 2020) in R. A backward-stepwise approach, which was based on the Akaike information criterion for small sample sizes and removed terms one at a time on the basis of the largest reduction in deviance, was used to select the top models. All statistical analyses were conducted in R.

Results

Chilkat River

Overwinter survival and smolt production Over the time series (BY 1999–2009), mean freshwater overwinter survival for Chinook salmon in the Chilkat River was 36% (standard error of the mean [SE] 10) and ranged from 21% (SE 5) for BY 2000 to 53% (SE 15) for BY 2005 (Fig. 2). Mean smolt abundance was 172,616 individuals and ranged from 105,300 individuals in 2000 to 282,700 individuals in 2003 (Fig. 2). There was no significant linear trend over time in annual estimates of overwinter survival

[10] Jaecks, T. 2016. Personal commun. Div. Sport Fish Commer. Fish., Alaska Dep. Fish Game, P.O. Box 115526, Juneau, AK 99811-5526.

[11] Jaecks, T., P. Richards, and P. Etherton. 2013. Spawning escapement of Chinook salmon in the Stikine River, 2013. Alaska Dep. Fish Game, Reg. Oper. Plan SF.1J.2013.05, 27 p. [Available from website.]

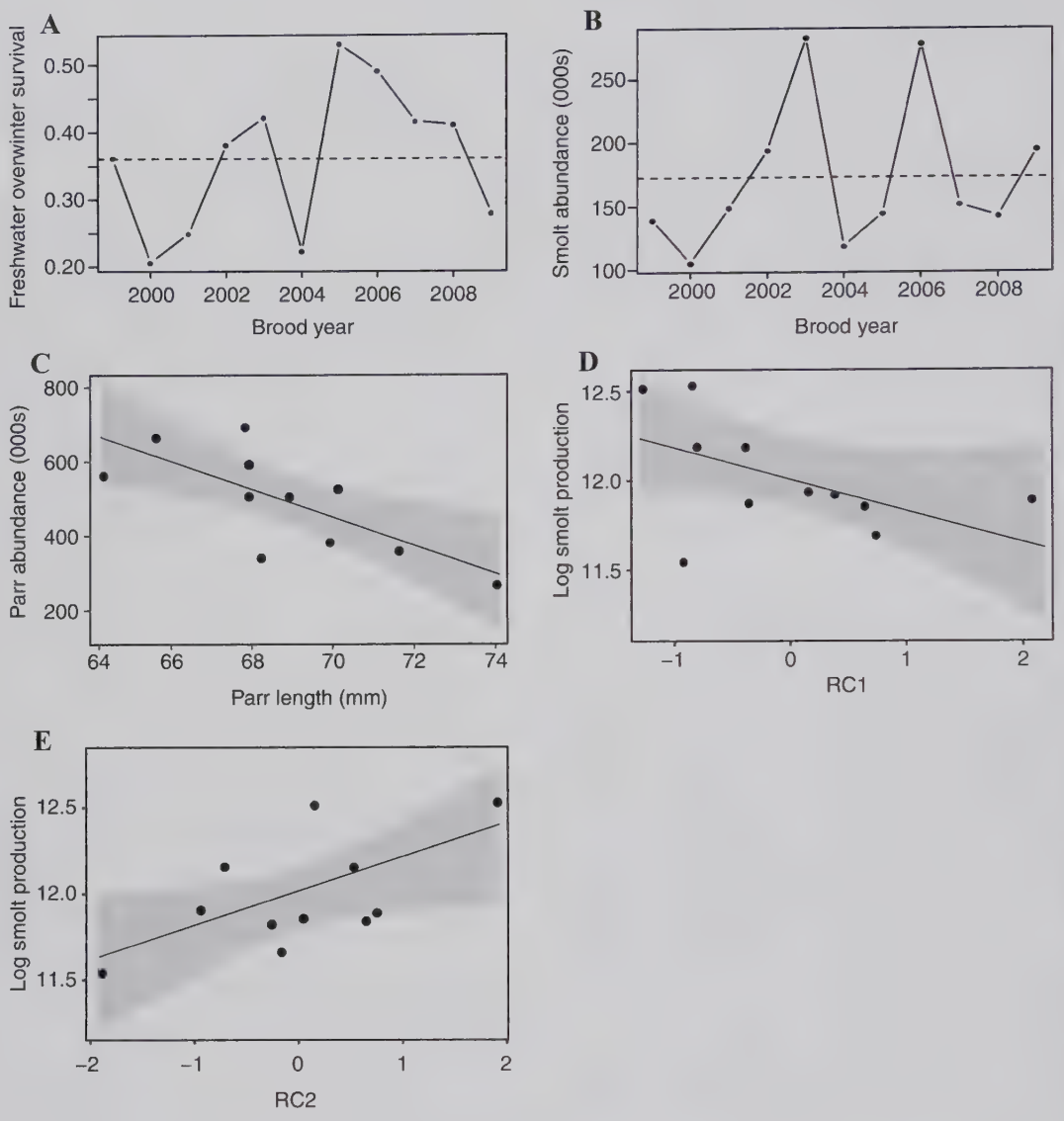

Figure 2

Time series of (**A**) overwinter survival and (**B**) smolt abundance by brood year (1999–2009), (**C**) the relationship between parr abundance and parr mid-eye fork length, and the relationships between log-transformed smolt production (estimated spring abundance) and the (**D**) first rotated component (RC1) and (**E**) second rotated component (RC2) for Chinook salmon (*Oncorhynchus tshawytscha*) during their freshwater period in the Chilkat River in Southeast Alaska. The horizontal dashed lines in panels A and B indicate mean freshwater overwinter survival and smolt abundance. The regression line and 95% confidence interval (gray areas) in panel C are based on a regression of parr length on parr abundance. The regression lines and 95% confidence intervals (gray areas) in panels D and E are based on the principal component regression of RC1 and RC2 on smolt production.

(coefficient of multiple determination [R^2]=0.12, P=0.29) or smolt abundance (R^2=0.05, P=0.49).

Overall mean parr mid-eye fork length was 69 mm, ranging from an annual mean of 64 mm in 2006 to 74 mm in 2005. Results from the simple linear regression indicate a significant negative relationship between parr length and parr abundance (R^2=0.54, P=0.01) (Fig. 2). Over the study period, river discharge was consistent in fall and was higher and more variable in spring. The mean temperature in fall was 3.2°C (range: 2.2–4.8°C), and the mean temperature in spring was −0.8°C (range: −3.8–2.5°C). There were no significant temporal trends in discharge (fall: P=0.45; spring: P=0.86) or temperature (fall: P=0.93; spring: P=0.74).

Two RCs were retained for analyses on the basis of a scree plot and accounted for 39% and 38% of the overall

variability in the data set. The first RC (RC1) loaded most heavily on parr length and fall discharge, and the second one (RC2) loaded most heavily on early spring discharge and temperature (Table 2). Results from the principal component regression model indicate that the 2 RCs explained little of the variation in overwinter survival (adjusted R^2=0.14, F=1.78, P=0.23). There were no significant relationships between overwinter survival and RC1 (P=0.51) or RC2 (P=0.12) (Table 3). In contrast, smolt production was significantly related to both RC1 (standardized regression coefficient [β]=–0.10, P=0.05) and RC2 (β=0.19, P=0.03), indicating that smolt production was enhanced when parr were smaller and discharge was lower during the previous fall and when discharge was higher and temperatures were warmer in the spring (Table 3, Fig. 2).

Marine survival Over the time series (BY 1999–2009), mean marine survival of Chinook salmon in the Chilkat River was 2.8% (SE 0.7) and ranged from 1.3% (SE 0.4) for BY 2002 and 1.3% (SE 0.7) for BY 2008 to 4.7% (SE 1.0) for BY 2000 (Fig. 3). Although not significant at the 95% level, there was a negative temporal trend in marine survival for fish in the Chilkat River (R^2=0.34, P=0.06).

The annual mean mid-eye fork length for smolt Chinook salmon in the Chilkat River was 73 mm (range: 69–79 mm), and there was no significant trend in smolt length over the study period. Mean summer SST over the study period was 12.0°C, and summer SSTs ranged from 10.5°C to 13.0°C. Mean temperature in the Chilkat River during the spring migration period (April–May) was 4.3°C (range: 3.3–5.5°C). The index value for standardized mean spring discharge in SEAK was –0.02 (range: –1.5–2.3). There was no significant temporal trend over this period (temperature: P=0.16; discharge: P=0.57). On average across BYs, smolt outmigration in the Chilkat River ended on ordinal date 136 (15 or 16 May), and the end date ranged from ordinal date 129 (8 May) in 2004 (BY 2002) to ordinal date 143 (23 May) in 2001 (BY 1999). Outmigration timing (end date of outmigration) was positively related to smolt length (r=0.73) and negatively related to spring discharge (r=–0.69) (Table 1).

Three PCs were retained and used to explain variation in log-transformed marine survival of Chinook salmon in the Chilkat River. The first PC (PC1) loaded heaviest on migration timing, smolt length, and discharge, the second PC (PC2) loaded primarily on SST, and the third PC (PC3) loaded heaviest on average river temperature (Table 4). Log-transformed marine survival of Chinook salmon in the Chilkat River was significantly negatively related to PC1, indicating that marine survival was higher when outmigration ended later and smolt length was greater and that marine survival was lower when spring discharge was higher (R^2=0.5, P=0.01) (Table 5, Fig. 3).

Table 2

Loadings of the first and second rotated components from principal component analysis of environmental and biological variables used to explain variation in overwinter survival and smolt production of Chinook salmon (*Oncorhynchus tshawytscha*) in the Chilkat River in Southeast Alaska. Data used in this analysis were for Chinook salmon from the brood years 1999–2009.

Component	RC1	RC2
Parr length	0.88	–0.31
Fall discharge	0.91	0.17
Spring discharge	0.18	0.87
Fall temperature	0.48	0.47
Spring temperature	–0.35	0.88
Proportion of variance explained	0.39	0.38
Cumulative proportion	0.39	0.77

Stikine River

For Chinook salmon in the Stikine River, mean marine survival was 1.7% (SE 0.3) and ranged from 0.6% (SE 0.1)

Table 3

Results from the principal component regression model used to examine the relationships between the first and second rotated components and overwinter survival and smolt production of Chinook salmon (*Oncorhynchus tshawytscha*) in the Chilkat River in Southeast Alaska. Model statistics include the standardized regression coefficient (β), standard error of the coefficient (SE), coefficient divided by its standard error (t), and the coefficient of multiple determination (R^2). Data used in this model were for Chinook salmon from the brood years 1999–2009.

Explanatory variable	Response variable	Model statistic				
		β	SE	t	P	R^2
Freshwater overwinter survival	RC1	0.04	0.10	0.42	0.68	0.005
	RC2	0.14	0.10	1.37	0.21	
Smolt production	RC1	–0.16	0.07	–2.26	0.05	0.520
	RC2	0.19	0.07	2.75	0.03	

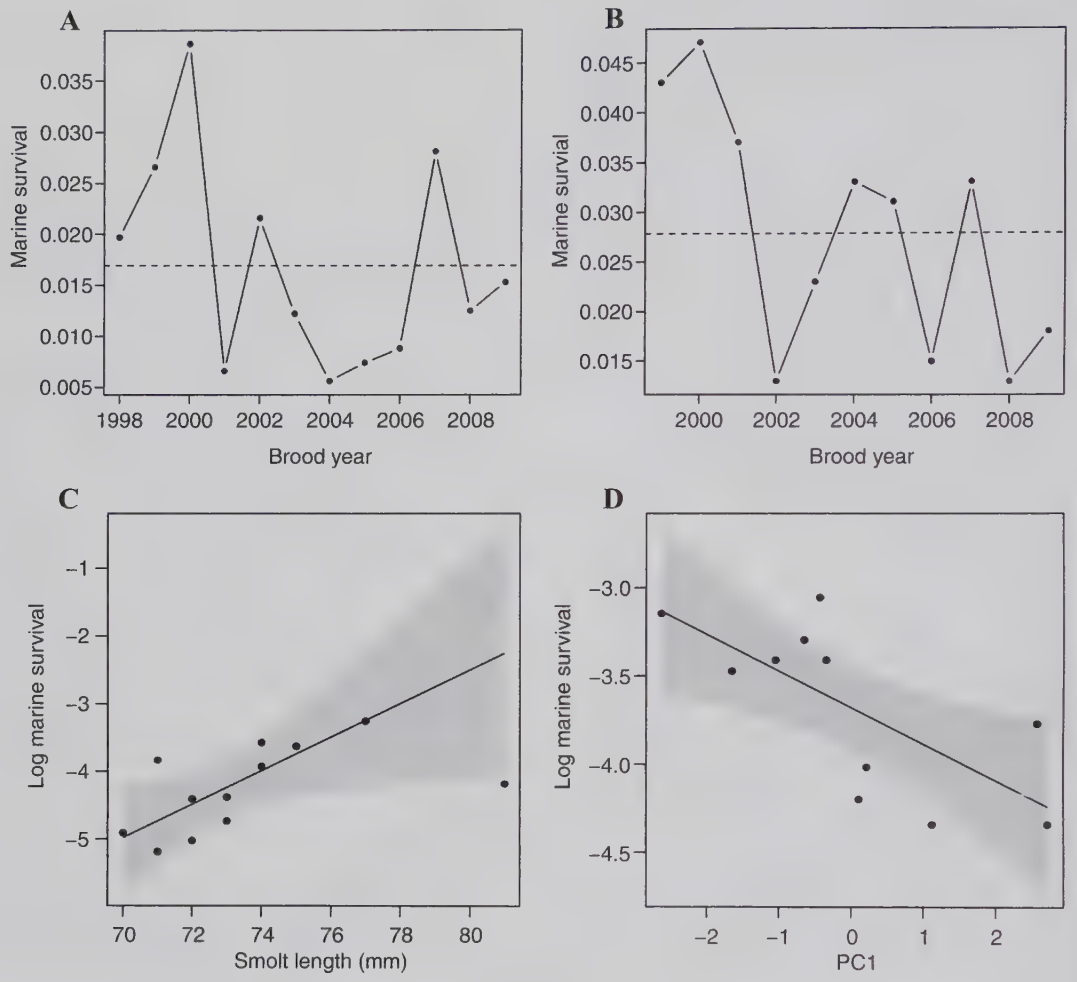

Figure 3

Time series of marine survival of Chinook salmon (*Oncorhynchus tshawytscha*) in the (**A**) Stikine River and (**B**) Chilkat River in Southeast Alaska. The horizontal dashed lines represent mean survival of Chinook salmon for all sample years, the brood years 1998–2009 for the Stikine River and the brood years 1999–2009 for the Chilkat River. The (**C**) relationship between log-transformed marine survival and smolt mid-eye fork length in the Stikine River and the (**D**) relationship between log-transformed marine survival and the first principal component (PC1) in the Chilkat River during the same sample periods are shown. Regression lines and 95% confidence intervals (gray areas) are presented in the bottom panels.

for BY 2004 to 3.9% (SE 0.6) for BY 2000. There was no significant temporal trend in marine survival of fish in the Stikine River (R^2=0.08, P=0.36) (Fig. 3).

Smolt Chinook salmon from the Stikine River were, on average, 74 mm in mid-eye fork length and ranged from 70 mm in 2005 to 81 mm in 2009. There was no significant trend in smolt length over the study period (BYs 1998–2009); however, mean smolt size in 2009 (81 mm) was substantially larger than in previous years and was considered an outlier in the data set. In summer (June–July) during the study period, mean SST was 12.1°C and SSTs ranged from 10.5°C to 13°C. Mean discharge in spring for the Stikine River was 1147 m^3/s (range: 679–1574 m^3/s), with no significant temporal trend (P=0.23).

Log-transformed marine survival of Chinook salmon in the Stikine River was significantly positively correlated to smolt length (R^2=0.26, P=0.05) (Table 5, Fig. 3). There were no significant relationships between marine survival and SST or between marine survival and spring discharge; therefore, neither relationship was included in the final model.

Discussion

Marine survival

Understanding factors influencing the survival and productivity of Chinook salmon during critical periods in

their life history can enhance the accuracy of run forecasts of management agencies that are critical to efforts to sustain healthy populations well into the future. In this study, available data from 2 rivers in SEAK were used. Results of this research highlight variation in biological and environmental factors linked to marine survival of Chinook salmon from different BYs and stocks. Marine survival of Chinook salmon from the Chilkat River was correlated with the timing of the end of the smolt outmigration period, smolt length, and spring river conditions, and marine survival for Chinook salmon from the Stikine River was correlated to smolt body size. Previous research on marine survival of Pacific salmon has emphasized the importance of the early marine period in determining BY strength (Holtby et al., 1990; Graham et al., 2019). Although different factors influenced marine survival of Chinook salmon in the Stikine and Chilkat Rivers during the study period, these results reinforce the importance of the early marine period.

Marine survival was higher in the BYs when mean smolt length was longer, indicating that size-selective processes influence marine survival of Chinook salmon from both the Stikine and Chilkat Rivers. The movements of juvenile Chinook salmon from these rivers upon ocean entry are not well understood. However, the data on CWT recoveries in studies conducted by the ADFG indicate that adult fish from the Stikine River move offshore into the Gulf of Alaska and the Bering Sea and that fish from the Chilkat River inhabit the inside waters of northern SEAK (Pahlke et al.[5]; Elliott and Peterson[2]). Similarities in the relationship between smolt body size and marine survival in these 2 stocks further indicate the importance of freshwater growth and the early marine period, regardless of stock size or behavior.

Results of research on Chinook salmon in the Yukon River, sockeye salmon (*O. nerka*) across Alaska, and wild and hatchery-born chum salmon (*O. keta*) in SEAK also indicate that fish encounter increased size-selective pressures upon marine entry (Koenings et al., 1993; Murphy et al., 2013; Duncan and Beaudreau, 2019). Upon marine entry, smaller fish may encounter higher rates of predation from common nearshore species in SEAK, such as the Pacific staghorn sculpin (*Leptocottus armatus*) and Dolly Varden (*Salvelinus malma*), and larger fish may be more capable of emigrating farther from shore where pelagic zooplankton are more abundant (Koenings et al., 1993; Duncan and Beaudreau, 2019). Although the mechanisms that enhance the survival of larger (>74 mm in mid-eye fork length) juvenile fish in the Stikine and Chilkat Rivers are unclear, the results of our study and these other studies may indicate that size-selective pressures during the marine entry period are similar across stocks of Pacific salmon in the region.

The relationship between smolt size and marine survival also highlights the importance of the freshwater period

Table 4

Loadings of the first, second, and third principal components from a principal component analysis of environmental and biological variables used to explain variation in log-transformed marine survival of Chinook salmon (*Oncorhynchus tshawytscha*) in the Chilkat River in Southeast Alaska. Environmental variables include sea-surface temperature (SST), river discharge in spring, and river temperature in spring. Biological variables include migration timing and smolt length. Data used in this analysis were for Chinook salmon from the brood years 1999–2009.

Explanatory variable	PC1	PC2	PC3
Migration timing	−0.54	0.33	−0.10
SST	0.25	0.85	<0.01
Smolt length	−0.49	0.31	−0.29
Spring discharge	0.53	0.27	0.24
Spring river temperature	−0.36	0.06	0.92
Proportion of variance explained	0.54	0.22	0.15
Cumulative proportion	0.54	0.75	0.91

Table 5

Results from the final principal component regression and linear regression models used to examine the relationships between log-transformed marine survival and principal component 1 (PC1) and smolt length for Chinook salmon (*Oncorhynchus tshawytscha*) in the Chilkat and Stikine Rivers, respectively. The statistics used to evaluate the models include standardized regression coefficient (β), standard error of the coefficient (SE), coefficient divided by its standard error (t), and the coefficient of multiple determination (R^2). Data used in the models were for Chinook salmon from the brood years 1999–2009 for those from the Chilkat River and from the brood years 1998–2009 for those from the Stikine River.

Explanatory variable: marine survival	Response variable	Model statistic				
		β	SE	t	P	R^2
Chilkat River	PC1	−0.21	0.07	−3.03	0.01	0.5
Stikine River	Smolt length	0.25	0.11	2.18	0.05	0.26

and the conditions that allow for greater growth and larger smolt sizes. Smolt outmigration timing has been shown to be stock specific and to correlate with optimal local marine conditions (Hvidsten et al., 1998). Optimal conditions lead to fish experiencing favorable SSTs for growth, increased abundance of food resources, or reduced interactions with predators (Hvidsten et al., 1998; Mortensen et al., 2000). In our study, the end date of outmigration, which could only be tested for Chinook salmon in the Chilkat River, was positively related to marine survival, indicating that smolts of BYs that outmigrated later in the season had higher marine survival. Antonsson et al. (2010) similarly found that Atlantic salmon (*Salmo salar*) that migrated later had higher survival, but Mortensen et al. (2000) found that the earliest and latest emigrating smolt pink salmon (*O. gorbuscha*) had the lowest marine survival rates. Early outmigrants experienced colder water temperatures and lower prey densities, and that exposure likely resulted in lower survival (Mortensen et al., 2000). For Chinook salmon in the Chilkat River, migrations that ended later likely provided additional time for some smolts to attain a larger size before outmigration, given that mean smolt length was longer in years when migrations ended later. Alternatively, the later migration period may have distributed smolts over a wider range of conditions, increasing the chance that some individuals encountered favorable marine conditions.

Increased discharge in spring during outmigration can influence migration timing in some stocks and may also be linked to marine survival. For smolt Chinook salmon in the Nechako River, in British Columbia, high discharge and river temperatures resulted in shorter migration periods (Sykes et al., 2009). Lawson et al. (2004) found that high discharge in spring could facilitate outmigration by increasing swimming speed and allowing fish to be transported downstream more passively, potentially conserving energy reserves and improving survival. In our study, higher spring discharge resulted in earlier outmigrations and lower marine survival for Chinook salmon from the Chilkat River. In contrast, discharge was not significantly related to the survival of fish from the Stikine River. River conditions may be more indicative of the environment experienced by smolts that remain in coastal waters during the marine entry phase, when a large portion of marine mortality occurs. For example, smolt Chinook salmon from the Fraser River fared worse during years when discharge into the Strait of Georgia was high because it caused increased turbulence, reduced stability, and low production in estuarine areas (Gargett, 1997). High seasonal discharge may cause similar patterns in the inside waters of SEAK where Chinook salmon from the Chilkat River reside and, therefore, may limit survival. Alternatively, the lack of a relationship between discharge and marine survival of Chinook salmon from the Stikine River could be evidence of a rapid migration upon ocean entry to offshore waters that are less affected by freshwater discharge.

Local SSTs were not related to marine survival of Chinook salmon from the Stikine and Chilkat Rivers. Mortensen et al. (2000) found that higher SSTs in Auke Bay were related to higher growth and survival of pink salmon from Auke Creek, but Briscoe et al. (2005) found no correlation between local SST and marine survival of jack and adult coho salmon (*O. kisutch*) in the same system. Increases in survival related to SSTs stem from optimal growth conditions because temperature is the primary function that controls metabolic and growth rates for ectotherms (Brett et al., 1969; Groot et al., 1995). Sea-surface temperatures can also affect ocean conditions, such as upwelling, food availability, and predator assemblages, all of which may aid or hamper growth and survival of Pacific salmon (Cole, 2000; Mortensen et al., 2000; Mueter et al., 2002b). Mueter et al. (2005) found that warmer coastal SSTs were associated with increased survival for chum, sockeye, and pink salmon in Alaska. Similar results have been reported for Chinook salmon in the Unuk River, northeast of Ketchikan, Alaska, with higher marine survival occurring with higher coastal SSTs (Graham, 2016).

The lack of a relationship between nearshore SSTs and marine survival of Chinook salmon in the Stikine and Chilkat Rivers could be because the majority of individuals grew elsewhere. As mentioned previously, it is possible that most of the smolts from the Stikine River migrate directly and more rapidly to more open-ocean areas rather than occupying more nearshore waters upon marine entry as assumed in our study. Marine survival of Chinook salmon from the Chilkat River, a stock that is believed to grow in the inside waters of northern SEAK, was correlated to migration timing and river conditions but not to nearshore SSTs. Conducting trawl surveys during the summer in Icy Strait, a known migration corridor for salmon in northern SEAK, Orsi et al. (2013) found few ocean age-0 Chinook salmon in summer trawl hauls, indicating that these fish may be nonmigratory upon marine entry and remain in more local areas. Alternatively, average SST from June and July could have been too broad a range to detect a process that occurred over days or weeks, rather than over months, for Chinook salmon from the 2 rivers (Briscoe et al., 2005).

Overwinter survival and smolt production

Freshwater indices of survival and production were tested only for Chinook salmon from the Chilkat River because of constraints in data availability. We found that lower discharge in fall and higher discharge in early spring were associated with increased smolt production in the Chilkat River. Results from previous research indicate high variability and seasonality in the relationships between the freshwater life stage of salmon and river discharge. Low discharge levels in the fall and winter have been reported to limit survival and smolt production, likely reducing migratory pathways in the fall and overwintering habitat availability in some systems (Lawson et al., 2004; Crozier and Zabel, 2006). High discharge in summer has been linked to low production of stream-type juvenile Chinook salmon in the Yukon River, in Alaska, possibly because high discharge caused velocity barriers that limited

habitat that was safe for drift foraging and increased risk-taking behaviors induced by foraging (Neuswanger et al., 2014). High spring flows have been determined to improve survival during smolt outmigration because higher discharge is associated with increased turbidity, which could protect fish visually from predators (Lawson et al., 2004). In our study, increased smolt production associated with low discharge in fall could indicate that these conditions enable increased fall foraging opportunities without limiting pre-winter migration corridors or habitat. Higher flows in early spring could increase habitat and drift-feeding opportunities while reducing competitive interactions between juvenile salmonids after the less productive winter period (Lawson et al., 2004).

Acclimation costs linked to changing water temperatures that occur in the fall and spring can result in the depletion of lipid reserves and lower body condition, possibly reducing salmonid survival during long winters (Cunjak et al., 1987). In our study, increased smolt production of Chinook salmon in the Chilkat River was correlated with warmer temperatures (>4°C) in early spring, potentially reflecting a survival advantage when winter periods are shorter and followed by warmer spring water temperatures. In contrast, Lawson et al. (2004) related air temperature to freshwater production of coho salmon in Oregon, near the southern end of their range, and found lower smolt production during years with higher annual temperatures. The variance in these results may be attributed to the lower range of temperatures in glacially fed streams, temperatures that do not reach the higher than optimal temperatures for streams, as they do in the streams in southern Oregon.

Body size of juveniles has also been proven to influence freshwater survival and production of salmonids. Larger body size has been linked to increased overwinter survival and production because higher lipid reserves enable larger individuals to tolerate harsh winter conditions, increase size-based predator avoidance abilities, and allow competitive advantages over smaller individuals for quality habitats (Quinn and Peterson, 1996; Meyer and Griffith, 1997; Zabel and Achord, 2004). In our study, higher smolt production was related to smaller parr body size for Chinook salmon, indicating density dependence in the freshwater environment because parr length was also negatively correlated with parr abundance. Armstrong and Griffiths (2001) found that the proportion of Atlantic salmon sheltering during the freshwater overwinter period decreased with abundance. In the Chilkat River, higher densities could have reduced the scope for growth because of competition for food or habitat refugia. Small body size may also be beneficial. For example, Carlson and Letcher (2003) observed that in 2 trout species, the brown trout (*Salmo trutta*) and brook trout (*Salvelinus fontinalis*), older, larger individuals had lower survival rates than younger, smaller individuals and suggested that this relationship may be a result of larger fish being more habitat limited in winter and, therefore, more susceptible to predation. Density-dependent effects during the freshwater phase that limit parr body size may also affect marine survival, given that smolt size was an important indicator of BY success for Chinook salmon from the Chilkat River.

Conclusions

The results of our study indicate that environmental mechanisms influencing survival of Chinook salmon in SEAK were stock specific, as has been observed for other stocks of Pacific salmon in this region (Malick et al., 2009). River conditions in spring appear to have influenced marine survival of Chinook salmon in the Chilkat River but not in the Stikine River, possibly as a result of the differences between stocks in offshore foraging locations. Smolt length may influence survival in both rivers, and results from this study reinforced the importance of environmental and biological factors on freshwater production and early marine survival for determining brood strength of stocks of Pacific salmon. Warmer water temperatures and increased river discharge projected to occur as a result of climate change may affect these critical survival periods if mismatches between feeding and growth conditions are exaggerated in both freshwater and marine systems. Because reductions in the productivity and abundance of stocks of Chinook salmon throughout SEAK have led to increased effort for stock assessments and to reductions in allowable catch, understanding critical periods in the life history of these stocks was key (ADFG CSRT[1]).

Acknowledgments

We thank T. Jaecks and P. Richards for providing ADFG data for Chinook salmon in the Chilkat and Stikine Rivers and the ADFG field crews for spending their summers collecting and reporting the data used in this study. We also thank M. Adkison of the University of Alaska for his input, guidance, and review throughout the project. This research would not have been possible without funding by the Alaska Sustainable Salmon Fund, the University of Alaska Fairbanks, and the ADFG.

Literature cited

Antonsson, T., T. Heidarsson, and S. S. Snorrason.
2010. Smolt emigration and survival to adulthood in two Icelandic stocks of Atlantic salmon. Trans. Am. Fish. Soc. 139:1688–1698.

Armstrong, J. D., and S. W. Griffiths.
2001. Density-dependent refuge use among over-wintering wild Atlantic salmon juveniles. J. Fish Biol. 58:1524–1530.

Beamish, R. J., and C. Mahnken.
2001. A critical size and period hypothesis to explain natural regulation of salmon abundance and the linkage to climate and climate change. Prog. Oceanogr. 49:423–437.

Biro, P. A., J. R. Post, and E. A. Parkinson.
2003. From individuals to populations: prey fish risk-taking mediates mortality in whole-system experiments. Ecology 84:2419–2431.

Biro, P. A., A. E. Morton, J. R. Post, and E. A. Parkinson.
2004. Over-winter lipid depletion and mortality of age-0 rainbow trout (*Oncorhynchus mykiss*). Can. J. Fish. Aquat. Sci. 61:1513–1519.

Bohlin, T., C. Dellefors, and U. Faremo.
1993. Timing of sea-run brown trout (*Salmo trutta*) smolt migration: effects of climatic variation. Can. J. Fish. Aquat. Sci. 50:1132–1136.

Brett, J. R., J. E. Shelbourn, and C. T. Shoop.
1969. Growth rate and body composition of fingerling sockeye salmon, *Oncorhynchus nerka*, in relation to temperature and ration size. J. Fish. Res. Board Can. 26:2363–2394.

Briscoe, R. J., M. D. Adkison, A. Wertheimer, and S. G. Taylor.
2005. Biophysical factors associated with the marine survival of Auke Creek, Alaska, coho salmon. Trans. Am. Fish. Soc. 134:817–828.

Brown, R. S., W. A. Hubert, and S. F. Daly.
2011. A primer on winter, ice, and fish: what fisheries biologists should know about winter ice processes and stream-dwelling fish. Fisheries 36:8–26.

Carlson, S. M., and B. H. Letcher.
2003. Variation in brook and brown trout survival within and among seasons, species, and age classes. J. Fish Biol. 63:780–794.

Cole, J.
2000. Coastal sea surface temperature and coho salmon production off the north-west United States. Fish. Oceanogr. 9:1–16.

Crozier, L. G., and R. W. Zabel.
2006. Climate impacts at multiple scales: evidence for differential population responses in juvenile Chinook salmon. J. Anim. Ecol. 75:1100–1109.

Cunjak, R. A.
1988. Physiological consequences of overwintering in streams: the cost of acclimatization? Can. J. Fish. Aquat. Sci. 45:443–452.

Cunjak, R. A., A. Curry, and G. Power.
1987. Seasonal energy budget of brook trout in streams: implications of a possible deficit in early winter. Trans. Am. Fish. Soc. 116:817–828.

Duncan, D. H., and A. H. Beaudreau.
2019. Spatiotemporal variation and size-selective predation on hatchery- and wild-born juvenile chum salmon at marine entry by nearshore fishes in Southeast Alaska. Mar. Coast. Fish. 11:372–390.

Gargett, A. E.
1997. The optimal stability 'window': a mechanism underlying decadal fluctuations in North Pacific salmon stocks? Fish. Oceanogr. 6:109–117.

Graham, C. J.
2016. Evaluation of growth, survival, and recruitment of Chinook salmon in Southeast Alaska rivers. M.S. thesis, 140 p. Univ. Alaska Fairbanks, Fairbanks, AK. [Available from website.]

Graham, C. J., T. M. Sutton, M. D. Adkison, M. V. McPhee, and P. J. Richards.
2019. Evaluation of growth, survival, and recruitment of Chinook salmon in Southeast Alaska rivers. Trans. Am. Fish. Soc. 148:243–259.

Groot, C., L. Margolis, and W. C. Clarke (eds.).
1995. Physiological ecology of Pacific salmon, 515 p. Univ. British Columbia Press, Vancouver, Canada.

He, X., and D. M. Lodge.
1990. Using minnow traps to estimate fish population size: the importance of spatial distribution and relative species abundance. Hydrobiologia 190:9–14.

Healey, M.
1991. Life history of Chinook salmon (*Oncorhynchus tshawytscha*). *In* Pacific salmon life histories (C. Groot and L. Margolis, eds.), p. 311–393. Univ. British Columbia Press, Vancouver, Canada.

Holtby, L. B., B. C. Andersen, and R. K. Kadowaki.
1990. Importance of smolt size and early ocean growth to interannual variability in marine survival of coho salmon (*Oncorhynchus kisutch*). Can. J. Fish. Aquat. Sci. 47:2181–2194.

Houde, E. D.
1987. Fish early life dynamics and recruitment variability. Am. Fish. Soc. Symp. 2:17–29.

Huusko, A., L. Greenberg, M. Stickler, T. Linnansaari, M. Nykänen, T. Vehanen, S. Koljonen, P. Louhi, and K. Alfredsen.
2007. Life in the ice lane: the winter ecology of stream salmonids. River Res. Appl. 23:469–491.

Hvidsten, N. A., T. G. Heggberget, and A. J. Jensen.
1998. Sea water temperatures at Atlantic salmon smolt entrance. Nord. J. Freshw. Res. 74:79–86.

Hvidsten, N. A., A. J. Jensen, A. H. Rikardsen, B. Finstad, J. Aure, S. Stefansson, P. Fiske, and B. O. Johnsen.
2009. Influence of sea temperature and initial marine feeding on survival of Atlantic salmon *Salmo salar* post-smolts from the Rivers Orkla and Hals, Norway. J. Fish Biol. 74:1532–1548.

Jackson, J. E.
2003. A user's guide to principal components, 592 p. John Wiley and Sons, New York.

Jonsson, B., and N. Jonsson.
1993. Partial migration: niche shift versus sexual maturation in fishes. Rev. Fish Biol. Fish. 3:348–365.

Koenings, J. P., H. J. Geiger, and J. J. Hasbrouck.
1993. Smolt-to-adult survival patterns of sockeye salmon (*Oncorhynchus nerka*): effects of smolt length and geographic latitude when entering the sea. Can. J. Fish. Aquat. Sci. 50:600–611.

Lawson, P. W., E. A. Logerwell, N. J. Mantua, R. C. Francis, and V. N. Agostini.
2004. Environmental factors influencing freshwater survival and smolt production in Pacific Northwest coho salmon (*Oncorhynchus kisutch*). Can. J. Fish. Aquat. Sci. 61:360–373.

Malick, M. J., M. D. Adkison, and A. C. Wertheimer.
2009. Variable effects of biological and environmental processes on coho salmon marine survival in southeast Alaska. Trans. Am. Fish. Soc. 138:846–860.

McCormick, S. D., L. P. Hansen, T. P. Quinn, and R. L. Saunders.
1998. Movement, migration, and smolting Atlantic salmon (*Salmo salar*). Can. J. Fish. Aquat. Sci. 55:77–92.

Meyer, K. A., and J. S. Griffith.
1997. First-winter survival of rainbow trout and brook trout in the Henrys Fork of the Snake River, Idaho. Can. J. Zool. 75:59–63.

Mohseni, O., and H. G. Stefan.
1999. Stream temperature/air temperature relationship: a physical interpretation. J. Hydrol. 218:128–141.

Mortensen, D., A. Wertheimer, S. Taylor, and J. Landingham.
2000. The relation between early marine growth of pink salmon, *Oncorhynchus gorbuscha*, and marine water temperature, secondary production, and survival to adulthood. Fish. Bull. 98:319–335.

Mueter, F. J., D. M. Ware, and R. M. Peterman.
2002a. Spatial correlation patterns in coastal environmental variables and survival rates of salmon in the north-east Pacific Ocean. Fish. Oceanogr. 11:205–218.

Mueter, F. J., R. M. Peterman, and B. J. Pyper.
2002b. Opposite effects of ocean temperature on survival rates of 120 stocks of Pacific salmon (*Oncorhynchus* spp.) in northern and southern areas. Can. J. Fish. Aquat. Sci. 59:456–463.

Mueter, F. J., B. J. Pyper, and R. M. Peterman.
2005. Relationships between coastal ocean conditions and survival rates of northeast Pacific salmon at multiple lags. Trans. Am. Fish. Soc. 134:105–119.

Murphy, J., K. Howard, L. Eisner, A. Andrews, W. Templin, C. Guthrie, K. Cox, and E. Farley.
2013. Linking abundance, distribution, and size of juvenile Yukon River Chinook salmon to survival in the northern Bering Sea. *In* 3rd international workshop on migration and survival mechanisms of juvenile salmon and steelhead in ocean ecosystems; Vancouver, 25–26 April (N. D. Davis and C. Chan, eds.), p. 25–30. North Pac. Anadromous Fish Comm. Tech. Rep. 9. [Available from website.]

Neuswanger, J., M. S. Wipfli, A. E. Rosenberger, and N. F. Hughes.
2014. Mechanisms of drift-feeding behavior in juvenile Chinook salmon and the role of inedible debris in a clear-water Alaskan stream. Environ. Biol. Fishes 97:489–503.

Orsi, J. A., M. V. Sturdevant, E. A. Fergusson, W. R. Heard, and E. V. Farley Jr.
2013. Chinook salmon marine migration and production mechanisms in Alaska. *In* 3rd international workshop on migration and survival mechanisms of juvenile salmon and steelhead in ocean ecosystems; Vancouver, 25–26 April (N. D. Davis and C. Chan, eds.), p. 240–243. North Pac. Anadromous Fish Comm. Tech. Rep. 9. [Available from website.]

Quinn, T. P.
2005. The behavior and ecology of Pacific salmon and trout, 562 p. Univ. Washington Press, Seattle, WA.

Quinn, T. P., and N. P. Peterson.
1996. The influence of habitat complexity and fish size on over-winter survival and growth of individually marked juvenile coho salmon (*Oncorhynchus kisutch*) in Big Beef Creek, Washington. Can. J. Fish. Aquat. Sci. 53:1555–1564.

R Core Team.
2020. R: a language and environment for statistical computing. R Foundation for Statistical Computing, Vienna, Austria. [Available from website, accessed March 2020.]

Rikardsen, A. H., M. Haugland, P. A. Bjørn, B. Finstad, R. Knudsen, J. B. Dempson, J. C. Holst, N. A. Hvidsten, and M. Holm.
2004. Geographical differences in marine feeding of Atlantic salmon post-smolts in Norwegian fjords. J. Fish Biol. 64:1655–1679.

Seber, G. A. F.
1982. The estimation of animal abundance and related parameters, 2nd ed., 654 p. Blackburn Press, London.

Sogard, S. M.
1997. Size-selective mortality in the juvenile stage of teleost fishes: a review. Bull. Mar. Sci. 60:1129–1157.

Sykes, G. E., C. J. Johnson, and J. M. Shrimpton.
2009. Temperature and flow effects on migration timing of Chinook salmon smolts. Trans. Am. Fish. Soc. 138:1252–1265.

Thompson, J. N., and D. A. Beauchamp.
2014. Size-selective mortality of steelhead during freshwater and marine life stages related to freshwater growth in the Skagit River, Washington. Trans. Am. Fish. Soc. 143:910–925.

Vega, S. L., T. M. Sutton, and J. M. Murphy.
2017. Marine-entry timing and growth rates of juvenile chum salmon in Alaskan waters of the Chukchi and northern Bering seas. Deep-Sea Res., II 135:137–144.

Wang, J., R. Zamar, A. Marazzi, V. Yohai, M. Salibian-Barrera, R. Maronna, E. Zivot, D. Rocke, D. Martin, M. Maechler et al.
2020. robust: port of the S+ "Robust Library." R package, vers. 0.5-0.0. [Available from website, accessed March 2020.]

Wootton, R. J.
1998. Ecology of teleost fishes, 2nd ed., 386 p. Kluwer Acad. Publ., Dordrecht, Netherlands.

Zabel, R. W., and S. Achord.
2004. Relating size of juveniles to survival within and among populations of Chinook salmon. Ecology 85:795–806.

National Marine
Fisheries Service
NOAA

Fishery Bulletin
established in 1881

Spencer F. Baird
First U.S. Commissioner
of Fisheries and founder
of *Fishery Bulletin*

Assessment of attraction and avoidance behaviors of fish in response to the proximity of transiting underwater vehicles

Matthew D. Campbell (contact author)[1]
Ariane Huddleston[2]
David Somerton (retired)[3]
M. Elizabeth Clarke[4]
Waldo Wakefield (retired)[5]
Steve Murawski[6]
Chris Taylor[7]
Hanumant Singh[8]
Yogesh Girdhar[9]
Mary Yoklavich (retired)[10]

Email address for contact author: matthew.d.campbell@noaa.gov

[1] Mississippi Laboratories
Southeast Fisheries Science Center
National Marine Fisheries Service, NOAA
3209 Frederic Street
Pascagoula, Mississippi 39567

[2] Science and Technology Center
Northern Gulf Institute
Mississippi State University
1021 Balch Boulevard
Stennis Space Center, Mississippi 39529

[3] Resource Assessment and Conservation Engineering
Alaska Fisheries Science Center
National Marine Fisheries Service, NOAA
7600 Sand Point Way NE, Building 4
Seattle, Washington 98115

[4] Northwest Fisheries Science Center
National Marine Fisheries Service, NOAA
2725 Montlake Boulevard East
Seattle, Washington 98112

[5] Newport Research Station
Northwest Fisheries Science Center
National Marine Fisheries Service, NOAA
2032 SE OSU Drive
Newport, Oregon 97365-5275

[6] College of Marine Science
University of South Florida
140 Seventh Avenue South
Marine Science Laboratory 118
St. Petersburg, Florida 33701

[7] Center for Coastal Fisheries and Habitat Research
National Center Coastal Ocean Sciences
National Ocean Service
101 Pivers Island Road
Beaufort, North Carolina 28516

[8] Department of Electrical and Computer Engineering
Northeastern University
360 Huntington Avenue
Boston, Massachusetts 02115

[9] Deep Submergence Laboratory
Woods Hole Oceanographic Institution
266 Woods Hole Road
Woods Hole, Massachusetts 02543-1050

[10] Fisheries Ecology Division
Southwest Fisheries Science Center
National Marine Fisheries Service, NOAA
110 McAllister Way
Santa Cruz, California 95060

Abstract—Underwater vehicles have many advantages for sampling fish; however, estimates can be biased by behavioral responses to sampling gear. To evaluate avoidance and attraction bias we assessed changes in fish abundance relative to a variety of sampling vehicles during transit through a test bed. Fish species were classified into five attraction and avoidance categories according to the behavioral responses exhibited. We observed that the rigor of behavioral responses varied by vehicle, vehicle range and altitude, transect number, and habitat complexity. The effect of each variable is dependent on behavioral guild, but vehicle range was the most consistent predictor of changes in abundance regardless of vehicle. Vehicles that surveyed the environment at higher relative altitudes off the seafloor and at slower speeds elicited weaker behavioral responses regardless of whether those reactions were attraction or avoidance. The testbed approach allowed assessment of responses that cannot be observed from the perspective of a sampling vehicle but was restricted by the number of species-specific interactions observed. Despite success in estimating behavioral responses, calibrating the effect against known densities of fish was not possible. However, the method used is a robust way for future investigations to quantify species-specific responses for gear calibration and to provide information that aids in the calculation of fish abundance.

Manuscript submitted 18 February 2021.
Manuscript accepted 13 September 2021.
Fish. Bull. 119:216–230 (2021).
Online publication date: 1 November 2021.
doi: 10.7755/FB.119.4.2

The views and opinions expressed or implied in this article are those of the author (or authors) and do not necessarily reflect the position of the National Marine Fisheries Service, NOAA.

High-relief, complex seafloor habitats (e.g., rock and coral reef) present a number of challenges for the deployment of traditional fishing gears, such as seines, gill nets, bottom trawls, and longlines. These habitats are rugged, are prone to snag and destroy sampling gear, and are often damaged by sampling gear (Hall-Spencer et al., 2002; Mangi and Roberts, 2006; Roberts et al., 2006). Further, gears such as traps and handlines have been used to sample populations of reef fish species, but their size selectivity limits their utility to a few species and to a narrow range of size and age composition (Parker et al., 2016). Because of these difficulties, the use of optical gears mounted on underwater stationary platforms and on vehicles are becoming increasingly common in efforts to sample complex reef environments (Yoklavich et al., 2007;

Patterson et al., 2009; Armstrong and Singh, 2012; Grasty, 2014; Bacheler and Shertzer, 2015). Attractive aspects of optical sampling gears include that they 1) do not require extraction of fish, 2) have negligible impact on the habitat, 3) collect habitat data, and 4) often allow calculation of sampling volume or area and therefore can be used to produce habitat-specific density estimates that can be scaled to calculate abundance (Royle et al., 2009; Trenkel and Lorance, 2011; Whitmarsh et al., 2017).

An artifact of many fisheries survey methods is that the unit of measurement is an observation rate or catch rate and therefore cannot be used to estimate fish densities (e.g., fish per unit area). Collection of rate data constrains analysts to development of relative abundance indices (Williams et al., 2018) that are rarely calibrated against known fish densities and therefore cannot provide data to calculate absolute abundance. In addition, gear bias can affect counts; for example, observations and counts of fish are negatively affected during scuba-diver surveys because of air bubbles from exhalation (Gray et al., 2016; Emslie et al., 2018). Using vehicles to conduct optical surveys is a popular sampling method because they can cover long distances while transiting, allowing estimation of area sampled and fish densities, but they too will have inherent sampling biases (Clarke et al., 2009; Stierhoff et al., 2013; Thanopoulou et al., 2018).

Estimates of fish densities are useful because they can be scaled over the area of known habitat to calculate absolute abundances for use in stock assessments (O'Connell and Carlile, 1993; Yoklavich et al., 2007). Although calculation of fish density might seem like a straightforward process, estimates can be affected by environmental conditions and fish behavior (Fig. 1).

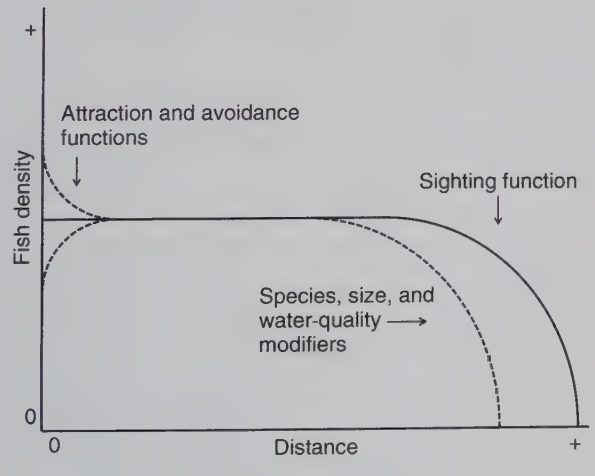

Figure 1

Diagram showing the theoretical effects of attraction and avoidance (dashed line above the sighting function) and sighting (solid line) functions on density estimation. The dashed line under the sighting function represents how fish density is theoretically modified by water quality, species, and size of the individuals observed.

Therefore, it is critical to estimate sighting functions and attraction and avoidance functions when conducting distance sampling and strip-transect surveys (Sale and Sharp, 1983; Ensign et al., 1995; Cheal and Thompson, 1997). Importantly, the need for estimating such functions has been shown to be true even for species with minimal or no avoidance behaviors (Kulbicki and Sarramégna, 1999).

As with any sampling gear, fish are likely to respond to the presence of stationary platforms and vehicles, and those responses have been recognized as a potential source of bias (Uzmann et al., 1977; Jagielo et al., 2003; Stoner et al., 2008). Each of these vehicles has its own characteristics related to movement speed, deployment altitude, acoustic signature, size, and visibility, all of which can introduce bias into the data collected (Koslow et al., 1995; Lorance and Trenkel, 2006; Stoner et al., 2008). In addition, fish are apt to respond to novelties in the environment in different ways in accordance with survival and foraging needs (Olla et al., 1998) and perhaps out of curiosity. Regardless of the underlying motivation, species-specific responses to sampling gears need to be quantified in order to deal with underlying biases and to generate reliable count, density, and abundance estimates.

Classes of vehicles commonly used in marine research include remotely operated vehicles (ROVs), autonomous underwater vehicles (AUVs), towed vehicles (TVs), and human occupied vehicles. Vehicles are used in sampling efforts predominately as part of line-transect methods, but the engineering specifications of vehicles and the execution of the line-transect surveys differ. These vehicle-specific differences can result in measurement biases of unknown direction and magnitude, the result of which is a need for gear calibration (Clarke et al., 2009). Further, it is recognized that, within a vehicle class, there will likely be many variations and exceptions (Yoklavich et al., 2015). Potential stimuli that could elicit attraction to, or avoidance of, vehicles include transit speed and altitude, visual profiles, and acoustic signatures. Ideally the specific stimuli causing a reaction can be identified, but more importantly fish responses in general need to be evaluated and quantified as a first step in understanding how to develop gear-calibration methods.

Because of the elevated interest in the use of vehicles to conduct surveys of high-relief, complex bottom types, the National Marine Fisheries Service (NMFS) initiated the Untrawlable Habitat Strategic Initiative (UHSI) in 2014. Participants in the UHSI were tasked with designing a multitiered field experiment to evaluate the sampling efficiency of camera systems mounted on stationary platforms, ROVs, AUVs, and TVs used to count fish and invertebrates in a sampling area or volume. The analysis in this study was focused on the change in abundance of reef fish species in a sampling volume due to the passage of a mobile survey vehicle. Our intent was to develop a functional relationship between vehicle range from the sampling volume and relative change in fish abundance (Fig. 1).

Materials and methods

Study area

The experiment was conducted in August 2014 and in July and August 2015 at the Florida Middle Grounds, on the West Florida Shelf in the northeastern Gulf of Mexico (GOM) between Cape San Blas and Tampa Bay, Florida (Fig. 2). The Florida Middle Grounds consist of high-relief outcrops of carbonate rock (relief ~2–5 m) that host diverse assemblages of alcyonarian corals, sponges, and macroalgae (Austin and Jones, 1974; Darcy and Gutherz, 1984; Rezak et al., 1985; Koenig et al., 2000). The Florida Middle Grounds are the center of a productive snapper-grouper fishery of the eastern GOM and also host a diverse assemblage of pelagic and demersal fishes (Pierce and Mahmoudi, 2001). Water clarity in summer months ranges between 10 and 30 m, and the depth range on the bank is 20–40 m (Koenig et al., 2000). Sampling depths ranged from 20 to 35 m, and sites were selected to maximize natural light and clear water to ensure quality photography and accurate fish identifications and measurements. At the beginning of the experiment, low-relief (1–3 m) reef sites were selected to ensure safe deployment of the sampling gear. As our ability to accurately position sampling gear improved with time and safe vehicle transits could be ensured, we deployed them on increasingly complex high-relief habitat (>3 m).

Platforms and deployment

To evaluate the response to vehicles, we deployed an array of 3 stationary, autonomous camera platforms (Fig. 3) that remained on the seafloor between 7 and 10 h at multiple sites. The stationary platforms consisted of the Modular Optical Underwater Sampling System (MOUSS) (Amin et al., 2017) outfitted with the following components: stereo cameras, long-baseline (LBL) sonar beacons, and batteries (hereafter referred to as *MOUSS platforms*). The MOUSS platforms were fabricated with stainless steel and ballasted by the weight of batteries, pressure housings, and lead weights. Optical data were collected with the stereo cameras, which were capable of measuring and positioning objects in 3 dimensions (Amin et al., 2017). Cameras were mounted on a base-bar with an 80-cm separation between cameras, at a 10° "toe-in" angle, and

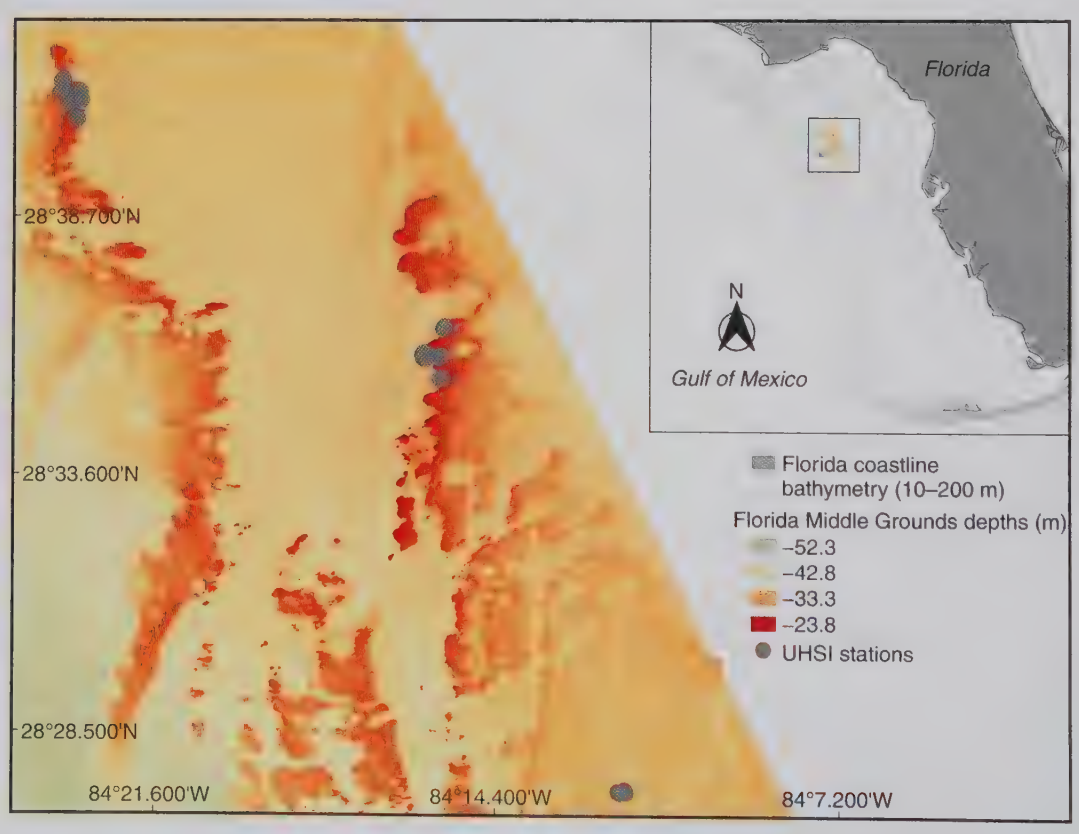

Figure 2

Bathymetric map of the study area in the Florida Middle Grounds, on the West Florida Shelf in the Gulf of Mexico, where mobile survey vehicles and stationary camera systems were deployed to assess changes in abundance of reef fish taxa in response to the passage of vehicles in August 2014 and in July and August 2015. Sampling stations (gray circles) of the Untrawlable Habitat Strategic Initiative (UHSI) were focused on ridge habitats.

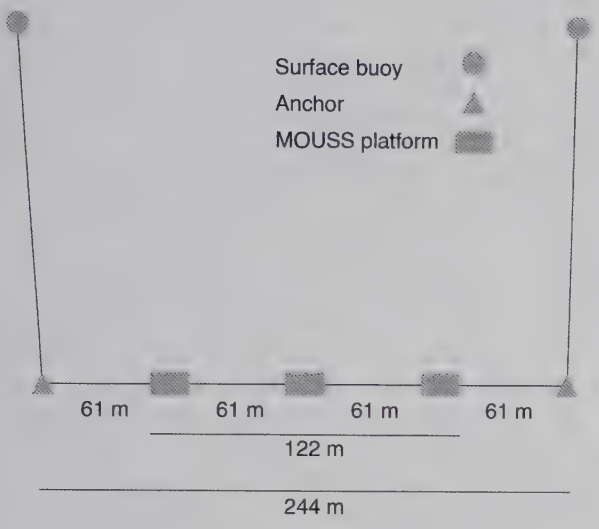

Figure 3

General schematic of 3 ground-tended Modular Optical Underwater Sampling System platforms (rectangles) set 61 m apart along a groundline. Anchors (triangles) and surface buoys (circles) were attached 61 m from the platforms at each end of the line. Total length between anchors was 244 m, and the total distance between end cameras was 122 m.

were 18 cm above the seafloor. Cameras have a 70° field of view (FOV) and use ambient light, and camera settings were optimized for expected light conditions in clear, shallow water (20–40 m). Still images were acquired at a rate of 5 frames per second and were later processed to make video files in MPEG format. Geographic position of each platform was determined by using repeated acoustic surveys that triangulated the LBL acoustic beacons, and those positions were used to aid navigation of each vehicle in front of the MOUSS platforms.

To ensure that the orientation of each of the 3 MOUSS platforms was consistent, they were deployed in a fashion similar to that of demersal longline traps, such as those used in the sablefish (*Anoplopoma fimbria*) fishery in U.S. waters (Afanasyev et al., 2014) (Fig. 3). Platforms were attached to a 9.5-mm bottom line that was continuously spooling off a winch while the ship maintained a constant heading during setting. The entire set was anchored on each end by steel weights (22 kg) located 61 m from the 2 outermost platforms. Two quick links were spliced into the longline at predetermined points 61 m apart, onto which the platforms were attached with high-strength snap shackles that were connected to platform harnesses. Anchor to anchor, the transect distance was 244 m, and the distance between end point cameras was 122 m (Fig. 3). This method of deployment allowed the main line to act as a yoke to keep the MOUSS platforms, and therefore camera orientation, roughly perpendicular to the ship's bearing. Cameras were normally deployed in ~30 min, and then the LBL beacons were surveyed to triangulate MOUSS platform position over a period that was typically 2–3 h. The deployment and triangulation process provided time for fish to become acclimated to the presence of the MOUSS platforms prior to the deployment of the survey vehicles.

Vehicles and transects

Survey vehicles evaluated in the experiment included a Phantom HD2+2[1] ROV (Deep Ocean Engineering, San Jose, CA), the Camera-based Assessment Survey System TV (Lembke et al., 2017), and the SeaBED AUV (Singh et al., 2004). For simplification we refer to the vehicles we used as *ROV*, *TV*, and *AUV*. Each vehicle has different deployment and operation properties that limited our ability to stage all vehicles simultaneously on the survey ship and to deploy all vehicles in a single day. Therefore, the survey was divided into 2 segments that were conducted back to back. As a result, general deployment areas could be surveyed with each vehicle, but exact locations were not replicated across survey legs, resulting in each vehicle operating in somewhat different habitats (i.e., depth, substrate type, and fish community and abundance varied by site). Thus, models used to evaluate fish responses were somewhat vehicle specific.

The ROV (140 × 69 × 66 cm, in length, width, and height, respectively) was constantly tethered to the ship to provide power for vehicle operations and was remotely piloted from the ship by using a combination of 2 live-feed cameras (front and rear), sector scanning sonar, and a compass. During ROV deployments, the ship was anchored and, as a result, no tether management system was required and the tether was sufficiently long (338 m) to navigate from anchor to anchor at all operational depths during the experiment. Following ROV launch, the vehicle was driven on the surface to the closest down-current buoy, and then the ROV descended to the anchor. Upon reaching the seafloor, the pilot oriented the ROV on the desired transect heading and parked the ROV on the seafloor for 15 min prior to beginning to survey the first transect. Transects were run parallel to the orientation of the 3 MOUSS platforms and camera FOV, from anchor to anchor in both directions, and with 15-min resting periods between each transect. Depending on sea state and time of day, 2–6 transects were surveyed at each site prior to recovery of the vehicle.

The TV (179 × 127 × 87 cm, in length, width, height, respectively) was towed behind the ship by using a winch and conducting wire that also powered the vehicle and provided real-time seafloor imagery to assist the pilot in navigation. Vehicle operations were conducted by a pilot who communicated with the ship's officers on the bridge about preferred heading and speed, and with deck personnel regarding winch payout and vehicle altitude.

[1] Mention of trade names or commercial companies is for identification purposes only and does not imply endorsement by the National Marine Fisheries Service, NOAA.

Real-time vehicle altitude data and seafloor depths from the shipboard echo sounders are necessary to appropriately control the vehicle and avoid obstacles. Live views from the vehicle are provided by forward- and side-facing cameras (AVT Prosilica GT1920, Allied Vision Technologies GmbH, Stadtroda, Germany) mounted at 35° angles and constantly lit with LED flood lights. Cameras collected images at a resolution of 1936 × 1456 pixels and at 12 frames per second. The vehicle collected real-time hydrological (e.g., salinity, temperature, and depth), vehicle altitude, and compass data that were stored in onboard computers. Transects were surveyed in parallel to the set direction of the MOUSS platforms and perpendicular to the camera FOV. Between transect runs, the vehicle altitude was increased to a safe height, and the vehicle then was towed in a large oval. Therefore, during surveying of transects, the TV always traveled in the same direction down the transect line with ~30 min elapsed time between each transect.

The AUV (1.90 × 0.34 ×1.50 m, in length, width, and height, respectively) operated free from the ship at all times during a dive, following a preprogrammed route. The AUV was equipped with onboard power, computing, acoustic beacons, and an acoustic Doppler profiler for bottom-tracking, conducting its operations, and navigating through the environment. The vehicle's stereo cameras were oriented to photograph the seafloor (i.e., downward facing) and coupled with a xenon camera strobe to capture imagery during transit. Environmental data (e.g., salinity, temperature, depth) and vehicle altitude and position data were collected and stored onboard the AUV. At the start of the mission, the AUV descended to the seafloor, navigated to the programmed transect start position, and transited the desired course. Transects were surveyed parallel to the set direction of the MOUSS platforms and at a preprogrammed constant altitude above the seafloor (either 2 or 4 m), in both directions, and at increasing distances from the camera with each successive transect. In 2014, to ensure the vehicle was observed with the MOUSS platforms, vehicle altitude was lowered to 2 m; therefore; vehicle altitude varied between sites although altitude during a dive was held constant. Each successive transect was separated by an interval of approximately 30 min from the previous transect, similar to the intervals used for surveys conducted with the TV.

Vehicle range from the MOUSS platform was calculated by using stereo-camera imagery data when the vehicle was observed and then by fitting a linear model to estimate values when the vehicle was outside of the MOUSS sampling volume. During vehicle passage, 5 vehicle position coordinates per second were measured in centimeters from the stereo-camera origin. We then used the point cloud positional data and a linear model to estimate vehicle position for periods when the vehicle was outside of the stereo-camera FOV. Positional data were then used to estimate vehicle range relative to when the vehicle passed across the y intercept of the cameras (i.e., where x=0) for each second from 1.03 min before and after that moment (i.e., up and down range from the camera origin). This linear model assumes that the vehicles transited in a relatively straight line and that error in position estimates was reduced by obtaining estimates for positions of 5 data points per second. Therefore, the total time for video annotation was 2.06 min. This time frame was selected because the fastest vehicle (the TV) transited across the stereo-camera FOV in 8 s and because abundance estimates from the MOUSS platforms were collected in 4-s bins.

In this way, several bins of count data can be captured during the time when the vehicle was just entering, within, or just departing the MOUSS platform sampling volume (i.e., the coincident sampling volume). Sometimes MOUSS platforms landed on uneven seafloor and were tilted in various orientations; as a result, measuring exact altitude of the vehicle during transit was not always possible. Therefore, we collected qualitative data as a measurement of vehicle transit altitude in lieu of measuring exact transit altitude. Qualitative vehicle altitude above the seafloor (RVA) was qualitatively ranked as low (~1–2 m; code: 1), middle (~2–5 m; code: 2), and high (>5 m; code: 3).

Video annotation and relative abundance

Fish were identified to the lowest taxon possible, and attraction and avoidance patterns relative to the vehicle were noted. When there were fewer than 50 individuals of a species in a given video frame all individuals were counted. When there were >50 fish, the total number was estimated by subsampling a portion of the school and extrapolating the subsample by the total area the school occupied on the video screen.

Videos were annotated in 2 different ways to test the following: 1) fish acclimation to stationary cameras after first deployment and 2) change in relative fish counts in relation to vehicle passage. To evaluate fish acclimation during the first hour of deployment, 2-min intervals were randomly selected from the first hour of MOUSS platform deployment and prior to vehicle deployment. Species-specific fish counts during this time were estimated in 4-s bins. To analyze fish response to mobile vehicles, species-specific fish counts were collected at 4-s intervals during a 2.06-min video segment for which the midpoint is defined as the video frame when the vehicle crossed the stereo-camera origin. Depending on vehicle speed, this method resulted in fish counts for 1 min prior to and following vehicle transit, with a 4-s interval when the vehicle passed directly in front of a MOUSS platform. The video frames in which the vehicle was captured with the stereo cameras were considered the coincident sampling volume, and the exposure time in the sampled volume was dependent on vehicle speed. Because speed varied by vehicle and condition, we excluded time as a factor in the models in favor of estimating vehicle range to the coincident sampling volume.

With a few exceptions, such as greater amberjack (*Seriola dumerili*), scamp (*Mycteroperca phenax*), and gray snapper (*Lutjanus griseus*), specific species were infrequently captured in images coincident to vehicle transit.

Thus, developing species-specific models was not possible for most species observed; however, general attraction and avoidance response behaviors were easily characterized. As a result, species were grouped into 5 behavioral guilds, and abundance data from the species belonging to those groups were pooled for analysis (Table 1). Behavioral guilds identified and analyzed included pelagic pursuers, benthic pursuers, down movers, lateral movers, and local reactive. Group composition is shown in Table 1 but in brief was as follows: the pelagic pursuers were composed of jacks (Carangidae) and mackerels (Scombridae); the benthic pursuers were composed of groupers (Serranidae) and wrasses (Labridae); lateral movers were composed of snappers (Lutjanidae) and porgies (Sparidae); down movers were composed of species of damselfish (Pomacentridae) and jawfish (Opistognathidae); and the local reactive guild was composed of species of filefish (Monacanthidae), butterflyfish (Chaetodontidae), and sand perch (*Diplectrum* spp.). Fifteen models were produced for each unique combination of the 3 vehicles and 5 behavioral guilds.

Changes in fish counts during the MOUSS platform acclimation time were evaluated by using generalized additive models (GAMs) with the GAM predict function of the package mgcv (vers. 3.6.1; Wood, 2011) in R (vers. 4.0.3; R Core Team, 2020). Fish acclimation models included the following variables: time (seconds) and habitat complexity (qualitatively rated 1–5 from low to high). Changes in relative abundance due to vehicle passage were also analyzed by using GAMs. Because all vehicles did not necessarily transit through equivalent transects (the TV and AUV had no shared transects), and therefore did not pass through equivalent underlying fish densities, changes were analyzed in separate models for each vehicle type (i.e., we did not create a single model with a vehicle variable). Additionally, the habitat complexity variable allowed us to model site-specific differences in abundance that could potentially mask responses to a vehicle. For example, without a variable that explains site-specific differences, high-abundance sites could potentially have disproportionate effects on outcomes. Models used to examine fish responses to vehicle passage included the following variables: RVA (low, middle, and high), transect number (integer), range (meters), and ranked habitat complexity (qualitatively rated 1–5 from low to high). Deployment of the entire transect course took significant effort. Thus, multiple transects were surveyed over the course of a day, and that daily number of transects was tracked as a sequential value called transect number. Transect number therefore is used to compile the total number of vehicle exposures that occurred on the transect course over a single deployment of the 3 MOUSS platforms on the transect course.

Table 1

Behavioral guild assignments based on movements of fish taxa in response to presence of mobile survey vehicles deployed in the Florida Middle Grounds during August 2014 and July and August 2015.

Pelagic pursuers	Benthic pursuers	Down movers
Seriola dumerili	*Mycteroperca venenosa*	Pomacentridae
Sphyraena barracuda	*Mycteroperca phenax*	*Pomacentrus* sp.
Seriola rivoliana	*Mycteroperca* sp.	*Chromis insolata*
Carangidae	*Epinephelus morio*	*Chromis enchrysura*
Seriola sp.	Serranidae	*Chromis* sp.
Caranx lugubris	*Halichoeres bathyphilus*	*Opistognathus aurifrons*
Scombridae	*Halichoeres bivittatus*	*Opistognathus* sp.
	Halichoeres sp.	
Lateral movers	**Local reactive**	
Rhomboplites aurorubens	*Monacanthus ciliatus*	
Lutjanus griseus	*Stephanolepis hispidus*	
Lutjanus campechanus	*Monacanthus* sp.	
Calamus calamus	*Monacanthus tuckeri*	
Calamus nodosus	*Stegastes leucostictus*	
Calamus penna	*Stegastes partitus*	
Calamus proridens	*Stegastes* sp.	
Calamus sp.	*Stegastes variabilis*	
Haemulon plumierii	*Chaetodon ocellatus*	
Haemulon sp.	*Chaetodon sedentarius*	
Pagrus pagrus	*Chaetodon* sp.	
Clepticus parrae	*Diplectrum formosum*	
	Decodon puellaris	

Results

General observations

The array of 3 MOUSS platforms was deployed during daylight hours at 13 distinct areas over 9 d in August 2014 and at 7 distinct areas over 5 d in July and August 2015. Deployments of MOUSS platforms varied in time from 7 to 10 h. Over the 9 d of dedicated sampling in 2014, 73 transects were surveyed with vehicles, resulting in 218 individual passes or observations in front of the MOUSS platforms. Over the 7 d of dedicated sampling in 2015, 57 transects were surveyed with vehicles, resulting in 171 individual passes or observations in front of the MOUSS platforms.

The target speed of the AUV was 1.0 kt (0.51 m/s), and target altitude was either 2 or 4 m. In 2014, to improve the likelihood of observing the AUV in images from the stereo camera, the transect altitude was lowered from 4 to 2 m. The AUV transited in straight lines but was vulnerable to heavy currents, which caused the vehicle to "crab," make frequent course corrections, and to transit at a more variable rate of speed. The target speed of the TV was approximately 3.5 kt at an altitude of 2 m, but sometimes the speed was as high as 5 kt when travelling down current and the altitude was as high as ~5 m in high-relief areas where the potential of hitting the reef was a concern. Because the TV is towed and control of the vessel is fairly precise at the surface (e.g., GPS navigation), the TV transited the straightest transects of all the vehicles. However, transect deployments had to be well planned and executed in order to avoid hitting obstacles (e.g., tending buoys or reef). The target speed and altitude of the ROV was 0.5–1.0 kt and 0.5–1.0 m above the seafloor, but sometimes speed was as high as 2 kt and altitude was as high as 2.5 m because of currents, tether orientation, and operator error. Currents, tether orientation, and pilot error sometimes caused the transect path to meander from the intended straight line. In general, the ROV was the vehicle most consistently observed on MOUSS cameras, and transects improved over time likely as a result of a combination of slow speeds and rapid feedback to the pilot.

Generalized additive models

Results from the fish acclimation GAMs indicate significant effects for both time and habitat complexity. The model explained 17.8% of deviance with a coefficient of determination (r^2) of 0.11. Although the information on model fit indicates that there is considerable unexplained variability, the trend indicates that fish counts declined during the acclimation period and reached an asymptote at around 45 min (Fig. 4). General observations indicate that jacks (*Seriola* spp.) and great barracuda (*Sphyraena barracuda*), when present, closely examined the stationary camera but lost interest quickly. In addition, the reef fish community observed immediately around the stereo cameras became more active at initial deployment but appeared to slowly become disinterested and begin to forage and interact with the habitat and each other at around 30 min after deployment.

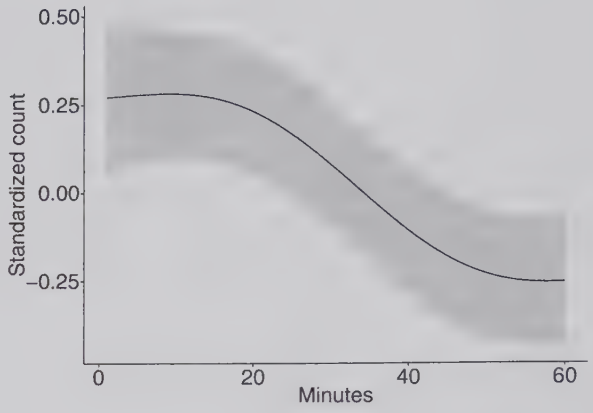

Figure 4

Changes in fish abundance during the acclimation period (first 60 min) following deployment of Modular Optical Underwater Sampling System platforms at selected reef sites in the Florida Middle Grounds. The gray shaded area represents the 95% confidence interval. Trends indicate a decrease in abundance with an asymptotic response occurring at around 45 min. The experiment was conducted during August 2014 and July and August 2015.

Results from vehicle interaction GAMs indicate that significant terms and overall fit of the models differed between behavioral guilds and between vehicles within each guild (Table 2). From a qualitative perspective, the pelagic pursuers group had strong attraction to all of the vehicles tested and was the most obvious group to characterize (Fig. 5). The model for the AUV had significant effects for RVA, vehicle range, and transect number, but habitat complexity was not significant. The AUV model explained 48.9% of the deviance with an r^2 of 0.43. The TV model had significant effects for vehicle range, transect number, and habitat complexity, but RVA was not significant. The TV model explained 59.3% of the deviance with an r^2 of 0.29. The ROV model showed significant effects for vehicle range, but vehicle altitude, transect number, and habitat complexity were not significant. The ROV model explained 81% of the deviance with an r^2 of 0.46. Pelagic pursuers had spikes in abundance when vehicles were close in proximity to the MOUSS platforms (~50 m) (Fig. 5). Passage of the slower-moving AUV and ROV resulted in a spike in relative fish abundance at closer ranges (~10 m) than passage of the fast-moving TV (~50 m). Relative abundance of pelagic pursuers increased with increasing AUV altitude but had no relationship to TV altitude. The effect of relative altitude could not be tested on the ROV because all passes were within the low category. Increasing the number of transects generally resulted in peak increases in relative abundance between the third and fourth transect for the AUV and TV, but this pattern was not evident for the ROV.

Table 2

Generalized additive model run results by behavioral guild and survey vehicle, used to assess changes in the relative abundance of fish due to vehicle passage at sites in the Florida Middle Grounds during August 2014 and July and August 2015. Vehicles evaluated included an autonomous underwater vehicle (AUV), a towed vehicle (TV), and a remotely operated vehicle (ROV). *P*-values are provided for each variable included in the models: relative vehicle altitude above the seafloor (RVA), transect number, habitat complexity, and vehicle range. Also given are the sample size (n), percentage of deviance explained, and coefficient of determination (r^2). Asterisks (*) indicate significant variables ($P<0.05$). NA indicates a variable that was not used in a particular model run.

Guild	Vehicle	n	Intercept	RVA	Transect number	Habitat complexity	Vehicle range (m)	Deviance explained	r^2
Pelagic pursuers	AUV	217	0.10	8.8×10^{-7} *	1.4×10^{-5} *	0.56	1.2×10^{-4} *	48.9%	0.43
	TV	527	$<2.0 \times 10^{-16}$ *	0.82	2.2×10^{-6} *	1.3×10^{-9} *	$<2.0 \times 10^{-16}$ *	59.3%	0.29
	ROV	62	NA	NA	NA	0.46	6.7×10^{-5} *	81.1%	0.46
Benthic pursuers	AUV	279	0.55	2.0×10^{-3} *	0.55	5.0×10^{-4} *	6.2×10^{-2}	46.7%	0.53
	TV	1798	2.0×10^{-4} *	3.4×10^{-7} *	$<2.0 \times 10^{-16}$ *	$<2.0 \times 10^{-16}$ *	2.2×10^{-11} *	34.0%	0.22
	ROV	1919	1.7×10^{-8} *	3.9×10^{-8} *	1.1×10^{-13} *	$<2.0 \times 10^{-16}$ *	1.7×10^{-3} *	13.9%	0.10
Down movers	AUV	186	3.7×10^{-12} *	2.0×10^{-4} *	4.8×10^{-11} *	$<2.0 \times 10^{-16}$ *	0.76	98.0%	0.99
	TV	744	$<2.0 \times 10^{-16}$ *	6.8×10^{-14} *	$<2.0 \times 10^{-16}$ *	$<2.0 \times 10^{-16}$ *	$<2.0 \times 10^{-16}$ *	60.8%	0.39
	ROV	1921	1.9×10^{-15} *	$<2.0 \times 10^{-16}$	1.9×10^{-7} *	$<2.0 \times 10^{-16}$ *	0.03 *	18.6%	0.14
Lateral movers	TV	217	NA	6.4×10^{-5}	5.0×10^{-4} *	1.9×10^{-5} *	0.42	26.8%	0.73
	ROV	1085	1.3×10^{-13} *	1.2×10^{-8}	$<2 \times 10^{-16}$ *	$<2.0 \times 10^{-16}$ *	$<2.0 \times 10^{-16}$ *	38.3%	0.14
Local reactive	TV	1767	0.20 *	3.4×10^{-2}	2.0×10^{-3} *	$<2.0 \times 10^{-16}$ *	1.4×10^{-8} *	11.6%	0.17
	ROV	1112	NA	$<2.0 \times 10^{-16}$	$<2.0 \times 10^{-16}$ *	$<2.0 \times 10^{-16}$ *	1.8×10^{-7} *	29.7%	0.42

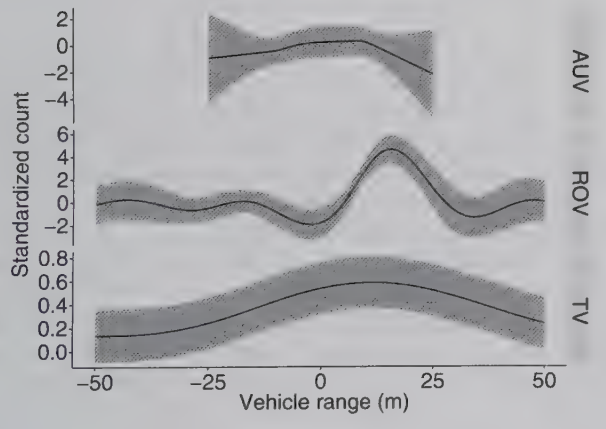

Figure 5

Change in standardized fish counts observed at selected reef sites in the Florida Middle Grounds for the pelagic pursuers guild as a function of vehicle range (meters) and by vehicle type. Survey vehicles used in this experiment included an autonomous underwater vehicle (AUV), a remotely operated vehicle (ROV), and a towed vehicle (TV). Predictions were made by using the GAM predict function in the R package mgcv, and parameters were set in the models as follows: first transect transited, the relative vehicle altitude from the seafloor was set at the middle level (2 m), and habitat complexity was set at the average qualitative rating (2.5). The gray shaded areas represent the 95% confidence intervals. Surveys were conducted during August 2014 and July and August 2015.

From a qualitative perspective, the benthic pursuers group exhibited strong attraction to all of the vehicles tested but in general were not fast enough to keep up with a transiting vehicle. Therefore, members of this guild tended to only briefly chase vehicles following passage (Fig. 6). For the benthic pursuers guild, results from the AUV model indicate significant effects for RVA and habitat complexity, but vehicle range was marginally significant and transect number was not significant. The AUV model explained 46.7% of the deviance with an r^2 of 0.52 (Table 2). The TV model had significant effects for RVA, vehicle range, transect number, and habitat complexity. The TV model explained 34.0% of the deviance with an r^2 of 0.22. The ROV model had significant effects for RVA, vehicle range, transect number, and habitat complexity. The ROV model explained 13.9% of the deviance with an r^2 of 0.10. For the benthic pursuers guild, relative abundance increased with decreasing vehicle range to the MOUSS sampling volume, peaking at a distance of around 0 m and remaining at elevated levels following vehicle passage (Fig. 6). In general, relative abundance of this group also increased as a function of transect number with varying results relative to vehicle type. For both slow-transiting vehicles (AUV and ROV), increasing RVA resulted in increased relative abundance; whereas, with the TV relative abundance decreased with increasing RVA.

From a qualitative perspective, the lateral movers group tended to flee laterally as the vehicle neared the MOUSS platform sampling volume (Fig. 7). For the lateral movers guild, results from the TV model indicate significant

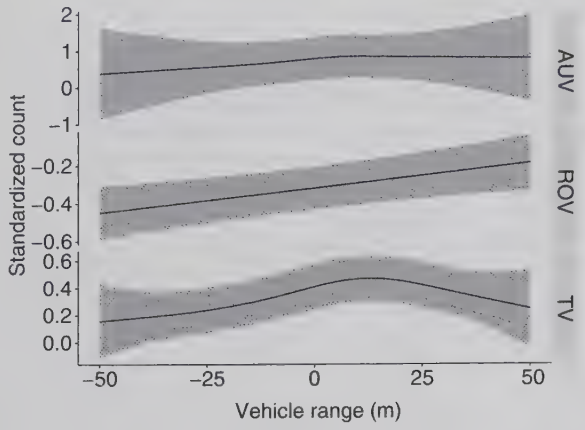

Figure 6

Change in standardized fish counts observed at selected reef sites in the Florida Middle Grounds of the benthic pursuers guild as a function of vehicle range (meters) and by vehicle type. Survey vehicles used in this experiment were an autonomous underwater vehicle (AUV), a remotely operated vehicle (ROV), and a towed vehicle (TV). Predictions were made by using the GAM predict function in the R package mgcv, and parameters were set in the models as follows: first transect transited, the relative vehicle altitude from the seafloor was set at the middle level (2 m), and habitat complexity was set at the average qualitative rating (2.5). The gray shaded areas represent the 95% confidence intervals. Surveys were conducted during August 2014 and July and August 2015.

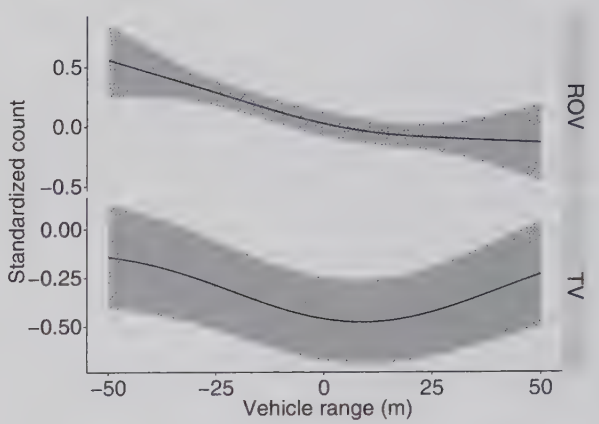

Figure 7

Change in standardized fish counts observed at selected reef sites in the Florida Middle Grounds of the lateral movers guild as a function of vehicle range (meters) and by vehicle type. Survey vehicles used in this experiment were a remotely operated vehicle (ROV) and a towed vehicle (TV). Predictions were made by using the GAM predict function in the R package mgcv, and parameters were set in the models as follows: first transect transited, the relative vehicle altitude from the seafloor was set at the middle level (2 m), and habitat complexity was set at the average qualitative rating (2.5). The gray shaded areas represent the 95% confidence intervals. Surveys were conducted during August 2014 and July and August 2015.

effects on relative abundance for RVA, transect number, and habitat complexity, but vehicle range was not significant. The TV model explained 26.8% of the deviance with an r^2 of 0.73 (Table 2). Results from the ROV model indicate significant effects on relative abundance for RVA, transect number, habitat complexity, and vehicle range. The ROV model explained 38.3% of the deviance with an r^2 of 0.14. There were not enough interactions with the AUV to analyze effects for the lateral movers guild. Lateral movers guild fish abundance decreased significantly with decreasing vehicle range to the MOUSS platform sampling volume (Fig. 7). Following passage of the TV, fish tended to return to the MOUSS platform sampling volume; whereas, they did not return following ROV passage. Relative abundance of the lateral movers guild decreased with increasing number of transects surveyed with the ROV. Relative vehicle altitude above the seafloor had opposite effects by vehicle, with low transect numbers for the TV resulting in increased relative abundance and with increased transect number for the ROV resulting in increased relative abundance. This result might be due to the differences in habitat preferences between vermilion snapper (semi-pelagic) and porgies (benthic) having been mixed into the same model.

From a qualitative perspective, the down movers guild exhibited negative reactions to the vehicles, and fish in this group fled down into available interstitial spaces in the local habitat but did not leave the MOUSS platform sampling volume (Fig. 8). Relative abundance of the down movers guild decreased with decreasing vehicle range, and the steepness of the decline and subsequent increase appears to be dependent on vehicle type. For the down movers guild, results from the AUV model indicate significant effects on relative abundance for RVA, transect number, and habitat complexity, but range was not significant. The AUV model explained 98.0% of the deviance with an r^2 of 0.98 (Table 2). Results from the TV model indicate significant effects on down movers guild relative abundance for RVA, transect number, habitat complexity, and vehicle range. The TV model explained 60.8% of the deviance with an r^2 of 0.38. Results from the ROV model indicate significant effects on relative abundance for RVA, transect number, habitat complexity, and vehicle range. The ROV model explained 18.6% of the deviance with an r^2 of 0.14. Strongest responses were observed for the TV and ROV (fastest vehicles), and the weakest responses were observed for the AUV (slowest vehicle). For both the AUV and ROV, down movers guild relative abundance decreased with increasing transect number. In contrast, results from the TV model indicate that relative abundance increased through the first 5 transects followed by decreasing relative abundance thereafter. Increasing RVA indicates increasing down movers guild

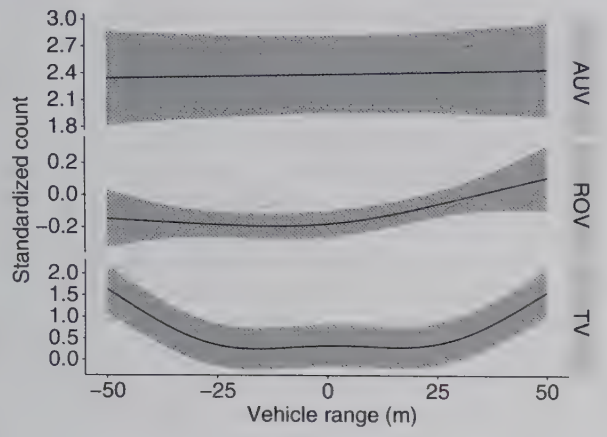

Figure 8

Change in standardized fish counts observed at selected reef sites in the Florida Middle Grounds of the down movers guild as a function of vehicle range (meters) and by vehicle type. Survey vehicles used in this experiment were an autonomous underwater vehicle (AUV), a remotely operated vehicle (ROV), and a towed vehicle (TV). Predictions were made by using the GAM predict function in the R package mgcv, and parameters were set in the models as follows: first transect transited, the relative vehicle altitude from the seafloor was set at the middle level (2 m), and habitat complexity was set at the average qualitative rating (2.5). The gray shaded areas represent the 95% confidence intervals. Surveys were conducted during August 2014 and July and August 2015.

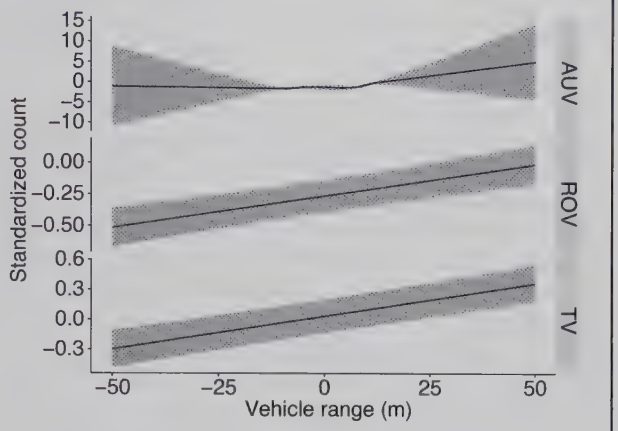

Figure 9

Change in standardized fish counts observed at selected reef sites in the Florida Middle Grounds of the local reactive guild as a function of vehicle range (meters) and by vehicle type. Survey vehicles used in this experiment were an autonomous underwater vehicle (AUV), a remotely operated vehicle (ROV), and a towed vehicle (TV). Predictions were made by using the GAM predict function in the R package mgcv, and parameters were set in the models as follows: first transect transited, the relative vehicle altitude from the seafloor was set at the middle level (2 m), and habitat complexity was set at the average qualitative rating (2.5). The gray shaded areas represent the 95% confidence intervals. Surveys were conducted during August 2014 and July and August 2015.

relative abundance for the AUV and ROV but indicates a decreasing trend in relative abundance for the TV.

From a qualitative perspective, relative abundance of the local reactive guild tended to change little in relation to vehicle passage (Fig. 9). However, observations on camera indicate that individuals of this group tended to increase activity with a vehicle present but did not flee the sampling volume in front of the MOUSS platforms (i.e., locally reactive). For the local reactive guild, results from the TV model indicate significant effects on relative abundance for RVA, transect number, habitat complexity, and vehicle range. The TV model explained 11.6% of the deviance with an r^2 of 0.17 (Table 2). Results from the ROV model indicate significant effects on relative abundance for RVA, transect number, habitat complexity, and vehicle range. The ROV model explained 29.7% of the deviance with an r^2 of 0.42. The AUV had too small of a sample size to evaluate this group. Vehicle altitude could only be evaluated for the TV and was negatively related to relative abundance.

Discussion

Species-specific gear interactions were difficult to capture; however, various patterns of fish response to the vehicles allowed classification of species into behavioral guilds. The use of GAMs proved to be an effective method to examine changes in relative abundance of fish as a function of vehicle range and relative altitude, transect number, and habitat complexity. The effect of each variable is dependent on the behavioral guild of interest, but vehicle range was a consistent predictor of relative changes in abundance regardless of vehicle and behavioral guild. In general, the best fitting models were associated with the strongest behavioral responses, such as the attraction behavior observed for the pelagic pursuers guild and the avoidance behavior observed for the down movers guild. Finally, although logistically difficult to conduct, the testbed method we used to evaluate fish responses to sampling gear was effective and potentially will provide a path forward to conducting gear calibrations in the future.

The consistency of vehicle range in the GAMs allowed the development of functional relationships between vehicle range and the change in relative abundance in the MOUSS platform sampling volume (Figs. 4–9). Although many studies have recognized or coarsely evaluated fish responses to sampling vehicles (Ralston et al., 1986; Richards, 1986; Koslow et al., 1995; Trenkel et al., 2004a, 2004b; Lorance and Trenkel, 2006; Ryer et al., 2009), no studies have included estimation of a functional relationship that predicts relative change in abundance to an approaching vehicle (i.e., far-field response). The testbed approach proved to be a robust method of deriving

attraction and avoidance functions that in future iterations of this research will be useful for conducting vehicle calibration studies and for modifying fish abundance and density estimates.

The benthic and pelagic pursuers guilds had strong attraction to the survey vehicles. Both guilds included several managed species that are important components of fisheries that operate in the GOM, including scamp, red grouper (*Epinephelus morio*), and greater amberjack. In addition to the obvious distinction of habitat preference, these guilds had distinct differences in ability to match vehicle speed while in pursuit. Pelagic pursuers concentrated behind vehicles and could easily maintain pace with them; however, their response was not persistent over repeated transects (Fig. 5). The strong attraction signal, coupled with the pelagic pursuers ability to match vehicle speed, indicates that the same fish could be observed with vehicles along the transect line, resulting in overestimation of fish abundance or density. Unfortunately, given the relatively short transect length in our surveys, we could not determine the distance over which pelagic pursuers continued to follow a vehicle.

Conversely, benthic pursuers gave short chase following vehicle passage and could not keep up with vehicles; however, they repeated the behavior in subsequent vehicle transects (Fig. 6). This finding indicates that new individuals from the benthic pursuers group are likely being observed with the vehicles down the transect line. Thus, density estimates for species of this guild likely will not require adjustment because the observed fish did not aggregate around the vehicles and, as a result, were not drawn down a transect line. Of higher concern for observing benthic pursuers guild fish like groupers is their coloration and mottling patterns (Burge et al., 2012; Watson et al., 2014) and their tendency to hide underneath structure, both of which makes them difficult to observe (Camp et al., 2013). Therefore, understanding detection probability and sighting functions may be more critical for estimating abundance or density for species in the benthic pursuers guild. In our experiment, the following behavior seems to be most strongly associated with piscivorous fish, perhaps as a stalking or investigatory type of behavior. Strong attraction to ROVs has also been observed for yellowtail rockfish (*Sebastes flavidus*) (Stoner et al., 2008) and Pacific hake (*Merluccius productus*) (Adams et al., 1995); however, neither study quantified the response. In general, attraction responses need to be well understood because they concentrate fish, could result in overestimation of density, and are thus not conservative.

Gear avoidance is one of the more common behaviors noted in studies (Adams et al., 1995; Koslow et al., 1995; Uiblein et al., 2003; Lorance and Trenkel, 2006) and was most clearly observed for the lateral and down movers guilds. Lateral movers guild fish, which include snapper and grunts, exhibited significant decreases in abundance with decreasing vehicle range, indicating a flight response to approaching vehicles. Avoidance behaviors have been linked to the looming effect in which fast, direct approaches increase the likelihood and strength of the flight response (Frid and Dill, 2002). An analysis of fine-scale data collected from frame-by-frame analysis of a subset of the UHSI videos revealed that vermilion snapper scaled their response from slow-swimming behavior and loosely aggregated schools when the vehicle was distant to tightly aggregated schools and fast-swimming behavior when the TV came into the sampling volume (Somerton et al., 2017). Both the ROV and TV displaced lateral movers guild fish from the MOUSS platform sampling volume prior to the vehicle's arrival; however, there was not enough AUV data to analyze. The persistence of the flight response was vehicle dependent; for instance, abundance quickly returned to pre-disturbance levels following TV transit; whereas, abundance remained depressed following ROV transit. The difference in the persistence of the effect could be related to the extended length of time the ROV tether remained in the vicinity of the MOUSS platform. Calibration experiments will be necessary for vehicle-based surveys that target fish species in this guild and that exhibit strong flight response as there is high likelihood that abundance and density will be underestimated.

Another clear case of vehicle avoidance was associated with the down movers guild. The flight response to the approaching vehicle was consistent and strongly oriented downward into protective habitat, but fish did not depart the sampling volume (i.e., present but no longer detected). Most of the species in the down movers guild in this analysis are in the family Pomacentridae (e.g., *Chromis* spp.), are generally small in body size, and are found in close proximity to reef habitat. The distinct downward response to the vehicle was also observed when predators, such as great barracuda swam through the sampling volume, and thus we presume this behavior to be related to predator avoidance and response to novel threats. It could be that the body size of the species in this group precludes them from outswimming a predator in open water and that a strategy to stay near protective habitat into which they can flee is advantageous. In addition, the response appears to be weakest in relation to the AUV and strongest for the TV and ROV. As with the response of the lateral movers, the looming effect is strongly associated with the speed of the vehicle (Frid and Dill, 2002) and might explain the observed differences in fish responses between vehicles. The AUV travels slower and at higher altitudes than the other vehicles and therefore has a decreased looming effect, which perhaps tempers the flight response into protective habitat (i.e., perceived threat is dampened). As with the lateral movers guild, gear calibrations are required for species in this group to compensate for changes in abundance due to the flight response.

The local reactive guild is composed largely of species of ornamental reef fish, such as butterflyfish (*Chaetodon* spp.), filefish (*Monacanthus* spp.), and damselfish (*Stegastes* spp.). For this guild, abundance increased as a function of vehicle range, and fish of this guild exhibited little attraction or avoidance to the vehicles and, as with fish of the down movers guild, did not leave the sampling volume. Review of video also revealed increased activity (i.e., reactive behavior) following vehicle passage. Further,

abundance increased with increasing number of transects. Because fish of the local reactive guild were not attracted to the vehicles but abundance increased as a function of vehicle range and over transects, vehicle passage could have altered the behavior of the fish, causing a coincident increase in detectability by the MOUSS platforms. In other words, detection rather than abundance is potentially changing, at least from the perspective of the MOUSS cameras.

Detection probability and sighting functions (i.e., range to positive identification of fish) have been shown to be critical for estimation of fish densities for strip-transect and distance sampling methods (Sale and Sharp, 1983; Ensign et al., 1995; Cheal and Thompson, 1997), even for species that have minimal or no avoidance behaviors (Kulbicki and Sarramégna, 1999). Although the functions developed in this work add critical information about how relative fish abundance changed prior to vehicle arrival, vehicle-specific sighting functions are equally important to develop even for species exhibiting minimal or no behavioral response. Further, it is important to understand that the MOUSS platforms in our experiment have their own detection probability and sighting functions; therefore, what is presented here is relative to the MOUSS platform observations. Thus, our modeling does not necessarily lead to unbiased estimates of abundance or biomass. Further research that could establish fish density in a known area, and therefore establish the standard in which the optical systems were deployed, would be a useful but extremely difficult undertaking. Finally, all of the key components necessary to estimate fish density will likely have important covariates to consider, variables such as light, water clarity, and habitat complexity. Light and water clarity were fairly constant over the course of the experiment; however, habitat complexity varied among sites. Both of these findings may or may not occur in basin-wide surveys but are critical considerations for those types of surveys (e.g., in the Gulf of Mexico).

Although we were able to estimate functions that were based on vehicle range and that included important covariates to help evaluate fish response (e.g., habitat complexity), we were unable to connect those responses to any specific vehicle stimuli (e.g., noise or light). Sensory mechanisms of fish that detect the sound, light, and motion of a vehicle are all critical components that likely incite fish reaction and potentially bias observations in undetermined directions and magnitude. For instance, in an experiment designed to observe soniferous fish behavior, ROV noise induced a strong negative behavioral response that affected observations during sampling (Rountree and Juanes, 2010). Similarly, responses to artificial lighting range from attraction to avoidance and are species specific (McIninch and Hocutt, 1987; Marchesan et al., 2005; Raymond and Widder, 2007). Furthermore, the order of stimuli detection and their associated thresholds in fish are uncertain. For instance, the sound produced by motors and propellers or the vibration of tow cables generate noise that could stimulate the lateral movers guild fish and cause a response prior to the fish detecting vehicle lights. Similarly, positioning beacons generate sound but generally operate at higher frequencies than fish can detect (Mann et al., 2001; Popper, 2003; Stoner et al., 2008).

Ultimately, noise-inducing equipment, such as tethers, tow cables, and propellers are critical components of vehicles; therefore, experiments should include a capacity to measure relevant stimuli in order to relate them to fish response. For instance, future iterations of this type of experiment and large-scale ocean observation systems (Rountree et al., 2020) would benefit from having a suite of acoustic sensors and light meters to identify specific vehicle noise and light production signatures. Light meters and turbidity sensors for detecting ambient conditions in the environment would also be useful for estimation of vehicle- and condition-specific sighting functions. Finally, experimental methods that place sampling platforms at specific locations and on specific habitat would likely result in more interactions with target species and enable development of species-specific range functions. Cameras that have increased FOV (e.g., 360° or full spherical) might be useful, given that it has been reported that they increase fish detection (Kilfoil et al., 2017; Campbell et al., 2018). Additionally, full-spherical cameras would be useful in vehicle detection when they transit behind or above the intended transect line, and thus more gear interactions could be captured.

The original statistical analysis was envisioned to create single-species models that include vehicle type as a variable in order to facilitate direct comparisons of vehicle performance. Logistics of the ship, however, caused us to stage the experiment in 2 separate periods. Therefore, in the experiment, each vehicle was tested in somewhat different habitats that had varied fish assemblages and densities, making it impossible to expose each vehicle to a standardized set of conditions. Because of the difficulty of sampling different sites, we created the habitat complexity variable in an effort to standardize site conditions and clarify changes in abundance that were associated with vehicle passage. Additionally, species-specific interactions in the coincident sampling volume in space and time were rare, thus making single-species models problematic to estimate. Other at-sea conditions also created situations where the AUV in particular was not deployed as frequently as the other vehicles and therefore had fewer interactions with target species. For these reasons, we felt that a direct comparison that used a singular model (i.e., inclusion of a vehicle variable) was not defensible. Importantly, our observations were that each vehicle had good and bad traits for sampling different habitats and had differential utility depending on target species. Thus, we made an effort to not compare vehicles qualitatively (i.e., good or bad). We envision that the outcomes of our work potentially would help researchers select a vehicle that best fits the target environment and species they intend to sample.

Critically, underlying fish density could not be controlled; therefore, statistical analysis, model estimation, and resultant explanatory capacity were shaped around the data that we were able to obtain. Recent efforts to

estimate species-specific absolute abundance, such as the Great Red Snapper Count (Stunz et al.[2]), rely on integration of data across a wide spectrum of instrumentation. Basin-scale efforts such as this require some form of calibration treatment obtained over a wide range of sampling conditions and habitats (e.g., water clarity and low to high relief) and across a variety of platforms and instruments capable of scaling to common units (e.g., fish density per unit area or volume). To achieve proper calibration, efforts such as those laid out in this paper will be necessary and will undoubtedly be very expensive in time, complexity, and expense. Without proper methods to calibrate instruments against known densities, efforts such as those undertaken in this experiment, while interesting, might not result in desired outcomes. Thus targets such as absolute abundance will remain elusive or will be heavily reliant on poorly understood assumptions about vehicle sampling properties and their associated biases.

Conclusions

The test-bed experiment was logistically difficult to conduct because many moving pieces had to be synchronized to produce coincident sampling volumes and useful data. Logistical difficulties included temporal synchronization of all sampling equipment, orientation of the MOUSS platforms perpendicular to the transect line transited by the vehicles, geolocation of cameras once deployed, and navigation of vehicles precisely down transect lines. Although the logistics of the experiment went smoothly and improved over time, it was equally difficult to detect interactions for specific fish species. Another issue is that manual annotation of videos is a slow process, and producing data sets therefore is a time intensive process that would be enhanced with automated approaches, particularly those that can be used to generate data on small spatio-temporal scales (Shafait et al., 2017). A field experiment that would encompass all of the potential variables of interest (e.g., species movement patterns, water conditions, and vehicle effects) would be difficult to coordinate and control; therefore, a logical next step is to evaluate the question in a simulation-modeling framework (Kim and Wardle, 1998).

Acknowledgments

The authors would like to acknowledge the NMFS Office of Science and Technology for continued support throughout this 5-year strategic initiative. We would like to thank the Mississippi Laboratories of the NMFS Southeast Fisheries Science Center, the University of South Florida, and the Florida Institute of Oceanography for providing personnel and dockside support to stage and conduct this complicated experiment. We would also like to thank the crews of RV *Pelican* (LUMCON, Cocodrie, LA) and RV *Weatherbird II* (FIO, St. Petersburg, FL).

[2] Stunz, G. W., W. F. Patterson III, S. P. Powers, J. H. Cowan Jr., J. R. Rooker, R. A. Ahrens, K. Boswell, L. Carleton, M. Catalano, J. M. Drymon et al. 2021. The great red snapper count: estimating the absolute abundance of age-2+ red snapper (*Lutjanus campechanus*) in the U.S. Gulf of Mexico, 152 p. Mississippi-Alabama Sea Grant Consort., Ocean Springs, MS. [Available from website.]

Literature cited

Adams, P. B., J. L. Butler, C. H. Baxter, T. E. Laidig, K. A. Dahlin, and W. W. Wakefield.
1995. Population estimates of Pacific coast groundfishes from video transects and swept-area trawls. Fish. Bull. 93:446–455.

Afanasyev, P. K., A. M. Orlov, and R. N. Novikov.
2014. Comparative characteristic of sablefish *Anoplopoma fimbria* in catches with passive and active fishing gear in the northwestern Pacific Ocean. J. Ichthyol. 54:146–164.

Amin, R., B. L. Richards, W. Misa, J. Taylor, G. C. Young, D. Miller, A. Rollo, C. Demarke, H. Singh, J. Childress et al.
2017. The Modular Optical Underwater Survey System (MOUSS) for in situ sampling of fish assemblages. *In* OCEANS 2017—Anchorage; Anchorage, 18–21 September, p. 1–8. Inst. Electr. Electr. Eng., Piscataway, NJ. [Available from website.]

Armstrong, R. A., and H. Singh.
2012. Mesophotic coral reefs of the Puerto Rico shelf. *In* Seafloor geomorphology as benthic habitat: GeoHab atlas of seafloor geomorphic features and benthic habitats (P. T. Harris and E. K. Baker, eds.), p. 365–374. Elsevier, London.

Austin, H. M., and J. I. Jones.
1974. Seasonal variation of physical oceanographic parameters on the Florida Middle Ground and their relation to zooplankton biomass on the West Florida Shelf. Fla. Sci. 37:16–32.

Bacheler, N. M., and K. W. Shertzer.
2015. Estimating relative abundance and species richness from video surveys of reef fishes. Fish. Bull. 113:15–26.

Burge, E. J., J. D. Atack, C. Andrews, B. M. Binder, Z. D. Hart, A. C. Wood, L. E. Bohrer, and K. Jagannathan.
2012. Underwater video monitoring of groupers and the associated hard-bottom reef fish assemblage of North Carolina. Bull. Mar. Sci. 88:15–38.

Camp, E. F., K. E. Lohr, S. C. Barry, P. G. Bush, C. A. Jacoby, and C. Manfrino.
2013. Microhabitat associations of late juvenile Nassau grouper (*Epinephelus striatus*) off Little Cayman, BWI. Bull. Mar. Sci. 89:571–581.

Campbell, M. D., J. Salisbury, R. Caillouet, W. B. Driggers, and J. Kilfoil.
2018. Camera field-of-view and fish abundance estimation: a comparison of individual-based model output and empirical data. J. Exp. Mar. Biol. Ecol. 501:46–53.

Cheal, A. J., and A. A. Thompson.
1997. Comparing visual counts of coral reef fish: implications of transect width and species selection. Mar. Ecol. Prog. Ser. 158:241–248.

Clarke, M. E., N. Tolimieri, and H. Singh.
2009. Using the Seabed AUV to assess populations of groundfish in untrawlable areas. *In* The future of fisheries science in North America (R. J. Beamish and B. J. Rothschild, eds.), p. 357–372. Springer, Dordrecht, Netherlands.

Darcy, G. H., and E. J. Gutherz.
1984. Abundance and density of demersal fishes on the West Florida Shelf, January 1978. Bull. Mar. Sci. 34:81–105.

Emslie, M. J., A. J. Cheal, M. A. MacNeil, I. R. Miller, and H. P. A. Sweatman.
2018. Reef fish communities are spooked by scuba surveys and may take hours to recover. PeerJ 6:e4886.

Ensign, W. E., P. L. Angermeier, and C. A. Dolloff.
1995. Use of line transect methods to estimate abundance of benthic stream fishes. Can. J. Fish. Aquat. Sci. 52:213–222.

Frid, A., and L. Dill.
2002. Human-caused disturbance stimuli as a form of predation risk. Conserv. Ecol. 6(1):11.

Grasty, S. E.
2014. Use of a towed camera system for estimating reef fish populations densities on the West Florida Shelf. M.S. thesis, 89 p. Univ. South Fla., St. Petersburg, FL. [Available from website.]

Gray, A. E., I. D. Williams, K. A. Stamoulis, R. C. Boland, K. C. Lino, B. B. Hauk, J. C. Leonard, J. J. Rooney, J. M. Asher, K. H. Lopes Jr. et al.
2016. Comparison of reef fish survey data gathered by open and closed circuit SCUBA divers reveals differences in areas with higher fishing pressure. PLoS ONE 11(12):e0167724.

Hall-Spencer, J., V. Allain, and J. H. Fosså.
2002. Trawling damage to Northeast Atlantic ancient coral reefs. Proc. R. Soc. Lond., B 269:507–511.

Jagielo, T., A. Hoffmann, J. Tagart, and M. Zimmermann.
2003. Demersal groundfish densities in trawlable and untrawlable habitats off Washington: implications for the estimation of habitat bias in trawl surveys. Fish. Bull. 101:545–565.

Kilfoil, J., M. Bond, M. D. Campbell, J. Kiszka, K. Gastrich, M. Heithaus, Y. Zhang, and A. Wirsing.
2017. Baited Remote Underwater Video surveys undercount sharks at high densities: insights from full-spherical camera technologies. Mar. Ecol. Prog. Ser. 585:113–121.

Kim, Y.-H., and C. S. Wardle.
1998. Modelling the visual stimulus of towed fishing gear. Fish. Res. 34:165–177.

Koenig, C. C., F. C. Coleman, C. B. Grimes, G. R. Fitzhugh, K. M. Scanlon, C. T. Gledhill, and M. Grace.
2000. Protection of fish spawning habitat for the conservation of warm-temperate reef-fish fisheries of shelf-edge reefs of Florida. Bull. Mar. Sci. 66:593–616.

Koslow, J. A., R. Kloser, and C. A. Stanley.
1995. Avoidance of a camera system by a deepwater fish, the orange roughy (*Hoplostethus atlanticus*). Deep-Sea Res., I 42:233–244.

Kulbicki, M., and S. Sarramégna.
1999. Comparison of density estimates derived from strip transect and distance sampling for underwater visual censuses: a case study of Chaetodontidae and Pomacanthidae. Aquat. Living Resour. 12:315–325.

Lembke, C., S. Grasty, A. Silverman, H. Broadbent, S. Butcher, and S. Murawski.
2017. The Camera-Based Assessment Survey System (C-BASS): a towed camera platform for reef fish abundance surveys and benthic habitat characterization in the Gulf of Mexico. Cont. Shelf Res. 151:62–71.

Lorance, P., and V. M. Trenkel.
2006. Variability in natural behaviour, and observed reactions to an ROV, by mid-slope fish species. J. Exp. Mar. Biol. Ecol. 332:106–119.

Mangi, S. C., and C. M. Roberts.
2006. Quantifying the environmental impacts of artisanal fishing gear on Kenya's coral reef ecosystems. Mar. Pollut. Bull. 52:1646–1660.

Mann, D. A., D. M. Higgs, W. N. Tavolga, M. J. Souza, and A. N. Popper.
2001. Ultrasound detection by clupeiform fishes. J. Acoust. Soc. Am. 109:3048–3054.

Marchesan, M., M. Spoto, L. Verginella, and E. A. Ferrero.
2005. Behavioural effects of artificial light on fish species of commercial interest. Fish. Res. 73:171–185.

McInnch, S. P., and C. H. Hocutt.
1987. Effects of turbidity on estuarine fish response to strobe lights. J. Appl. Ichthyol. 3:97–105.

O'Connell, V. M., and D. W. Carlile.
1993. Habitat-specific density of adult yelloweye rockfish (*Sebastes ruberrimus*) in the eastern Gulf of Alaska. Fish. Bull. 91:304–309.

Olla, B. L., M. W. Davis, and C. H. Ryer.
1998. Understanding how the hatchery environment represses or promotes the development of behavioral survival skills. Bull. Mar. Sci. 62:531–550.

Parker, D., H. Winker, A. T. F. Bernard, E. R. Heyns-Veale, T. J. Langlois, E. S. Harvey, and A. Götz.
2016. Insights from baited video sampling of temperate reef fishes: how biased are angling surveys? Fish. Res. 179:191–201.

Patterson, W. F., III, M. A. Dance, and D. T. Addis.
2009. Development of a remotely operated vehicle based methodology to estimate fish community structure at artificial reef sites in the northern Gulf of Mexico. Proc. Gulf Caribb. Fish. Inst. 61:263–270.

Pierce, D. J., and B. Mahmoudi.
2001. Nearshore fish assemblages along the central west coast of Florida. Bull. Mar. Sci. 68:243–270.

Popper, A. N.
2003. Effects of anthropogenic sounds on fishes. Fisheries 28(10):24–31.

R Core Team.
2020. R: a language and environment for statistical computing. R Foundation for Statistical Computing, Vienna, Austria. [Available from website, accessed January 2021.]

Ralston, S., R. M. Gooding, and G. M. Ludwig.
1986. An ecological survey and comparison of bottom fish resource assessments (submersible versus handline fishing) at Johnston Atoll. Fish. Bull. 84:141–155.

Raymond, E. H., and E. A. Widder.
2007. Behavioral responses of two deep-sea fish species to red, far-red, and white light. Mar. Ecol. Prog. Ser. 350:291–298.

Rezak, R., T. J. Bright, and D. W. McGrail.
1985. Reefs and banks of the northwestern Gulf of Mexico: their geological, biological, and physical dynamics, 259 p. Wiley, New York.

Richards, L. J.
1986. Depth and habitat distributions of three species of rockfish (*Sebastes*) in British Columbia: observations from the submersible PISCES IV. Environ. Biol. Fish. 17:13–21.

Roberts, J. M., A. J. Wheeler, and A. Freiwald.
2006. Reefs of the deep: the biology and geology of cold-water coral ecosystems. Science 312:543–547.

Rountree, R. A., and F. Juanes.
2010. First attempt to use a remotely operated vehicle to observe soniferous fish behavior in the Gulf of Maine, Western Atlantic Ocean. Curr. Zool. 56:90–99.

Rountree, R. A., J. Aguzzi, S. Marini, E. Fanelli, F. C. De Leo, J. Del Rio, and F. Juanes.
2020. Towards an optimal design for ecosystem-level ocean observatories. *In* Oceanography and marine biology: an annual review, vol. 58 (S. J. Hawkins, A. L. Allcock, A. E. Bates, A. J. Evans, L. B. Firth, C. D. McQuaid, B. D. Russell, I. P. Smith, S. E. Swearer, and P. A. Todd, eds.), p. 79–106. Taylor and Francis Group, Boca Raton, FL.

Royle, J. A., J. D. Nichols, K. U. Karanth, and A. M. Gopalaswamy.
2009. A hierarchical model for estimating density in camera-trap studies. J. Appl. Ecol. 46:118–127.

Ryer, C. H., A. W. Stoner, P. J. Iseri, and M. L. Spencer.
2009. Effects of simulated underwater vehicles lighting on fish behavior. Mar. Ecol. Prog. Ser. 391:97–106.

Sale, P. F., and B. J. Sharp.
1983. Correction for bias in visual transect censuses of coral reef fishes. Coral Reefs 2:37–42.

Shafait, F., E. S. Harvey, M. R. Shortis, A. Mian, M. Ravanbakhsh, J. W. Seager, P. F. Culverhouse, D. E. Cline, and D. R. Edgington.
2017. Towards automating underwater measurement of fish length: a comparison of semi-automatic and manual stereo–video measurements. ICES J. Mar. Sci. 74:1690–1701.

Singh, H., A. Can, R. Eustice, S. Lerner, N. McPhee, and C. Roman.
2004. Seabed AUV offers new platform for high-resolution imaging. EOS Trans. Am. Geophys. Union 85:289–296.

Somerton, D. A., K. Williams, and M. D. Campbell.
2017. Quantifying the behavior of fish in response to a moving camera vehicle by using benthic stereo cameras and target tracking. Fish. Bull. 115:343–354.

Stierhoff, K. L., J. L. Butler, S. A. Mau, and D. W. Murfin.
2013. Abundance and biomass estimates of demersal fishes at the Footprint and Piggy Bank from optical surveys using a remotely operated vehicle (ROV). NOAA Tech. Memo. NMFS-SWFSC-521, 32 p.

Stoner, A. W., C. H. Ryer, S. J. Parker, P. J. Auster, and W. W. Wakefield.
2008. Evaluating the role of fish behavior in surveys conducted with underwater vehicles. Can. J. Fish. Aquat. Sci. 65:1230–1243.

Thanopoulou, Z., M. Sini, K. Vatikiotis, C. Katsoupis, P. G. Dimitrakopoulos, and S. Katsanevakis.
2018. How many fish? Comparison of two underwater visual sampling methods for monitoring fish communities. PeerJ 6:e5066.

Trenkel, V. M., and P. Lorance.
2011. Estimating *Synaphobranchus kaupii* densities: contribution of fish behaviour to differences between bait experiments and visual strip transects. Deep-Sea Res., I 58:63–71.

Trenkel, V. M., P. Lorance, and S. Mahévas.
2004a. Do visual transects provide true population density estimates for deepwater fish? ICES J. Mar. Sci. 61:1050–1056.

Trenkel, V. M., R. I. C. C. Francis, P. Lorance, S. Mahévas, M.-J. Rochet, and D. M. Tracey.
2004b. Availability of deep-water fish to trawling and visual observation from a remotely operated vehicle (ROV). Mar. Ecol. Prog. Ser. 284:293–303.

Uiblein, F., P. Lorance, and D. Latrouite.
2003. Behaviour and habitat utilisation of seven demersal fish species on the Bay of Biscay continental slope, NE Atlantic. Mar. Ecol. Prog. Ser. 257:223–232.

Uzmann, J. R., R. A. Cooper, R. B. Theroux, and R. L. Wigley.
1977. Synoptic comparison of three sampling techniques for estimating abundance and distribution of selected megafauna: submersible vs camera sled vs otter trawl. Mar. Fish. Rev. 39(12):11–19.

Watson, A. C., L. A. Siemann, and R. T. Hanlon.
2014. Dynamic camouflage by Nassau groupers *Epinephelus striatus* on a Caribbean coral reef. J. Fish Biol. 85:1634–1649.

Whitmarsh, S. K., P. G. Fairweather, and C. Huveneers.
2017. What is big BRUVver up to? Methods and uses of baited underwater video. Rev. Fish Biol. Fish. 27:53–73.

Williams, K., C. N. Rooper, A. De Robertis, M. Levine, and R. Towler.
2018. A method for computing volumetric fish density using stereo cameras. J. Exp. Mar. Biol. Ecol. 508:21–26.

Wood, S. N.
2011. Fast stable restricted maximum likelihood and marginal likelihood estimation of semiparametric generalized linear models. J. R. Stat. Soc., B 73:3–36.

Yoklavich, M. M., M. S. Love, and K. A. Forney.
2007. A fishery-independent assessment of an overfished rockfish stock, cowcod (*Sebastes levis*), using direct observations from an occupied submersible. Can. J. Fish. Aquat. Sci. 64:1795–1804.

Yoklavich, M., J. Reynolds, and D. Rosen.
2015. A comparative assessment of underwater visual survey tools: results of a workshop and user questionnaire. NOAA Tech. Memo. NMFS-SWFSC-547, 34 p.

National Marine Fisheries Service
NOAA

Fishery Bulletin
established in 1881

Spencer F. Baird
First U.S. Commissioner of Fisheries and founder of *Fishery Bulletin*

Comparison of a bottom longline survey and a bottom trawl survey for 2 groundfish species in the Gulf of Maine to evaluate habitat-related availability of large fish

W. David McElroy (contact author)[1]
Jessica Blaylock[2]
Gary R. Shepherd (retired)[3]
Christopher M. Legault[3]
Paul C. Nitschke[3]
Katherine A. Sosebee[3]

Email address for contact author: dave.mcelroy@noaa.gov

[1] Cooperative Research Branch
Northeast Fisheries Science Center
National Marine Fisheries Service, NOAA
166 Water Street
Woods Hole, Massachusetts 02543

[2] Fisheries Monitoring Operations Branch
Northeast Fisheries Science Center
National Marine Fisheries Service, NOAA
166 Water Street
Woods Hole, Massachusetts 02543

[3] Population Dynamics Branch
Northeast Fisheries Science Center
National Marine Fisheries Service, NOAA
166 Water Street
Woods Hole, Massachusetts 02543

Abstract—Understanding fishery-independent survey selectivity is fundamental to relating relative abundance indices to total population size. The selectivity of a survey in an assessment model represents a combination of gear selectivity and availability of fish to the gear. Concerns have been raised about possible bias in sampling of the bottom trawl survey (BTS) of the NOAA Northeast Fisheries Science Center (NEFSC) caused by the challenges associated with towing in rough-bottom habitat. These difficulties may affect the availability of some fish, such as large (≥100 cm in total length [TL]) Atlantic cod (*Gadus morhua*). To evaluate the potential presence of BTS habitat-related bias, we compared catches of Atlantic cod and white hake (*Urophycis tenuis*) from BTS sampling in the Gulf of Maine with catches from the NEFSC bottom longline survey, which focuses on rough-bottom habitats in the same region. Differences between survey catches were apparent for large white hake (≥90 cm TL), supporting the premise of availability differences between surveys for white hake and the assumption of dome-shaped selectivity for the BTS. In contrast, results for Atlantic cod did not support the hypothesis of habitat-related bias in sampling of the BTS, supporting continued use of asymptotic selectivity for Atlantic cod in the BTS.

Manuscript submitted 16 November 2020.
Manuscript accepted 22 September 2021.
Fish. Bull. 119:231–242 (2021).
Online publication date: 3 November 2021.
doi: 10.7755/FB.119.4.3

The views and opinions expressed or implied in this article are those of the author (or authors) and do not necessarily reflect the position of the National Marine Fisheries Service, NOAA.

Fishery-independent scientific surveys can be used to produce relative abundance indices for fish stocks, as well as demographic and biological data, that are free of biases associated with commercial catches, and as such they are an integral part of many stock assessments (Hilborn and Walters, 1992). In the northeastern United States, the NOAA Northeast Fisheries Science Center (NEFSC) uses data from its bottom trawl survey (BTS) to inform assessments of finfish and marine invertebrate stocks. The BTS was designed to sample the northwestern Atlantic Ocean between Cape Hatteras, North Carolina, and Nova Scotia, Canada (Grosslein[1]; Azarovitz, 1981) and follows a stratified random design with stratification determined by depth and geographic region (Stauffer, 2004). Stock assessments by the NEFSC assume that the BTS data can be used to produce representative estimates of the characteristics of each stock, including trends in abundance, distribution across habitats, sex structure, and size and age compositions.

The catch of a given species from a fishing event depends on a combination of 2 main factors: fish availability and gear selectivity (Crone et al.[2]; Maunder et al., 2014). Availability refers to the probability that the fish are in proximity to the gear and are vulnerable to possible capture. As such, availability is primarily determined by the spatial distribution of different sizes of fish relative to the distribution of survey sampling. Gear selectivity (hereafter referred to as *selectivity*) refers to the probability that a fish of a given length

[1] Grosslein, M. D. 1969. Groundfish survey methods. Bur. Commer. Fish., Woods Hole Lab. Ref. Doc. 69-02, 34 p. [Available from website.]

[2] Crone, P., M. Maunder, J. Valero, J. McDaniel, and B. Semmens (eds.). 2013. Selectivity: theory, estimation, and application in fishery stock assessment models. Workshop Ser. Rep. 1, 9 p. Cent. Adv. Popul. Assess. Methodol., La Jolla, CA.[Available from website.]

will be captured if the gear encounters it. Several factors can affect selectivity, including fishing gear characteristics and fish behavior (Crone et al.[2]). Selectivity influences the relationship between the size composition of the fish caught in the survey and the size composition of the population (Crone et al.[2]; Maunder et al., 2014). Therefore, understanding a fishery-independent survey's selectivity, along with its underlying assumptions, is fundamental to the interpretation of the resulting index of relative abundance and of its ability to track the population trends and cohorts. This selectivity can be modeled as curves describing the probability of capture at length and may have 4 general shapes: increasing, asymptotic, dome-shaped, and saddle-shaped (Sampson and Scott, 2012). The most common selectivity curve used in stock assessments is *flat-topped* selectivity, a form of asymptotic selectivity in which the proportion of a demographic group that is vulnerable to the gear increases over the lifespan of the group until all members are fully vulnerable (Cadrin et al., 2016).

The Atlantic cod (*Gadus morhua*), hereafter primarily referred to as *cod*, has historically been the focal species of the New England groundfish fishery. In the Gulf of Maine (GOM), commercial landings, mostly caught with trawl and gill nets, exceeded 10,000 metric tons (t) in the early 1990s. However, this level of exploitation has not been sustainable because population abundance has been in a downward trajectory since the 1980s (NEFSC, 2013a). According to the most recent assessment (NEFSC[3]), the GOM cod stock is overfished and experiencing overfishing with spawning stock biomass at 6–9% of the biomass target. In response to the stock condition, annual quotas have been reduced to <1000 t in recent years (GARFO[4]).

One of the consequences of continued overfishing has been the truncation of the size and age compositions of the GOM cod stock. Data from the NEFSC BTS, which has involved sampling in the area since 1963 (Grosslein[1]; Azarovitz, 1981), indicate that large cod (≥100 cm in total length [TL]) were consistently present from the onset of the survey until the mid-1980s, when they represented on average about 8% of the annual catches (Fig. 1) (data from the NEFSC 2019 GOM Atlantic cod stock assessment [NEFSC[3]], available from website). Since then, their encounter rate has gradually declined and they have become rare in BTS catches (<1% on average) over the past 10 years. The commercial landings indicate a consistent but low presence of cod ≥100 cm TL, typically composing 1–2% of the annual landings since the early 1980s (Fig. 1). In addition to a reduction in abundance of fish at this size range, there has been a truncation of the age structure of cod caught in the BTS and in the commercial fishery beyond age 8, despite a potential maximum age greater than 20 years (NEFSC[3]).

The white hake (*Urophycis tenuis*) is another important groundfish species in the GOM with recent annual commercial landings around 2000 t, predominantly caught with trawl gear. The stock was considered overexploited in 2008 (NEFSC, 2008) and is currently overfished (with biomass at less than half of the biomass at maximum sustainable yield), although fishing mortality has been reduced to a level below the threshold for overfishing (NEFSC[3]). The commercial fishery routinely encounters white hake older than 9 years (NEFSC, 2013b; NEFSC[3]), indicating that mature individuals are present in the population. However, large white hake (≥90 cm TL) have been uncommon in the size composition of the BTS since the beginning of the time series in 1963 (Fig. 1) (data from the NEFSC 2019 white hake stock assessment [NEFSC[3]], available from website).

Consequently, the recent stock assessment applied a dome-shaped selectivity pattern at age for indices of abundance and biomass derived from data collected during the spring and fall BTS (NEFSC, 2013b, 2017; NEFSC[3]); this selectivity pattern assumes that the largest or oldest members of a demographic group are not fully vulnerable to survey gear because of gear avoidance (Sampson and Scott, 2012; Cadrin et al., 2016). In contrast, white hake ≥90 cm TL have composed a significant portion of the commercial landings since the mid-1990s, with at least 6% of landings exceeding 90 cm TL in most years since 2000 (Fig. 1). The difference in commercial versus survey selectivity is presumably a result of commercial fleets targeting fishing locations and of different tow speeds and durations (K. Sosebee, personal commun.).

The truncated size (and age) distribution of adult cod as well as a decline in weight at age for fish at ages 3 and above have been a concern for fishery managers for some time (NEFSC, 2008, 2017). Previous discussions and analyses considered several possible reasons for the truncation, such as the presence of fixed gears (e.g., lobster gear) in inshore areas that would make potential cod habitat unavailable for sampling during the BTS or decreased selectivity of large fish in the fishery; however, no supporting evidence was found (NEFSC, 2013a). An alternative explanation may be linked to the history of the GOM cod stock. A significant decline in abundance, as experienced by this stock, can affect the spatial distribution of a stock. Range contraction and density-dependent habitat selection can occur in depleted stocks (Holt, 1987; Lawton, 1993), and both processes have been documented for cod (Swain and Wade, 1993; Hutchings and Reynolds, 2004; Tamdrari et al., 2010). Other factors, such as prey distribution and climate change, may also influence the spatial distribution of groundfish in general and of cod in particular (Nye et al., 2009; Ames and Lichter, 2013; Orio et al., 2019). Given the combined circumstances of overfishing and changes in environmental conditions in the ecosystem of the GOM (NEFSC[5]), it is possible that the spatial

[3] NEFSC (Northeast Fisheries Science Center). In preparation. Operational assessment of 14 Northeast groundfish stocks, updated through 2018. Northeast Fish. Sci. Cent. Ref. Doc. [Available from website.]

[4] GARFO (Greater Atlantic Regional Fisheries Office). 2019. Northeast multispecies (groundfish) fishing year 2019 commercial regulations. 18 July 2019. [Available from website.]

[5] NEFSC (Northeast Fisheries Science Center). 2019. State of the ecosystem 2019: New England, 31 p. Report to the New England Fisheries Management Council. [Available from website.]

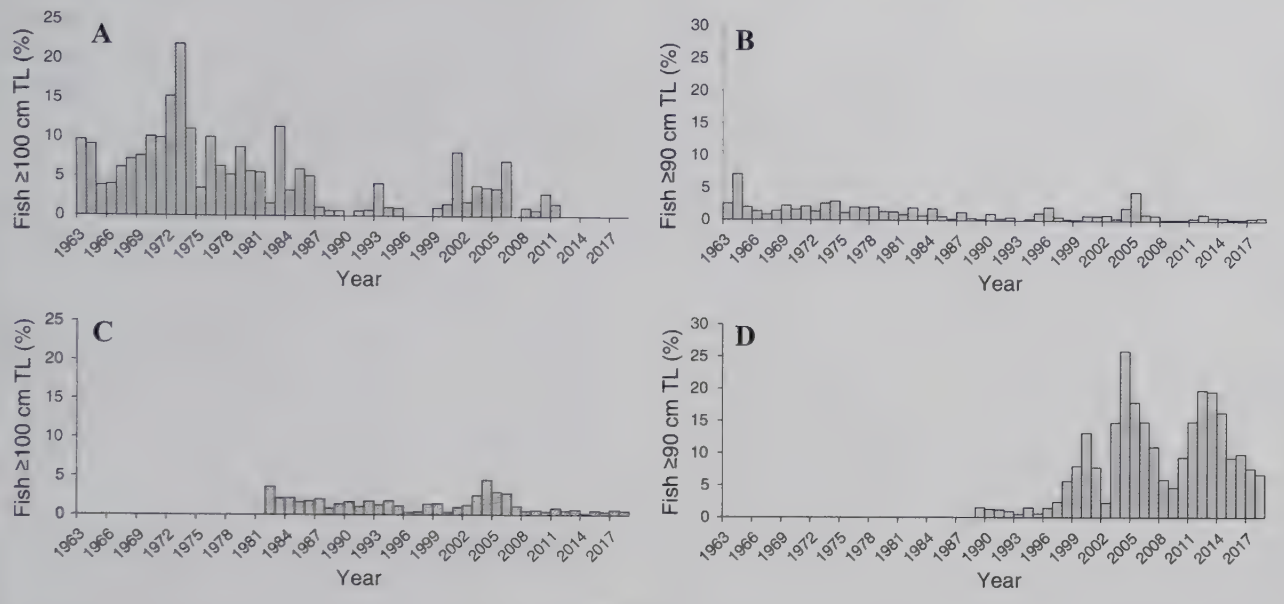

Figure 1

Percentage of large Atlantic cod (*Gadus morhua*) (≥100 cm in total length [TL]) (left panels) and white hake (*Urophycis tenuis*) (≥90 cm TL) (right panels) captured in the Gulf of Maine (**A** and **B**) in the NOAA Northeast Fisheries Science Center bottom trawl survey (BTS) during 1963–2018 and (**C** and **D**) in the commercial fishery, based on commercial landings (CL) data used in the stock assessments, during 1982–2018 for Atlantic cod and during 1989–2018 for white hake. Because of changes over time in size regulations of the fishery for the Gulf of Maine Atlantic cod stock, the percentages represented are relative to the total number of individuals ≥50 cm TL. The percentages of white hake are relative to fish of all sizes because there is no size limit for this stock.

distribution of cod has changed over the last 50 years and that some portion of the stock (e.g., large cod, ≥100 cm TL) has shifted to habitat that cannot consistently be sampled as part of the BTS.

Although the BTS research vessel has an otter trawl outfitted with large roller (*rockhopper*) gear 40.6 cm in diameter (Politis et al.[6]) to accommodate the variety of bottom habitat types in the sampling area, towing of the trawl gear in highly structured habitat is limited on the basis of the likelihood of the gear getting stuck on the rugged bottom. Consequently, organisms that inhabit rough-bottom habitats are less available to BTS sampling. There is a concern, particularly among industry stakeholders, that large cod may have a reduced distribution and are limited to hard-bottom habitats that are difficult to sample with mobile trawl gear. If large adult cod have moved to hard-bottom locations, it would result in a change in their vulnerability to the survey gear and could explain the truncation of the size distribution evident in the BTS data. Although adult cod are known to inhabit areas with substrates of sand, gravel, or mud, they do have an affinity for rocky bottoms, and their distribution among habitats can vary among seasons and sizes (Scott, 1982; Fahay et al., 1999). If the spatial distribution of large cod in the GOM has changed, it could indicate that BTS selectivity for cod may be more dome-shaped, like the selectivity for white hake, rather than flat-topped, which is the type of selectivity used in the stock assessment for cod (NEFSC, 2013a, 2017). The consequences of incorrectly specifying a flat-topped selectivity curve when a dome-shaped curve is warranted would be an underestimation of stock abundance and biomass.

In 2014, the NEFSC started a bottom longline survey (LLS) to address concerns about the presence of fish species in rough-bottom habitat in the GOM that may experience low encounter rates with the trawl survey. The LLS was designed following a stratified random design similar to that of the BTS, but the LLS survey area was further stratified by bottom type, with classification of smooth and rough bottom (McElroy et al., 2019). Because of the concentrated effort of the LLS in rough-bottom habitats, data from the LLS provide a perspective on availability of groundfish in the GOM complementary to the BTS.

With respect to cod, the LLS stratification design offers an opportunity to evaluate the presence of large cod in the rough-bottom areas of the GOM. If data from the LLS indicate that large cod are more prevalent in the rough-bottom habitats than across the BTS sampling area, it would provide support for considering dome-shaped selectivity for the BTS in the GOM cod stock assessment. On the other hand, if large cod are not caught at a higher rate

[6] Politis, P. J., J. K. Galbraith, P. Kostovick, and R. W. Brown. 2014. Northeast Fisheries Science Center bottom trawl survey protocols for the NOAA ship *Henry B. Bigelow*. Northeast Fish. Sci. Cent. Ref. Doc. 14-06, 138 p. [Available from website.]

in the LLS compared with the rate of capture in the BTS, it would be unclear whether it is due to low selectivity in the longline gear or simply due to the absence (i.e., low availability) of these fish. To address this question, we used white hake as a control for the selectivity of the longline gear. Atlantic cod and white hake, the latter of which has an accepted dome-shaped selectivity for the BTS, are generally similar gadoids in size (both can exceed 100 cm TL), prey types, and prey size (Scharf et al., 2000). Therefore, we would expect both species to have comparable probability of capture with the LLS gear. In other words, if large white hake (≥90 cm TL) are caught in the LLS, we would expect large cod to be caught as well, if these fish are present. Conversely, if large white hake are caught in the LLS but large cod are not, we would deduce that large cod are not present in the area. This approach offers an avenue to examine whether data from the LLS supports the presence of large cod in the rough-bottom habitat of the GOM.

The objectives of this study were to evaluate the relative size distributions of Atlantic cod and white hake in the LLS and BTS and to test the hypothesis that availability by size is different between the predominantly smooth-bottom habitats sampled with bottom trawl gear and the rough-bottom habitats sampled with longline gear. Specifically, we will focus on the upper end of the size distributions of the LLS and BTS catches to explore whether they differ for each species. Depending on the results, as explained previously, our findings may indicate the need for reconsideration of the selectivity curve used for the BTS in the GOM Atlantic cod stock assessment. In addition, results of our analysis can also validate the current BTS selectivity assumed for the white hake assessment.

Materials and methods

The NEFSC has been conducting the BTS in the fall since 1963 and in the spring since 1968 (Azarovitz, 1981). This survey follows a stratified random sampling design, with stratification by depth and region, for selection of sampling stations in federal waters on the continental shelf from Cape Hatteras to the Scotian Shelf (Stauffer, 2004; Politis et al.[6]). Stations are randomly selected within each stratum prior to each survey cruise, with the number of stations selected per stratum being proportional to the area of the stratum, typically with a minimum of 3 stations per stratum (Politis et al.[6]). Although several factors are considered before a tow begins (e.g., presence of shipwrecks or fixed gear and strength of bottom current), bottom type does not specifically affect the determination of a tow location. Since 2009, the NEFSC has used the NOAA Ship *Henry B. Bigelow* as the primary research vessel for the BTS. The NOAA Ship *Pisces* was used in the fall of 2017; however, because the 2 vessels are the same size and class it is assumed that changes in vessel did not affect selectivity. Each vessel used a 4-seam, 3-bridle bottom trawl with a rockhopper sweep (Politis et al.[6]) that can be used in a variety of habitat types. At each station, data on the abundance, biomass, and size distribution of fish were collected for each species. Fish TL was measured (to the nearest 0.5 cm) by using digital fish measuring boards.

The LLS, which is an industry-based survey implemented by the NEFSC (McElroy et al., 2019), has occurred concurrently with the spring and fall BTS since 2014. The further stratification of sampling by bottom type for the LLS is based on rugosity. Bottom type was defined as either smooth or rough, with rough-bottom habitats having a terrain ruggedness index value (Riley et al., 1999) greater than the 70th percentile within each stratum (McElroy et al., 2019). With the participation of 2 commercial fishing vessels, the sampling of the LLS occurs between 42.0°N and 43.5°N, an area that encompasses all or portions of 6 BTS strata (Fig. 2). Sampling density is higher in the LLS than in the BTS, and stations are more heavily allocated to rough-bottom substrata in the LLS (Politis et al.[6]; McElroy et al., 2019). In the current allocation of stations sampled in the LLS, 84% of stations are in rough-bottom strata, and the sampling in the BTS when stratified post hoc by using the LLS strata includes 20–35% of stations in the rough-bottom strata per year (Suppl. Table) (online only).

Tub-trawl longlines are used for the LLS with gear similar to those used commercially for groundfish species, such as cod and white hake, in the region. The longline gear is deployed with 1000 12/0 semicircle E-Z baiter hooks[7] (O. Mustad and Son AS, Gjøvik, Norway) on 38-cm gangions that are baited with squid on a 1.85-km (1-nmi) mainline and soaked for 2 h across the slack tide (McElroy et al., 2019). The hook size and soak time were chosen to be relatively comparable with some commercial groundfish operations, and the soak time was standardized across the slack tide to get a portion of both sides of a tide. The mainline length was chosen to be consistent with the mean tow distance of the BTS. At each station, data on the abundance, biomass, and size distribution of fish were collected for each species. Fish TL was measured (to the nearest 0.5 cm) by using digital fish measuring boards.

Length frequencies of cod and white hake caught in the LLS and BTS were generated by using TL by season for the period 2014–2018. For the BTS, data from all stations meeting gear and operational acceptance criteria (Politis et al.[6]) were included from stock assessment strata sets for each species: offshore strata 26–30 and 36–40 for the GOM cod stock (NEFSC, 2013a) and offshore strata 21–30 and 36–40 for the white hake stock (NEFSC, 2013b) (Fig. 2). Use of stock assessment strata for the BTS reflects the intent of the analysis to relate the findings about availability of cod and white hake in the rough-bottom habitat of the GOM based on data from the LLS to the respective stocks as a whole, rather than simply comparing BTS and LLS results in the overlapping area. For the LLS, data from all stations that met gear and operational acceptance criteria (McElroy et al., 2019) were

[7] Mention of trade names or commercial companies is for identification purposes only and does not imply endorsement by the National Marine Fisheries Service, NOAA.

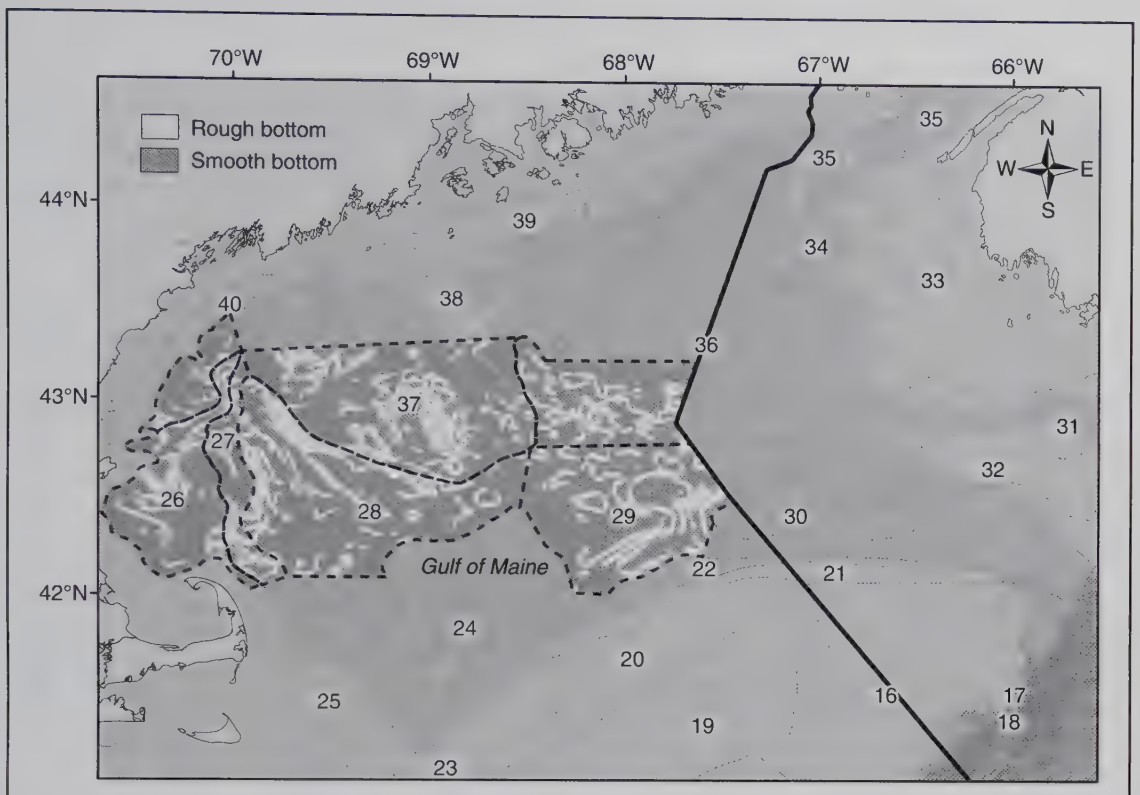

Figure 2

A map of the strata of the bottom longline survey (LLS) (dashed black lines) and offshore strata of the bottom trawl survey (BTS) (thin gray lines, numbered in the center). The LLS strata include all of BTS strata 26, 27, and 37 and portions of BTS strata 28, 29, and 36. The thick black line indicates the boundary between the exclusive economic zones of the United States and Canada. Both surveys are implemented by the NOAA Northeast Fisheries Science Center following a stratified random design, with stratification determined by depth and geographic region in the BTS and by depth, geographic region, and bottom type (rough or smooth) in the LLS. Sources for base map: Esri, Garmin, GEBCO, NOAA NGDC, and other contributors.

included from LLS strata that were located on rough bottom where towing is difficult. Stations of the LLS on smooth bottom were omitted because of concerns about low catchability due to poor bait retention on soft bottom (McElroy et al., 2019).

For each species, year, and season, we first calculated estimates of aggregate (i.e., all lengths combined) stratified mean abundance indices (for the BTS, see Cochran, 1977; for the LLS, see McElroy et al., 2019). Second, we used the length frequencies from the raw data to derive estimates of stratified mean abundance indices at length (i.e., mean numbers at each length). The indices of abundance at length were then standardized to produce estimates of the proportion of numbers at length as a representation of length distributions. The Bhattacharyya coefficient (BC) (Bhattacharyya, 1943) was calculated as a measure of overlap between the length–frequency distributions of the 2 surveys, for each species and season. This coefficient provides a robust measure of relative similarity in distribution ranging from 0.0, indicating no overlap, to 1.0, indicating identical distributions (Winner et al., 2018).

Results

Sampling coverage of the study area was comparable between the 2 gear types. The LLS data sets used in analysis included data from 33–38 stations in each season in each year, 349 stations in total (Table 1). In 2017 and 2018, modifications to the method of station allocation for the LLS resulted in increased sampling in rough-bottom habitat (McElroy et al., 2019). The BTS data sets used in analysis included at least 50 stations in the spring and fall for GOM Atlantic cod and white hake (Table 1) during 2014–2017, for a total of 550 stations sampled. Because of operational difficulties, fewer stations were sampled in the BTS in 2018, resulting in a reduced sample size.

On average, the species of interest were adequately represented in the catches of both the LLS and BTS. During the LLS, catches of cod occurred at 73% of stations in the spring, and at 70% of stations in the fall, yielding lengths of 1603 individuals in the spring and of 1330 individuals in the fall (Table 1). For white hake, the rate of encounter in the LLS averaged 50% in the spring and 74% in the fall, producing lengths of 882 individuals in the spring

Table 1

The number of stations, number of stations with catch, and number of sampled Atlantic cod (*Gadus morhua*) and white hake (*Urophycis tenuis*) for which lengths were recorded in the Gulf of Maine as part of the NOAA Northeast Fisheries Science Center bottom longline survey (LLS) and bottom trawl survey (BTS) during 2014–2018, by season and year. Data were selected from strata with rough bottom for the LLS and from strata used in the stock assessments for these species for the BTS (for strata used in the assessments, see NEFSC, 2013a, 2013b).

			LLS			BTS		
Species	Season	Year	No. of stations sampled	No. of stations with catch	No. of fish with lengths recorded	No. of stations sampled	No. of stations with catch	No. of fish with lengths recorded
Atlantic cod	Spring	2014	33	26	285	61	19	112
		2015	33	26	346	65	29	696
		2016	33	22	401	66	32	299
		2017	38	28	251	52	27	143
		2018	38	25	320	30	11	48
		Total			1603			1298
	Fall	2014	33	23	184	58	18	215
		2015	33	26	333	66	20	55
		2016	33	28	252	65	16	199
		2017	37	23	245	50	20	121
		2018	38	20	316	37	8	134
		Total			1330			724
White hake	Spring	2014	33	11	48	82	51	465
		2015	33	14	129	91	61	599
		2016	33	15	160	91	75	718
		2017	38	24	329	77	48	583
		2018	38	24	216	47	36	379
		Total			882			2744
	Fall	2014	33	22	267	82	68	578
		2015	33	24	264	89	78	1175
		2016	33	27	302	91	76	1022
		2017	37	27	337	68	56	709
		2018	38	28	556	60	47	453
		Total			1726			3937

and of 1726 individuals in the fall. Atlantic cod were present in sampling of the BTS at 43% and 30% of stations in the spring and fall, respectively (Table 1). There was a difference between seasons in sample size in the BTS for cod, with lengths of 1298 individuals measured in the spring and of 724 individuals measured in the fall. White hake were more prevalent than cod in catches of the BTS, with white hake caught at 70% of the stations sampled in the spring and at 83% of the stations sampled in the fall. Lengths were collected from 2744 and 3937 white hake sampled during the BTS in the spring and fall, respectively. The number of lengths recorded during the BTS were low for both species in 2018 compared with in 2014–2017, especially for cod (Table 1).

Overall, the size distribution of cod captured in the LLS was similar to that in the BTS (Table 2, Fig. 3). Mean length of cod in the BTS was 50.7 cm TL (standard deviation [SD] 15.2; range: 15–93 cm TL) in the spring and 53.4 cm TL (SD 23.0; range: 13–93 cm TL) in the fall; whereas, the mean length of cod in the LLS was 50.0 cm TL (SD 10.5; range: 24–91 cm TL) in the spring and 58.9 cm TL (SD 16.4; range: 26–103 cm TL) in the fall. Length distributions for cod from both surveys were very comparable, particularly for cod over 40 cm TL (Fig. 3). The distribution for cod caught in the BTS in spring was characterized as bimodal, split around the length of 25 cm TL, with fish below that size not fully represented. The distribution for cod caught in the BTS in fall was also bimodal, split around the length of 35 cm TL, with a large contribution from fish <35 cm TL. The size distribution for cod caught in the LLS in both seasons combined was unimodal with limited representation of fish <40 cm TL.

Although there were annual variations among years for both surveys (Table 2, Suppl. Figs. 1 and 2 [online only]), distributions of cod length in the spring generally had high overlap from 40 to 70 cm TL, and the overlap of distributions in the fall was similar but with slightly higher proportions of fish with lengths of 40–65 cm TL in the LLS. The proportion of cod ≥70 cm TL had high similarity between the surveys in the fall, with the exception of a few fish in the LLS that were ≥95 cm TL. The distributions of fish caught in the BTS and LLS largely overlapped in

Table 2

Percentage of the stratified mean abundance indices by size group, season, and year, for the Atlantic cod (*Gadus morhua*) and white hake (*Urophycis tenuis*) sampled in the Gulf of Maine in 2014–2018 during the NOAA Northeast Fisheries Science Center bottom longline survey (LLS) and bottom trawl survey (BTS). Data were selected from strata with rough bottom for the LLS and from strata used in the stock assessments for these species for the BTS (for strata used in the assessments, see NEFSC, 2013a, 2013b). TL=total length.

			LLS				BTS			
Species	Season	Year	<80 cm TL	80–89 cm TL	90–99 cm TL	≥100 cm TL	<80 cm TL	80–89 cm TL	90–99 cm TL	≥100 cm TL
Atlantic cod	Spring	2014	99.8	0.2	0.0	0.0	95.8	1.7	2.5	0.0
		2015	100.0	0.0	0.0	0.0	99.3	0.7	0.0	0.0
		2016	99.7	0.3	0.0	0.0	98.5	1.5	0.0	0.0
		2017	98.9	1.1	0.0	0.0	91.6	7.0	1.4	0.0
		2018	97.9	1.8	0.3	0.0	91.4	7.3	1.3	0.0
	Fall	2014	97.9	1.5	0.6	0.0	97.5	2.5	0.0	0.0
		2015	92.5	6.3	0.8	0.4	83.4	15.3	1.3	0.0
		2016	94.4	5.6	0.0	0.0	93.3	5.3	1.4	0.0
		2017	96.7	2.3	1.0	0.0	90.1	8.6	1.3	0.0
		2018	86.7	10.7	2.3	0.3	97.6	2.4	0.0	0.0
White hake	Spring	2014	87.2	6.4	6.5	0.0	97.2	1.9	0.4	0.5
		2015	96.4	2.4	1.2	0.0	99.4	0.4	0.2	0.0
		2016	98.7	0.0	0.6	0.6	99.4	0.4	0.1	0.0
		2017	98.7	1.3	0.0	0.0	98.2	1.2	0.5	0.2
		2018	94.1	4.4	0.9	0.6	98.4	1.5	0.0	0.1
	Fall	2014	85.8	8.2	4.0	2.0	97.8	2.0	0.0	0.2
		2015	95.1	2.7	1.2	1.0	99.1	0.5	0.1	0.2
		2016	96.4	1.7	0.7	1.2	99.4	0.2	0.3	0.0
		2017	70.3	11.3	9.2	9.2	99.1	0.8	0.0	0.1
		2018	93.3	4.7	1.1	0.9	96.8	0.6	2.3	0.2

spring with occasional higher proportions of cod ≥70 cm TL in the catches of the BTS. The biggest differences between the surveys were observed in catches of cod with sizes of 15–38 cm TL. Atlantic cod <35 cm TL were regularly represented in BTS catches but were very limited in LLS catches. This difference was particularly evident in the fall, when cod at sizes of 25–38 cm TL were common in catches of the BTS (Fig. 3). Cod ≥80 cm TL were uncommon (<10% of the sampled fish; Table 2, Fig. 3) in both surveys (except for the LLS in fall 2018 and for the BTS in fall 2015) but were more frequent in the fall than in the spring for both surveys. Cod ≥90 cm TL were rare (<3% of the sampled fish) in most surveys and occurred more often in the fall. Only 2 cod ≥100 cm TL were captured in either survey during the 5 years of data examined.

The BC, used for the comparisons of annual length distributions of Atlantic cod (Table 3) between the BTS and LLS, indicates variable but high overlap (BC=0.77–0.91) in the spring in all years except 2018 (BC=0.50). The BC indicates that overlap in distributions of the 2 surveys was generally less in the fall than in the spring but still relatively high in most years (BC=0.62–0.87) except, again, in 2018 (BC=0.55). The BCs for surveys in 2016 are the most consistent across the 2 seasons (0.90 and 0.87 for spring and fall, respectively) and among the highest observed. The BCs for distributions combined across the period 2014–2018 indicate that overlap was high in both spring (BC=0.96) and fall (BC=0.89). The distributions for combined years were more complete than the distributions for individual years because the former were based on data from a larger sample than that for each individual year.

For white hake, length distributions aggregated across years were dissimilar between the LLS and BTS (Table 2, Fig. 3). White hake in the spring LLS were most commonly 40–75 cm TL (Fig. 3), and in the fall LLS the peak in the length distribution was typically 55–80 cm TL. In contrast, the peak abundance in the BTS was observed for fish with lengths around 32 cm TL in the spring, with a couple of peaks in the catches at sizes around 45 and 55 cm TL (Fig. 3). In catches of white hake in the fall BTS, the most prevalent sizes were around 35–50 cm, with secondary peaks of abundance for fish at 20–30 cm TL and 60–65 cm TL (Fig. 3). Recent recruits, at sizes around 10 cm TL, occurred in the fall BTS, and white hake <40 cm TL were rarely observed in LLS catches. White hake ≥80 cm TL were regularly observed at a low frequency in the spring LLS, but they were common in the catches of the fall LLS (Table 2, Suppl. Figs. 1 and 2 [online only]). In contrast, white hake ≥80 cm TL, and particularly those ≥90 cm TL, were infrequent in the BTS across both seasons relative to the LLS.

White hake ≥90 cm TL composed 2–18% of the fish sampled in the LLS among years in the fall, and although such

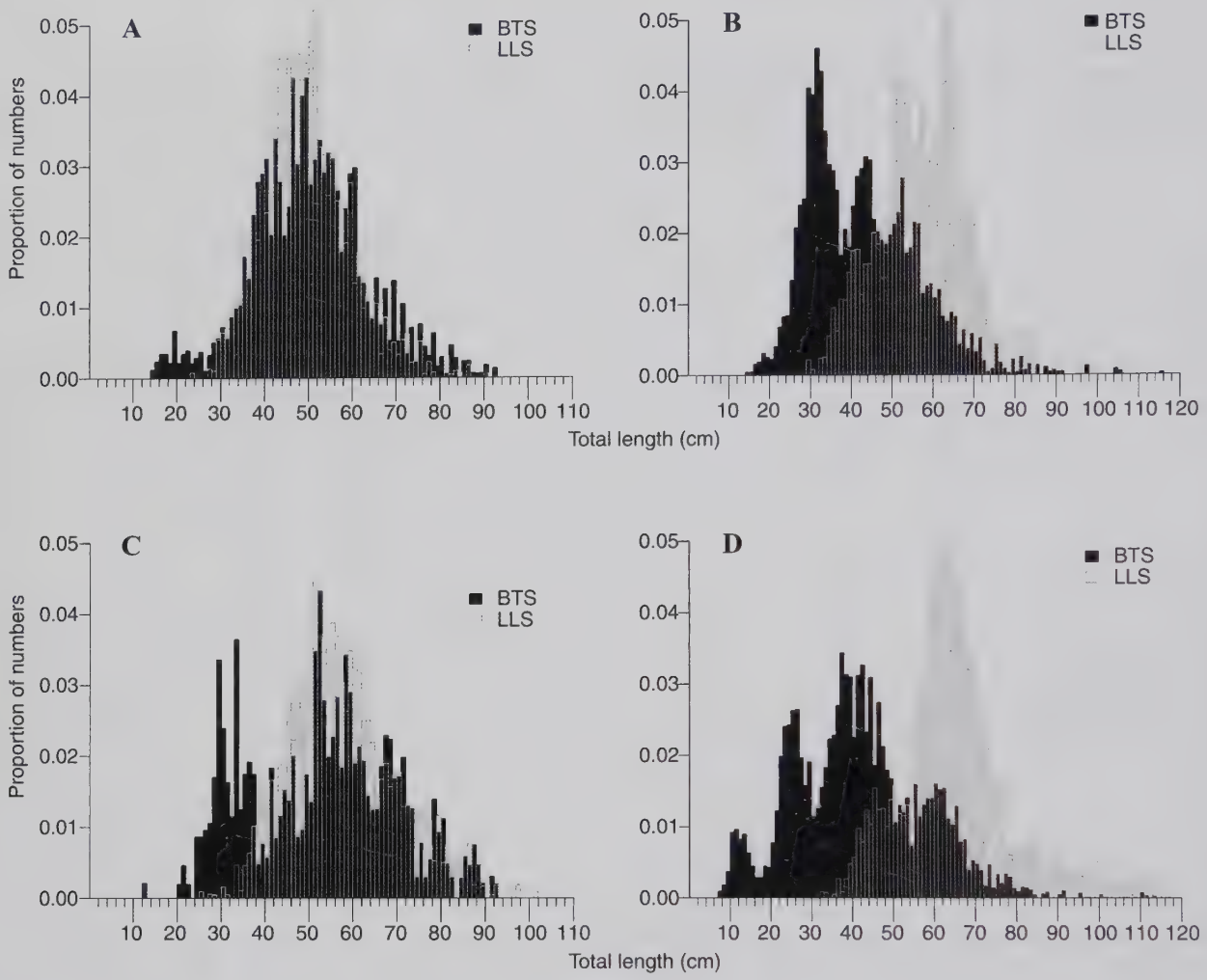

Figure 3

Length–frequency distributions of Atlantic cod (*Gadus morhua*) (left panels) and white hake (*Urophycis tenuis*) (right panels) captured in the Gulf of Maine in the NOAA Northeast Fisheries Science Center bottom trawl survey (BTS, black bars) and bottom longline survey (LLS, open bars) during (**A** and **B**) the spring and (**C** and **D**) the fall for the years 2014–2018 combined. Proportions at length were derived from indices of stratified mean abundance at length for each survey.

white hake were present in the spring they were less common (0–7% of the sampled fish; Table 2). White hake ≥100 cm TL were rarely captured in the spring LLS, and they were caught in low numbers (1–2% of the sampled fish) in the fall, with the exception of some high catches in fall 2017 (9.2% of the sampled fish; Table 2). The interannual variation of the LLS catch was more evident in the fall than in the spring, with higher catches of white hake ≥80 cm TL in 2014 (Suppl. Figs. 1B and 2B) (online only) and particularly in 2017 (Suppl. Figs. 1H and 2H) (online only). The catch of white hake ≥80 cm TL in the BTS was limited in both seasons (averaging 1.5% of the catch in the spring and 1.6% of the catch in the fall), and fish ≥90 cm TL were rare in all seasons and years examined (Table 2, Suppl. Figs. 1 and 2 [online only]).

The BC for the comparison of the BTS and LLS annual length distributions of white hake (Table 3) indicates lower overlap than was observed for cod. The BCs for white hake in spring surveys (BC=0.53–0.84) indicate that overlap in distributions was usually higher and more variable than that for the fall surveys (BC=0.50–0.67). The finding of greater variation in spring is consistent with the prevalence of white hake at more stations in the fall surveys than in the spring surveys (Table 1). The BC for the distributions combined across 2014–2018 is 0.77 for the spring surveys and only 0.65 for the fall surveys. The distributions for combined years of white hake catches were based on data from a larger sample size, filled in gaps, and decreased the differences by providing a more complete distribution than that for individual years, as was found with cod. However, the differences in distributions between the LLS and BTS were still greater for white hake than for cod.

Table 3

Bhattacharyya coefficients (BCs) representing the degree of overlap in length distributions between the NOAA Northeast Fisheries Science Center bottom longline survey (LLS) and bottom trawl survey (BTS) for Atlantic cod (*Gadus morhua*) and white hake (*Urophycis tenuis*) sampled in the Gulf of Maine during 2014–2018 by season and year and for all years combined. Data were selected from strata with rough bottom for the LLS and from strata used in the stock assessments for these species for the BTS (for strata used in the assessments, see NEFSC, 2013a, 2013b). The BC may range from 0.00 (no overlap) to 1.00 (identical distributions).

	Atlantic cod		White hake	
Year	Spring	Fall	Spring	Fall
2014	0.86	0.62	0.53	0.58
2015	0.91	0.75	0.64	0.58
2016	0.90	0.87	0.73	0.67
2017	0.77	0.83	0.84	0.60
2018	0.50	0.55	0.63	0.50
2014–2018	0.96	0.89	0.77	0.65

Discussion

The intent of this study was to evaluate the presence of large cod (≥100 cm TL) in the rough-bottom habitat of the GOM, as indicated by a comparison of catches of cod and white hake in the LLS and BTS conducted by the NEFSC in 2014–2018. Possible aggregation of large cod in rough-bottom habitat due to presumed density-dependent range contraction could warrant reconsideration of the flat-topped BTS gear selectivity currently used in the GOM cod stock assessment. Using white hake as a control, we evaluated whether the LLS and BTS data support use of a dome-shaped selectivity curve for cod in the BTS by comparing length distributions of the 2 species in each survey. Our results indicate that large cod were not more prevalent in the rough-bottom habitat sampled for the LLS than in the BTS sampling area; therefore, no evidence was found to support a dome-shaped selectivity pattern for cod in the BTS. On the other hand, our approach provided a unique opportunity for validation of the selectivity curve used for white hake. Large white hake (≥90 cm TL) were sparse in the BTS but present in the LLS, supporting the continued use of a dome-shaped selectivity for the BTS in the assessment for this species.

Patterns of the size distributions for the 2 gadoid species in this study are distinct between the LLS and BTS, which sample different compositions of habitats. The largest divergence in the distributions for both species occurred at small sizes (<35 cm TL), which were present in trawl catches but poorly represented in longline catches. These differences were expected given the contrasting capture mechanisms of each gear. In particular, hook and bait size, as well as mouth gape, swimming ability, and other behaviors, limit the longline selectivity for small fish, and trawls capture most fish that cannot outswim or pass through the net (Engås et al., 1996; Millar and Fryer, 1999). The efficiency of trawl gear at catching small fish increases when a lined codend is used, and the codend of the trawl net used in the BTS is lined. Cod at the upper end of the size range had similar distributions between the 2 surveys, with few large cod observed in catches with either gear. In contrast, large white hake were more abundant in the LLS than in the BTS. This pattern was relatively consistent among years despite some interannual and seasonal variation. Both gear types could have additional selectivity characteristics that contribute to the size patterns observed. However, the presence of large white hake in the LLS, which is concentrated on rough-bottom habitats, confirms that this survey is capable of catching large gadoids that are not selected by trawl gear in the areas sampled for the BTS. Therefore, given the comparable low catches of large cod in both surveys, our results indicate that BTS gear selectivity or ineffective sampling in rough-bottom habitat are not likely the cause of the absence of large cod in the BTS in recent years.

Commercial landings data support the observation of the absence of large cod in BTS catches in the GOM over a 40-year time frame. Big cod were infrequent throughout the period in both the BTS and commercial landings data sets, and when the occurrence of big fish increased, the length frequencies were still comparable between BTS catches and landings. Although the proportion of large white hake in commercial landings has varied over the past 20 years, these fish nevertheless represented a much greater proportion of the annual commercial landings than of the BTS catches in the same period. The size of fish in commercial landings for both species could be influenced by changes in market demand, fishing costs, and regulatory changes. The general expectation is that the market demand for large cod is always high for this quintessential New England seafood. Regulatory rules and low quotas could have been disincentives for cod landings in recent years and have contributed to the paucity of large cod in the commercial landings; however, these market and regulatory factors would not account for the lack of large cod in the BTS time series. In contrast, catches of large white hake have been consistently low across the BTS time series, and their proportional occurrence in the commercial landings is very high. These differences in the occurrence of large white hake have provided some of the justification for the application of a dome-shaped selectivity to the BTS time series in the assessment for white hake (NEFSC, 2013b). Although neither gear type provides complete selectivity across all fish lengths, data from the LLS provide complementary and independent validation that habitat-related availability to the BTS is likely for large white hake.

The size distribution of white hake in the LLS may reflect preference for rough-bottom habitat, particularly for large individuals, and fine-scale differences in station locations relative to rough-bottom habitat. Studies characterizing the habitat of white hake have been limited, but

results from most of the studies indicate a preference for mud, fine-grained sand, or soft bottom (Scott, 1982; Chang et al., 1999). However, these studies relied upon fishery-independent trawl data. Ames (2012) looked at historical seasonal movements based on interviews with fishermen and described fishing grounds not only as mostly mud bottom but also as around the ledges, rises, and banks of the northern GOM. Habitat and distribution of white hake changes with life stage (Macdonald et al., 1984; Chang et al., 1999), possibly contributing to some of the observed differences in catch composition for white hake between gears. Differences in survey catches could also be driven by behavioral factors that influence availability of the large white hake to different survey gears or by an interaction between behavior, habitat, and the response to fishing gear presence. The use of baited hooks may attract large white hake that avoid trawls behaviorally or have a habitat preference for structure.

Another possibility is that small-scale habitat variation (e.g., a few boulders or a wreck in a muddy area) may facilitate trawl gear avoidance. In a study in the Gulf of St. Lawrence, white hake were captured in channel bottoms, but the highest rate of capture was on deepwater slopes (Nozères et al.[8]). This preference for slope habitat is consistent with what was observed in the LLS, which has a bottom-type stratification derived from depth data and includes many of the sloped edges of the ledges, banks, and other structured habitats in the GOM (McElroy et al., 2019). The actual bottom type can vary greatly because the LLS classification is broad within the 2 categories of rough and smooth. The results of our study indicate at least some presence proximal to structured or slope habitats in the deeper waters of the GOM for large white hake, a habitat preference that may influence their availability to the BTS.

Habitat preference of Atlantic cod may have less influence on their availability to longline gear compared with their availability to bottom trawl gear. Cod are known for their preference for sand, gravel, rocks, ledges, slopes, and wrecks (Scott, 1982; Fahay et al., 1999; Wieland et al., 2009). However, they are also captured on other bottom types, such as mud (Macdonald et al., 1984; Wieland et al., 2009). Scott (1982) found higher concentrations of cod on sand and gravel bottoms on the Scotian Shelf but reported there was not a high preference. In a study in which multiple gear types were used, Wieland et al. (2009) found that cod prefer rough-bottom habitat, with some variation by season and gear type potentially influenced by seasonal movements. The authors also found no relationship between bottom type and cod size but cautioned that the study could not explore other factors, such as current strength or prey distribution, that could affect cod distribution. The results of the analysis presented here between the BTS and LLS indicate that there was no difference in the size composition for the upper end of the size distribution. Cod appear to lack a size-related habitat preference sufficient enough to limit their availability to the BTS or to limit the survey's ability to capture the full size range of the individuals present. It remains possible that size-related habitat preference is a function of population density and patterns observed now reflect the current low abundance. It seems reasonable that under conditions of reduced abundance, cod would be expected to concentrate in their preferred habitats (e.g., rocky habitat), but this notion was not supported by the catches of the LLS.

The LLS is an example of successful cooperative research that can benefit assessments and management. Although the LLS time series is short compared with that of the BTS at this time, it will be long enough in the coming years to be evaluated within a stock assessment model. Analysis of data from the LLS may result in additional indices of abundance for a few of the common fish species in the region. The emphasis on more structured habitat will particularly benefit species strongly associated with those habitats, including a number of data-poor species and those considered species of concern by the National Marine Fisheries Service, such as cusk (*Brosme brosme*) and thorny skate (*Amblyraja radiata*), which are both well represented in LLS catches. This fixed-gear survey represents a supplemental source of biological and demographic information that can be examined in conjunction with data from the BTS to gain a deeper understanding of the status of fish communities in the GOM and to advance research and management. Greater diversity of comparable surveys in which different gear types are used also provides data for a broader suite of species, further benefiting ecosystem-based management approaches.

Conclusions

The choice of selectivity for a fishery-independent survey is critical to a stock assessment because it can influence model outputs and subsequent management decisions. The results of the analysis in this study provide a unique exploration of selectivity patterns for 2 groundfish species through a comparison of catches from 2 overlapping surveys with different gear types and sampling stratifications. Our results indicate that the size selectivity for white hake differs between the 2 surveys, with large white hake readily observed in the LLS but not well represented in BTS catches. These fish may not be available to the BTS because of habitat or other factors, such as gear avoidance. Our findings validate the continued use of a dome-shaped selectivity for the BTS in the white hake stock assessment. In contrast, results indicate that catches were similar between the 2 surveys for cod in the upper end of the size distribution. A lack of large cod in the LLS, which focuses on sampling rough-bottom habitat, indicates that a similar absence of large cod in BTS catches is not due to habitat-related availability. Therefore, our findings do not support the hypothesis of habitat-related bias in the catches of cod

[8] Nozères, C., J. Gauthier, H. Bourdages, and Y. Lambert. 2015. Review of white hake (*Urophycis tenuis*) in the northern Gulf of St. Lawrence in support of a recovery potential assessment. DFO Can. Sci. Advis. Sec. Res. Doc. 2015/076, 56 p. [Available from website.]

in the BTS. It remains to be determined if other factors could influence the gear selectivity or availability of large cod; however, the results of analysis in this study support the continued use of the asymptotic (flat-topped) selectivity for the BTS in the GOM cod stock assessment.

Acknowledgments

We thank captains P. Lynch (F/V *Mary Elizabeth*) and E. Hesse (F/V *Tenacious II*) and their crews for contributions to the LLS. We thank the NEFSC Cooperative Research Branch staff, particularly C. Alexander, B. Gervelis, G. Gianesin, and D. St. Amand, for their support of the LLS. Special thanks to L. O'Brien, M. Martin, and P. Rago for contributions to the design of the LLS. We are grateful to staff of the NEFSC Ecosystems Surveys Branch for tireless efforts on the BTS. Thanks to A. Wood and P. Politis for comments on an earlier draft.

Literature cited

Ames, E. P.
2012. White hake (*Urophycis tenuis*) in the Gulf of Maine: population structure insights from the 1920s. Fish. Res. 114:56–65.

Ames, E. P., and J. Lichter.
2013. Gadids and alewives: structure within complexity in the Gulf of Maine. Fish. Res. 141:70–78.

Azarovitz, T. R.
1981. A brief historical review of the Woods Hole Laboratory trawl survey time series. *In* Bottom trawl surveys (W. G. Doubleday and D. Rivard, eds.), p. 62–67. Can. Spec. Publ. Fish. Aquat. Sci. 58. [Available from website.]

Bhattacharyya, A.
1943. On a measure of divergence between two statistical populations defined by their probability distribution. Bull. Calcutta Math. Soc. 35:99–109.

Cadrin, S. X., G. R. DeCelles, and D. Reid.
2016. Informing fishery assessment and management with field observations of selectivity and efficiency. Fish. Res. 184:9–17.

Chang, S., W. W. Morse, and P. L. Berrien.
1999. Essential fish habitat source document: white hake, *Urophycis tenuis*, life history and habitat characteristics. NOAA Tech. Memo. NMFS-NE-136, 23 p. [Available from website.]

Cochran, W. G.
1977. Sampling techniques, 3rd ed., 448 p. John Wiley and Sons, New York.

Engås, A., S. Løkkeborg, A. V. Soldal, and E. Ona.
1996. Comparative fishing trials for cod and haddock using commercial trawl and longline at two different stock levels. J. Northwest Atl. Fish. Sci. 19:83–90.

Fahay, M. P., P. L. Berrien, D. L. Johnson, and W. W. Morse.
1999. Essential fish habitat source document: Atlantic cod, *Gadus morhua*, life history and habitat characteristics. NOAA Tech. Memo. NMFS-NE-124, 41 p. [Available from website.]

Hilborn, R., and C. J. Walters.
1992. Quantitative fisheries stock assessment: choice, dynamics and uncertainty, 570 p. Chapman and Hall, New York.

Holt, R. D.
1987. Population dynamics and evolutionary processes: the manifold roles of habitat selection. Evol. Ecol. 1:331–347.

Hutchings, J. A., and J. D. Reynolds.
2004. Marine fish population collapses: consequences for recovery and extinction risk. BioScience 54:297–309.

Lawton, J. H.
1993. Range, population abundance and conservation. Trends Ecol. Evol. 8:409–413.

Macdonald, J. S., M. J. Dadswell, R. G. Appy, G. D. Melvin, and D. A. Methven.
1984. Fishes, fish assemblages, and their seasonal movements in the lower Bay of Fundy and Passamaquoddy Bay, Canada. Fish. Bull. 82:121–139.

Maunder, M. N., P. R. Crone, J. L. Valero, and B. X. Semmens.
2014. Selectivity: theory, estimation, and application in fishery stock assessment models. Fish. Res. 158:1–4.

McElroy, W. D., L. O'Brien, J. Blaylock, M. H. Martin, P. J. Rago, J. J. Hoey, and V. A. Sheremet.
2019. Design, implementation, and results of a cooperative research Gulf of Maine longline survey, 2014–2017. NOAA Tech. Memo. NMFS-NE-249, 68 p. [Available from website.]

Millar, R. B., and R. J. Fryer.
1999. Estimating the size-selection curves of towed gears, traps, nets and hooks. Rev. Fish Biol. Fish. 9:89–116.

NEFSC (Northeast Fisheries Science Center).
2008. Assessment of 19 Northeast groundfish stocks through 2007: report of the 3rd groundfish assessment review meeting (GARM III), Northeast Fisheries Science Center, Woods Hole, Massachusetts, August 4–8, 2008. Northeast Fish. Sci. Cent. Ref. Doc. 08-15, 884 p. [Available from website.]
2013a. 55th Northeast regional stock assessment workshop (55th SAW) assessment report. Northeast Fish. Sci. Cent. Ref. Doc. 13-11, 845 p. [Available from website.]
2013b. 56th Northeast regional stock assessment workshop (56th SAW) assessment report. Northeast Fish. Sci. Cent. Ref. Doc. 13-10, 868 p. [Available from website.]
2017. Operational assessment of 19 Northeast groundfish stocks, updated through 2016. Northeast Fish. Sci. Cent. Ref. Doc. 17-17, 259 p. [Available from website.]

Nye, J. A., J. S. Link, J. A. Hare, and W. J. Overholtz.
2009. Changing spatial distribution of fish stocks in relation to climate and population size on the Northeast United States continental shelf. Mar. Ecol. Prog. Ser. 393:111–129.

Orio, A., U. Bergström, A.-B. Florin, A. Lehmann, I. Šics, and M. Casini.
2019. Spatial contraction of demersal fish populations in a large marine ecosystem. J. Biogeogr. 46:633–645.

Riley, S. J., S. D. DeGloria, and R. Elliot.
1999. A terrain ruggedness index that quantifies topographic heterogeneity. Intermt. J. Sci. 5:23–27.

Sampson, D. B., and R. D. Scott.
2012. An exploration of the shapes and stability of population-selection curves. Fish Fish. 13:89–104.

Scharf, F. S., F. Juanes, and R. A. Rountree.
2000. Predator size-prey size relationships of marine fish predators: interspecific variation and effects of ontogeny and body size on trophic-niche breadth. Mar. Ecol. Prog. Ser. 208:229–248.

Scott, J. S.
1982. Selection of bottom type by groundfishes of the Scotian Shelf. Can. J. Fish. Aquat. Sci. 39:943–947.

Stauffer, G.
2004. NOAA protocols for groundfish bottom trawl surveys of the nation's fishery resources. NOAA Tech. Memo. NMFS-F/SPO-65, 205 p. [Available from website.]
Swain, D. P., and E. J. Wade.
1993. Density-dependent geographic distribution of Atlantic cod (*Gadus morhua*) in the southern Gulf of St. Lawrence. Can. J. Fish. Aquat. Sci. 50:725–733.
Tamdrari, H., M. Castonguay, J.-C. Brêthes, and D. Duplisea.
2010. Density-independent and -dependent habitat selection of Atlantic cod (*Gadus morhua*) based on geostatistical aggregation curves in the northern Gulf of St. Lawrence. ICES J. Mar. Sci. 67:1676–1686.
Wieland, K., E. M. F. Pedersen, H. J. Olesen, and J. E. Beyer.
2009. Effect of bottom type on catch rates of North Sea cod (*Gadus morhua*) in surveys with commercial fishing vessels. Fish. Res. 96:244–251.
Winner, K., M. J. Noonan, C. H. Fleming, K. A. Olson, T. Mueller, D. Sheldon, and J. M. Calabrese.
2018. Statistical inference for home range overlap. Methods Ecol. Evol. 9:1679–1691.

National Marine Fisheries Service
NOAA

Fishery Bulletin
established in 1881

Spencer F. Baird
First U.S. Commissioner of Fisheries and founder of *Fishery Bulletin*

Recruitment and survival of juvenile Gulf sturgeon (*Acipenser oxyrinchus desotoi*) in the Apalachicola River in Florida

Adam G. Fox (contact author)[1]
Nathaniel Q. Hancock[1,2]
J. Andrew Marbury[1,3]
Adam J. Kaeser[4]
Douglas L. Peterson (retired)[1]

Email address for contact author: agfox@uga.edu

[1] Warnell School of Forestry and Natural Resources
University of Georgia
180 East Green Street
Athens, Georgia 30602

[2] Northern District Office
North Carolina Division of Marine Fisheries
100 Kitty Hawk Lane
Elizabeth City, North Carolina 27909

[3] DeLeon Springs Fisheries Field Laboratory
Northeast Region
Florida Fish and Wildlife Conservation Commission
5450 U.S. Highway 17
DeLeon Springs, Florida 32130

[4] Panama City Fish and Wildlife Conservation Office
U.S. Fish and Wildlife Service
1601 Balboa Avenue
Panama City, Florida 32405-3792

Abstract—The Gulf sturgeon (*Acipenser oxyrinchus desotoi*) is an anadromous fish found in drainages of the Gulf coast from Louisiana to Florida and is federally listed as threatened under the Endangered Species Act. Estimates of abundance of adult Gulf sturgeon from several studies have been reported, but direct quantification of juvenile abundance has not been attempted—although such information regarding annual recruitment and juvenile population trends is critical. Our objectives were to quantify recruitment of Gulf sturgeon in the Apalachicola River in Florida by estimating age-1 juvenile abundance and to investigate their survival. During May–August in 2013–2018, we used entanglement gear to conduct a mark-recapture assessment of juvenile Gulf sturgeon. Using Huggins closed population models, we estimated that the Apalachicola River produces 28–210 age-1 juveniles annually (mean: 70 individuals [standard deviation 69.4]). Acoustic telemetry data collected from a subset of age-1 fish indicate that the study area was closed during sampling. We conservatively estimated overwinter survival on the basis of detections and recapture of age-2+ fish acoustically tagged at age 1. Survival varied among years from 33% to 90%. These results indicate that direct estimates of recruitment of Gulf sturgeon to age 1 are feasible, but it is difficult to determine whether this population is recruitment limited without similar data for other populations of Gulf sturgeon.

Manuscript submitted 13 April 2021.
Manuscript accepted 14 October 2021.
Fish. Bull. 119:243–254 (2021).
Online publication date: 12 November 2021.
doi: 10.7755/FB.119.4.4

The views and opinions expressed or implied in this article are those of the author (or authors) and do not necessarily reflect the position of the National Marine Fisheries Service, NOAA.

The Gulf sturgeon (*Acipenser oxyrinchus desotoi*) is a large-bodied, anadromous fish found in drainages of the Gulf coast of the United States from Louisiana to Florida. Like most members of Acipenseridae, the Gulf sturgeon has a late age at maturity, a protracted spawning interval, and a long lifespan (Huff[1]; Nelson et al., 2013). These life history traits make sturgeon particularly vulnerable to anthropogenic disturbances (Rochard et al., 1990), and, as a result of population declines caused by overharvesting and habitat alteration, the Gulf sturgeon was listed as threatened under the Endangered Species Act in 1991 (Federal Register, 1991).

Reproducing populations of Gulf sturgeon currently exist in 7 coastal river systems from the Suwannee River, in Florida, to the Pearl River, in Louisiana (USFWS and NMFS, 2009). Research and monitoring of these populations has largely focused on the capture of juveniles (>900 mm in total length [TL]) and adult fish (≥1350 mm TL), by using gill nets with large mesh (≥12.7 cm stretch) (Sulak et al., 2016). Results of these efforts indicate that the Suwannee River has the largest population, with an estimated abundance of 5000–10,000 adults and juveniles (Chapman et al., 1997; Sulak and Clugston, 1999; Sulak et al., 2016). As summarized by Sulak et al. (2016), most recent estimates of juvenile and adult abundance in other rivers are substantially lower. Although quantifying juvenile and adult abundance does provide insights into long-term population trends, these estimates are not useful in assessing the effects of recovery actions aimed at improving the reproductive success of Gulf sturgeon because these changes will not be reflected in the adult population for many years.

[1] Huff, J. A. 1975. Life history of the Gulf of Mexico sturgeon, *Acipenser oxyrinchus desotoi*, in the Suwannee River, Florida. Fla. Dep. Nat. Resour., Mar. Resour. Publ. 16, 30 p. [Available from Fla. Dep. Environ. Protection, 3900 Commerce Blvd., Tallahassee, FL 32399-3000.]

Monitoring recruitment to age 1 could provide an alternative method for investigation of bottlenecks to population growth that occur during reproduction and early life and could provide managers with forward-looking, quantitative measures for monitoring biological responses to restoration actions that target such bottlenecks (Pine et al., 2001; Schueller and Peterson, 2010). Indeed, some of the core goals of the Programmatic Damage Assessment and Restoration Plan (DHNRDAT[2]), which was developed to restore injury caused by the Deepwater Horizon Oil Spill of 2010, are to improve access to spawning habitats and to boost the reproductive success of Gulf sturgeon by increasing rates of survival during early life.

One approach to gathering recruitment data for sturgeon species is to capture larval sturgeon as they disperse from spawning areas. This method has been used to collect larvae of several sturgeon species (Braaten et al., 2008; Dumont et al., 2011; McAdam, 2011), although it requires precise knowledge of spawning locations and timing to effectively target larvae with fishing gear. Spawning has been confirmed at a handful of sites across the range of the Gulf sturgeon (Parauka and Giorgianni[3]; Heise et al., 2004; Kreiser et al., 2008; Flowers et al., 2009; Sulak et al.[4]). However, larvae do not appear to disperse from spawning areas in a synchronized, predictable fashion, as has been observed for other sturgeon species (Kynard and Parker, 2004), and it remains to be determined whether they can be reliably captured with drift nets.

A second method for monitoring recruitment involves the capture of young-of-the-year (YOY) sturgeon by using bottom-trawling gear. This method has proven effective for large river species like the pallid sturgeon (*Scaphirhynchus albus*) and shovelnose sturgeon (*S. platorynchus*) (Herzog et al., 2005; Doyle et al., 2007), where occupied habitats have been identified (Braaten and Fuller, 2007). However, given the dispersal behavior of Gulf sturgeon, YOY are likely distributed throughout the entire system during their first summer after hatching (Kynard and Parker, 2004; Sulak et al., 2016), rendering capture with trawling gear unlikely. Indeed, efforts to capture Gulf sturgeon with bottom-trawling gear have had little success (Sulak and Clugston, 1999; Kirk and Killgore[5]).

A third method for gathering recruitment data is to estimate the abundance of age-1 juveniles by using gill nets and a mark-recapture approach. This method is now routinely used to assess populations of Atlantic sturgeon (*Acipenser oxyrinchus oxyrinchus*) (Schueller and Peterson, 2010; Bahr and Peterson, 2016; Hale et al., 2016) and is also effective for monitoring small populations (e.g., Farrae et al., 2009). Despite success with Atlantic sturgeon, a fellow subspecies of *A. oxyrinchus*, quantitative estimation of age-1 juvenile recruitment has not been attempted for any population of Gulf sturgeon (USFWS and NMFS, 2009). Several researchers have back-calculated recruitment by using data on the age structure of populations (Sulak and Clugston, 1999; Randall and Sulak, 2007; Pine and Martell[6]), but those studies provided only general information about historical population trends and shed no light on current trends in recruitment of Gulf sturgeon.

In addition, little is known about the seasonal habitat requirements of juvenile Gulf sturgeon, although habitat and access may be impediments to species recovery (USFWS and GSMFC[7]; Zehfuss et al., 1999; Flowers et al., 2009). During the summer months, both adult and juvenile (i.e., age 1 and older) Gulf sturgeon reside in main-channel aggregation sites of their natal rivers (Wooley and Crateau, 1985; Hightower et al., 2002), and the majority of individuals do not actively forage (Sulak et al., 2012). During late fall, juvenile Gulf sturgeon move downriver to forage for benthic macrofauna in the estuary (Mason and Clugston, 1993; Sulak and Clugston, 1999; Sulak et al., 2009), while adults disperse more widely to feed in the nearshore, marine waters of the Gulf of Mexico (Odenkirk, 1989; Sulak and Clugston, 1999).

Abiotic conditions may limit habitat access and utilization by juveniles; young juveniles have a lower tolerance for salinity than older fish (Altinok et al., 1998; Kynard and Parker, 2004). Juvenile Gulf sturgeon may remain inshore for up to 6 years (Clugston et al., 1995), possibly because of an intolerance to full ocean salinity. Regarding one potential determinant of year-class strength of Gulf sturgeon, Randall and Sulak (2007) proposed the *salinity barrier* hypothesis, which is that growth and survival of juvenile sturgeon may be enhanced during years when elevated river discharge reduces the salinity of the receiving estuary for longer durations, thereby providing juveniles greater access to benthic resources during the foraging period. Monitoring the year-class strength of

[2] DHNRDAT (Deepwater Horizon Natural Resource Damage Assessment Trustees). 2016. Deepwater Horizon oil spill: final programmatic damage assessment and restoration plan and final programmatic environmental impact statement. [Available from website.]

[3] Parauka, F. M., and M. Giorgianni. 2002. Availability of Gulf sturgeon spawning habitat in northwest Florida and southeast Alabama river systems, 77 p. [Unpublished technical report. Available from Panama City Field Off., U.S. Fish Wildl. Serv., 1601 Balboa Ave., Panama City, FL 32405.]

[4] Sulak, K. J., M. Randall, J. P. Clugston, and W. Clark. 2013. Critical spawning habitat, early life history requirements, and other life history and population attributes of the Gulf sturgeon (*Acipenser oxyrinchus desotoi*) in the Suwannee River, Florida, 99 p. Final report to the Florida Fish and Wildlife Conservation Commission. Proj. Rep. TAL-NG95-125-2013. [Available from the Fla. Fish Wildl. Conserv. Comm., 620 S. Meridian St., Tallahassee, FL 32399.]

[5] Kirk, J. P., and K. J. Killgore. 2008. Gulf sturgeon movements in and near the Mississippi River Gulf outlet. U.S. Army Corps Eng., ERDC/EL TR-08-18, 9 p. [Available from website.]

[6] Pine, W. E., III, and S. Martell. 2009. Status of Gulf sturgeon *Acipenser oxyrinchus desotoi* in the Gulf of Mexico, 34 p. [Unpublished report prepared for 2009 Gulf sturgeon annual working group meeting; Cedar Key, 17–19 November.]

[7] USFWS and GSMFC (U.S. Fish and Wildlife Service and the Gulf States Marine Fisheries Commission). 1995. Gulf sturgeon recovery/management plan, 170 p. Southeast Reg., USFWS, Atlanta, GA. [Available from website.]

age-1 juvenile cohorts over time could enable an investigation of environmental factors, like salinity, that have been thought to influence recruitment during the first year of life of Gulf sturgeon (e.g., Nilo et al., 1996).

Yet another unknown is the overwinter survival rate of juvenile Gulf sturgeon during the foraging period. While foraging in the estuary, juvenile sturgeon may be taken by bottom fisheries, such as shrimp trawling fisheries (Wooley and Crateau, 1985; Collins et al., 2000). Although this potential source of mortality has been noted over the years (USFWS and GSMFC[7]; USFWS and NMFS, 2009), estimation of the overwinter survival of juvenile sturgeon has not been attempted. Monitoring the overwinter survival of age-1 Gulf sturgeon may provide insight into what happens to young juveniles after they recruit to the population and may allow comparisons of mortality across river systems that experience different pressures (e.g., bycatch in other fisheries or dredging).

The goal of this 6-year study, therefore, was to investigate juvenile Gulf sturgeon in order to elucidate gaps associated with this life stage. We selected the Apalachicola River system for this investigation because information on where to target juvenile Gulf sturgeon was available from historical records of their incidental capture during monitoring of adults. The specific objectives of this study were to estimate the abundance of age-1 annual cohorts as a quantified measure of recruitment and to calculate a conservative estimate of the survival of age-1 juveniles during their estuarine overwintering period.

Materials and methods

Study site

The Apalachicola River is the largest river by discharge in the state of Florida (Iseri and Langbein, 1974). The river is formed by the confluence of the Flint and Chattahoochee Rivers, although this junction is now inundated by the reservoir created by construction of the Jim Woodruff Lock and Dam (JWLD). Downstream of the JWLD, the Apalachicola River flows freely for 171 river kilometers (rkm) through the Florida Panhandle to Apalachicola Bay in the Gulf of Mexico (Fig. 1). Sampling efforts were concentrated in the Brothers River, a tributary that flows into the Apalachicola River 21 rkm upstream of the bay. The Brothers River has a deep (9–15 m) channel that has been identified as a summer habitat for juvenile Gulf sturgeon (Wooley and Crateau, 1985; Kirk and Killgore[5]; A. Kaeser, unpubl. data). Additional sampling was conducted in several areas located in the lower and upper sections of the main stem Apalachicola

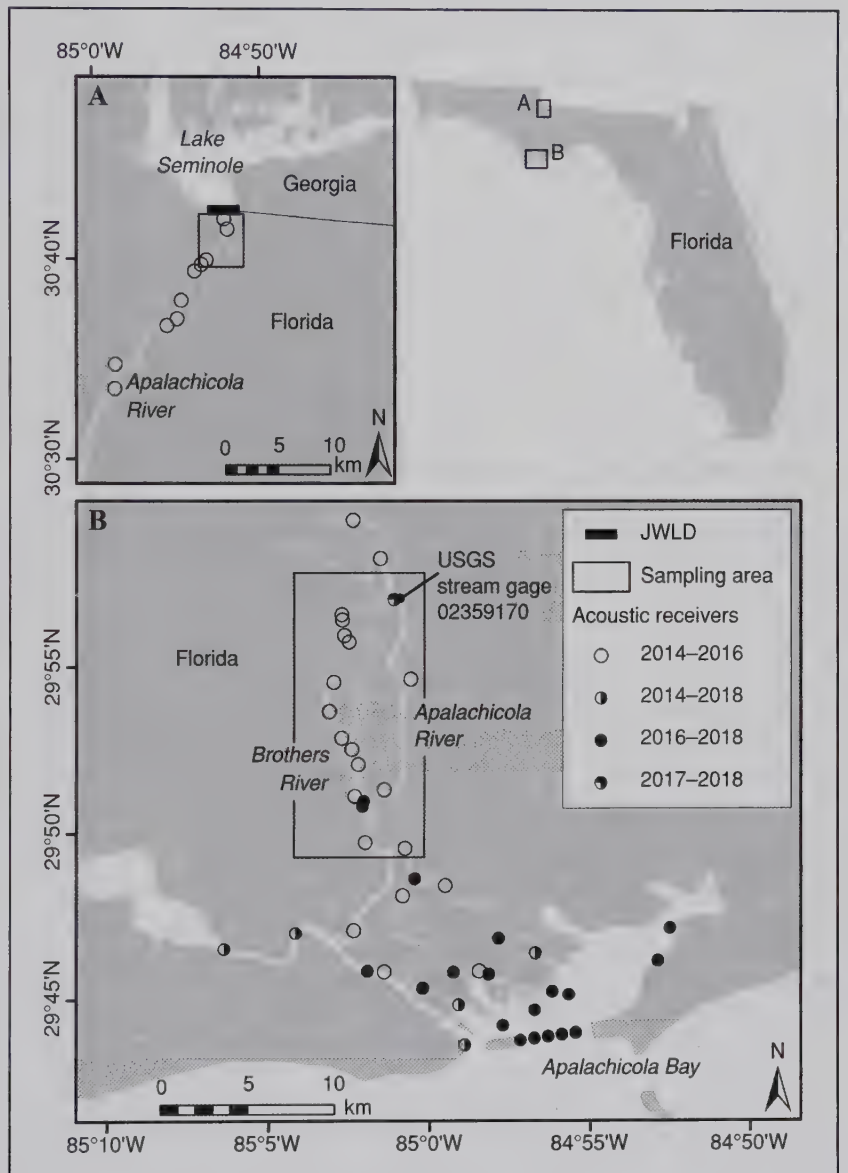

Figure 1

Maps of the study site in the Apalachicola River in Florida: (**A**) the Apalachicola River downstream of the Jim Woodruff Lock and Dam (JWLD, indicated by a black rectangle) and (**B**) the Brothers River and lower Apalachicola River. Sampling for juvenile Gulf sturgeon (*Acipenser oxyrinchus desotoi*) in 2014–2018 occurred within the boxes outlined in black. Circles indicate locations of acoustic receivers within the array installed for this study—open for receivers deployed during 2014–2016, black for those deployed during 2016–2018, half black for those deployed during 2014–2018, and three-fourths black for the receiver deployed during 2017–2018. In panel B, the location of U.S. Geological Survey (USGS) stream gage 02359170 on the Apalachicola River near Sumatra, Florida, is indicated.

River where juvenile and adult Gulf sturgeon have previously been captured (A. Kaeser, unpubl. data), as well as in other nearby reaches of the river (Fig. 1).

Fish tagging

From May through August of 2013–2018, we sampled for Gulf sturgeon 4–5 d/week. Each day, we deployed 6–12 anchored monofilament gill nets throughout the river channel at depths of 4–18 m. All nets comprised three 50-m panels consisting of 7.6-, 8.9-, and 10.2-cm monofilament mesh (stretch measure). Net design was based on nets proven to capture juvenile Atlantic sturgeon in rivers in Georgia (Schueller and Peterson, 2010). Nets were typically soaked for 60–120 min, depending on conditions. To ensure that sampling occurred within the recommended water-quality ranges (Kahn and Mohead, 2010), we used a YSI Pro2030[8] meter (YSI Inc., Yellow Springs, OH) to measure water temperature (in degrees Celsius), dissolved oxygen (in milligrams per liter), and salinity (using the practical salinity scale) at each netting location. River discharge data were obtained from the nearest U.S. Geological Survey stream gage (02359170 on the Apalachicola River near Sumatra, Florida; data available from website.).

As nets were retrieved, all captured Gulf sturgeon were immediately removed and placed into a floating net pen where they could recover before being brought on board the vessel for data collection. Each individual was examined for marks indicating previous capture; if no mark was present, the fish was marked with a passive integrated transponder (PIT) tag inserted into the musculature at the base of the dorsal fin or under the fourth dorsal scute. The fish was then weighed to the nearest gram, measured to the nearest millimeter (in fork length [FL]), and released at the site of capture within 30 min of initial capture.

Fish ages were first assigned from modal distributions on length–frequency histograms of catch of Gulf sturgeon for each year of the study, by using the method described by Peterson et al. (2000) and Schueller and Peterson (2010). To validate assigned ages, we obtained sections of second marginal fin rays from the pectoral fins of a subsample of captured fish; these samples were prepared by using techniques described by Baremore and Rosati (2014). Ages were determined on the basis of consensus of 3 independent readers (if consensus could not be reached, we removed that sample from the validation data set). Because there was essentially no overlap in lengths at age, we were able to assign a length range for age-1 and age-2 Gulf sturgeon.

Acoustic telemetry

To investigate the closure of the summer aggregation site in the Brothers River during the fishing period and to examine overwinter survival, we tagged up to 20 age-1 juveniles (age estimated on the basis of length) with a surgically implanted acoustic transmitter (Vemco V7-4X, Innovasea Systems Inc., Boston, MA) in May and June of each study year. To implant the transmitter, we placed each fish in a V-shaped surgical platform, with a battery-powered pump supplying fresh river water to its gills. An incision of 2–3 cm was made along the midline of the abdomen by using a sterile scalpel, and through this incision the sanitized transmitter (~1.6 g) was inserted into the body cavity. The incision was then closed with a 2/0 absorbable monofilament suture (Monoswift L943, CP Medical, Norcross, GA) by using a single interrupted pattern (Boone et al., 2013; Baremore and Rosati, 2014). After the surgical procedure, each fish was placed in a floating pen. Once a fish had regained its orientation and ability to swim, it was released at its capture site. Ping rate and battery life of transmitters varied among the study years (Table 1). The transmitters deployed in 2017 had a 120-d delay before they began transmitting, extending the battery life of those tags through the summer of 2018, allowing us to confirm fish survival and improve estimates of overwinter survival.

To detect the tagged juveniles after their release, we deployed an array of acoustic receivers throughout the Brothers and Apalachicola Rivers, their distributaries, and the East Bay subunit of Apalachicola Bay (Fig. 1). The array consisted of 30 stationary acoustic receivers (Vemco VR2W, Innovasea Systems Inc.). Receivers were anchored to the bottom with concrete weights and held upright (hydrophone upward) in the water column with a PVC float. Receivers were attached to trees, navigational markers, or other pilings by using stainless steel cables. Some were secured to pilings with aluminum U-channel, and others were deployed in open water, where they were anchored with cinder blocks. Every 2–3 months throughout the study period, the entire receiver

Table 1

Specifications for acoustic transmitter tags implanted in age-1 juvenile Gulf sturgeon (*Acipenser oxyrinchus desotoi*) captured and tagged from May through August in 2013–2018 in the Brothers River and other areas of the Apalachicola River system in Florida. All tags were Vemco V7-4X transmitters with a frequency of 69 kHz. Minimum and maximum delays, and delay before activation, were set by the manufacturer. Transmitter lifespan was estimated by the manufacturer.

Year	Min. delay between signals (s)	Max. delay between signals (s)	Lifespan (d)	Delay before activation (d)
2014	80	160	305	0
2015	170	310	426	0
2016	170	310	426	0
2017	80	160	374	120

[8] Mention of trade names or commercial companies is for identification purposes only and does not imply endorsement by the National Marine Fisheries Service, NOAA.

array received routine maintenance and data were downloaded from each receiver. Routine maintenance included replacing batteries and cleaning of any biofouling. Supplemental telemetry data were obtained by periodically sweeping the study area with a portable receiver and hydrophone (Vemco VR100, Innovasea Systems Inc.) to detect fish between receivers or outside of the array. Between December and May in 2016, our receiver array was restructured to include more receivers outside of the Brothers River, leaving a gate (i.e., receivers that covered the river channel) where the Brothers River flowed into the Apalachicola River; in the spring of 2017, another gate was added at the cut connecting the upper Brothers River to the main stem Apalachicola River. The purpose of these gates was to detect fish as they left or reentered the aggregation site.

Data from the acoustic receiver array were carefully checked for any spurious detections (e.g., simultaneous detections of a single fish at disparate receiver stations), and such detections were removed. Raw detection data were converted into detection days (one detection per fish per receiver per day). If a fish was not detected on a study day but was known to be alive because of detections on subsequent days, that fish was assigned the location of its last known detection until it was detected elsewhere (this method was applied by Fox and Peterson, 2019, to telemetry data from tagged juvenile Atlantic sturgeon). We used these telemetry data to determine whether and how often tagged fish left the Brothers River during our mark-recapture sampling season or to determine if fish tagged elsewhere in the system entered the Brothers River—the lack of such movements into or out of the Brothers River would indicate closure of the aggregation site. Additionally, we used telemetry data to calculate overwinter survival, as described later in the "Survival analysis" section.

Abundance estimation

To estimate the annual abundance of age-1 juvenile Gulf sturgeon, we fit a Huggins closed capture model (Huggins, 1989, 1991) to mark-recapture data from the gill-net surveys. Models were fit to data by using the RMark package (Laake[9]) in statistical software R (vers. 3.5.1; R Core Team, 2018). Each week of the study was considered a sampling period in the capture history for each year, and in each sampling period, an individual was classified as either absent or present, regardless of the actual number of times it was captured that week. The model includes the assumption that the population was closed, meaning that there were no births or deaths and that no immigration or emigration occurred throughout each summer in the study period, and the assumption that tags were not lost or overlooked. We primarily used telemetry data to look for violations to the assumption of closure, but we also used the program CloseTest (vers. 3; Stanley and Burnham, 1999) for an alternative way to investigate closure.

After we compiled individual capture histories for each juvenile caught during the study, each fish was assigned to an age group (i.e., age 1, age 2, or age 3+) on the basis of its length. A set of candidate models was produced to estimate juvenile cohort abundances in each of the 6 study years. The candidate set of models and their main settings were as follows:

- M_o, in which capture probability was constant;
- M_t, in which capture probability varied with time;
- M_a, in which capture probability varied by fish age;
- M_{t+a}, in which capture probability varied by an additive effect of time and age; and
- M_{t*a}, in which capture probability varied by an interactive effect of time and age.

In all models, capture probability was set as equal to recapture probability because no evidence indicates that capture history had any influence on recapture probability for sturgeon—this method has been used in other studies in which recruitment of sturgeon was estimated to age 1 (e.g., Bahr and Peterson, 2016). Akaike information criterion (Akaike, 1973), corrected for small sample size (AIC_c) (Hurvich and Tsai, 1989), was then used to evaluate the relative likelihood of each model. For each year of the study, all models were averaged by using Akaike information criterion model weight to estimate abundance of age-1 Gulf sturgeon, to reduce bias in the event of several candidate models being plausible (i.e., the top model carried a weight <0.90) (Burnham and Anderson, 2002).

Survival analysis

We estimated overwinter survival by comparing the number of acoustically tagged age-1 juveniles detected leaving the summer aggregation sites in the fall and winter with the number of fish from that cohort that returned the following spring. Detection of the fish that by then were age 2 was done through acoustic detection or physical capture. Survival was calculated as the percentage of tagged age-1 fish that were confirmed to still be alive at age 2 (or an older age). Because this survival analysis does not include detection probabilities, it has a necessarily conservative approach, in that survival is likely underestimated because it is not possible to distinguish between fish that died and fish that remained alive but were not detected.

Results

Over 6 years of sampling, we set 1834 nets for a total of 2205 net-hours of sampling effort within the Brothers River. Because anchored gill nets did not sample Gulf

[9] Laake, J. 2013. RMark: an R interface for analysis of capture-recapture data with MARK. AFSC Process. Rep. 2013-01, 25 p. Alaska Fish. Sci. Cent., Natl. Mar. Fish. Serv., Seattle, WA. [Available from website.]

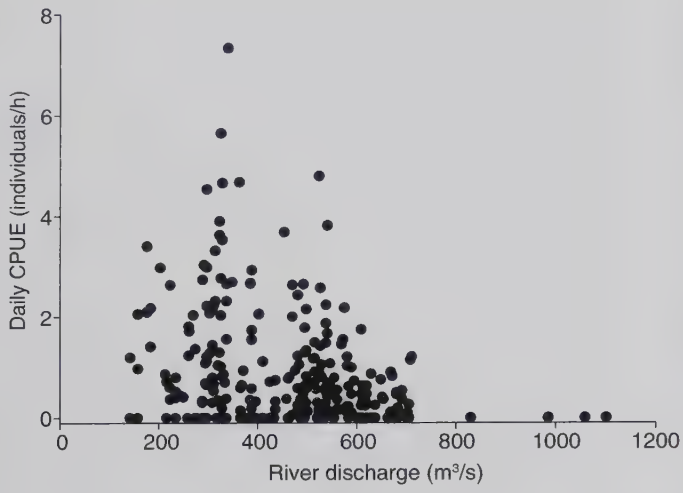

Figure 2

The relationship of catch per unit of effort (CPUE) for sampling of Gulf sturgeon (*Acipenser oxyrinchus desotoi*) and discharge of the Apalachicola River in Florida between May and August in 2013–2018. Catch per unit of effort was calculated as number of sturgeon captured per hour of netting effort. River discharge data are from U.S. Geological Survey (USGS) stream gage 02359170 on the Apalachicola River near Sumatra, Florida. Data in this figure are a subset of all catch data, consisting of catch for the 2 sites most frequently sampled in the Brothers River tributary, which had a wide variety of river discharge conditions in 2013–2018.

sturgeon effectively when river discharge exceeded ~850 m^3/s (Fig. 2), we generally did not set nets when flows exceeded this threshold. Therefore, sampling period varied among study years, from just 4 weeks in 2013 to 15 weeks in 2018 (Table 2). In 2013, netting locations were dispersed entirely within the Brothers River. During 2014–2018, 192 net-hours (10% of all net-hours in the period) were expended in other areas of the Apalachicola River system. Water quality in netting areas remained relatively consistent throughout all summer sampling periods (Suppl. Table 1) (online only). The interquartile temperature range was 26.7–29.1°C, and the interquartile range for dissolved oxygen was 4.34–5.79 mg/L. Salinity in all sampling locations was <0.1, with the exception of several sets in the lower Apalachicola River, from which no sturgeon were caught.

Over the 6 years of sampling, 2029 Gulf sturgeon were captured in the Apalachicola and Brothers Rivers, including 1100 unique individuals (Table 2). Of those fish, 288 were identified as age-1 juveniles. Results of length–frequency analysis (validated by pectoral fin ray analysis) indicate that age-1 fish had FL of 370–530 mm, although there was some variation among years in median length (Suppl. Fig. 1) (online only). Most age-1 juveniles (number of samples [n]=282, 97.9%) were captured within the Brothers River. During this study, only 6 age-1 fish were ever captured in other reaches of the Apalachicola River—all were observed just below the JWLD in 2017 and 2018 (although we sampled in that area in 2015–2018).

In May and early June during 2014–2017, we tagged 50 age-1 juveniles with acoustic transmitters (Fig. 3). All but 1 fish were captured within the Brothers River; the exception was a fish captured at the JWLD. We detected 76% (n=38) of tagged fish on our acoustic array after tagging; detection rates varied, with 42–100% of fish detected per study year and 21–25, 360 detections per fish. We also physically recaptured 16 acoustically tagged individuals within the year they were tagged or in subsequent years. In 2016, we found infections of the sutured surgery site on several tagged fish that were

Table 2

Effort, catch, and other details for sampling of Gulf sturgeon (*Acipenser oxyrinchus desotoi*) in the Apalachicola River, in Florida, during May–August in 2013–2018. The total number of Gulf sturgeon captured includes all ages and all recaptured fish. Abundance of age-1 fish was calculated by using Huggins closed capture models, and values are presented as point estimates of number of individuals with 95% confidence intervals (CIs). We tested for closure of the age-1 population by using the program CloseTest; P-values ≤0.05 indicate statistical significance and a population that was not closed.

	Effort			Total no. of fish captured	No. of age-1 juveniles		Abundance of age-1 fish		
Year	Nets set	Net-hours	Sampling periods		Marked	Recaptured	Abundance	95% CI	CloseTest P-value
2013	167	287	4	101	33	12	46	37–70	0.34
2014	291	465	9	602	151	62	218	190–241	0.63
2015	318	348	9	341	25	6	54	34–119	0.75
2016	270	270	9	333	34	23	51	35–67	0.06
2017	291	311	13	198	24	22	28	24–36	0.72
2018	497	524	15	156	21	9	31	21–48	0.11

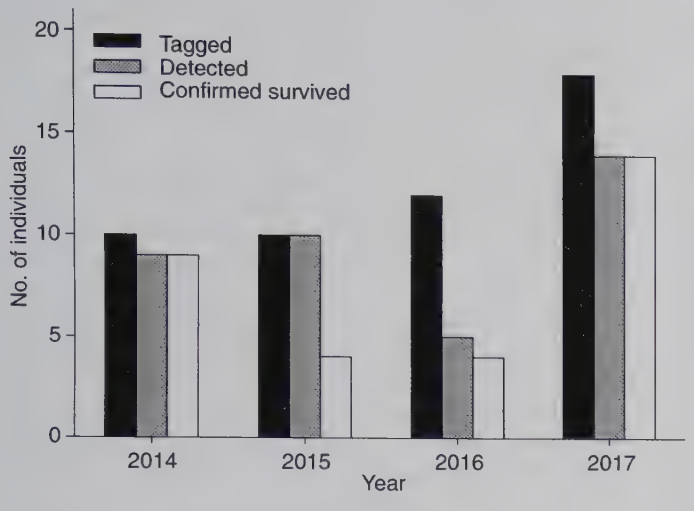

Figure 3

Deployment and detection of acoustic tags on and fate of age-1 Gulf sturgeon (*Acipenser oxyrinchus desotoi*) captured and tagged in the Apalachicola River in Florida during 2014–2017. Black bars indicate the number of age-1 fish implanted with acoutic transmitters in each year of this study, and gray bars indicate how many of those transmitters were subsequently detected by the acoustic receiver array. Open bars indicate the number of individuals confirmed to have survived to at least age 2, through a combination of detections with telemetry data and physical recapture of fish.

recaptured in nets—something we did not observe in any other study year.

During summer months, individuals tagged in the Brothers River remained there almost exclusively. In 2014, one fish was briefly detected by a receiver in the main stem Apalachicola River near the mouth of the Brothers River but returned to the Brothers River within about 3 h of that detection. In 2017, another tagged fish was detected at a receiver at the mouth of the Brothers River and may have entered the Apalachicola River (it was never detected by receivers there); that fish was detected again at the same gate receiver 18 d later. Recapture of fish (in gill nets) and sporadic active tracking of tagged fish confirmed their presence in the Brothers River even when fish were not detected by the acoustic receiver array (e.g., they were between 2 receivers and out of the detection range of both). During opportunistic hydrophone sweeps, tagged age-1 fish were never detected outside of the Brothers River. The juveniles moved out of the Brothers River in the fall and were detected with receivers in the main stem Apalachicola River and its distributaries as they moved toward Apalachicola and East Bays. Tagged fish were detected moving back up these same channels toward and into the Brothers River the following spring. The single Gulf sturgeon acoustically tagged at the JWLD was never detected in the Brothers River, but it was detected with receivers in the Apalachicola Estuary as it moved downriver in the fall.

Recruitment

Model selection on the basis of AICc values indicates that the M_{t+a} model (with the additive effect of time and age) held almost all of the weight in most years of the study; the M_{t*a} model (with the interactive effect of time and age) held the most weight in only 2 years (Suppl. Table 2) (online only). For the age-1 cohort, weighted averaging of all models resulted in estimated abundance of 28–54 individuals in each year of the study, except for 2014, for which the estimated abundance of age-1 fish was 210 individuals (Fig. 4).

Survival

Of the 38 acoustic transmitters that we deployed on Gulf sturgeon and later detected in our array, 24 transmitters were last detected in March or later of the following calendar year (i.e., the fish implanted with the transmitters survived the winter after tagging). An additional 7 tagged fish that were never detected by the array were physically recaptured ≥1 sampling season after tagging. We have confirmed that 31 fish (62% of all tagged fish) survived to at least age 2. Our conservative estimates of overwinter survival varied annually from a low of 33.3% to a high of 90.0% (mean: 60.2% [standard deviation (SD) 27.8]) (Fig. 3).

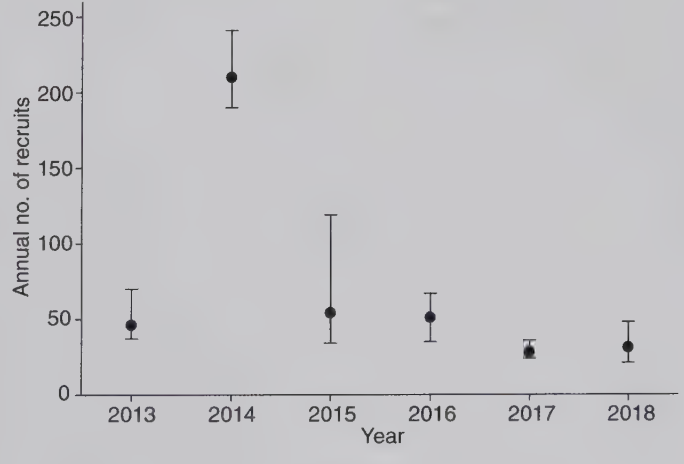

Figure 4

Estimates of abundance of age-1 juvenile Gulf sturgeon (*Acipenser oxyrinchus desotoi*), by year that a cohort was sampled, in the Apalachicola River in Florida during 2013–2018. Abundance is measured as the number of recruits. Error bars indicate 95% confidence intervals.

Discussion

Recruitment

This study is the first to directly estimate annual recruitment of any population of Gulf sturgeon. Across the 6 years of this study, age-1 recruits were observed every year, and mean annual recruitment was relatively stable. The Apalachicola River produced approximately 50 age-1 Gulf sturgeon in most years, although recruitment was substantially greater in 2014, when we estimated that there were 210 age-1 sturgeon.

Although there are no direct recruitment estimates for Gulf sturgeon to which our results can be compared, Pine and Martell[6] used an age-structured, mark-recapture model to back-calculate recruitment on the basis of the adult population, and they reported annual recruitment in the Apalachicola River to be 100–300 individuals/year, slightly greater than our estimates. However, direct recruitment estimates do exist for Atlantic sturgeon in several southern rivers. The largest populations of Atlantic sturgeon in the southeastern United States have annual recruitment that is an order of magnitude greater than what we generally observed in the Apalachicola River: the Altamaha River, in Georgia, produces 500–2500 age-1 juveniles every year (Schueller and Peterson, 2010), and the Savannah River, in Georgia and South Carolina, produces 500–600 juveniles annually (Bahr and Peterson, 2016). Recruitment of Gulf sturgeon in the Apalachicola River appears more similar to that observed in small rivers in Georgia's coastal plain, rivers where annual recruitment is <100 age-1 juveniles per year, if any, such as in the Ogeechee River (Farrae et al., 2009), Satilla River (Fritts et al., 2015), and St. Marys River (Fox et al., 2018). These populations are considered particularly small and imperiled (ASSRT, 2007).

Although recruitment of Gulf sturgeon in the Apalachicola River was substantially lower than recruitment of Atlantic sturgeon in similar large, Piedmont river systems (e.g., the Savannah and Altamaha Rivers), all 3 river systems did produce new recruits every year, indicating that spawning occurred every year. In contrast, small populations of Atlantic sturgeon (e.g., those in the Satilla and St. Marys Rivers) did not produce age-1 recruits every year. This comparison to recruitment of Atlantic sturgeon indicates that, although Gulf sturgeon in the Apalachicola River spawn successfully every year, recruitment may be limited. Analysis of recruitment across other populations of Gulf sturgeon will be necessary to determine how the population in the Apalachicola River compares to others of the same subspecies.

We tagged fish largely within the Brothers River; therefore, our recruitment estimates pertain primarily to the population of juveniles that reside in this part of the river system. Over many years of historical sampling by the U.S. Fish and Wildlife Service (A. Kaeser, unpubl. data), juvenile Gulf sturgeon have been captured in only one other location outside the Brothers River—below the JWLD. Moreover, in this study, we set nets in the Apalachicola River, including in many reaches with characteristics (e.g., depth, salinity, and temperature) similar to those of the Brothers River and, in most years, caught no age-1 juveniles outside of the Brothers River. Our capture of several age-1 juveniles below the JWLD indicates that juveniles can (sometimes) be found at this location. Because our estimates are specific to the geography we sampled, we acknowledge that the presence of age-1 fish in undiscovered aggregation sites, should they exist, would mean that we have underestimated true, population-level recruitment in the Apalachicola River system. However, unless there are unknown aggregation sites that contain dozens or hundreds of unsampled age-1 fish, it seems likely that our estimates either accurately represent or provide a robust indicator of recruitment to age 1 in the river system. Annual recruitment in the Apalachicola River appears to be measured in dozens of fish, not hundreds or thousands.

The validity of the abundance estimates produced in this study relies heavily on the assumption of population closure (demographic and geographic)—no births, deaths, immigration, or emigration can occur during the sampling period (Huggins, 1989). Under this assumption, capture rates could fluctuate throughout the sampling season (as they did during this study), resulting in more accurate estimates than values produced with an open model (Stanley and Richards, 2005). Although the assumption of closure can never be proven per se, there are several reasons why we believe the population was essentially closed during our sampling. For numerous studies (e.g., Wooley and Crateau, 1985; Hightower et al., 2002) in which the life history of Gulf sturgeon was examined, results indicate that all juveniles returned to aggregation sites in their natal river during summer months. We conducted our sampling mainly in the summer at the aggregation site in the Brothers River. CloseTest results (Table 2) indicate that age-1 cohorts likely met the closure assumption in most years of the study—the lack of closure in 2016 could have been a result of elevated mortality due to exceptionally warm water temperatures (see discussion of survival in the next section).

The telemetry data collected during this study largely support the assumption of closure for the Brothers River. No tagged age-1 juveniles were detected outside the aggregation site in that river for more than a short period (<4 h), and no individuals marked (i.e., acoustically tagged) near the JWLD were observed in the Brothers River during the summer in which they had been tagged. The JWLD appears to have a separate aggregation site that is occupied by only a few, if any, age-1 fish. However, if the population was not closed, our estimates of annual recruitment would be lower than the true number of recruits.

Mark-recapture models also include the assumption that marks (i.e., tags) were not lost or overlooked. In lake sturgeon (*Acipenser fulvescens*), PIT tag retention is 99% (Briggs et al., 2019), and we would expect similar results for other species in Acipenseridae. Each Gulf sturgeon we captured was thoroughly scanned for PIT tags, and many

marked fish were captured more than once within a single summer. Although we cannot prove that no fish rejected PIT tags, the repeated capture of tagged fish within and among summers indicates that sturgeon retained their PIT tags and that tags were not overlooked.

Survival

Overwinter survival of juvenile Gulf sturgeon from age 1 to age 2 appears quite variable, with high survival in some years (e.g., 90% in 2014) and substantially lower rates in others (e.g., 40% in 2015 and 33% in 2016). However, these estimates are conservative (i.e., biased lower than the true values) because we were unable to differentiate actual mortality of tagged fish from transmitter failure or lack of detection. We were able to supplement acoustic detections with physical recapture events to confirm that—after as long as several years at large—some fish had actually survived. Although we are unable to ascertain the fates of individuals that were not detected or recaptured at age 2 or beyond, it is unlikely that these fish utilized another aggregation site outside of our receiver array because they were not detected moving upriver in the spring or in the main stem Apalachicola River. No tagged juveniles were detected outside of the Brothers River in surveys with the portable receiver, and many tagged fish were eventually recaptured in gill nets within the aggregation site in the Brothers River.

The probability of detecting tagged fish in our array was undoubtedly <1. Although results of preliminary testing of the detection range of receivers indicate that receivers could detect a Vemco V7-4X transmitter at ranges of up to 800 m, we recognize that in most cases detection range is probably substantially smaller. Detection range also likely varied with condition and orientation of receivers, with river conditions at each site in the array, and even with ambient weather. Therefore, fish could certainly have swum past acoustic receivers in the array without detection. Additionally, distribution of receivers within the array changed over the course of this study. Beginning in 2016, many receivers in the Brothers River were moved to locations lower in the estuary. Our transmitter specifications also differed among study years, both in signal delay and activation delay, creating additional differences in probability of detection across study years.

Despite imperfect detection, our survival analysis required only that we detect each tagged fish at least once in the year after tagging—to indicate that it had survived and moved back upriver. Most surviving tagged fish likely would have been detected at least once during the several months in which this detection could occur. Indeed, 77.5% of all fish confirmed to have survived to ages ≥2 were detected by the array (and most of those fish were detected hundreds of times). Additionally, if a fish did survive, each year it remained at large provided an additional sampling season in which we might catch it and confirm survival. Continued long-term monitoring of Gulf sturgeon in the Apalachicola River may yet reveal the survival of some fish that are currently presumed dead by this model, increasing the rate of survival beyond what we report in this paper.

This study was not intended to identify sources of overwinter mortality for Gulf sturgeon in the Apalachicola River. However, some mortalities may have resulted from transmitter implantation, especially in substandard environmental conditions. In 2016, water temperatures reached as high as 31.3°C (Suppl. Table 1) (online only). Although we did not conduct surgeries in temperatures above 28°C, exposure to very warm water shortly after being tagged may have facilitated the infections we observed at surgery sites of recaptured fish in 2016. These infections likely explain the decreased survival of tagged fish in 2016. Commercial fisheries in the area may also be responsible for some mortality of Gulf sturgeon. Wooley and Crateau (1985) documented incidental capture of juvenile and adult Gulf sturgeon (>800 mm TL) in shrimp trawls and other commercial fishing gears; juveniles are also potentially susceptible to these threats.

Despite the conservative bias and potential inaccuracies of our estimates of overwinter survival, examining mean annual survival still has utility. During this study, the mean annual survival rate was 60.3% (SD 27.8)—which translates to annual mortality of 39.7% (*mortality*=1–*survival*). This rate of mortality is roughly comparable to previous estimates of mortality for juvenile Gulf sturgeon: Morrow et al. (1998) found an annual mortality of 34% for fish at ages 3–9 in the Pearl River, and Pine et al. (2001) estimated that annual mortality was 25% for Gulf sturgeon at ages 1–3 in the Suwannee River. If we omit data for 2016 from our survival analysis (presuming that low survival in that year was due to surgery site infections), mean mortality across this study was 30.7%., a value that is even more congruent with the reports in the literature. Tate and Allen (2002) simulated responses of populations of Gulf sturgeon to several rates of juvenile mortality and found that, at 30% annual mortality, populations remained stable over 200 years but that, at 35% annual mortality, the population slowly collapsed. Refining the accuracy of survival estimates remains an important goal for researchers and managers of Gulf sturgeon, and the ability in future studies to adjust survival estimates for imperfect detection should lead to estimates of true overwinter survival that are more accurate and higher than those we have reported.

Conclusions

The results of this study indicate that direct estimates of annual recruitment of Gulf sturgeon are feasible. In the Apalachicola River, we observed age-1 juveniles recruiting to the population in every year of our study, but abundance of age-1 fish was low: only about 50 individuals in 5 of the 6 years of this study.

The methods employed in this study can be used to obtain recruitment data for other populations of Gulf sturgeon, once juvenile aggregation sites have been located.

To capture juveniles, we recommend that researchers set small-mesh gill nets and initially focus sampling on river reaches with water-quality characteristics similar to those of the aggregation site in the Brothers River (see Suppl. Table 1) (online only). Sampling with anchored nets should occur only in appropriate flows—we recommend that researchers attempt to determine the relationship between discharge and catch per unit of effort of juvenile Gulf sturgeon in each river in order to maximize sampling efficiency. Once age-1 fish have been located, acoustic telemetry can be used to identify the extent of aggregation sites. Mark-recapture sampling then should target the identified aggregation sites, with additional sampling occurring in other river reaches.

Quantitative estimates of recruitment of Gulf sturgeon in other rivers will allow direct comparison between populations, as well as comparisons across time within each population. Additionally, telemetry data from age-1 fish will help fill important data gaps about juvenile habitat utilization. Researchers and managers will be able to assess the effects of restoration actions (e.g., dam removal, fish passage, and habitat restoration) or environmental catastrophes (e.g., oil spills and hurricanes) on recruitment quickly, rather than having to wait a decade to see any changes reflected in the adult population. Additionally, multiyear sets of recruitment data will allow investigation of how variation in annual recruitment relates to environmental conditions, such as temperature and river discharge (both of which, in the Apalachicola River, are influenced by the JWLD).

Acknowledgments

We would like to thank the USFWS for funding this work and the USFWS Panama City Field Office, St. Joseph Bay State Buffer Preserve, and D. Higginbotham for providing support. This project was conducted under Florida Fish and Wildlife Conservation Commission special activity licenses SAL-14-1481-SRP and SAL-15-1481A-SRP. The findings and conclusions in this article are those of the authors and do not necessarily represent the views of the USFWS.

Literature cited

Akaike, H. 1973.
Information theory and an extension of the maximum likelihood principle. *In* Second international symposium on information theory; Tsaghkadzor, 2–8 September 1971 (B. N. Petrov and F. Csáki, eds.), p. 267–281. Akadémiai Kiadó, Budapest, Hungary.

Altinok, I., S. M. Galli, and F. A. Chapman.
1998. Ionic and osmotic regulation capabilities of juvenile Gulf of Mexico sturgeon, *Acipenser oxyrinchus desotoi*. Comp. Biochem. Physiol., A 120:609–616.

ASSRT (Atlantic Sturgeon Status Review Team).
2007. Status review of Atlantic sturgeon (*Acipenser oxyrinchus oxyrinchus*). Report to National Marine Fisheries Service, Northeast Regional Office. [Available from website.]

Bahr, D. L., and D. L. Peterson.
2016. Recruitment of juvenile Atlantic sturgeon in the Savannah River, Georgia. Trans. Am. Fish. Soc. 145:1171–1178.

Baremore, I. E., and J. D. Rosati.
2014. A validated, minimally deleterious method for aging sturgeon. Fish. Bull. 112:274–282.

Boone, S. S., S. M. Hernandez, A. C. Camus, D. L. Peterson, C. A. Jennings, J. L. Shelton, and S. J. Divers.
2013. Evaluation of four suture materials for surgical incision closure in Siberian sturgeon. Trans. Am. Fish. Soc. 142:649–659.

Braaten, P. J., and D. B. Fuller.
2007. Growth rates of young-of-year shovelnose sturgeon in the Upper Missouri River. J. Appl. Ichthyol. 23:505–515.

Braaten, P. J., D. B. Fuller, L. D. Holte, R. D. Lott, W. Viste, T. F. Brandt, and R. G. Legare.
2008. Drift dynamics of larval pallid sturgeon and shovelnose sturgeon in a natural side channel of the upper Missouri River, Montana. North Am. J. Fish. Manage. 28:808–826.

Briggs, A. S., J. C. Boase, J. A. Chiotti, J. Hessenauer, and T. C. Wills.
2019. Retention of loop, Monel, and passive integrated transponder tags by wild, free-ranging lake sturgeon (*Acipenser fulvescens* Rafinesque, 1817). J. Appl. Ichthyol. 35:629–635.

Burnham, K. P., and D. R. Anderson.
2002. Model selection and multimodel inference: a practical information theoretic approach, 2nd ed., 488 p. Springer, New York.

Clugston, J. P., A. M. Foster, and S. H. Carr.
1995. Gulf sturgeon, *Acipenser oxyrinchus desotoi*, in the Suwannee River, Florida, USA. *In* Proceedings of the international symposium on sturgeons (A. D. Gershanovich and T. I. J. Smith, eds.), p. 215–224. VNIRO Publ., Moscow, Russia.

Collins, M. R., S. G. Rogers, T. I. J. Smith, and M. L. Moser.
2000. Primary factors affecting sturgeon populations in the southeastern United States: fishing mortality and degradation of essential habitats. Bull. Mar. Sci. 66:917–928.

Doyle, W., C. Paukert, A. Starostka, and T. Hill.
2007. A comparison of four types of sampling gear used to collect shovelnose sturgeon in the lower Missouri River. J. Appl. Ichthyol. 24:637–642.

Dumont, P., J. D'Amours, S. Thibodeau, N. Dubuc, R. Verdon, S. Garceau, P. Bilodeau, Y. Mailhot, and R. Fortin.
2011. Effects of the development of a newly created spawning ground in the Des Prairies River (Quebec, Canada) on the reproductive success of lake sturgeon (*Acipenser fulvescens*). J. Appl. Icthyol. 27:394–404.

Farrae, D. J., P. M. Schueller, and D. L. Peterson.
2009. Abundance of juvenile Atlantic sturgeon in the Ogeechee River, Georgia. Proc. Annu. Conf. Southeast Assoc. Fish Wildl. Agencies 63:172–176.

Federal Register.
1991. Endangered and threatened wildlife and plants; threatened status for the Gulf sturgeon. Fed. Regist. 56(189):49653–49658. [Available from website.]

Flowers, H. J., W. E. Pine III, A. C. Dutterer, K. G. Johnson, J. W. Ziewitz, M. S. Allen, and F. M. Parauka.
2009. Spawning site selection and potential implications of modified flow regimes on viability of Gulf sturgeon populations. Trans. Am. Fish. Soc. 138:1266–1284.

Fox, A., and D. Peterson.
2019. Movement and out-migration of juvenile Atlantic sturgeon in Georgia, USA. Trans. Am. Fish. Soc. 148:952–962.

Fox, A. G., I. I. Wirgin, and D. L. Peterson.
2018. Occurrence of Atlantic sturgeon in the St. Marys River, Georgia. Mar. Coast. Fish. 10:606–618.

Fritts, M. W., C. Grunwald, I. Wirgin, T. L. King, and D. L. Peterson.
2015. Status and genetic character of Atlantic sturgeon in the Satilla River, Georgia. Trans. Am. Fish. Soc. 145:69–82.

Hale E. A., I. A. Park, M. T. Fisher, R. A. Wong, M. J. Stangl, and J. H. Clark.
2016. Abundance estimate for and habitat use by early juvenile Atlantic sturgeon within the Delaware River Estuary. Trans. Am. Fish. Soc. 145:1193–1201.

Heise, R. J., W. T. Slack, S. T. Ross, and M. A. Dugo.
2004. Spawning and associated movement patterns of Gulf sturgeon in the Pascagoula River drainage, Mississippi. Trans. Am. Fish. Soc. 133:221–230.

Herzog, D. P., V. A. Barko, J. S. Scheibe, R. A. Hrabik, and D. E. Ostendorf.
2005. Efficacy of a benthic trawl for sampling small-bodied fishes in large river systems. North Am. J. Fish. Manage. 24:594–603.

Hightower, J. E., K. P. Zehfuss, D. A. Fox, and F. M. Parauka.
2002. Summer habitat use by Gulf sturgeon in the Choctawhatchee River, Florida. J. Appl. Ichthyol. 18:595–600.

Huggins, R.
1989. On the statistical analysis of capture. Biometrika 76:133–140.
1991. Some practical aspects of a conditional likelihood to capture experiments. Biometrics 47:725–732.

Hurvich, C. M., and C. Tsai.
1989. Regression and time series selection in small samples. Biometrika 76:297–307.

Iseri, K. T., and W.B. Langbein.
1974. Large rivers of the United States. U.S. Geol. Surv. Circ. 686, 10 p. [Available from website.]

Kahn, J., and M. Mohead.
2010. A protocol for use of shortnose, Atlantic, Gulf, and green sturgeons. NOAA Tech. Memo. NMFS-OPR-45, 62 p.

Kreiser, B. R., J. Berg, M. Randall, F. Parauka, S. Floyd, B. Young, and K. Sulak.
2008. Documentation of a Gulf sturgeon spawning site on the Yellow River, Alabama. Gulf Caribb. Res. 20:91–95.

Kynard, B., and E. Parker.
2004. Ontogenetic behavior and migration of Gulf of Mexico sturgeon, *Acipenser oxyrinchus desotoi*, with notes on body color and development. Environ. Biol. Fishes 70:43–55.

Mason, W. T., Jr., and J. P. Clugston.
1993. Foods of the Gulf sturgeon in the Suwannee River, Florida. Trans. Am. Fish. Soc. 122:378–385.

McAdam, S. O.
2011. Effects of substrate condition on habitat use and survival by white sturgeon (*Acipenser transmontanus*) larvae and potential implications for recruitment. Can. J. Fish. Aquat. Sci. 68:812–822.

Morrow, J. V., Jr., J. P. Kirk, K. J. Killgore, H. Rogillio, and C. Knight.
1998. Status and recovery potential of Gulf sturgeon in the Pearl River system, Louisiana–Mississippi. North Am. J. Fish. Manage. 18:798–808.

Nelson, T. C., P. Doukakis, S. T. Lindley, A. D. Schreier, J. E. Hightower, L. R. Hildebrand, R. E. Whitlock, and M. A Webb.
2013. Research tools to investigate movements, migrations, and life history of sturgeons (Acipenseridae), with an emphasis on marine-oriented populations. PLoS ONE 8(8):e71552.

Nilo, P., P. Dumont, and R. Fortin.
1996. Climatic and hydrological determinants of year-class strength of St. Lawrence River lake sturgeon (*Acipenser fulvescens*). Can. J. Fish. Aquat. Sci. 54:774–780.

Odenkirk, J. S.
1989. Movements of Gulf of Mexico sturgeon in the Apalachicola River, Florida. Proc. Annu. Conf. Southeastern Assoc. Fish Wildl. Agencies 43:230–238.

Peterson, D. L., M. B. Bain, and N. Haley.
2000. Evidence of declining recruitment of Atlantic sturgeon in the Hudson River. North Am. J. Fish. Manage. 20:231–238.

Pine, W. E., III, M. S. Allen, and V. J. Dreitz.
2001. Population viability of the Gulf of Mexico sturgeon: Inferences from capture-recapture and age-structured models. Trans. Am. Fish. Soc. 130:1164–1171.

R Core Team.
2020. R: a language and environment for statistical computing. R Foundation for Statistical Computing, Vienna, Austria. [Available from website, accessed July 2018.]

Randall, M. T., and K. J. Sulak.
2007. Relationship between recruitment of Gulf sturgeon and water flow in the Suwannee River, Florida. Am. Fish. Soc. Symp. 56:69–83.

Rochard, E., G. Castelnaud, and M. Lepage.
1990. Sturgeons (Pisces Acipenseridae); threats and prospects. J. Fish. Biol. 37:123–132.

Schueller, P., and D. L. Peterson.
2010. Abundance and recruitment of juvenile Atlantic sturgeon in the Altamaha River, Georgia. Trans. Am. Fish. Soc. 139:1526–1535.

Stanley, T. R., and K. P. Burnham.
1999. A closure test for time-specific capture-recapture data. Environ. Ecol. Stat. 6:197–209.

Stanley, T. R., and J. D. Richards.
2005. Software review: a program for testing capture-recapture data for closure. Wildl. Soc., B 33:782–785.

Sulak, K. J., and J. P. Clugston.
1999. Recent advances in life history of Gulf of Mexico sturgeon, *Acipenser oxyrinchus desotoi*, in the Suwannee River, Florida, USA: a synopsis. J. Appl. Ichthyol. 15:116–128.

Sulak, K. J., and M. T. Randall, R. E. Edwards, T. M. Summers, K. E. Luke, W. T. Smith, A. D. Norem, W. M. Harden, R. H. Lukens, F. Parauka et. al.
2009. Defining winter trophic habitat of juvenile Gulf sturgeon in the Suwannee and Apalachicola rivermouth estuaries, acoustic telemetry investigations. J. Appl. Ichthyol. 25:505–515.

Sulak, K. J., J. J. Berg, and M. Randall.
2012. Feeding habitats of the Gulf sturgeon, *Acipenser oxyrinchus desotoi*, in the Suwannee and Yellow rivers, Florida, as identified by multiple stable isotope analyses. Environ. Biol. Fishes 95:237–258.

Sulak, K. J., P. Parauka., W. T. Slack, R. T. Ruth, M. T. Randal, K. Luke, M. F. Mettee, and M. E. Price.
2016. Status of scientific knowledge, recovery progress, and future research directions for the Gulf sturgeon, *Acipenser oxyrinchus desotoi* Vladykov, 1955. J. Appl. Ichthyol. 32:87–161.

Tate, W. B., and M. S. Allen.
2002. Simulated impacts of juvenile mortality on Gulf of Mexico sturgeon populations. Sci. World J. 2:270–274.

USFWS and NMFS (U.S. Fish and Wildlife Service and National Marine Fisheries Service).
2009. Gulf sturgeon (*Acipenser oxyrinchus desotoi*) 5-year review: summary and evaluation, 49 p. Southeast Reg., Panama City Ecol. Serv. Off., USFWS, Panama City, FL, and Southeast Reg., Off. Prot. Resour., Natl. Mar. Fish. Serv., St. Petersburg, FL. [Available from website.]

Wooley, C. M. and E. J. Crateau.
1985. Movement, microhabitat, exploitation and management of Gulf of Mexico sturgeon, Apalachicola River, Florida. North Am. J. Fish. Manage. 5:590–605.

Zehfuss, K. P., J. E. Hightower, and K. H. Pollock.
1999. Abundance of Gulf sturgeon in the Apalachicola River, Florida. Trans. Am. Fish. Soc. 128:130–143.

National Marine Fisheries Service
NOAA

Fishery Bulletin
established in 1881

Spencer F. Baird
First U.S. Commissioner of Fisheries and founder of *Fishery Bulletin*

Postrelease movements of leatherback turtles (*Dermochelys coriacea*) following incidental capture in fishing gear in the Atlantic Ocean

Emily P. Bond
Michael C. James (contact author)

Email address for contact author: mike.james@dfo-mpo.gc.ca

Population Ecology Division
Fisheries and Oceans Canada
P.O. Box 1006
Dartmouth, Nova Scotia B2Y 4A2, Canada

Abstract—Fisheries bycatch is posited to be a leading cause of decline in abundance of Atlantic leatherback turtles (*Dermochelys coriacea*). However, although this species regularly interacts with fisheries across its range, movements and postrelease survival of leatherbacks remain largely unstudied. Such research is lacking because sampling opportunities are unpredictable and logistically challenging. Here, movements of 4 leatherbacks equipped with satellite tags following incidental capture in fixed-gear fisheries in Nova Scotia, Canada, are presented, alongside results from previous postentanglement tracking of 15 leatherbacks tagged throughout the Atlantic Ocean. Mean tracking duration after tagging was 232.58 d (standard deviation 165.61; sample size=19), comparable with what has been reported for fishery-independent deployments of satellite tags on leatherbacks. This result indicates that, provided they are released carefully and completely from fishing gear, many leatherbacks survive entanglement events without apparent long-term effects.

Manuscript submitted 16 February 2021.
Manuscript accepted 20 September 2021.
Fish. Bull. 119:255–260 (2021).
Online publication date: 17 November 2021.
doi: 10.7755/FB.119.4.5

The views and opinions expressed or implied in this article are those of the author (or authors) and do not necessarily reflect the position of the National Marine Fisheries Service, NOAA.

It is challenging to quantify the effects of anthropogenic threats to marine species, especially for highly migratory animals, such as marine mammals, sharks, and sea turtles (Lascelles et al., 2014). However, the use of electronic tagging technologies, including satellite telemetry, can provide insight into bycatch risk (Witt et al., 2011; Kindt-Larsen et al., 2016) and has provided indirect (Henderson et al., 2020) and direct evidence for mortality associated with fishery interactions (Byrne et al., 2017; Benson et al., 2018). Application of satellite transmitters to incidentally caught sea turtles has also facilitated evaluation of postrelease mortality after fishery interactions (Chaloupka et al., 2004; Swimmer et al., 2006; Snoddy and Williard, 2010).

In the Atlantic Ocean, leatherback turtles (*Dermochelys coriacea*) interact with numerous fisheries and gear types (Wallace et al., 2010). The capture of reproductive leatherbacks in artisanal gill nets is especially concerning for the Northwest Atlantic leatherback turtle subpopulation because of the high potential for mortality (Wallace et al., 2013; NMFS and USFWS, 2020). In Trinidad, where one of the largest nesting assemblages of leatherbacks is found, coastal gill-net fisheries are estimated to kill 1000 leatherbacks annually (Lee Lum, 2006). Although additional studies are needed to quantify the extent of this risk and mortality rates in coastal waters near nesting beaches, bycatch in coastal gill-net fisheries has also been identified as a threat in French Guiana (TEWG, 2007), Colombia (Patiño-Martinez et al., 2008), and Brazil (Lewison and Crowder, 2007).

Atlantic Canada, a region that includes the provinces of New Brunswick, Nova Scotia, Prince Edward Island, and Newfoundland and Labrador, is a primary foraging area for leatherbacks in the Northwest Atlantic Ocean, where incidental capture in fixed-gear fisheries has been identified as a primary threat to this species (Hamelin et al., 2017). However, capture rates, rates of mortality during capture, and postrelease mortality of leatherbacks in this area are not well understood. Here, satellite tracking data are presented for leatherbacks released following incidental entanglement in fixed-gear fisheries in Atlantic Canada. Given the rarity of opportunities to satellite tag leatherbacks entangled in fixed fishing gear, additional published satellite tracks

of leatherbacks released following incidental entanglement (sample size [n]=15) were also reviewed. These tracks include records from the Northwest Atlantic Ocean, Southwest Atlantic Ocean, and Northeast Atlantic Ocean.

Materials and methods

Four leatherbacks were tagged in coastal waters off Nova Scotia, Canada (turtles A–D in Table 1). These 4 turtles were found entangled in lines associated with fish traps

Table 1

Details of fishery interactions and satellite tracking for leatherback turtles (*Dermochelys coriacea*) satellite tagged and released following incidental capture in fishing gear in 2003–2012 in the Northwest Atlantic Ocean (NWA), Southwest Atlantic Ocean (SWA), and Northeast Atlantic Ocean (NEA). Mean travel rates are given with standard deviation in parentheses. A dash indicates a field that was not reported in the reviewed study. CCL=curved carapace length.

Turtle	Date deployed	Gear type	Location	Sex	CCL (cm)	Tag attachment type	Days tracked	Mean travel rate (km/h)	Source
A	16-Jul-2003	Fish trap (line entanglement)	Nova Scotia, Canada (NWA)	U	134.0	Harness	537	1.13 (0.79)	This study
B	12-Aug-2003	Fish trap (line entanglement)	Nova Scotia, Canada (NWA)	U	140.0	Harness	210	1.19 (0.54)	This study
C	18-Jul-2008	Fish trap (line entanglement)	Nova Scotia, Canada (NWA)	M	148.2	Direct	311	1.38 (0.76)	This study
D	4-Jul-2012	Fish trap (line entanglement)	Nova Scotia, Canada (NWA)	F	144.0	Direct	212	1.43 (0.96)	This study
E	12-Feb-2006	Driftnet	São Paulo, Brazil (SWA)	F	153.0	Harness	97		Almeida et al. (2011)
F	15-Jun-2005	Pelagic longline (mainline or branch lines)	High seas (SWA)	F	148.0	Harness	313		López-Mendilaharsu et al. (2009)
G	31-Jul-2006	Pelagic longline (mainline or branch lines)	High seas (SWA)	M	159.0	Harness	237		López-Mendilaharsu et al. (2009)
H	14-Aug-2006	Pelagic longline (mainline or branch lines)	High seas (SWA)	U	126.0	Harness	349		López-Mendilaharsu et al. (2009)
I	29-Oct-2006	Artisanal bottom-set gill net	Rio de la Plata Estuary, Uruguay (SWA)	F	155.5	Harness	631		López-Mendilaharsu et al. (2009)
J	1-Sep-2005	Lobster pot (line entanglement)	0.2 km from Cuas Harbour, Ireland (NEA)	F	–	Harness	375		Doyle et al. (2008)
K	29-Jun-2006	Salmon drift net	0.5 km from Cuas Harbour, Ireland (NEA)	M	–	Direct	233		Doyle et al. (2008)
L	19-Aug-2007	Fixed gear (line entanglement)	Nantucket Sound, USA (NWA)	M	140.7	Direct	34		Dodge et al. (2014); Dodge[1]
M	29-Aug-2007	Fixed gear (line entanglement)	Cape Cod Bay, USA (NWA)	M	143.2	Direct	18		Dodge et al. (2014); Dodge[1]
N	29-Aug-2007	Fixed gear (line entanglement)	Nantucket Sound, USA (NWA)	U	123.0	Direct	16		Dodge et al. (2014); Dodge[1]
O	22-Sep-2007	Fixed gear (line entanglement)	Cape Cod Bay, USA (NWA)	U	137.5	Direct	183		Dodge et al. (2014); Dodge[1]
P	1-Oct-2007	Fixed gear (line entanglement)	Cape Cod Bay, USA (NWA)	F	136.0	Direct	35		Dodge et al. (2014); Dodge[1]
Q	23-Aug-2008	Fixed gear (line entanglement)	Nantucket Sound, USA (NWA)	M	146.4	Direct	234		Dodge et al. (2014); Dodge[1]
R	28-Aug-2008	Fixed gear (line entanglement)	Nantucket Sound, USA (NWA)	U	140.0	Direct	191		Dodge et al. (2014); Dodge[1]
S	3-Sep-2009	Fixed gear (line entanglement)	Nantucket Sound, USA (NWA)	M	155.0	Direct	203		Dodge et al. (2014); Dodge[1]

[1] Dodge, K. 2021. Personal commun. Fish. Sci. Emerg. Tech., New England Aquar., 1 Central Wharf, Boston, MA 02110.

(Table 1), and they presented with rope wrapped multiple times around the front flippers, or the flippers and neck, as is commonly documented among leatherbacks entangled in fixed-gear fisheries in Atlantic Canada (Hamelin et al., 2017). Following complete removal of all entangling fishing gear, each turtle was visually examined for injuries, and its condition was assessed. Turtles were measured and photographed. Sex was determined for individuals with curved carapace length (CCL) ≥145 cm on the basis of phallus display or tail morphology, and turtles with CCL <145 cm were classified as juveniles (Eckert, 2002). Tissue samples were obtained by using a 5-mm biopsy punch (Acuderm Inc.[1], Fort Lauderdale, FL), and identification tags (Monel flipper tags and passive integrated transponders) were applied.

Turtles were equipped with satellite transmitters (models SSC3 [n=1], SPOT3 [n=1], or MK10-AF [n=2], Wildlife Computers Inc., Redmond, WA), by using harnesses (n=2) or direct attachment (n=2) (Hamelin and James, 2018). After tagging, turtles were immediately released. Location data were transmitted through the Argos satellite network, and locations classified as LC3, LC2, LC1, and LC0 and estimated to be within 150 m, 150–350 m, 350–1000 m, and >1000 m of true locations were retained for analysis (Fig. 1). Data processing and analyses were conducted by using statistical software R, vers. 3.6.1 (R Core Team, 2019), and tracking data were plotted by using ArcMap 10.7 (Esri, Redlands, CA). Protocols for disentanglement, sampling, and satellite-tag attachment were approved by the Dalhousie University Committee on Laboratory Animals or the Fisheries and Oceans Canada Maritimes Animal Care Committee to meet standards established by the Canadian Council on Animal Care. Data and interaction details for turtles E–S (Table 1) were obtained from previously published tracks of satellite-tagged leatherbacks following their release from fishing gear.

Results and discussion

Turtles A–D were active and responsive at the time of release; they displayed only minor abrasions and vigorous movements. Satellite tracking durations spanned 210–537 d, with an average of 9754 km (standard deviation [SD] 3790.6) travelled and mean travel rates from 1.130 km/h (SD 0.791) to 1.430 km/h (SD 0.960) (Table 1). Turtle B immediately swam south and departed continental shelf waters after release. However, the other turtles remained in northern continental shelf waters off Canada and the United States throughout the summer–fall foraging season, before eventually migrating to low latitudes for the winter (Fig. 1). Such behavior is consistent with movement patterns exhibited by free-swimming leatherbacks tracked following directed-capture sampling in Canada or from nesting beaches (James et al., 2005). Tags on 3 turtles ceased transmitting data during the winter following tag deployment; however, turtle A was tracked through a second foraging season in waters off Atlantic Canada (for a total tracking duration of 537 d).

Travel rates for turtles A–D were similar to those of leatherbacks tracked following directed capture off Nova Scotia (Jonsen et al., 2006) and after departing nesting beaches in Trinidad (Eckert, 2006) and French Guiana (Fossette et al., 2008). Three of the 4 turtles were not observed again after tagging. However, Turtle D was subsequently recorded nesting at Matura Beach, Trinidad, in 2014, 2017, and 2019 (when replacement satellite tags were deployed) and was tracked back to waters off Atlantic Canada in 2017, 2019, and 2020. Turtle D's foraging, migratory, and nesting history spanning 8 years from the first tag deployment is compelling evidence for a lack of long-term behavioral or fitness effects associated with the original capture and tagging of this individual.

The mean tracking duration for leatherbacks after they were disentangled and released (all deployments, Table 1) was 232.58 d (SD 165.61; n=19). Most (74%) leatherbacks were tracked for over 100 d, with many completing large-scale migrations throughout the deployment period (Doyle et al., 2008; Almeida et al., 2011; Dodge et al., 2014) (Fig. 1). The mean tracking duration of leatherbacks after disentanglement and release in our analysis was not significantly different from the tracking durations of live-captured leatherbacks documented by Hamelin and James (2018) (P=0.538). Importantly, the sample considered here includes leatherbacks interacting with a variety of fisheries throughout the Atlantic Ocean and encompasses turtles that presented as vigorous and lacking apparent external injuries at the time of tagging (turtles A–D) (Doyle et al., 2008) and others that had clearly sustained injuries (Innis et al., 2010; Dodge et al., 2014). The tracking results here (turtles A–S, Table 1), coupled with the high rate of scarring likely caused by fishery interactions observed among nesting and foraging leatherbacks (Archibald and James, 2018), indicate that many leatherbacks can recover from entanglement events. Dodge et al. (2014) established that some of the turtles they tracked were previously entangled, and at least one tagged turtle had sustained injuries from constricting and cutting lines (Innis et al., 2010). Others, however, only had minor abrasions. It is unclear if the short tracking durations (<50 d, Table 1) among the leatherbacks considered from other studies correspond to turtles that had severe entanglement injuries and were judged by Innis et al. (2010) to be in relatively poor health.

The satellite tracking data reviewed and presented here are from a variety of satellite transmitter models with varying sensor options, sampling and transmission regimes, and battery capacities. Biofouling, broken antennas, and premature detachment can contribute to cessation of satellite tag transmissions, affecting tracking durations (Hays et al., 2007). These confounding factors,

[1] Mention of trade names or commercial companies is for identification purposes only and does not imply endorsement by the National Marine Fisheries Service, NOAA.

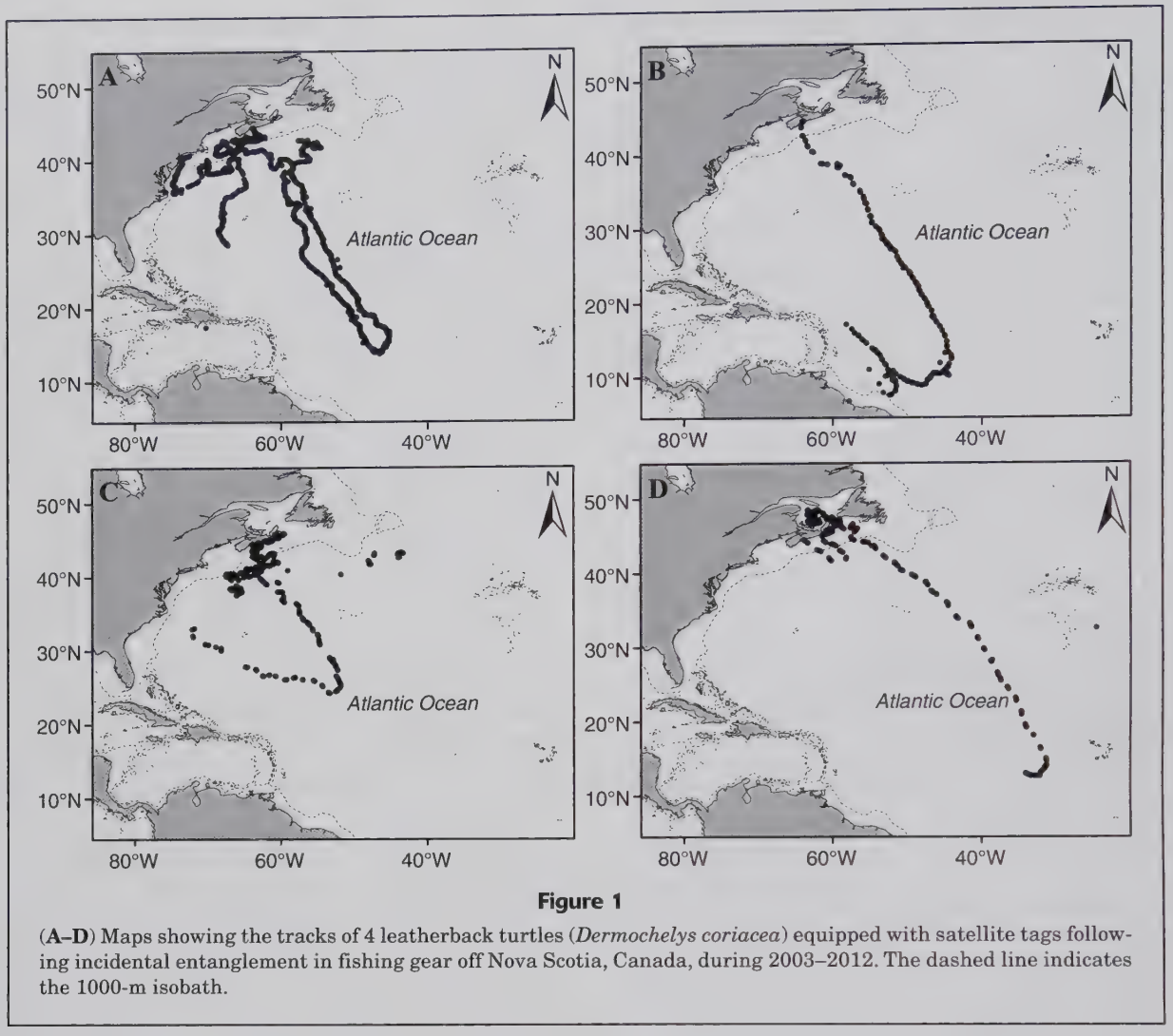

Figure 1

(**A–D**) Maps showing the tracks of 4 leatherback turtles (*Dermochelys coriacea*) equipped with satellite tags following incidental entanglement in fishing gear off Nova Scotia, Canada, during 2003–2012. The dashed line indicates the 1000-m isobath.

which are normally impossible to diagnose remotely, make it difficult to identify events of true turtle mortality, especially when environmental data, such as depth, temperature, or light level, are not available.

Uncertainty regarding how representative the sample we considered is of post-entanglement outcomes for leatherbacks results from the relatively low number of entangled turtles equipped with satellite tags and the lack of standardized biomedical assessment criteria for classifying entanglement condition across all turtles. Innis et al. (2010) and Dodge et al. (2014) deliberately included turtles with apparent entanglement injuries in their studies, and an attending veterinarian conducted detailed animal health assessments. Comparable assessments were not available for the sample from Canada. Therefore, it is possible that the results from Canada may reflect biases associated with turtles that, although entangled, appeared relatively healthy at the time of tagging. This is possible because, to meet animal care permitting requirements, only turtles that appeared active and responsive were equipped with satellite tags off Nova Scotia.

The data presented here indicate that some leatherbacks survive entanglement events and complete long-distance migrations. However, opportunistic satellite tagging of entangled leatherbacks is logistically challenging. Therefore, to date, only small sample sizes have been achieved and under inconsistent study protocols. These limitations have precluded quantification of postrelease mortality of leatherbacks following bycatch in various fisheries. Targeted studies of fates of incidentally captured leatherbacks at the time of release and after release are urgently required to effectively quantify the threat of incidental entanglement. Such research should apply standardized protocols for leatherback health assessment and should consider the role of different environmental conditions, gear types, and entanglement severity on fates of turtles. In the interim, survival outcomes for leatherbacks interacting with fisheries could be enhanced through efforts to reduce the duration of entanglement events. This may be accomplished through reduced soak times, regular checking of gear, and implementation of prompt and humane disentanglement protocols.

Acknowledgments

We thank D. Themelis and P. Emery for comments that improved this manuscript. We are grateful to the Canadian Sea Turtle Network and fishermen in Nova Scotia who assisted with associated fieldwork.

Literature cited

Almeida, A. P., S. A. Eckert, S. C. Bruno, J. T. Scalfoni, B. Giffoni, M. López-Mendilaharsu, and J. C. A. Thomé.
2011. Satellite-tracked movements of female *Dermochelys coriacea* from southeastern Brazil. Endanger. Species Res. 15:77–86.

Archibald, D. W., and M. C. James.
2018. Prevalence of visible injuries to leatherback sea turtles *Dermochelys coriacea* in the Northwest Atlantic. Endanger. Species Res. 37:149–163.

Benson, J. F., S. J. Jorgensen, J. B. O'Sullivan, C. Winkler, C. F. White, E. Garcia-Rodriguez, O. Sosa-Nishizaki, and C. G. Lowe.
2018. Juvenile survival, competing risks, and spatial variation in mortality risk of a marine apex predator. J. Appl. Ecol. 55:2888–2897.

Byrne, M. E., E. Cortés, J. J. Vaudo. G. C. McN. Harvey, M. Sampson, B. M. Wetherbee, and M. Shivji.
2017. Satellite telemetry reveals higher fishing mortality rates than previously estimated, suggesting overfishing of an apex marine predator. Proc. R. Soc., B 284:20170658.

Chaloupka, M., D. Parker, and G. Balazs.
2004. Modelling post-release mortality of loggerhead sea turtles exposed to the Hawaii-based pelagic longline fishery. Mar. Ecol. Prog. Ser. 280:285–293.

Dodge, K. L., B. Galuardi, T. J. Miller, and M. E. Lutcavage.
2014. Leatherback turtle movements, dive behavior, and habitat characteristics in ecoregions of the Northwest Atlantic Ocean. PLoS One 9(3):e91726.

Doyle, T. K., J. D. R. Houghton, P. F. O'Súilleabháin, V. J. Hobson, F. Marnell, J. Davenport, and G. C. Hays.
2008. Leatherback turtles satellite-tagged in European waters. Endanger. Species Res. 4:23–31.

Eckert, S. A.
2002. Distribution of juvenile leatherback sea turtle *Dermochelys coriacea* sightings. Mar. Ecol. Prog. Ser. 230:289–93.
2006. High-use oceanic areas for Atlantic leatherback sea turtles (*Dermochelys coriacea*) as identified using satellite telemetered location and dive information. Mar. Biol. 149:1257–1267.

Fossette, S., H. Corbel, P. Gaspar, Y. Le Maho, and J. Y. Georges.
2008. An alternative technique for the long-term satellite tracking of leatherback turtles. Endanger. Species Res. 4:33–41.

Hamelin, K. M., and M. C. James.
2018. Evaluating outcomes of long-term satellite tag attachment on leatherback sea turtles. Anim. Biotelem. 6:18.

Hamelin, K. M., M. C., James, W. Ledwell, J. Huntington, and K. Martin.
2017. Incidental capture of leatherback sea turtles in fixed fishing gear off Atlantic Canada. Aquat. Conserv. 27:631–642.

Hays, G. C., C. J. A. Bradshaw, M. C. James, P. Lovell, and D. W. Sims.
2007. Why do Argos satellite tags deployed on marine animals stop transmitting? J. Exp. Mar. Biol. Ecol. 349:52–60.

Henderson, A. F., C. R. McMahon, R. Harcourt, C. Guinet, B. Picard, S. Wotherspoon, and M. A. Hindell.
2020. Inferring variation in southern elephant seal at-sea mortality by modelling tag failure. Front. Mar. Sci. 7:517901.

Innis, C., C. Merigo, K. Dodge, M. Tlusty, M. Dodge, B. Sharp, A. Myers, A. McIntosh, D. Wunn, C. Perkins et al.
2010. Health evaluation of leatherback turtles (*Dermochelys coriacea*) in the northwestern Atlantic during direct capture and fisheries gear disentanglement. Chelonian Conserv. Biol. 9:205–222.

James, M. C., C. A. Ottensmeyer, and R. A. Myers.
2005. Identification of high-use habitat and threats to leatherback sea turtles in northern waters: new directions for conservation. Ecol. Lett. 8:195–201.

Jonsen, I. D., R. A. Myers, and M. C. James.
2006. Robust hierarchical state–space models reveal diel variation in travel rates of migrating leatherback turtles. J. Anim. Ecol. 75:1046–1057.

Kindt-Larsen, L., C. W. Berg, J. Tougaard, T. K Sørensen, K. Geitner, S. Northridge, S. Sveegaard, and F. Larsen.
2016. Identification of high-risk areas for harbour porpoise *Phocoena phocoena* bycatch using remote electronic monitoring and satellite telemetry data. Mar. Ecol. Prog. Ser. 555:261–271.

Lascelles, B., G. Notarbartolo Di Sciara, T. Agardy, A. Cuttelod, S. Eckert, L. Glowka, E. Hoyt, F. Llewellyn, M. Louzao, V. Ridoux et al.
2014. Migratory marine species: their status, threats and conservation management needs. Aquat. Conserv. 24(S2):111–127.

Lee Lum, L.
2006. Assessment of incidental sea turtle catch in the artisanal gillnet fishery in Trinidad and Tobago, West Indies. Appl. Herpetol. 3:357–368.

Lewison, R. L., and L. B. Crowder.
2007. Putting longline bycatch of sea turtles into perspective. Conserv. Biol. 21:79–86.

López-Mendilaharsu, M., C. F. Rocha, P. Miller, A. Domingo, and L. Prosdocimi.
2009. Insights on leatherback turtle movements and high use areas in the Southwest Atlantic Ocean. J. Exp. Mar. Biol. Ecol. 378:31–39.

NMFS and USFWS (National Marine Fisheries Service and U.S. Fish and Wildlife Service).
2020. Endangered Species Act status review of the leatherback turtle (*Dermochelys coriacea*), 378 p. Report to the National Marine Fisheries Service Office of Protected Resources and U.S. Fish and Wildlife Service. [Available from website.]

Patiño-Martinez, J., A. Marco, L. Quiñones, and B. Godley.
2008. Globally significant nesting of the leatherback turtle (*Dermochelys coriacea*) on the Caribbean coast of Colombia and Panama. Biol. Conserv. 141:1982–1988.

R Core Team.
2019. R: a language and environment for statistical computing. R Foundation for Statistical Computing, Vienna, Austria. [Available from website, accessed July 2019.]

Snoddy, J. E., and A. S. Williard.
2010. Movements and post-release mortality of juvenile sea turtles released from gillnets in the lower Cape Fear River, North Carolina, USA. Endanger. Species Res. 12:235–247.

Swimmer, Y., R. Arauz, M. McCracken, L. McNaughton., J. Ballestero, M. Musyl,, K. Bigelow, and, R. Brill.
2006. Diving behavior and delayed mortality of olive ridley sea turtles *Lepidochelys olivacea* after their

release from longline fishing gear. Mar. Ecol. Prog. Ser. 323:253–261.

TEWG (Turtle Expert Working Group).
2007. An assessment of the leatherback turtle population in the Atlantic Ocean. NOAA Tech. Memo. NMFS-SEFSC-555, 116 p.

Wallace, B. P., R. L. Lewison, S. L. McDonald, R. K. McDonald, C. Y. Kot, S. Kelez, R. K. Bjorkland, E. M. Finkbeiner, S. Helmbrecht, and L. B. Crowder.
2010. Global patterns of marine turtle bycatch. Conserv. Lett. 3:131–142.

Wallace, B. P., C. Y. Kot, A. D. DiMatteo, T. Lee, L. B. Crowder, and R. L. Lewison.
2013. Impacts of fisheries bycatch on marine turtle populations worldwide: toward conservation and research priorities. Ecosphere 4(3):1–49.

Witt, M. J., E. Augowet Bonguno, A. C. Broderick, M. S. Coyne, A. Formia, A. Gibudi, G. A. Mounguengui Mounguengui, C. Moussounda, M. NSafou, S. Nougessono et al.
2011. Tracking leatherback turtles from the world's largest rookery: assessing threats across the South Atlantic. Proc. R. Soc., B 278:2338–2347.

National Marine Fisheries Service
NOAA

Fishery Bulletin
established in 1881

Spencer F. Baird
First U.S. Commissioner of Fisheries and founder of *Fishery Bulletin*

Age validation of the northern stock of black sea bass (*Centropristis striata*) in the Atlantic Ocean

Elise R. Koob (contact author)[1]
Scott P. Elzey[1]
John W. Mandelman[2]
Michael P. Armstrong[1]

Email address for contact author: elise.koob@mass.gov

[1] Annisquam River Marine Fisheries Station
Massachusetts Division of Marine Fisheries
30 Emerson Avenue
Gloucester, Massachusetts 01930

[2] Anderson Cabot Center for Ocean Life
New England Aquarium
1 Central Wharf
Boston, Massachusetts 02110

Abstract—Inaccurate age determinations can have serious effects on age-structured stock assessments that are used to manage fish populations. A recent push toward using an age-based model for the northern stock of black sea bass (*Centropristis striata*) led to an increase in direct aging effort in the northeastern United States. Yet, no large-scale otolith age validation study for this stock exists. We examined the annual periodicity of otolith growth in this species through marginal increment analysis with otoliths of fish from 3 age groups (fish of ages 1–2, ages 3–4, and ages 5+) and from 2 regions, north and south of the Hudson Canyon. Additionally, we validated the assignment of the first annulus through modal length–frequency analysis of young-of-the-year fish. The marginal increment ratio differed between age groups throughout the year, supporting the separation of these samples for age validation purposes. Higher ratios were observed in black sea bass from the region south of the Hudson Canyon throughout most of the year; however, fish from north of the canyon appear to accrete more otolith material during winter. Annual growth increments were deposited once per year, in spring or early summer, for all fish. In addition, absolute age was validated for the first time for this stock.

Manuscript submitted 9 April 2021.
Manuscript accepted 13 October 2021.
Fish. Bull. 119:261–273 (2021).
Online publication date: 17 November 2021.
doi: 10.7755/FB.119.4.6

The views and opinions expressed or implied in this article are those of the author (or authors) and do not necessarily reflect the position of the National Marine Fisheries Service, NOAA.

The range of the northern stock of black sea bass (*Centropristis striata*) off the coast of the northeastern United States extends from Cape Hatteras, North Carolina, to the Gulf of Maine (Mercer, 1978). This species can live to 15 years of age and reach approximately 60 cm in total length (TL) (Shepherd and Lambert, 1996). Black sea bass support an important commercial fishery and a valued recreational fishery that is worth over half the total annual landings (Musick and Mercer, 1977; NEFSC, 2017). This stock experienced a recent range expansion, linked to warming ocean trends (Bell et al., 2015; McBride et al., 2018), into coastal Maine waters—an area where this species had been rarely seen historically (Bigelow and Schroeder, 1953). The importance of this fishery, and the gaps in data on growth, age, migration patterns, and stock structure of black sea bass, led to a push for additional research on this species.

The accuracy of age data is crucial to stock assessments; errors in these estimates can undermine fisheries management and lead to overexploitation (Campana, 2001). A catch-at-age stock assessment model for the northern Atlantic stock of black sea bass was rejected in 2012, because of insufficient age data (NEFSC, 2012; ASMFC[1]). In response, agencies along the Atlantic coast of the United States began to collect and age samples of black sea bass, and a statistical catch-at-age model was accepted in 2016 (NEFSC, 2017). However, despite the increase in direct aging, there has been little effort to complete a large-scale age validation study for this stock.

Age estimates for black sea bass are primarily done by using otoliths, which are often the most accurate aging structure (Casselman, 1983). Calcium carbonate layers are accreted onto otoliths daily, and a seasonal banding pattern is formed, with bands differentiated as opaque or translucent (Campana and Thorrold, 2001). Age is determined

[1] ASMFC (Atlantic States Marine Fisheries Commission). 2013. Proceedings of the 2013 black sea bass ageing workshop, 17 p. ASMFC, Arlington, VA. [Available from website.]

by counting band pairs (one opaque and one translucent band) from the otolith core (birth) to the otolith edge (age at capture), making the assumption that one band pair equals 1 year in a fish's life (Beamish and McFarlane, 1983). Errors occur when growth layers identified as annuli (yearly growth bands) do not truly correspond to 1 year of growth (McBride, 2015). Validation of an aging method is a process that verifies that putative annuli occur once per year. Although there have been attempts to validate otolith aging methods for the northern stock of black sea bass, these studies were limited by small ranges, few age classes, or modest sample sizes (Mercer, 1978; Robillard et al.[2]). Thus far, no large-scale age validation study has been done for the northern stock of black sea bass with samples representative of those included in the stock assessment process (i.e., samples caught with a variety of gear types and from a variety of locations, sources, and age classes). Furthermore, no work has yet been published that validates the first annulus on otoliths for black sea bass in the northern stock, an imperative step to validating absolute age (Campana, 2001).

Verifying the location of the first annulus is a necessary step in validating aging methods; otherwise, age estimates could be biased in either direction (Campana, 2001). Additionally, the identification of the first annulus is often a primary source of error in aging practices (Campana, 2001) and is a known issue in reading otoliths of black sea bass (Dery and Mayo, 1988; ASMFC[1]). Reported discrepancies between identification of age-0 versus age-1 fish contributed to the exclusion of fall indices in the latest stock assessment (NEFSC, 2017).

The goal of this study was to identify the timing of annulus deposition and validate the current otolith aging method for the entire geographic range and observed age classes of the northern stock of black sea bass in the Atlantic Ocean, by using marginal increment analysis (MIA) and first annulus validation for young of the year (YOY).

Materials and methods

Sample collection and selection

The most common method of age validation is MIA, which measures growth from the last fully completed annulus to the edge of the aging structure (i.e., measures the marginal increment) at different times throughout the year (Campana, 2001). Marginal increment analysis requires samples to be collected across an entire year, preferably monthly, as well as across the observed age range of the selected species (Beamish and McFarlane, 1983; Campana, 2001). Constraints related to obtaining adequate sample sizes for individual ages led to the creation of 3 age bins, ages 1–2 (AB1), ages 3–4 (AB2), and ages 5 and older (AB3), which also account for growth differences among the age groups (Pilling et al., 2000; Winner et al., 2017). Age determinations supplied by collaborating institutions were used to classify samples to begin processing. Otoliths without an age estimate were assigned to classes on the basis of an age–length key created from samples previously aged by staff of the Massachusetts Division of Marine Fisheries (MA-DMF) (senior author, unpubl. data).

To capture potential growth variability between regions, a goal of 40 samples per age bin was chosen for MIA. Sagittal otoliths from samples of black sea bass were provided by collaborators across the northeastern United States who acquired them from both fishery-dependent and fishery-independent sources (Table 1, Fig. 1). A total of 1440 otoliths from black sea bass were initially subsampled for this study; however, 49 of those otoliths were excluded because they were broken or poorly sectioned and could not be reliably aged or measured. Additionally, marginal increment ratios (MIRs) could not be calculated for fish that were age 1 prior to annulus formation as a result of the use of 1 January as the year-class advancement date (Dery and Mayo, 1988) and were removed from analysis (number of samples [n]=23). Samples of black sea bass used for MIA (n=1335) were collected every month of the year, and they ranged in size from 100 to 605 mm TL and in age from 1 to 12 years (Table 2, Fig. 2). Sex data was available for 854 samples: 490 females (110–500 mm TL) and 364 males (130–546 mm TL).

Assessment of the first annulus can be completed 1) by measuring the completed first annulus of YOY in the season of annulus formation and 2) by tracking the modal length frequency of the smallest fish in the population to confirm that measured samples are YOY (Campana, 2001; Carvalho et al., 2017). Age-0 samples for first annulus validation were collected in the fall during the MA-DMF resource assessment survey (September 2017, n=30) and during the Northeast Fisheries Science Center (NEFSC) bottom-trawl survey (October 2016, archive, n=3). Age-1 samples caught in the summer and used in MIA were also used for comparison. These samples were collected during the MA-DMF ventless-trap survey (July and August 2015–2017, otolith archive, n=36). Total lengths ranged from 35 to 120 mm for age-0 fish and from 110 to 207 mm for age-1 fish.

A reference collection (n=100) with ages spanning from 0 to 10 years was created by using otoliths archived by the MA-DMF. These samples were used to assess reader error before and after otolith aging was completed for this project and were independent of the samples used in MIA.

Sample preparation

Age estimates made by using whole otoliths tend to underestimate fish age and use of otolith sections has resulted in higher accuracy (Hyndes et al., 1992; Fowler and Short, 1998). Therefore, sectioned otoliths were used in this study. Additionally, completing marginal increment measurements

[2] Robillard, E., J. W. Gregg, J. Dayton, and J. Gartland. 2016. Validation of black sea bass, *Centropristis striata*, ages using oxytetracycline marking and scale margin increments, 17 p. Stock Assess. Rev. Comm., SARC 62 working paper. [Available from Northeast Fish. Sci. Cent., Natl. Mar. Fish. Serv., NOAA, 166 Water St., Woods Hole, MA.]

Table 1

States of the northeastern United States in whose waters off the Atlantic coast black sea bass (*Centropristis striata*) were captured during 2013–2017, number of samples (n), sampling years, range of final age estimates for samples, and fishery type in which and gear type by which fish were captured. Otoliths from sampled fish were used in marginal increment analysis and first annulus validation. Gear types include bottom trawl, ventless trap, gill net, and hook and line. The following collaborators were the sources of samples: Massachusetts Division of Marine Fisheries (MA-DMF), North Carolina Department of Environment and Natural Resources (NC-DENR), NOAA Northeast Fisheries Science Center (NEFSC), Northeastern University, Rhode Island Department of Environmental Management (RI-DEM) in collaboration with the Commercial Fisheries Research Foundation (CFRF) and Virginia Institute of Marine Science (VIMS), and Rutgers University.

Capture location	n	Sampling years	Final age range (years)	Fishery type	Gear type	Source
Massachusetts	538	2013–2017	0–8	Independent	Trawl, trap	MA-DMF
Massachusetts–North Carolina	201	2013–2016	2–11	Dependent	Trawl	NC-DENR
Massachusetts–North Carolina	377	2015–2017	0–6	Independent; Dependent	Trawl	NEFSC
Maine and Massachusetts	90	2013–2016	1–5	Independent; Dependent	Trap, hook and line	Northeastern University
Rhode Island	69	2017	2–7	Dependent	Trawl, trap, gill net	RI-DEM, CFRF, VIMS
New Jersey	93	2017	1–12	Independent	Trap, hook and line	Rutgers University

on whole otoliths is difficult because of their curvature and the presence of broad, diffuse bands; whereas, sectioned otoliths have a crisp line at the distal edge of an annulus from which to measure. Left-sided otoliths were selected preferentially for consistency. Otoliths were embedded with epoxy resin and hardener (West System[3], Gougeon Brothers Inc., Bay City, MI) in silicone molds. Transverse sections (0.5 mm thick) were cut along the dorsoventral plane, containing the otolith core (Fig. 3A), by using an IsoMet Low Speed Saw with a diamond blade (Buehler, Lake Bluff, IL). All otolith preparation used these methods, including preparation of samples for MIA, first annulus analysis, and the reference collection.

Otolith aging and measurements

In black sea bass, the outside edge of the opaque growth zone formed in winter is considered the annulus (Dery and Mayo, 1988). A date of 1 January was used for year-class advancement. Age determinations were made under a compound microscope (100× magnification) by placing sectioned otoliths on a glass slide with mineral oil. Each otolith was aged independently by 2 experienced readers without knowledge of fish size, capture location, or any previous age interpretations. If ages differed between readers, a consensus reading was required for final age determination. These ages were used to group samples into the 3 age bins for analysis, replacing the initial determination used to bin samples during the sample selection. Final ages for the reference collection were made following these same methods. To assess precision and bias, each person read otoliths in the reference collection (with samples randomized prior to each reading) before and after MIA samples were read.

Annulus measurements were made by using Image-Pro Premier, vers. 9.1 (Media Cybernetics Inc., Rockville, MD), a compound microscope-camera system (Axiostar Plus microscope, ZEISS Microscopy, Jena, Germany, and QImaging MicroPublisher camera, Teledyne Photometrics, Tucson, AZ). A straight line was drawn along the dorsal side of the sulcal groove, from the otolith core to otolith edge (radius), and the distal edge of each opaque band was marked (Fig. 3B). Measurements (in millimeters) from otolith core to each marked annulus were generated by the software on the basis of a coordinate plane.

Statistical analysis

All analyses and visualizations for this project were run by using statistical software R, vers. 3.6.1 (R Core Team, 2019). Paired ages from readings of black sea bass otoliths were evaluated for precision and aging bias by using Chang's coefficient of variation (CV) (Chang, 1982) and a modification of the Bland–Altman bias plot (McBride, 2015). Additionally, the precision of the age estimates of each reader was assessed by comparing each reader's reference collection session and the reference collection final ages. A CV below 5% is recommended for precision among readers for aging studies (Campana, 2001; McBride, 2015). Coefficients of variation were produced by using the FSA package, vers. 0.8.25 (Ogle et al., 2019), in R.

Marginal increments are expressed as a proportion of the previous year's growth (Hood et al., 1994; Winner

[3] Mention of trade names or commercial companies is for identification purposes only and does not imply endorsement by the National Marine Fisheries Service, NOAA.

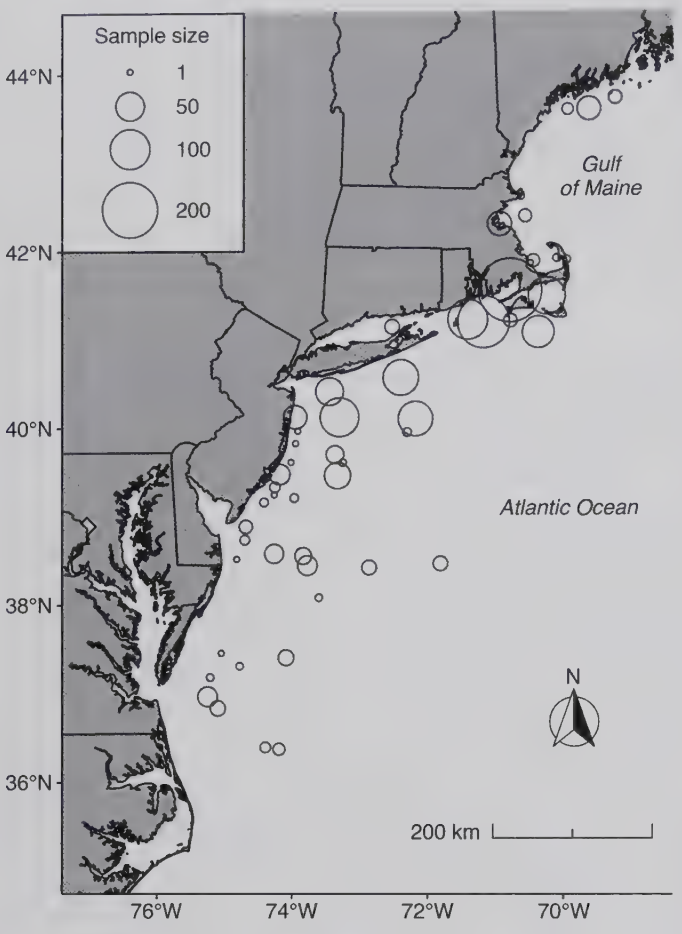

Figure 1

Map of locations where black sea bass (*Centropristis striata*) were caught in the Atlantic Ocean off the northeastern United States during 2013–2017. Sagittal otoliths were removed from sampled fish and used for marginal increment analysis and first annulus validation. Size of circles indicates the number of samples collected at each location.

et al., 2017), as the MIR (Vilizzi and Walker, 1999; Zlokovitz et al., 2003). If annuli are formed once per year, monthly MIR should indicate a sinusoidal pattern with only one minimum per year, when annulus formation is complete and new growth begins (Wenner et al., 1986; Pilling et al., 2000). Marginal increment ratios were calculated following Condini et al. (2014) by dividing the marginal increment (completed edge growth) by the measurement of the presumed previous year's growth (full band pair, one translucent band and one opaque band) (Fig. 3B):

$$MIR = (R_t - R_{t-1}) / (R_{t-1} - R_{t-2}),$$

where R_t = the otolith radius (core to edge);
R_{t-1} = the measurement from otolith core to the distal edge of the last opaque band; and
R_{t-2} = the measurement from otolith core to the distal edge of the penultimate opaque band.

A 2-way analysis of variance (ANOVA) was used to assess average MIRs between different times of year and among age bins, as recommended by Campana (2001). The Akaike information criterion (AIC) was used to identify the best model for analysis, varying predictors (*Month Bin*, *Age Bin*, and *Region*), additivity, and interactions. Month bins (e.g., January–February and March–April) were used instead of individual months because missing data would have precluded interactive models from running. Missing data were also the reason that region (i.e., capture location) could be included only as an additive predictor and not as an interactive one. The regions designated for this analysis were north and south of the Hudson Canyon, as described in the report for the latest stock assessment (NEFSC, 2017). This canyon begins 100 km from the mouth of the Hudson River and extends approximately 600 km to the southeast (NEFSC, 2017). Additionally, monthly average MIRs were used to visually assess the timing of annulus formation for each age bin.

The possibility of differences in growth of black sea bass between regions (Dery and Mayo, 1988), as well as the recent separation of the northern stock into 2 subunits north and south of the Hudson Canyon, motivated an analysis that included *Region* as an interactive predictor. In a 3-way ANOVA, seasons were used instead of month bins because of missing data. Seasons, chosen on the basis of information available about migration of black sea bass (they arrive inshore by April and leave by October or November; Drohan et al., 2007), were as follows: January, February, and March (winter); April, May, and June (spring); July, August, and September (summer); and October, November, and December (fall). Regions were designated as described previously, although a difference in sample sizes should be noted (north: n=970; south: n=365). Methods used to account for this unbalanced design are described at the end of this section. The AIC was used to identify the best model for analysis, varying predictors (*Season*, *Age Bin*, and *Region*), additivity, and interactions.

Because an ANOVA does not account for the cyclical nature of MIRs and because this lack of adjustment is a noted source of concern for MIA studies based solely on this statistical test (Okamura et al., 2013), a circular-linear model (see Okamura et al., 2013) was fit to the data from this study to analyze how many cycles (i.e., annuli) exist in a time span of 1 year. This method was used to assess AIC values for 3 models: models with no cycle (model N), 1 cycle (model A), and 2 cycles (model B) in the MIR data. This method was used separately for each age bin as well as for each region (with age bins combined). This analysis was completed in R, by using

Table 2

Number of samples of black sea bass (*Centropristis striata*), by month of capture and age estimate, from which sagittal otoliths were removed and used for marginal increment analysis. Ages in this table represent the final age assignments used in this study. Age bin 1 (AB1), age bin 2 (AB2), and age bin 3 (AB3) are provided to indicate which ages are included in each bin. Samples were collected in the Atlantic Ocean off the northeastern United States during 2013–2017. Blank cells indicate no otolith samples were available for that age bin and month combination.

Age bin	Age (years)	Month												
		Jan	Feb	Mar	Apr	May	Jun	Jul	Aug	Sep	Oct	Nov	Dec	Total
AB1	1				1		2	15	21	17	21	7		84
	2		13	22	24	42	43	29	23	29	32	18	6	281
AB2	3	15	17	20	7	24	13	21	20	22	15	10	16	200
	4	25	32	25	12	16	36	32	27	22	20	30	25	302
AB3	5	42	46	39	41	27	27	27	28	27	7	2	19	332
	6	1	4	9	5	16	15	12	11	10	1		4	88
	7		2	4	1	6		4	1	2			7	27
	8	1			2	1	1	1	1	1			5	13
	9	3	1		2									6
	11												1	1
	12			1										1
Total		87	115	120	95	132	137	141	132	130	96	67	83	1335

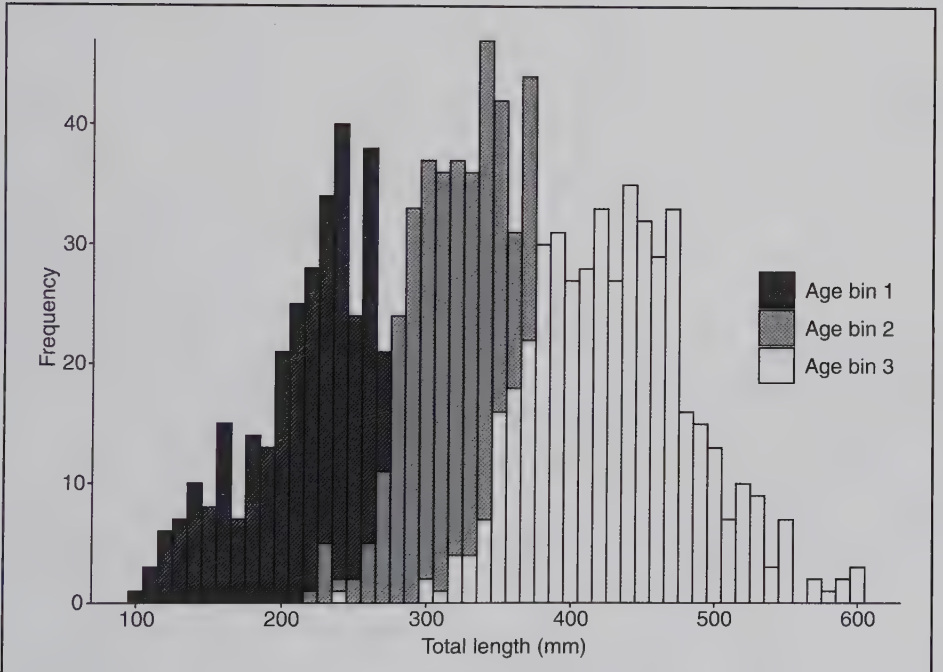

Figure 2

Length–frequency histograms for each age bin of black sea bass (*Centropristis striata*) from which sagittal otoliths were removed and used in marginal increment analysis. Samples were captured in the Atlantic Ocean off the northeastern United States between 2013 and 2017. Age bin 1 includes ages 1–2, age bin 2 comprises ages 3–4, and age bin 3 includes ages 5+.

code included in the supplemental material (SIII) of Okamura et al. (2013).

Measurements of otoliths from samples of age-0 black sea bass collected in the fall and age-1 black sea bass collected in summer were compared by using Welch's 2-sample *t*-test for first annulus validation. For age-1 fish sampled in summer, measurements were also compared with the first annulus measurements of all samples used

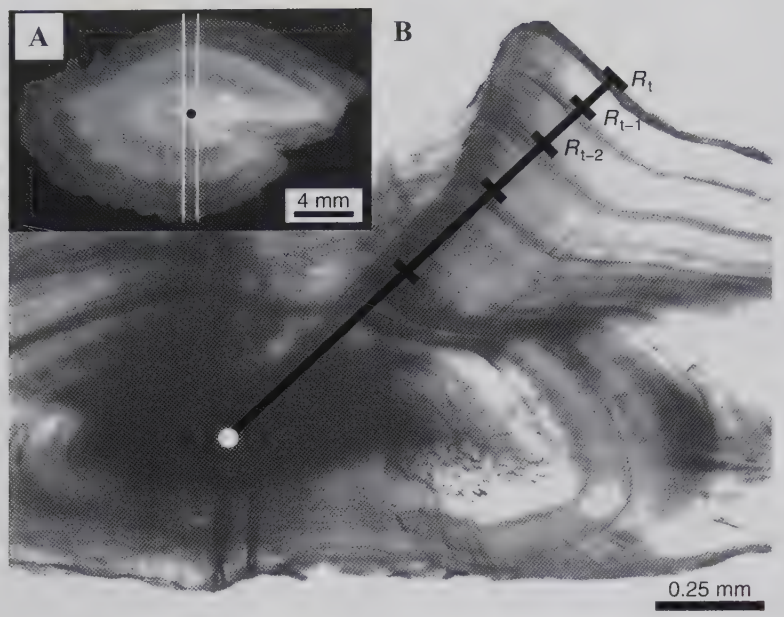

Figure 3

(**A**) Position of the transverse dorsoventral section (0.5 mm thick) taken through the core (black dot) of a whole sagittal otolith from a black sea bass (*Centropristis striata*) collected from Massachusetts in May 2015. (**B**) Measurements for marginal increment analysis on a sectioned otolith taken from the core (white dot) to the distal edge of each annulus (black bars); the black sea bass from which this otolith was removed was captured from Massachusetts in May 2014. The measurements are R_t, which depicts the otolith radius (core to edge); R_{t-1}, the distance to the final annulus (core to the last opaque band); and R_{t-2}, the distance to the penultimate annulus (core to the penultimate opaque band). The equation used to determine the marginal increment ratio (MIR) is $MIR=(R_t-R_{t-1})/(R_{t-1}-R_{t-2})$.

in MIA to confirm proper identification of the samples collected for this study. Length–frequency plots of the smallest fish (first 2 length modes) captured during the fall resource assessment survey (September 2016–2017) and the summer ventless trap survey (July–August 2016–2017) were evaluated to confirm identification of the fall age-0 and summer age-1 samples as YOY. Differences in first annulus measurements between otoliths from fish collected in the regions north and south of the Hudson Canyon were also compared with Welch's 2-sample *t*-test.

Assumptions for all statistical tests were evaluated by using visual diagnostic plots and were found to conform to assumptions of normality and homogeneity of variance. Type III sums of squares were used for both ANOVAs because of the unbalanced data. Post hoc multiple comparison analyses were conducted by using estimated marginal means, because sample sizes were not balanced among factor levels (Lenth, 2019), and Tukey's honestly significant difference test. A significance level of 0.05 was used in all statistical tests in this study. Model selection, ANOVAs, post hoc analyses, and visualizations were done by using R and the following packages in R: car, vers. 3.0-3 (Fox and Weisberg, 2019), emmeans, vers. 1.4.1 (Lenth, 2019), multcomp, vers. 1.4-10 (Hothorn et al., 2008), and ggplot2, vers. 3.2.1 (Wickham, 2016).

Results

Marginal increment analysis

Initial independent age determinations agreed for 1222 otoliths (89%); a consensus reading was required for the remaining samples. Precision was high and bias was low between readers in this study (CV=2.2%) (Fig. 4). Additionally, the precision of each reader was high (CVs <2%) for both individuals from the reference collection, before and after samples collected for this study were examined. For samples that had been aged previously, final age estimates from this study were compared with previous estimates from collaborators, and age determinations differed for 107 fish (11%) and had a CV of 2.5%. There was no bias.

The interactive model with the predictors of *Month Bin* and *Age Bin* had the lowest AIC value and was selected for further analysis. An interaction between *Month Bin* and *Age Bin* for MIR (F=13.795, df=10, P<0.0001) revealed the lowest mean MIR occurred for AB1, followed by AB2 and AB3 (P<0.01) for the month bins January–February, March–April, and May–June; however, the remaining month bins had slightly different patterns. The MIRs for AB1 and AB2 were similar in July–August (P=0.3143) and November–December (P=0.3178) but were smaller than those for AB3 (P<0.001). Also, MIRs for AB2 and AB3 were similar in September–October (P=0.8206) but were larger than those for AB1 (P<0.001).

Campana (2001) noted that a minimum in the MIR should occur once per year and be significantly different from the MIR in other times of the year. Figure 5, A–C, shows that the minimum MIR in each age bin (indicated with the letter *a* above boxes for month bins) occurred once per year and was different from that of other month bins (P<0.0001). The only exception was for AB3, which appeared to have a minimum that extended from July–August through September–October (P=0.9849); whereas the minimums for AB1 and AB2 were both in July–August only. Plots of raw data show the monthly MIR for AB3 declined in July prior to reaching a minimum in August (Fig. 6C). Similarly, a depression in MIR occurred in May–June for AB1 (Figs. 5A and 6A). For all age bins, MIR gradually increased throughout the year after the minimum occurred.

The model with 2-way interactions between *Age Bin*, *Season*, and *Region* had the lowest AIC value and was

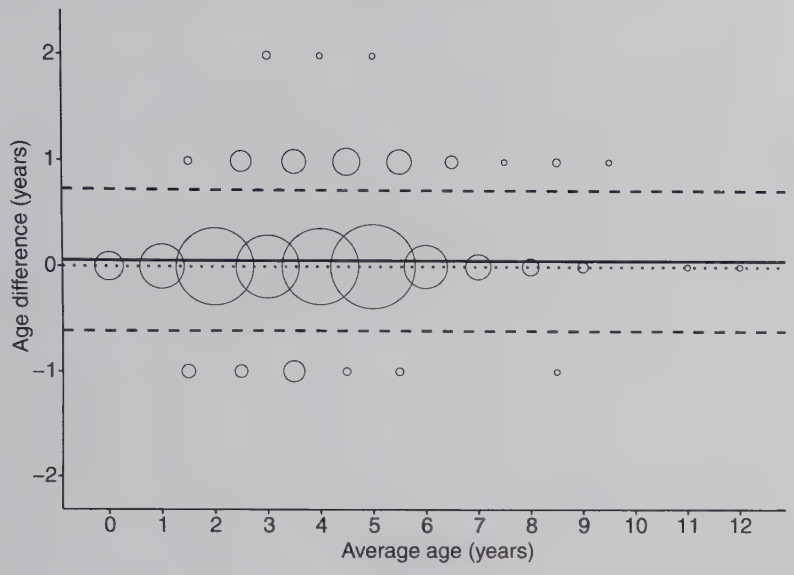

Figure 4

Bland–Altman bias plot of differences in age determinations between readers (reader 2–reader 1) of sagittal otoliths from black sea bass (*Centropristis striata*) caught in the Atlantic Ocean off the northeastern United States during 2013–2017. The dotted black line (located at 0) represents no bias in age estimates, the solid black line indicates the degree and direction of bias in age estimates for samples used in this study, and the dashed black lines indicate 95% confidence limits. Size of circles indicates the number of samples.

selected for further analysis. No interaction between *Age Bin* and *Region* was observed (F=1.717, df=2, P=0.1800); however, there was an interaction between *Season* and *Region* (F=3.593, df=3, P=0.0132). Marginal increment ratios were higher in the winter, spring, and fall for otoliths from fish sampled south of the Hudson Canyon than those for otoliths from fish collected north (P<0.010, P<0.05, and P<0.0001, for each season respectively), but MIRs for regions were similar in summer (P=0.4486). Figure 7, A and B, shows that there was one minimum MIR per year for each region and that it occurred in summer and was different from the MIRs for all other seasons (P<0.0001). This minimum occurred once per year for each region and was verified by plotting monthly means (Fig. 6, D and E). An interaction was also detected between *Season* and *Age Bin* (F=16.602, df=6, P<0.0001), corroborating results from the previous model, meaning there were differences in MIR between age bins in each season (P<0.0100). The only variant was that MIRs for AB1 and AB2 in summer were similar (P=0.4830), an outcome that was also observed in the model with the predictor *Month Bin*.

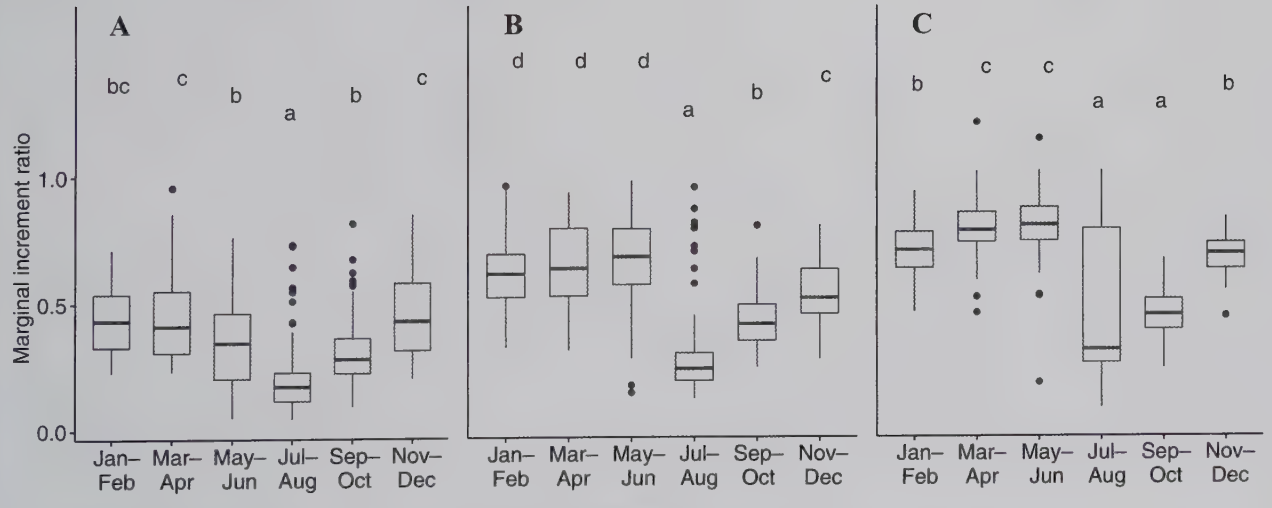

Figure 5

Box plots of marginal increment ratios for sagittal otoliths from black sea bass (*Centropristis striata*) captured in the Atlantic Ocean off the northeastern United States during 2013–2017, by month bin for (**A**) age bin 1 (ages 1–2), (**B**) age bin 2 (ages 3–4), and (**C**) age bin 3 (ages 5+). Letters above the boxes denote significant differences (significance level=0.05; tested with Tukey's honestly significant difference by using estimated marginal means). In each box plot, the thick horizontal line indicates the median, the areas above and below the median represent the 25th and 75th percentiles, the thin vertical lines indicate the 95% confidence limits, and the points indicate outliers.

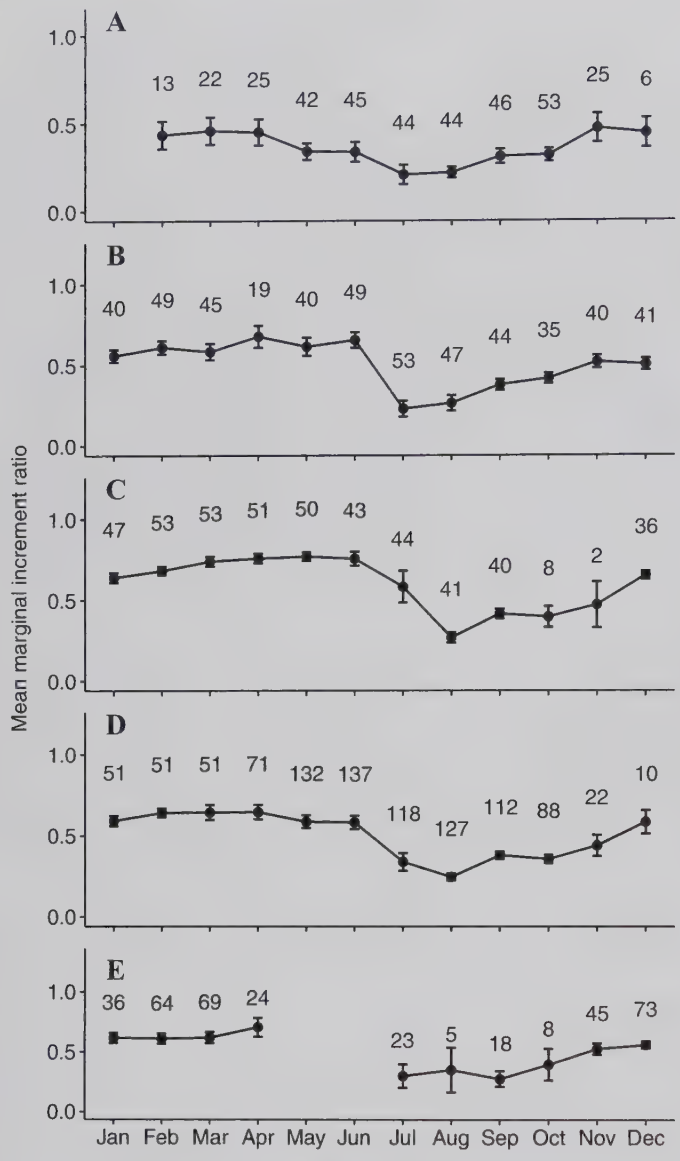

Figure 6

Monthly mean marginal increment ratios for black sea bass (*Centropristis striata*) caught in the Atlantic Ocean off the northeastern United States during 2013–2017, for (**A**) age bin 1 (ages 1–2), (**B**) age bin 2 (ages 3–4), and (**C**) age bin 3 (ages 5+) and for the regions (**D**) north and (**E**) south of the Hudson Canyon. Numerals above data points denote the number of samples for each month. Error bars indicate 2 standard errors of the mean.

Results of assessment with AIC values for the Okamura et al. (2013) circular-linear models (hereafter referred to as *the Okamura analysis*) indicate that 1 cycle was completed within a time span of 1 year for each age bin and both regions (i.e., model A had the lowest AIC values for all iterations). This finding confirms results from the interactive models and mean MIR visualizations, which indicate that the MIR reaches one minimum per year (Figs. 5, 6, and 7).

Young of the year: measurements and length–frequency analysis

Radius measurements of otoliths from age-0 samples collected in the fall were smaller than the first annulus measurements of age-1 samples (t =–11.92, df=67, P≤0.0001). The mean radius of otoliths from age-0 fish was 0.36 mm, compared with a mean annulus measurement of 0.60 mm for otoliths from age-1 samples. The first annulus measurements of otoliths from age-1 samples collected in summer were similar to the first annulus measurements of otoliths from all MIA samples (t=1.01, df=37, P=0.3205). Measurements of the first annulus (for all samples used in MIA, n=1299) range from 0.41 mm to 0.92 mm with a mean of 0.61 mm. Mean first annulus measurements were similar between regions (t=–1.19, df=629, P=0.2365), at 0.61 mm for otoliths of samples from the region north of the Hudson Canyon and 0.62 mm for otoliths of fish from the region to the south.

Results of modal length–frequency analysis done with data from the resource assessment and ventless trap surveys confirm that samples used for first annulus validation were YOY (Fig. 8). A distinct modal separation between ages was apparent in the samples used for MIA, and length modes of the smallest fish overlapped in each survey. Measured lengths of age-0 fish collected in the fall and used in this study were from 35 to 120 mm TL, comparable to the length range for the first mode of fish captured in the fall during the resource assessment survey, from 20 mm TL to approximately 125 mm TL (Fig. 8A). Age-1 fish caught in summer and used in this study had lengths of 110–207 mm TL; whereas, lengths of the smallest mode of black sea bass collected in summer during the ventless trap survey were 60 mm TL to approximately 180 mm TL (Fig. 8B).

Discussion

Annulus periodicity and timing

The results of this study verify that one opaque band and one translucent band were deposited per year in otoliths of black sea bass. One clear minimum MIR was observed, and otolith growth continued throughout the year for samples in each age bin and from both regions. This sinusoidal pattern is consistent with results of other MIA studies that have confirmed that one annulus is deposited per year (Wenner et al., 1986; Vilizzi and Walker, 1999; Pilling et al., 2000). Additionally, the Okamura analysis confirmed these results, also indicating that 1 cycle occurred per year in each age group and in each region.

Annulus deposition is considered finished when new translucent growth is observed at the otolith edge. In other

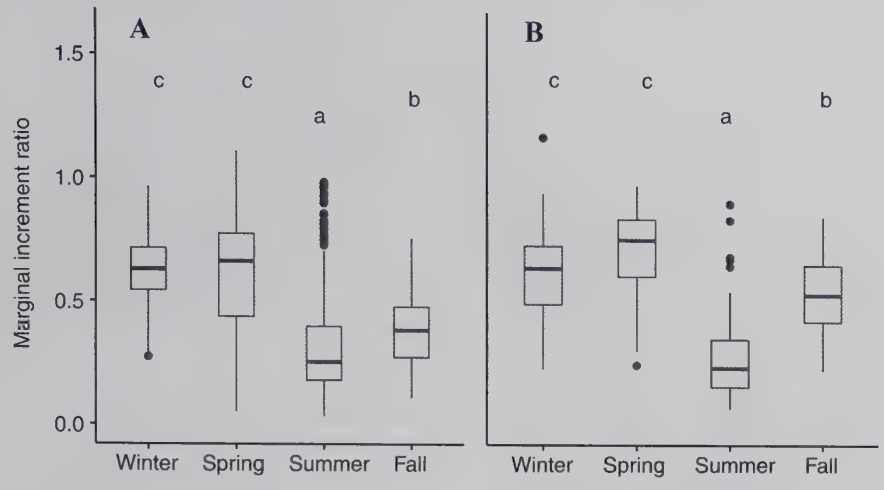

Figure 7

Box plots of marginal increment ratios for sagittal otoliths from black sea bass (*Centropristis striata*) captured in the Atlantic Ocean off the northeastern United States during 2013–2017, by season for the regions (**A**) north and (**B**) south of the Hudson Canyon. Letters above the boxes denote significant differences (significance level=0.05; tested with Tukey's honestly significant difference by using estimated marginal means). In each box plot, the thick horizontal line indicates the median, the areas above and below the median represent the 25th and 75th percentiles, the thin vertical lines indicate the 95% confidence limits, and the points indicate outliers.

words, the opaque annulus is being completed when MIRs are at a maximum before dropping to a minimum, which indicates new growth. The timing of annulus completion in this study was dependent on age bin. Maximum MIR for AB1 was observed in March–April (Fig. 6A); however, the decline in May–June (prior to the minimum in July) indicates that some fish were completing the annulus in these months. Therefore, annulus completion occurred between April and June for AB1. This variability was not surprising given the extensive spatial range from which these samples were collected (from Maine to Virginia). Miller et al. (2016) reported that overwintering adult black sea bass gathered along a defined shelf contour but that juveniles were scattered across the shelf and were exposed to a wider range of temperatures and salinities. Variation between individuals in this youngest age group, therefore, may be magnified by the environmental conditions experienced while overwintering.

The maximum MIR for AB2 was observed in June, followed by a stark decline to a minimum in July and August and a continuation of growth thereafter (Fig. 6B). Annulus completion largely occurred in June for this age bin, and new, translucent material began to be deposited on otoliths in July. Reduced variability in the timing of annulus deposition in this age group, compared with that in AB1, was likely a result of a more consistent growth rate between ages and regions.

Maximum and minimum MIRs for AB3 occurred in June and August, respectively (Fig. 6C). The mean MIR in July fell between these extremes, similar to the pattern observed in May–June in AB1. This finding indicates that some otoliths had new, translucent growth in July (a small amount of growth at the otolith margin); whereas, for others the opaque annulus was still being deposited (a large amount of growth at the otolith margin). The delay in annulus deposition for some samples in AB3 (with the minimum MIR occurring in August, as compared with in July for AB1 and AB2) could be related to energy allocated to spawning rather than to growth during this period. Morales-Nin and Ralston (1990) observed a decline in otolith growth as spawning season progressed and stated, "during the maturity period the metabolic energy seems to be diverted from growth, causing the formation of thin increments [as] seasonal growth rings." The northern stock of black sea bass typically spawns between April and October, with spawning peaking in June–July (Mercer, 1978; Wuenschel et al., 2013; McBride et al., 2018). Of the 44 black sea bass in AB3 that were measured in July, 25 samples were classified as fish in spawning condition (i.e., maturity data associated with otolith samples indicated the fish were ripe or ripe and running).

In other studies of black sea bass in the northern stock, annulus formation appears to have been associated with spawning period (Mercer, 1978; Alexander, 1981; Caruso, 1995); however, this connection may be coincidental (Beckman and Wilson, 1995). Instead, annulus deposition timing is likely the result of a combination of environmental and physiological processes (Fowler and Short, 1998). Additionally, black sea bass have a variety of reproductive strategies, including maturation as young, small males

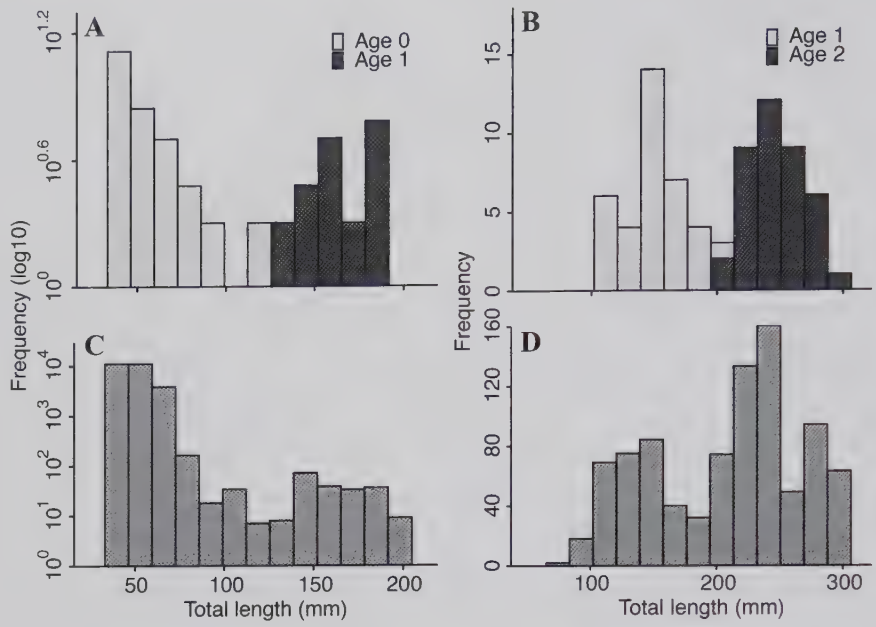

Figure 8

Length–frequency distributions of black sea bass (*Centropristis striata*) from the Atlantic Ocean off the northeastern United States whose sagittal otoliths were used in marginal increment analysis and first annulus validation: (**A**) age-0 and age-1 fish captured in the fall (September and October 2016–2017) and (**B**) age-1 and age-2 fish captured in summer (July and August 2015–2017). Length–frequency distributions are also presented for (**C**) black sea bass ≤220 mm in total length (TL) captured in the fall (September 2016–2017) during the Massachusetts Division of Marine Fisheries (MA-DMF) resource assessment survey and (**D**) black sea bass ≤310 mm TL captured in summer (July and August 2015–2017) during the MA-DMF ventless trap survey.

(Provost et al., 2017), that could also affect otolith growth in young age groups (<3 years) as well. Instead, the variability in annulus deposition for AB3 in this study could be due to the difficulty of accurately measuring growth at the otolith edge of older fish. The decline in otolith growth with increasing age made it challenging to discern the start of translucent edge growth; therefore, an apparent delay in annulus deposition could be an artifact of the measurement method. Mercer (1978) noted a delay in annulus deposition in age-5 black sea bass captured off the mid-Atlantic coast; however, sample sizes were low, and whole otoliths were used. As discussed previously, measurements on whole otoliths are less precise because of diffuse banding patterns and otolith curvature.

Otolith annulus deposition for black sea bass in the northern stock has been reported to occur in a range of months, from May and June (Dery and Mayo, 1988; Robillard et al.[2]) to August (Alexander, 1981). Mercer (1978) concluded that opaque deposition occurred in April and May, but the results from that study were highly variable; the drop in mean marginal increment in that study occurred from March through July in the ages examined (ages 1–5). Wenner et al. (1986) conducted marginal increment analysis on otoliths from black sea bass in the southern Atlantic stock and found that annual deposition of growth bands occurred in April and May for ages 0–10 combined. The timing of annulus deposition on otoliths from black sea bass in our study appears to generally agree with these previous reports (spring or early summer); however, detailed comparisons were difficult because of limitations in sampling locations, gear types, age range representation, or sample sizes in these studies.

First annulus validation

None of the previously mentioned published works on aging of black sea bass in the northern stock include validation of the first annulus. Hales and Able (1995) and McBride et al. (2018) conducted studies to validate the otolith daily aging method; however, in both studies fish less than 1 year old were used. Marginal increment analysis can be used to verify annual banding deposition patterns in an aging structure; however, if the first annulus had not been validated, values produced by using that aging method could have been incorrect by a consistent amount. In this study, the location of the first annulus was validated by measuring annuli on otoliths from YOY: the mean measurement for the first annulus in age-1 samples was larger than the expected total radius of an age-0 fish caught in the previous fall. Additionally, the first annulus measurements from

age-1 fish and the first annulus measured on all samples used in MIA were similar, indicating that it was identified correctly in the MIA.

The age-0 and age-1 samples in this study were confirmed to be YOY by comparing their modal length frequencies to the length frequencies of the smallest black sea bass caught in the fall during the resource assessment survey and in the summer during the ventless trap survey (Fig. 8). The similarities between the length frequencies are clear, and the designation of the samples in this study as YOY was appropriate. It should be noted that the samples measured for first annulus validation in this study were all from waters of Massachusetts. The similarity in first annulus measurement between these samples and all the samples used in MIA, as well as the previously mentioned similarity in mean first annulus measurements between regions, north and south of the Hudson Canyon, indicates that the first annulus validation completed in this study is applicable to the whole northern stock.

Age-bin separation

Results of this study confirm that separating samples into age bins was necessary for accurate age validation for this species. As a fish ages, somatic growth slows and otolith growth bands become closer together (Beamish and McFarlane, 1983). Otolith growth in a fish's first year is expected to be greater than growth in its second year, which will be greater than growth in its third year, and so on until, at a certain size or age, growth becomes more consistent. Differences in mean MIR between age bins throughout the year indicate that otolith deposition varies with age. For example, otoliths from fish in AB1 had a lower mean MIR than those from the other 2 age bins throughout most of the year. Additionally, the peak MIR for this age bin was less than 0.5. Marginal increment ratios that approach 1.0 would indicate that the completed edge growth on an otolith equals the growth of the penultimate annulus. The low peak MIR for AB1 signifies that there was rapid growth in the penultimate annulus followed by a decline in growth in the following year, as expected for this age group.

Conversely, AB3 had the highest MIRs throughout the year and came closer to approaching 1.0 at the time of annulus completion (mean MIR: 0.76, in May–June). Otoliths in this age bin have a higher proportion of edge growth compared with that of the penultimate annulus because growth has slowed, and annuli measurements were more consistent. This pattern is supported by the observed somatic growth of black sea bass with age, where the rapid growth experienced by younger fish slows considerably by ages 5–6 (NEFSC, 2017; McMahan et al., 2020). As expected, MIRs for AB2 fall between the values for AB1 and AB3 throughout most of the year. The effect of the interaction between *Age Bin* and *Month Bin* in the first model did not affect annulus validation, but it does further indicate the varied growth patterns throughout the year for otoliths from black sea bass in these age bins.

Regional differences within the northern stock

The documented variability of otolith growth for black sea bass by location (Dery and Mayo, 1988), as well as the recent separation of the northern stock into 2 subunits, motivated an analysis of possible differences in otolith growth between the regions north and south of the Hudson Canyon. The interaction between *Age Bin* and *Season* corroborated findings from the model with the predictor *Month Bin* discussed previously. No interaction between *Age Bin* and *Region* indicates that there was no regional difference in otolith edge growth within each age bin. The interaction between *Season* and *Region*, however, indicates that there was variability in otolith edge growth between regions throughout the year.

Higher MIRs were observed for otoliths from fish caught in the region south of the Hudson Canyon in the winter, spring, and fall, but there was no difference in MIRs between regions in summer. The similarity of MIRs in summer is not surprising because the absolute amount of growth following annulus deposition is small (Mercer 1978; Robillard et al.[2]). Differences throughout the rest of the year indicate that fish from south of the Hudson Canyon completed a higher proportion of the previous year's growth at these times than fish from the north, indicating that overall annual otolith growth may be lower for fish from the region south of the Hudson Canyon. Additionally, fish from the south had an 81% increase in edge growth from summer to fall, compared with a 23% increase achieved by fish from the north in the same period. Instead, fish from north of the Hudson Canyon had a 60% increase in growth from fall to winter; whereas, the increase in growth for the region south was 14%.

These findings are in line with those of previous research, but additional work is needed. In several studies, black sea bass were larger and had faster growth rates throughout the year at higher latitudes (Alexander, 1981; Dery and Mayo, 1988; Kolek[4]; Caruso, 1995; McMahan et al., 2020). McMahan et al. (2020) postulated that black sea bass from northern regions (e.g., north of Cape Cod) may either have adapted to grow in lower temperatures or have countergradient variation, with more growth achieved in the shorter growing season (i.e., winter). The differences in migration patterns between the 2 populations (i.e., east–west for fish south of the Hudson Canyon and north–south for fish in the north region) likely result in exposure to different temperatures throughout the year. This temperature variability could explain the differences in otolith growth between the 2 groups of fish in this study; however, a closer look at growth is needed to address this topic and should be considered for future research.

Although there were differences in otolith deposition between fish from the 2 regions, the otolith aging method

[4] Kolek, D. 1990. Homing of black sea bass, *Centropristis striata*, in Nantucket Sound, with comments on seasonal distribution, growth rates, and fisheries of the species. MADMF Black Sea Bass Investig. Intern. Rep., 9 p. [Available from Mass. Div. Mar. Fish., 251 Causeway St., Boston, MA 02114.]

was validated for each region (one minimum MIR in summer, with 1 cycle present in the Okamura analysis). Annulus deposition was completed in June for black sea bass from the region north of the Hudson Canyon, with otolith growth for some fish lagging into July (Fig. 6D). Annulus deposition for otoliths from fish caught south of the Hudson Canyon was completed on or after April but before July, indicating a similar timing of late spring or early summer for fish in this region.

Conclusions

Results from this study indicate that one opaque annulus per year is deposited on otoliths of black sea bass in late spring or early summer. Younger fish (ages 1–4) completed annulus formation earlier in the season than older fish, although this finding is likely an artifact of measurement difficulty for the older age groups. For fish in all age groups, annulus formation was completed and new translucent material had begun by July or August. Although there were slight differences in material deposition between regions, the otolith aging method was validated for samples captured from both regions. Additionally, the first annulus was confirmed in this study, validating, in conjunction with MIA, the absolute age of black sea bass in the northern stock.

The results of this study help ensure the accuracy and precision of aging practices for black sea bass by validating the otolith aging method used by agencies and organizations across the Atlantic coast of the northeastern United States. In this study, we included samples that reflect age data used in black sea bass stock assessments (i.e., samples captured from the entire spatial range of the northern stock, with a variety of methods, in various types of fisheries, and from multiple age groups). Age data produced by using a validated age determination method will reduce uncertainty in the stock assessment. Several agencies from the northeastern United States supply age estimates for the assessment of the northern stock of black sea bass. Scales have largely been phased out because of the preference for otoliths; however, variation exists between the use of whole otoliths, sectioned otoliths, or a combination of both (ASMFC[5]). Sectioned otoliths—which were used for age validation in this study—tend to be clearer, easier to interpret, and provide more accurate age determinations (Hyndes et al., 1992; Fowler and Short, 1998). We therefore recommend abiding by the results presented here for aging of black sea bass in the future.

Acknowledgments

We thank E. Robillard, S. Sutherland, and G. Shepherd of the NEFSC, D. Zemeckis and M. Burglund of Rutgers University, M. McMahan of Northeastern University, T. VanMiddlesworth of the North Carolina Department of Environment and Natural Resources, N. Lengyel of the Rhode Island Department of Environmental Management, T. Heimann of the Commercial Fisheries Research Foundation, and J. Garland of the Virginia Institute of Marine Science for samples and contacts and K. Fine for otolith aging. Funding was received from the National Marine Fisheries Service (award no. NA17NMF4740143), in cooperation with the Atlantic Coastal Cooperative Statistics Program, and from the U.S. Fish and Wildlife Service's Sport Fish Restoration Program (award no. F17AF00216 and no. F18AF00918).

[5] ASMFC (Atlantic States Marine Fisheries Commission). 2018. Report of the quality assurance/quality control fish ageing workshop, 50 p. ASMFC, Washington, D.C. [Available from website.]

Literature cited

Alexander, M. S.
1981. Population response of the sequential hermaphrodite black sea bass, *Centropristis striata*, to fishing. M.S. thesis, 104 p. State Univ. NY Stony Brook, Stony Brook, NY.

Beamish, R. J., and G. A. McFarlane.
1983. The forgotten requirement for age validation in fisheries biology. Trans. Am. Fish. Soc. 112:735–743.

Beckman, D. W., and C. A. Wilson.
1995. Seasonal timing of opaque zone formation in fish otoliths. *In* Recent developments in fish otolith research. Belle W. Baruch Lib. Mar. Sci. 19 (D. H. Secor, J. M. Dean, and S. E. Campana, eds.). p. 27–43. Univ. South Carolina Press, Columbia, SC.

Bell, R. J., D. E. Richardson, J. A. Hare, P. D. Lynch, and P. S. Fratantoni.
2015. Disentangling the effects of climate, abundance, and size on the distribution of marine fish: an example based on four stocks from the Northeast US shelf. ICES J. Mar. Sci. 72:1311–1322.

Bigelow, H. B., and W. C. Schroeder.
1953. Fishes of the Gulf of Maine. Fish. Bull. 53:1–577.

Campana, S. E.
2001. Accuracy, precision and quality control in age determination, including a review of the use and abuse of age validation methods. J. Fish Biol. 59:197–242.

Campana, S. E., and S. R. Thorrold.
2001. Otoliths, increments, and elements: keys to a comprehensive understanding of fish populations? Can. J. Fish. Aquat. Sci. 58:30–38.

Caruso, P. G.
1995. The biology and fisheries of black sea bass (*Centropristis striata*) in Massachusetts waters. M.S. thesis, 118 p. Univ. Rhode Island, Kingston, RI.

Carvalho, M. G., C. Moreira, H. Queiroga, P. T. Santos, and A. T. Correia.
2017. Age, growth and sex of the shanny, *Lipophrys pholis* (Linnaeus, 1758) (Teleostei, Blenniidae), from the NW coast of Portugal. J. Appl. Ichthyol. 33:242–251.

Casselman, J. M.
1983. Age and growth assessment of fish from their calcified structures—techniques and tools. *In* Proceedings of the international workshop on age determination of oceanic pelagic fishes: tunas, billfishes, and sharks; Miami, 15–18 February 1982 (E. D. Prince and L. M. Pulos, eds.), p. 1–17. NOAA Tech. Rep. NMFS 8.

Chang, W. Y. B.
1982. A statistical method for evaluating the reproducibility of age determination. Can. J. Fish. Aquat. Sci. 39:1208–1210.

Condini, M. V., C. Q. Albuquerque, and A. M. Garcia.
2014. Age and growth of dusky grouper (*Epinephelus marginatus*) (Perciformes: Epinephelidae) in the southwestern Atlantic, with a size comparison of offshore and littoral habitats. Fish. Bull. 112:311–321.

Dery, L. M., and J. P. Mayo.
1988. Black sea bass, *Centropristis striata*. *In* Age determination methods for northwest Atlantic species (J. Pentilla and L. M. Dery, eds.), p. 59–69. NOAA Tech. Rep. NMFS 72.

Drohan, A. F., J. P. Manderson, and D. B. Packer.
2007. Essential fish habitat source document: black sea bass, *Centropristis striata*, life history and habitat characteristics, 2nd ed. NOAA Tech. Memo. NMFS-NE-200, 68 p.

Fowler, A. J., and D. A. Short.
1998. Validation of age determination from otoliths of the King George whiting *Sillaginodes punctata* (Perciformes). Mar. Biol. 130:577–587.

Fox, J., and S. Weisberg.
2019. An R companion to applied regression, 3rd ed., 608 p. Sage Publ., Thousand Oaks, CA.

Hales, L. S., Jr., and K. W. Able.
1995. Effects of oxygen concentration on somatic and otolith growth rates of juvenile black sea bass, *Centropristis striata*. *In* Recent developments in fish otolith research. Belle W. Baruch Lib. Mar. Sci. 19 (D. H. Secor, J. M. Dean, and S. E. Campana, eds.), p. 135–153. Univ. South Carolina Press, Columbia, SC.

Hood, P. B., M. F. Godcharles, and R. S. Barco.
1994. Age, growth, reproduction, and the feeding ecology of black sea bass, *Centropristis striata* (Pisces: Serranidae), in the eastern Gulf of Mexico. Bull. Mar. Sci. 54:24–37.

Hothorn, T., F. Bretz, and P. Westfall.
2008. Simultaneous inference in general parametric models. Biom. J. 50:346–363.

Hyndes, G. A., N. R. Loneragan, and I. C. Potter.
1992. Influence of sectioning otoliths on marginal increment trends and age and growth estimates for the flathead *Platycephalus speculator*. Fish. Bull. 90:276–284.

Lenth, R.
2019. Emmeans: estimated marginal means, aka least-squares means. R package, vers. 1.4.1. [Available from website, accessed July 2019.]

McBride, R. S.
2015. Diagnosis of paired age agreement: a simulation of accuracy and precision effects. ICES J. Mar. Sci. 72:2149–2167.

McBride, R. S., M. K. Tweedie, and K. Oliveira.
2018. Reproduction, first-year growth, and expansion of spawning and nursery grounds of black sea bass (*Centropristis striata*) into a warming Gulf of Maine. Fish. Bull. 116:323–336.

McMahan, M. D., G. D. Sherwood, and J. H. Grabowski.
2020. Geographic variation in life-history traits of black sea bass (*Centropristis striata*) during a rapid range expansion. Front. Mar. Sci. 7:567758.

Mercer, L. P.
1978. The reproductive biology and population dynamics of black sea bass, *Centropristis striata*. Ph.D. diss., 196 p. Coll. William Mary, Williamsburg, VA. [Available from website.]

Miller, A. S., G. R. Shepherd, and P. S. Fratantoni.
2016. Offshore habitat preference of overwintering juvenile and adult black sea bass, *Centropristis striata*, and the relationship to year-class success. PLoS ONE 11(1):e0147627.

Morales-Nin, B., and S. Ralston.
1990. Age and growth of *Lutjanus kasmira* (Forskål) in Hawaiian waters. J. Fish Biol. 36:191–203.

Musick, J. A., and L. P. Mercer.
1977. Seasonal distribution of black sea bass, *Centropristis striata*, in the Mid-Atlantic Bight with comments on the ecology and fisheries of the species. Trans. Am. Fish. Soc. 106:12–25.

NEFSC (Northeast Fisheries Science Center).
2012. 53rd Northeast Regional Stock Assessment Workshop (53rd SAW) assessment summary report. Northeast Fish. Sci. Cent. Ref. Doc. 12-03, 33 p. [Available at website.]
2017. 62nd Northeast Regional Stock Assessment Workshop (62nd SAW) assessment report. Northeast Fish. Sci. Cent. Ref. Doc. 17-03, 261 p. [Available at website.]

Ogle, D. H., P. Wheeler, and A. Dinno.
2019. FSA: fisheries stock analysis. R package, vers. 0.8.25. [Available from website, accessed September 2019.]

Okamura, H., A. E. Punt, Y. Semba, and M. Ichinokawa.
2013. Marginal increment analysis: a new statistical approach of testing for temporal periodicity in fish age verification. J. Fish Biol. 82:1239–1249.

Pilling, G. M., R. S. Millner, M. W. Easey, C. C. Mees, S. Rathacharen, and R. Azemia.
2000. Validation of annual growth increments in the otoliths of the lethrinid *Lethrinus mahsena* and the lutjanid *Aprion virescens* from sites in the tropical Indian Ocean, with notes on the nature of growth increments in *Pristipomoides filamentosus*. Fish. Bull. 98:600–611.

Provost, M. M., O. P. Jensen, and D. L. Berlinsky.
2017. Influence of size, age, and spawning season on sex change in black sea bass. Mar. Coast. Fish. 9:126–138.

R Core Team.
2019. R: a language and environment for statistical computing. R Foundation for Statistical Computing, Vienna, Austria. [Available from website, accessed July 2019.]

Shepherd, G. R., and M. C. Lambert.
1996. Assessment of black sea bass north of Cape Hatteras, North Carolina. Northeast Fish. Sci. Cent. Ref. Doc. 95-17, 57 p. [Available from website.]

Vilizzi, L., and K. F. Walker.
1999. Age and growth of the common carp, *Cyprinus carpio*, in the River Murray, Australia: validation, consistency of age interpretation, and growth models. Environ. Biol. Fishes 54:77–106.

Wenner, C. A., W. A. Roumillat, and C. W. Waltz.
1986. Contributions to the life history of black sea bass, *Centropristis striata*, off the southeastern United States. Fish. Bull. 84:723–741.

Wickham, H.
2016. ggplot2: elegant graphics for data analysis, 2nd ed., 260 p. Springer-Verlag, New York.

Winner, B. L., T. C. MacDonald, and K. B. Amendola.
2017. Age and growth of sheepshead (*Archosargus probatocephalus*) in Tampa Bay, Florida. Fish. Bull. 115:155–166.

Wuenschel, M. J., R. S. McBride, and G. R. Fitzhugh.
2013. Relations between total gonad energy and physiological measures of condition in the period leading up to spawning: results of a laboratory experiment on black sea bass (*Centropristis striata*). Fish. Res. 138:110–119.

Zlokovitz, E. R., D. H. Secor, and P. M. Piccoli.
2003. Patterns of migration in Hudson River striped bass as determined by otolith microchemistry. Fish. Res. 63:245–259.

National Marine
Fisheries Service
NOAA

Fishery Bulletin
established in 1881

Spencer F. Baird
First U.S. Commissioner
of Fisheries and founder
of *Fishery Bulletin*

Discriminating between high- and low-quality field depletion experiments through simulation analysis

Leanne M. Poussard (contact author)[1]
Eric N. Powell[1]
Daniel R. Hennen[2]

Email address for contact author: leanne1poussard@gmail.com

[1] Gulf Coast Research Laboratory
University of Southern Mississippi
703 East Beach Drive
Ocean Springs, Mississippi 39564

[2] Northeast Fisheries Science Center
National Marine Fisheries Service, NOAA
166 Water Street
Woods Hole, Massachusetts 02543

Abstract—Between 1997 and 2011, the National Marine Fisheries Service conducted 50 depletion experiments to examine efficiency of survey gear for capturing clam species and to estimate stock density for populations of Atlantic surfclams (*Spisula solidissima*) and ocean quahogs (*Arctica islandica*) by using commercial hydraulic dredges. The Patch model was formulated to estimate gear efficiency and organism density from the depletion experiment data. The range of efficiencies estimated is substantial, leading to uncertainty in the application of these estimates in stock assessment. Known values of 4 measures of experimental performance for each of the 50 depletion experiments conducted in the field were compared with values of those same characteristics from 9000 simulated depletion experiments, values that were assumed to represent a suite of conditions that might also occur in the corresponding field experiment. These comparisons allow analyses of the quality of field experiments that would otherwise not be possible and provide evidence for weighting the results of field experiments beyond traditional measures of uncertainty. The characteristics of performance were used to identify a subset of field experiments that were more likely to have produced inaccurate estimates of gear efficiency, potentially introducing bias and, as a result, lowering the efficiency estimates in the entire depletion data set.

Manuscript submitted 31 March 2021.
Manuscript accepted 4 November 2021.
Fish. Bull. 119:274–293 (2021).
Online publication date: 24 November 2021.
doi: 10.7755/FB.119.4.7

The views and opinions expressed or implied in this article are those of the author (or authors) and do not necessarily reflect the position of the National Marine Fisheries Service, NOAA.

The implementation of a definitive measure of dredge efficiency for analyzing shellfish survey data substantially improves the estimation of abundance. Commonly, depletion experiments are used to estimate gear efficiency and population density for sessile and sedentary species in a target area (Leslie and Davis, 1939; Skalski et al., 1983; Lasta and Iribarne, 1997; Gedamke et al., 2005; Wilberg et al., 2013). These experiments are conducted by dredging over the same area and tracking the decline in catch of a target organism per dredge tow. Other dredge efficiency quantification methods, such as use of an underwater camera in between dredge tows, have also been used (Chai et al., 1992; Ragnarsson and Thórarinsdóttir, 2002; Morson et al., 2018). For a range of dry dredges, estimates exist for their efficiency for catching epibenthic animals, including oyster (Powell et al., 2007; Morson et al., 2018), clam (Pezzuto et al., 2010), crab (Vølstad et al., 2000; Wilberg et al., 2013), and scallop (Lasta and Iribarne, 1997; Beukers-Stewart and Beukers-Stewart[1]) species. By comparison, highly efficient hydraulic dredges are the primary gear type used to capture infaunal clam species (Da Ros et al., 2003; Hauton et al., 2007; Moschino et al., 2003; Gilkinson et al., 2005; Meseck et al., 2014). Hydraulic dredges increase the catchability of the target organism by using water pressure to liquefy the sediment (Da Ros et al., 2003; Gilkinson et al., 2003; Hauton et al., 2007; Meseck et al., 2014).

The ocean quahog (*Arctica islandica*) and the Atlantic surfclam (*Spisula solidissima*) support substantial fisheries that operate on the continental shelf of the northeastern United States and are captured exclusively by using hydraulic dredges because of the depths at which they are found. A typical hydraulic dredge is a large rectangular

[1] Beukers-Stewart, B. D., and J. S. Beukers-Stewart. 2009. Principles for the management of inshore scallop fisheries around the United Kingdom. Report to Natural England, Scottish Natural Heritage and Countryside Council for Wales. Univ. York, Mar. Ecosyst. Manage. Rep. 1, 58 p. [Available from website.]

box, 2.4–4.0 m wide and constructed of evenly spaced steel bars, and is towed over a seabed (Meyer et al., 1981; Lambert and Goudreau, 1996). A manifold at the head of a dredge distributes high-pressure water from a shipboard pump through a connecting hose. The water is focused with a series of jets onto the seabed, liquefying the sediment and unearthing the clams for capture by the dredge. Hydraulic dredges, widely used in clam fisheries (Parker, 1971; Hauton et al., 2007; Sala et al., 2017), are necessary for the commercial capture of the ocean quahog and Atlantic surfclam because of the depth and distance from shore at which these species are found and the fact that the fishery depends on the high volume and low unit cost of its catch. Therefore, rapid and efficient capture methods are economically essential.

A series of depletion experiments were conducted by the National Marine Fisheries Service (NMFS) between 1997 and 2011 on commercial clam vessels targeting populations of Atlantic surfclams and ocean quahogs off the northeastern and mid-Atlantic coasts of the United States to estimate the efficiency of both commercial hydraulic dredges. The exact locations of these depletion experiments are specified in appendix 3 of NEFSC (2017a, 2017b) (Fig. 1). As is often the case, estimates of dredge efficiency varied widely between individual experiments (Vølstad et al., 2000; Powell et al., 2007; Hennen et al., 2012; Wilberg et al., 2013; Morson et al., 2018). Very little is known about how environmental and sampling conditions influence the efficiency of a hydraulic dredge, factors that are likely the source of variation between experiments. Consequently, estimates of gear efficiency based on depletion experiments are a key source of uncertainty in the stock assessments for the Atlantic surfclam and ocean quahog.

The Patch model was developed to analyze the results of depletion experiments to estimate the efficiency of capture of sedentary species, such as the Atlantic surfclam and ocean quahog (Rago et al., 2006). The Patch model has been rigorously tested in previous studies (Hennen et al., 2012) and has been used to inform stock assessments of species, such as the Atlantic surfclam, ocean quahog, monkfish (*Lophius americanus*) (NEFSC, 2010a), and Atlantic sea scallop (*Placopecten magellanicus*) (NEFSC, 2010b; NMFS, 2011), that are commercially fished along the mid-Atlantic coast of the United States. Over 14 years, 50 depletion experiments were carried out along the continental shelf off the coasts of Massachusetts, Long Island in New York, and New Jersey and off the Delmarva Peninsula in Delaware, Maryland, and Virginia to determine the efficiency of hydraulic dredges used in the fisheries that target Atlantic surfclams and ocean quahogs. The Patch model provides estimates of capture efficiency and average density of organisms in the target area by tracking the relative reduction in catch for each dredge tow. Theoretically, capture efficiency is a measurable characteristic of the gear as well as of the species (Hennen et al., 2012).

In a field depletion experiment, the dredge is towed over the same ground repeatedly while covering the majority of a predetermined area. Depletion experiments are conducted in a rectangular area on average about 10 dredge widths wide (23–24 m) and about 400–1000 m long. A series of intersecting dredge tows are conducted across the selected area, with the path of the dredge tow beginning at one short end of the rectangle and finishing at the opposite end (Fig. 2). The tow paths are not parallel, rather the paths overlap and intersect at various points in the area by design in order to meet the requirements of the Patch

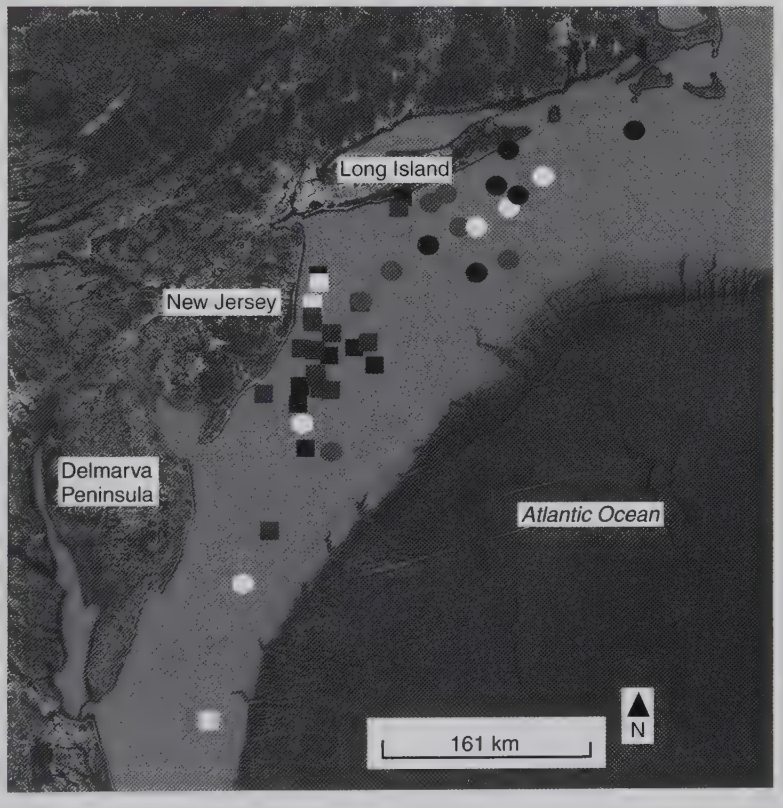

Figure 1

Map of the locations of the 50 depletion experiments that targeted ocean quahogs (*Arctica islandica*) (circles) and Atlantic surfclams (*Spisula solidissima*) (squares) off the mid-Atlantic coast of the United States between 1997 and 2011. White symbols indicate experiments with efficiency estimates under 0.4, gray symbols indicate experiments with efficiency estimates between 0.4 and 0.7, and black symbols indicate experiments with efficiency estimates above 0.7. Sources for Google Earth base map: data SIO, NOAA, U.S. Navy, NGA, GEBCO; image Landsat/Copernicus.

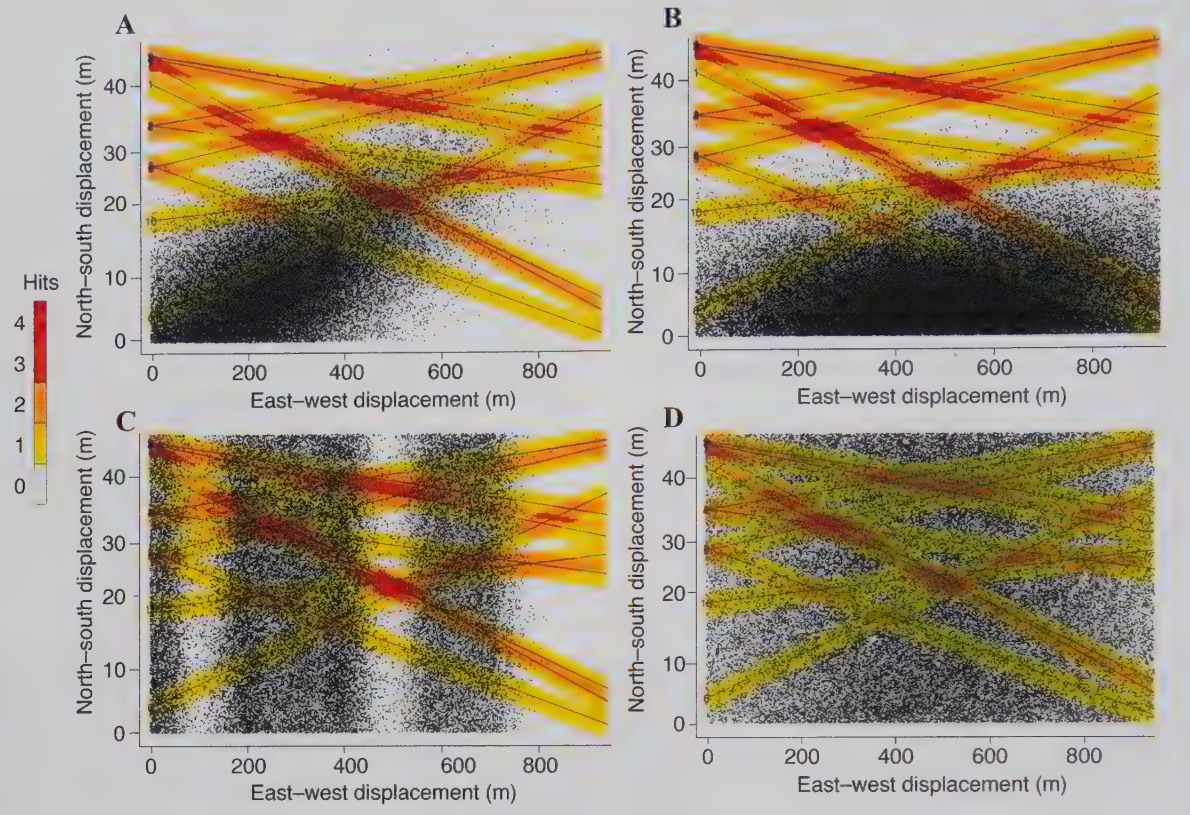

Figure 2

Distributions of ocean quahogs (*Arctica islandica*) and Atlantic surfclams (*Spisula solidissima*) from the analysis done with simulation of depletion experiments. Four types of distribution are shown: (**A**) a biased clam distribution with the highest densities in half the area, (**B**) a distribution with clams in a triangle wedge from southwest to northeast across the area, (**C**) a distribution with clams in even vertical bands, and (**D**) a clam distribution that is not patchy and is relatively uniform. The colored straight lines indicate paths of dredge tows passing through the area. Colors denote the amount of overlap (number of hits) of the dredge paths. Black dots indicate individual clams. Data used in the simulations are from depletion experiments conducted during 1997–2011 for populations of ocean quahogs and Atlantic surfclams off the mid-Atlantic coast of the United States.

model. The experiment requires the assumptions that all catches are random samples and that no organisms are transported into or out of the study site during the experiment (Leslie and Davis, 1939). The catch and the incremental dredge positions are recorded for each dredge tow. Over the course of the depletion experiment, catch per tow decreases; this rate of decline is proportional to the efficiency of the dredge (Hennen et al., 2012). If the rate of decline is steep, the dredge is highly efficient, and if it is shallow, the dredge may not be efficient.

Field depletion experiments can take hours to complete and require much effort on the part of scientists and crew on the ship. Therefore, it is important to know if experiments produce reliable efficiency estimates for the gear used and to evaluate poor performance that might be avoided in future endeavors. Poussard et al. (2021) used simulation analysis to determine best practices for depletion experiments and evaluated which range of experiment protocols were most likely to provide high-quality estimates of capture efficiency. Here, we report results of the use of the simulation data to identify the quality of field depletion experiments. The depletion experiment data set analyzed, obtained from NMFS (Hennen[2]), is unique at the time of this writing. No other data set from depletion experiments is this expansive.

Analyzing data from the NMFS hydraulic dredge depletion experiments provides an improved understanding of the sources of uncertainty in efficiency estimates, including the characteristics of experimental protocol and environmental factors affecting gear efficiency. In our study, first the characteristics of these experiments (e.g., dredge size, depth, and geographic region) were summarized, and then results of simulated depletion experiments were compared with those of the field depletion

[2] Hennen, D. 2019. Personal commun. Northeast Fish. Sci. Cent., Natl. Mar. Fish. Serv., NOAA, 166 Water St., Woods Hole, MA 02543.

experiments conducted on Atlantic surfclam and ocean quahog stocks by using a series of experimental quality measurements. The simulated depletion experiments have the advantage of being fully controlled, and the accuracy and precision of the measurement estimates they provide can be evaluated. In this analysis, a set of simulated experiments was matched to each field experiment. This set of simulated experiments was assumed to represent a suite of conditions that might also occur in the corresponding field experiment. The results of these comparisons allow examination of the quality of field experiments and provide evidence for weighting the results of field experiments beyond traditional measures of uncertainty.

Materials and methods

The Patch model

For estimation of the catchability coefficient (q), depletion experiments allow correction of survey catch by using the equations $N=SA/q$ and $q=\frac{\alpha e}{A}$, where N is stock abundance or biomass and SA is the swept area average of all tows in the experiment area. The q is obtained from α, the area swept by the sampling gear; e, the dredge efficiency; and A, the spatial domain of the estimates (Paloheimo and Dickie, 1964). The α is calculated as the distance the dredge is towed multiplied by the width of the dredge. See Figure 2 for a visual representation of the dredge tows in an experiment area.

The expected catch of organisms in any tow i, $E(C_i)$, given initial density of the target organisms (D_0) and the cumulative catch from previous tows, T_{i-1}, can be calculated as follows:

$$E(C_i) = q(D_0 - T_{i-1}), \quad (1)$$

assuming each tow covers the same spatial domain. In reality, this relationship is more complex because each tow covers only a portion of the area of the experiment. Incorporating the portion of the area that has already been hit by the dredge prior to tow i, also known as the *hit matrix* (Hennen et al., 2012), gives the expected catch per tow i as follows:

$$E(C_i) = (EAS_i)D_0, \quad (2)$$

where EAS is the effective area swept, defined as the total area swept by the dredge in tow i, taking into account the portion of the experimental area hit by the dredge in previous tows. The EAS is calculated as follows:

$$EAS = ea_i \sum_{j=1}^{i} f_{i,j}(1 - e\gamma)^{j-1}, \quad (3)$$

where e = the capture efficiency as estimated by the Patch model;
a_i = the area swept by tow i;
$f_{i,j}$ = the fraction of the area a_i hit by the dredge j times in previous tows; and
γ = the ratio of cell size to dredge width.

Rago et al. (2006) divided the experimental area into cells twice the width of the dredge. Hennen et al. (2012) removed γ by reducing the cells to points, eliminating the need to calculate cell size and, as a result, improving accuracy and precision of efficiency estimates. In this study, the latter method was used.

The negative binomial distribution was used to describe the dispersion of animals in the area of the experiment in order to account for extra variation in observed catches and for catch from previous tows when estimating catch in tow i. In this method, the cumulative spatial pattern of removal of animals is used to define capture probability for each organism. The negative binomial distribution of catch can be expressed as a function of D_0, k (the dispersion parameter), and EAS (Rago et al., 2006):

$$P(C_i \mid D_0, k, EAS) = \left(\frac{k}{D_0(EAS) + K}\right)^k \left(\frac{D_0(EAS)}{D_0(EAS) + k}\right)^{C_i} \times \prod_{j=1}^{C_i} \frac{k + j - 1}{j}. \quad (4)$$

The log likelihood (LL) function allows estimation of the dispersion parameter, initial density, and capture efficiency, given the hit matrix, catch, and area swept:

$$\begin{aligned} LL(D_0, k, e, \gamma \mid C_i, EAS) = {} & k\sum_{i=1}^{n} \log(k) \\ & - \log(D_0(EAS) + k) \\ & + \sum_{i=1}^{n} (\log(D_0(EAS)) \\ & - \log(D_0(EAS) + k) \\ & + \sum_{i=1}^{n} \sum_{j=1}^{C_i} \log(k + j - 1) \\ & - \sum_{i=1}^{n} C_i!, \end{aligned} \quad (5)$$

where n = the total number of tows in the sequence; and
! = a factorial.

Simulated data sets

Poussard et al. (2021) reported the results of 5400 depletion experiments simulated in a block design in which animal density, "true" dredge efficiency, the number of tows per experiment, and the dispersion of animals on the bottom were varied. For the purposes of the study we describe here, 3600 additional simulations with 15 and 25 dredge tows were conducted in order to provide a simulated data set that is comparable to the data from experiments conducted in the field, for a total of 9000 simulations (Table 1). The simulated data set included 5 options for the number of dredge tows for each experiment, 4 dispersions of individual clams in the area, 3 clam densities, and 3 values for the true efficiency of the dredge. Fifty simulations were conducted for each combination of factors (e.g., 50 simulations were conducted with 25 tows that had a dredge efficiency of 0.9 and clams distributed evenly through the area with a density of 3.00 individuals/m^2, and 50 more simulations were

Table 1

Characteristics from the analysis done with simulation of depletion experiments in a block design. All combinations of the 4 parameters were simulated: 50 simulations for each tetradic combination were conducted. The type of clam distribution is denoted as follows: uniform across the area (NP), patches oriented across the narrow dimension (P), patches oriented longitudinally (HP), and patches of a triangular nature emanating from one side of the rectangle (T). True efficiency is efficiency of the dredge for capture of shellfish. The data set used in the simulations came from depletion experiments conducted for populations of ocean quahogs (*Arctica islandica*) and Atlantic surfclams (*Spisula solidissima*) off the mid-Atlantic coast of the United States between 1997 and 2011.

Characteristic	Values				
True efficiency	0.9	0.6	0.2		
Clam density (individuals/m^2)	0.75	1.50	3.00		
Clam distribution	NP	HP	P	T	
No. of tows	40	25	20	15	10

conducted with all the same factors except with a density of 1.50 individuals/m^2, and so on). Fifty tow patterns were randomly generated for each tow number.

Here we discuss 4 useful measures for comparing depletion experiments, along with the estimates of efficiency and density. The 4 characteristics are the EAS (Equation 3), the coefficient of variation (CV) for the efficiency estimate (CV_E), the CV of the k parameter (CV_K) (the negative binomial dispersion parameter), and the overlap score (OS) describing tow overlap (Equation 7). The CVs were calculated by using the delta method standard deviation of estimates from the Patch model divided by the means of the estimates obtained from the log likelihood equation (Equation 5).

The OS is a measure that describes tow overlap that does not depend on estimated efficiency or the spatial dimensions of the site. The OS is derived directly from the hit matrix (Hennen et al., 2012), where the n rows equal the number of tows in the experiment and the m columns are the number of points touched m times previously. The highest possible amount of overlap for any depletion site would be the exact duplication of the longest tow in each sequence (the row with the most total points touched), repeated n times (OS_{max}). For tow i, the OS is calculated with this equation:

$$OS_i = \sum_{h=i}^{m} (p_{i,h} h), \tag{6}$$

where $p_{i,h}$ = the number of points in hit matrix row i and column h.

The OS for each tow sequence is then calculated with this equation:

$$OS = \frac{\sum_i^n OS_i}{OS_{max}} \times 100. \tag{7}$$

The value of OS varied nonlinearly with tow number. As a consequence, the values were detrended by using the mean OS value for that tow number to standardize all OS values of the same tow number. A higher value of OS equates to more dredge overlap in the tow structure of an experiment for a given number of tows.

For the simulations, where the true efficiency (*TrueEff*) was already known (efficiency values were 0.2, 0.6, and 0.9), Poussard et al. (2021) calculated the percent error in efficiency from the Patch model estimate of efficiency, *EstEff*, and the inherent efficiency specified in the simulation, *TrueEff*, as follows:

$$Error = \frac{EstEff - TrueEff}{TrueEff} \times 100. \tag{8}$$

On the basis of the results of their analysis of simulated depletion experiments, Poussard et al. (2021) concluded that a depletion experiment is more likely to produce accurate gear efficiency estimates if it employs a high number of dredge tows (e.g., 40 tows per experiment compared with 10 or 15 tows), maximizes the amount of intersection in tow paths, occurs over a homogenous as opposed to patchy distribution of clams, and uses a highly efficient dredge. The results of these simulations were compared with those of the field depletion experiments by using the set of 4 characteristics to match the field experiments to simulated experiments with similar characteristics. The known errors in the set of comparable simulated experiments were then used as a proxy for the reliability of each of the 50 field experiments.

Application of simulations: error estimates

Field experiments varied in the length of the depletion site and the width of the dredge used. For statistical analysis, EAS was standardized to a dredge width of 3.81 m and a site length of 960 m, consistent with the simulation data set of Poussard et al. (2021), by using a proportional standardization. All EAS values used were the average values per tow, rather than the total values, to take into account the large range in tow numbers among experiments.

A principal components analysis was conducted on the simulation data set to determine if the 4 measures that describe depletion performance (EAS, CV_E, CV_K, and OS) were correlated and, if so, to derive new orthogonal metrics. The data were standardized to a mean of 0 and a standard deviation of 1, and factors were designated by using Varimax rotation. Factor loadings indicate each of the 4 characteristics loaded on separate axes with loads exceeding 0.95; therefore, the 4 measures in their original form are approximately orthogonal and provide independent information for evaluating experimental performance.

Field experiments were matched to a subset of the simulated depletion experiments through an iterative process. For each field experiment, the values of the 4 characteristics were compared with values from the 9000 simulations. Data from field experiments were compared with the simulation data set by determining whether the

values of each of the 4 characteristics for a given field depletion experiment fell above or below the mean value for the characteristic from the simulation data set. This comparison generated a 4-digit integer sequence (e.g., 1011) for any given field experiment with the numeral 1 assigned if the field experiment measure fell above the mean of the simulated experiment measures and a with the numeral 0 assigned if the measure fell below the mean.

The same set of integer sequences were calculated for each simulation and compared with the mean of the characteristics for all simulated experiments. Then the subset of simulations that have the same sequence as the field experiment was extracted from the data set. The means of the measures for this subset were again calculated and compared with those of the field experiment, generating a new 4-digit sequence. This sequence, in turn, was used to extract a subset of simulated experiments of identical sequence. This process was repeated sequentially on each extracted subset, with the mean values for the simulated experiments being updated by using only the extracted subset, until none of the final subset of simulations had the same 4-digit value as the chosen field experiment. This group of simulations was considered the most comparable to the field experiment in question out of all the simulations. This "most comparable" subset typically numbered 2–20 of the 9000 simulations and was used to describe the average values for the simulated 4 characteristics and the average error in efficiency most appropriate for comparison with the known values (Tables 2 and 3).

Each simulation in the extracted subset of simulations was run by using a specified dispersion of clams. The distributions of clams were organized as follows: a relatively

Table 2

Parameters from 19 simulations that were most comparable with data from the depletion experiment OQ08-02. Type of clam distribution is denoted as uniform (NP), vertical bands (P), clams in half the area (HP), and diagonal across the area (T). Characteristics used to describe the experiments are the effective area swept (EAS), the coefficient of variation (CV) for the efficiency estimate (CV_E), and the CV of the k parameter (CV_K), which is the negative binomial dispersion parameter. The estimated efficiency of depletion experiment OQ08-02 is 0.79507. The data set used in the simulations came from depletion experiments conducted during 1997–2011 for ocean quahogs (*Arctica islandica*) off the mid-Atlantic coast of the United States. See Figure 1 for the locations where the experiments were conducted.

	Parameter		
Simulation and OQ08-02 values	CV_E	CV_K	EAS (m^2)
Average values from simulations	5.477	41.966	21,331.1
Values from experiment OQ08-02	9.361	35.067	24,604.8

Mean absolute error in efficiency estimate:	0.1003	Range:	0.0001–0.4000

	Parameter					
Error in efficiency estimate	Density (individuals/m^2)	Clam distribution	True efficiency	CV_E estimate	CV_K estimate	EAS (m^2)
0.6667	0.75	HP	0.6	0.0090	38.4412	22,601.94
0.6667	1.50	HP	0.6	0.0090	38.6189	22,601.94
0.6667	3.00	HP	0.6	0.0190	37.5421	22,771.00
0.1517	0.75	P	0.6	13.4774	47.8368	22,551.50
0.0633	0.75	P	0.6	14.3416	46.6667	22,696.44
0.1500	0.75	P	0.6	7.3768	47.6762	23,019.59
0.1050	1.50	P	0.6	9.4721	46.1634	22,653.81
0.0633	1.50	P	0.6	6.3793	47.7372	22,696.44
0.0883	1.50	P	0.6	5.4058	47.5397	23,019.59
0.6667	0.75	T	0.6	0.0710	41.7476	22,601.94
0.6667	0.75	T	0.6	0.0200	41.2644	22,771.00
0.6667	1.50	T	0.6	0.0190	41.0180	22,771.00
0.6667	3.00	T	0.6	0.1210	41.6268	22,601.94
0.0905	0.75	NP	0.6	5.7007	42.9225	20,596.54
0.0572	0.75	NP	0.6	4.9920	41.7308	20,775.93
0.0359	0.75	NP	0.6	6.4963	40.6921	20,679.71
0.0778	0.75	P	0.6	7.6546	48.6502	20,596.54
0.0017	0.75	P	0.6	6.5863	48.5524	20,807.33
0.0483	3.00	P	0.6	7.0053	38.5597	20,807.33

Table 3

Parameters from 19 simulations that were most comparable with data from the depletion experiment SC04-01. Type of clam distribution is denoted as vertical bands (P), clams in half the area (HP), and diagonal across the area (T). Characteristics used to describe the experiments are the effective area swept (EAS), the coefficient of variation (CV) for the efficiency estimate (CV_E), and the CV of the k parameter (CV_K), which is the negative binomial dispersion parameter. The estimated efficiency of depletion experiment SC04-01 is 0.53334. The data set used in the simulations came from depletion experiments conducted during 1997–2011 for Atlantic surfclams (*Spisula solidissima*) off the mid-Atlantic coast of the United States. See Figure 1 for the locations where the experiments were conducted.

	Parameter		
Simulation and SC04-01 values	CV_E	CV_K	EAS (m^2)
Average values from simulations	14.564	25.703	16,443.2
Values from SC04-01	19.835	28.085	12,824.4
Mean absolute error in efficiency estimate:	0.1471	Range:	0.0000–0.5817

			Parameter			
Error in efficiency estimate	Density (individuals/m^2)	Clam distribution	True efficiency	CV_E estimate	CV_K Estimate	EAS (m^2)
0.3083	1.50	HP	0.6	24.2038	26.5866	20,807.33
0.2533	1.50	HP	0.6	26.1968	26.7742	20,807.33
0.4250	3.00	HP	0.6	27.2515	26.4758	16,443.15
0.4633	3.00	HP	0.6	18.3371	26.4220	12,824.38
0.4133	3.00	HP	0.6	18.7500	26.8293	18,932.27
0.2533	0.75	T	0.6	19.0160	28.5385	19,145.44
0.4450	0.75	T	0.6	14.9942	28.6364	18,949.80
0.3250	0.75	T	0.6	13.2075	28.5484	18,931.71
0.2233	1.50	T	0.6	19.2098	28.5821	18,729.82
0.3467	1.50	T	0.6	19.9257	28.7838	18,815.12
0.0867	1.50	T	0.6	23.6196	28.9172	18,931.71
0.0033	3.00	T	0.6	23.4114	28.8820	18,581.26
0.3400	3.00	T	0.6	19.9005	28.8194	18,815.12
0.4167	3.00	T	0.6	14.7059	28.0702	18,891.53
0.0317	1.50	NP	0.6	1.7609	25.3618	18,729.82
0.0250	1.50	NP	0.6	1.3886	26.9719	18,932.27
0.0083	3.00	NP	0.6	1.3091	24.6763	18,891.53
0.0383	0.75	P	0.6	2.4398	26.3924	18,757.88
0.0233	1.50	P	0.6	2.2964	25.0700	13,600.72

uniform distribution across the depletion rectangle (NP), patches oriented across the narrow dimension (P), patches oriented longitudinally (HP), and patches of a triangular nature emanating from one side of the rectangle (T) (Fig. 2). The fraction of chosen simulations assigned to each field experiment falling into each of these categories was obtained to describe possible similarities in clam dispersion characteristics in the area occupied by the field depletion experiment.

Comparisons between field experiments and simulations were made by using 4 error terms chosen to determine which of the field depletion experiments diverged the most from the most comparable simulations identified with the 4-integer test. Two error terms, henceforth referred to as *Err1* and *Err2*, describe how closely the 4 experiment measures derived from the field experiments (EAS, CV_E, CV_K, and OS) agreed with the same measures obtained from the extracted subset of the simulations:

$$Err1 = \sum_{j=1}^{4} \frac{abs(observed - expected)}{expected} \text{ and} \tag{9}$$

$$Err2 = \sum_{j=1}^{4} \frac{(observed - expected)^2}{expected}, \tag{10}$$

where the observed measurement value is obtained from the field experiment and the expected measurement is the average value of the extracted simulations.

The error term *Err3* is the average percent error from the simulation subset obtained by comparing the field

estimate of efficiency with the known efficiency used in the simulation (Equation 8). The error term *Err3* was modified as a simple difference between the averages (observed and true efficiencies) obtained from the simulation subset as *Err4*:

$$Err4 = abs(ObsEff - TrueEff). \quad (11)$$

Caveat lector. No characteristic can be used to definitively estimate the accuracy of a field depletion experiment because the true efficiency perforce is unknown. Estimates of the 4 error terms relate attributes of a large set of simulated experiments, in which combinations of 4 different depletion experiment characteristics are used to describe how precisely the Patch model estimate of efficiency returned the known efficiency specified in the simulation. In this study, comparing field experiments directly to the simulations permitted inference of the quality of field experiments. Comparisons were made by using estimates of the 4 error terms to identify field experiments that have characteristics that resemble the 4 performance characteristics in the simulations of Poussard et al. (2021).

Statistics

Unless otherwise indicated, statistical evaluation of the quality of field depletion experiments was done with SAS 9[3] (SAS Institute Inc., Cary, NC). Field experiments that had estimates for 1 or more of the 4 error terms at or above the 80th percentile were compared with the remaining experiments that had 1 or more error estimate below the 80th percentile by using a Wilcoxon rank sum test (Sokal and Rohlf, 1998) to determine if the flagged subset of field experiments was a random subset of all field experiments, as determined by the error estimates and other characteristics as earlier described.

The relationship between descriptors of Patch model performance, including efficiency and density estimates, and descriptors of the experiment, such as location, depth, and target species in the field experiments, were resolved by using correspondence analysis (Clausen, 1998). For this purpose, continuous variables were classified into quartiles (1–4), and error terms were entered as 1 (below the 80th percentile) or 2 (at or above the 80th percentile). The variables used to specify the coordinate system for the correspondence analysis and a series of supplementary variables assigned coordinate positions include dredge efficiency and its CV, clam density and its CV, the k parameter, EAS, OS, latitude, depth, species, region, dredge width, and the 4 error terms. Of note, the error terms were all designated as supplementary variables, meaning that they did not determine the axes in the correspondence analysis and were added retrospectively to provide context.

Pearson's correlation coefficients were calculated by using statistical software R (vers. 3.6.0; R Core Team, 2019) for variables describing the field experiments to determine how factors, such as dredge width, experiment area width, number of tows, year, and latitude correlated with Patch model estimates of efficiency, density, and the k parameter.

[3] Mention of trade names or commercial companies is for identification purposes only and does not imply endorsement by the National Marine Fisheries Service, NOAA.

Results

Characteristics of field depletion experiments

The mean and median estimates of efficiency, density, and the k parameter for the 50 field depletion experiments are provided in Table 4. The mean estimate of efficiency for the 31 depletion experiments that targeted Atlantic surfclams is 0.635, and the mean efficiency estimate for the 19 depletion experiments that targeted ocean quahogs is 0.586 (Fig. 3). The mean density estimate for depletion experiments with Atlantic surfclams is 1.50 individuals/m^2, and the mean density estimate for depletion experiments with ocean quahogs is 1.18 individuals/m^2. These densities are well above the average stock density for both species because the depletion experiments were purposely sited in high-density areas. The mean estimate of k for the experiments with Atlantic surfclams is 12.10, and the mean for the experiments with ocean quahogs is 7.72.

Most depletion experiments that targeted ocean quahogs were conducted at higher latitudes and at deeper depths than depletion experiments that targeted Atlantic surfclams (Table 5). For depletion experiments with ocean quahogs, higher efficiency estimates were produced at the most northern locations (Fig. 1). Depletion experiments with Atlantic surfclams produced efficiency estimates that were higher off the coast of New Jersey than off the coasts of Long Island and the Delmarva Peninsula (Fig. 1).

Over the 14 years that depletion experiments were conducted, method and gear changed. Dredge width, for example, gradually increased from 2.55 to 3.81 m. The number of dredge tows used in each experiment varied through the years as well. The majority of experiments, especially in later years, used between 15 and 20 tows, but some experiments between 1997 and 2000 used as few as 4 tows and as many as 39 tows.

Correlation analysis

Efficiency estimates for depletion experiments that targeted ocean quahogs are significantly positively correlated with latitude (Fig. 1) and the width of the dredge (Fig. 4). Efficiency is incorporated into the equation to calculate EAS; therefore, the correlation between efficiency and EAS was expected, and correlations between efficiency and other variables were reflected by correlations between EAS and those same variables. Year was incorporated into the correlation analysis to examine how characteristics changed over time. As noted, dredge width increased with year, and tow number and depth decreased over time. The CV_E is

Table 4

Mean, median, standard deviation, and coefficient of variance (CV) for estimates from the Patch model for the following parameters: dredge efficiency; clam density; the *k* parameter, which is the negative binomial dispersion parameter; effective area swept (EAS); and the number of tows of the dredge. Estimates are based on the 50 depletion experiments conducted in the field between 1997 and 2011 for populations of ocean quahogs (*Arctica islandica*) and Atlantic surfclams (*Spisula solidissima*) off the mid-Atlantic coast of the United States. The standard deviation and CV values for efficiency and density are the averages of the delta method uncertainties associated with parameter estimation. *n*=number of experiments.

	Parameter				
Statistic	Efficiency	Density (individuals/m^2)	*k* parameter	EAS (m^2)	No. of tows
Ocean quahog (*n*=19)					
Mean	0.586	1.184	7.724	13,688.81	17.433
Median	0.629	0.094	6.165	13,746.99	17.270
Standard deviation	0.113	0.646	3.045	13,471.86	3.713
Coefficient of variance	0.357	16.907	0.613	13,471.86	0.189
Atlantic surfclam (*n*=31)					
Mean	0.635	1.496	12.097	13,570.90	22.330
Median	0.590	0.738	5.689	7325.56	19.143
Standard deviation	0.131	1.786	3.011	14,653.21	5.829
Coefficient of variance	0.206	12.855	0.351	0.104143	0.193

negatively correlated with the number of tows and strongly positively correlated with the CV of the density estimate (CV_D) (Figs. 4 and 5). In depletion experiments with Atlantic surfclams, as opposed to experiments with ocean quahogs, the CV_K is significantly positively correlated with the CV_D (Fig. 5). In the case of the Atlantic surfclam, no correlation exists between latitude and the efficiency estimates, but density estimates are negatively correlated with the latitude and efficiency estimates.

Error estimates and Wilcoxon rank sum tests

Field depletion experiments with parameter estimates that fall at or above the 80th percentile of their respective most comparable simulated experiments, for 1 or more of the 4 error estimates, are denoted by asterisks in Table 5. We used the 80th percentile, corresponding to a 90th percentile one-sided threshold, to retain a high probability of including marginal experiments in the group flagged as suspect, recognizing that this threshold may entrap some experiments of higher quality. Effectively, the goal was to err on the side of removing a few "good" field depletion experiments rather than keep a few "bad" ones.

Of the 50 depletion experiments, 24 experiments had estimates for 1 or more of the 4 error terms that fall at or above the 80th percentile. Experiments with estimates for error terms *Err1* (Equation 9) and *Err2* (Equation 10) at or above the 80th percentile are experiments that differed substantially from the chosen subset of simulations for 1 or more of the 4 characteristics that describe the depletion experiments, the CV_E, the CV_K, the number of tows, and the EAS. These field experiments were not well described by the most similar subset of simulations. The possibility that the range of values for EAS might influence the differential in the results for *Err1* and *Err2* was tested by recomputing *Err2* by using $\log_e(EAS)$. The set of experiments flagged by *Err2* did not change.

The error terms *Err3* (Equation 8) and *Err4* (Equation 11) provide an alternate method from *Err1* and *Err2* to identify field experiments that potentially produced unreliable efficiency estimates. In this case, error in efficiency estimates from a subset of similar simulations, each with a known error in their efficiency estimate, were compared. Field experiments most similar to simulated experiments that yielded high values for *Err3* and *Err4* were flagged.

When field experiments produced parameter estimates that fall at or above the 80th percentile for an error term, they were flagged by that error term (Table 6). When these field experiments were compared with the experiments that produced estimates that fall below the 80th percentile, some differences in Patch model estimates of gear efficiency and clam density came to light, highlighting that the 4 error measures are operationally different and can be used to evaluate experiment performance in different ways. For example, the experiments that were flagged by *Err2*, *Err3*, and *Err4* produced lower average and median efficiency estimates than those from experiments flagged by *Err1*.

The relationships between data from the field experiments flagged by one or more error terms and the rest of the data set were evaluated by using Wilcoxon rank sums tests (Table 7). Experiments flagged by *Err1* did not differ significantly from the remaining experiments for any of the measured depletion parameters. In each case, the

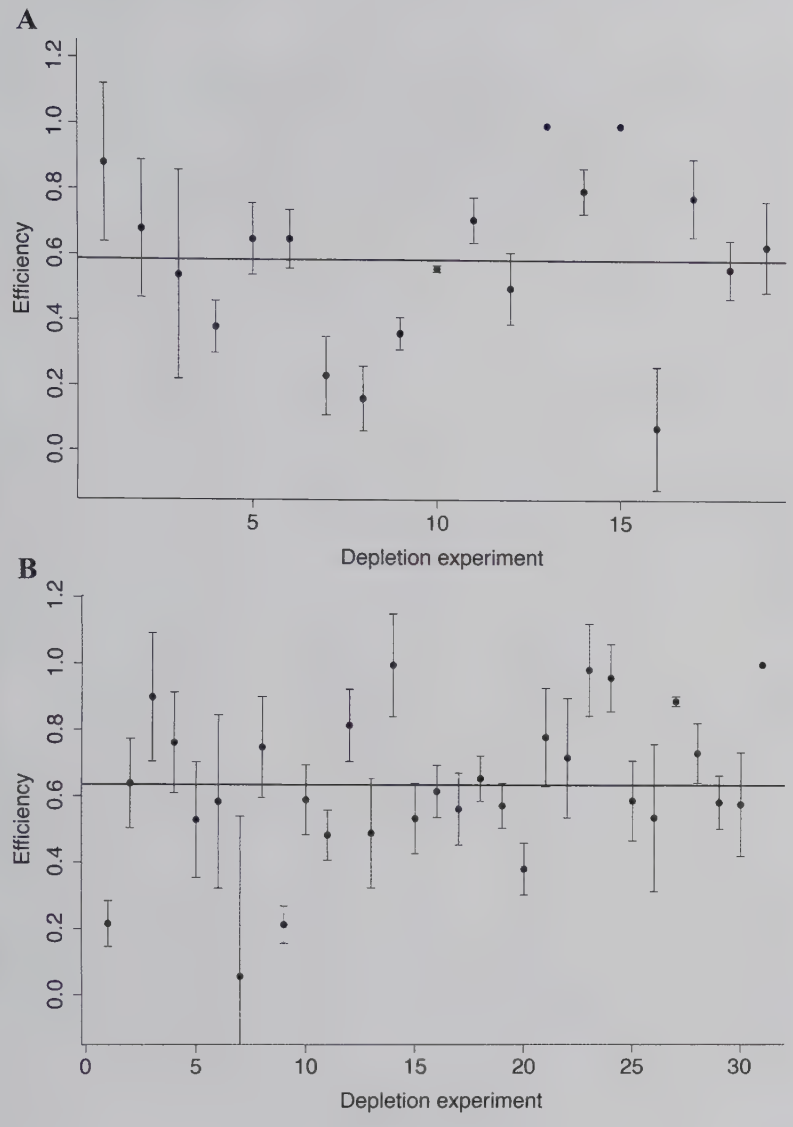

Figure 3

Estimates of capture efficiency of hydraulic dredges (**A**) for each of the 19 depletion experiments that targeted ocean quahogs (*Arctica islandica*) and (**B**) for each of the 31 depletion experiments that targeted Atlantic surfclams (*Spisula solidissima*) between 1997 and 2011 off the mid-Atlantic coast of the United States. The black horizontal line indicates the mean efficiency for the group of experiments in each panel. Error bars indicate standard deviations.

identified experiments were distributed randomly within the full set of field experiments with respect to the different error terms tested. If the experiments flagged by *Err1* were removed from the analysis, the mean and median efficiency estimates of the remaining field depletion experiments were not significantly different from the mean and median estimates for the entire data set. In dramatic contrast, for experiments flagged by *Err2*, *Err3*, and *Err4*, the efficiency estimates from the Patch model differed substantially from the estimates from the remaining field experiments. In addition, experiments flagged by *Err3* and *Err4* had CV_K and EAS values that were substantially different from the values from the experiments that were not flagged (Table 8). Interestingly, all 9 experiments flagged by *Err3* were among the 10 flagged by *Err4*, yet experiments flagged by *Err3* produced significantly different CV_E and CV_D estimates and the group of experiments flagged by *Err4* did not.

Correspondence analysis

A plot of correspondence analysis shows that variance in descriptor characteristics is primarily explained by the first 2 axes (Fig. 6). The 4 error terms are included as supplementary variables. The dispersions of clams (Fig. 2) were also added as supplementary variables; however, they are not included in the figures because each falls near the center of the correspondence plot. Dimension 1 (Figs. 6 and 7) was determined primarily on the basis of characteristic values from the Patch model, including estimates of efficiency, CV_E, CV_D, width of the dredge, and EAS (Table 9). Low EAS (which indicates more dredge overlap, low efficiency, or small experimental area), low efficiency estimates, high CV_E and CV_D, and small dredge sizes (2.54 m [8.33 ft] and 3.05 m [10.00 ft] wide), along with experiments with estimates of *Err2*, *Err3*, and *Err4* that fall at or above the 80th percentile, fall on the positive (right) side of dimension 1. High efficiency estimates, high EAS, the largest dredge size (3.81 m [12.50 ft]), and low CV_E and CV_D fall on the negative (left) side of dimension 1.

Dimension 2 (Figs. 6 and 7) is categorized by species (the ocean quahog and Atlantic surfclam) and other variables that relate to the location of the depletion experiments for the 2 species, such as depth, latitude, and region. The positive values are variables that relate to depletion experiments that targeted ocean quahogs, variables such as higher latitudes and deeper depths. Negative values are variables that relate to depletion experiments that targeted Atlantic surfclams: lower latitudes and shallower depths. Experiments with ocean quahogs were typically conducted farther north (Fig. 1) than experiments with Atlantic surfclams, and the species is generally found at deeper depths than the Atlantic surfclam. Dimension 3 (Figs. 7 and 8) is characterized by the CV_K, and high efficiency estimates and high EAS fall on the positive side.

Table 5

Characteristics and other details for depletion experiments that were conducted in the field and targeted ocean quahogs (*Arctica islandica*) and Atlantic surfclams (*Spisula solidissima*) between 1997 and 2011 off the mid-Atlantic coast of the United States. The regions are Long Island (LI) in New York; New Jersey (NJ); Southern New England (SNE); and the Delmarva Peninsula in Delaware, Maryland, and Virginia. Experiments with an error estimate at or above the 80th percentile are denoted with an asterisk (*) followed by the number of the error term (1, 2, 3, or 4). The overlap score describes the overlap of tows of the dredge in an experiment.

Experiment ID	Region	Dredge width (m)	No. of tows	Overlap score	Year	Latitude	Longitude
SC1997-2 (*3,*4)	NJ	2.54	39	0.5237	1997	40.05317	−73.83917
SC1997-3	NJ	3.30	13	1.2586	1997	39.39317	−73.91033
SC1997-4 (*1)	NJ	3.30	18	0.9197	1997	39.39317	−73.91033
SC1997-5	NJ	2.54	17	0.7535	1997	39.36500	−73.89833
SC1997-6 (*1)	NJ	2.54	19	0.6972	1997	39.36500	−73.89833
SC1999-2	NJ	3.30	4	1.4151	1999	39.68133	−73.74667
SC1999-3 (*2)	NJ	3.30	5	1.1389	1999	39.68133	−73.74667
SC1999-4	NJ	3.30	6	1.7098	1999	39.52133	−73.77867
SC1999-5 (*1)	DMV	3.30	28	0.7257	1999	36.90200	−74.97583
SC1999-6 (*2)	NJ	3.30	4	1.1338	1999	39.56333	−73.91167
SC1999-7	NJ	3.30	10	0.7994	1999	39.76800	−73.91633
OQ00-01 (*2)	LI	3.81	22	0.6107	2000	40.60217	−71.98750
OQ00-02 (*1)	LI	3.81	16	0.6647	2000	40.39450	−72.54300
OQ00-03 (*2,*3,*4)	LI	3.05	27	0.4191	2000	40.58300	−72.79683
OQ02-01 (*3,*4)	LI	3.05	24	0.7954	2002	40.72762	−71.73730
OQ02-02	LI	3.05	22	0.6755	2002	40.10312	−73.19108
OQ02-03	NJ	3.05	20	0.7304	2002	38.81491	−73.81335
OQ02-04 (*3*4)	DMV	3.05	24	0.7645	2002	37.88755	−74.64486
SC02-02	NJ	3.30	16	0.7788	2002	40.10908	−73.84423
SC02-03 (*3*4)	NJ	3.30	20	1.0199	2002	39.26923	−73.78116
SC02-04	DMV	3.30	18	0.7992	2002	38.85791	−74.02778
SC04-01	NJ	3.30	24	0.9250	2004	39.28611	−73.87778
SC04-02	NJ	3.30	20	0.8534	2004	39.58278	−74.02778
SC04-03 (*1)	DMV	3.05	20	1.0088	2004	38.27075	−74.37920
OQ05-01 (*1*2*3*4)	LI	3.05	20	1.2952	2005	40.51903	−72.07617
OQ05-02 (*1)	LI	3.05	21	1.3401	2005	40.38957	−72.38950
OQ05-03 (*2*3*4)	LI	3.05	20	1.1380	2005	40.64220	−72.65170
OQ05-04 (*2)	LI	3.05	17	1.1259	2005	40.68170	−72.18147
OQ05-06 (*2*3*4)	LI	3.05	20	1.0803	2005	40.05550	−72.41673
SC05-01	NJ	3.05	20	1.1754	2005	39.26530	−74.37947
SC05-02	NJ	3.05	17	1.0985	2005	39.56383	−73.90364
SC05-03 (*1*2)	NJ	3.05	20	1.0094	2005	39.89733	−73.90591
SC05-04 (*3*4)	DMV	3.05	20	1.2129	2005	39.56972	−73.54946
SC05-05	NJ	3.05	17	1.0779	2005	39.43615	−73.37320
OQ08-01	LI	3.05	17	0.8493	2008	40.93762	−72.04765
OQ08-02	LI	3.05	17	0.8783	2008	40.27445	−72.84397
OQ08-03	SNE	3.81	17	0.7940	2008	41.02307	−70.85472
SC08-01	NJ	3.81	13	0.8097	2008	39.30475	−74.05158
SC08-02	NJ	3.81	18	1.2103	2008	39.18136	−74.07645
SC08-03 (*1)	NJ	3.81	21	0.8772	2008	39.60343	−73.42194
SC08-04	NJ	3.81	17	0.9867	2008	39.81033	−73.9149
SC08-09	NJ	3.81	17	0.9607	2008	39.31328	−74.05285
OQ11-01 (*2)	NJ	3.81	10	1.0210	2011	39.03003	−74.05774
OQ11-02	NJ	3.81	20	0.9027	2011	39.89356	−73.48104
OQ11-02S	NJ	3.81	18	1.1519	2011	39.8925	−73.47500
OQ11-05	LI	3.81	22	0.9783	2011	40.13542	−72.12010
SC11-02 (*4)	NJ	3.81	20	0.9027	2011	39.89356	−73.48104
SC11-02S	NJ	3.81	18	0.9543	2011	39.89250	−73.47500
SC11-03 (*1)	LI	3.81	14	1.0206	2011	40.56700	−73.08100
SC11-04	LI	3.81	17	0.9260	2011	40.64100	−73.03600

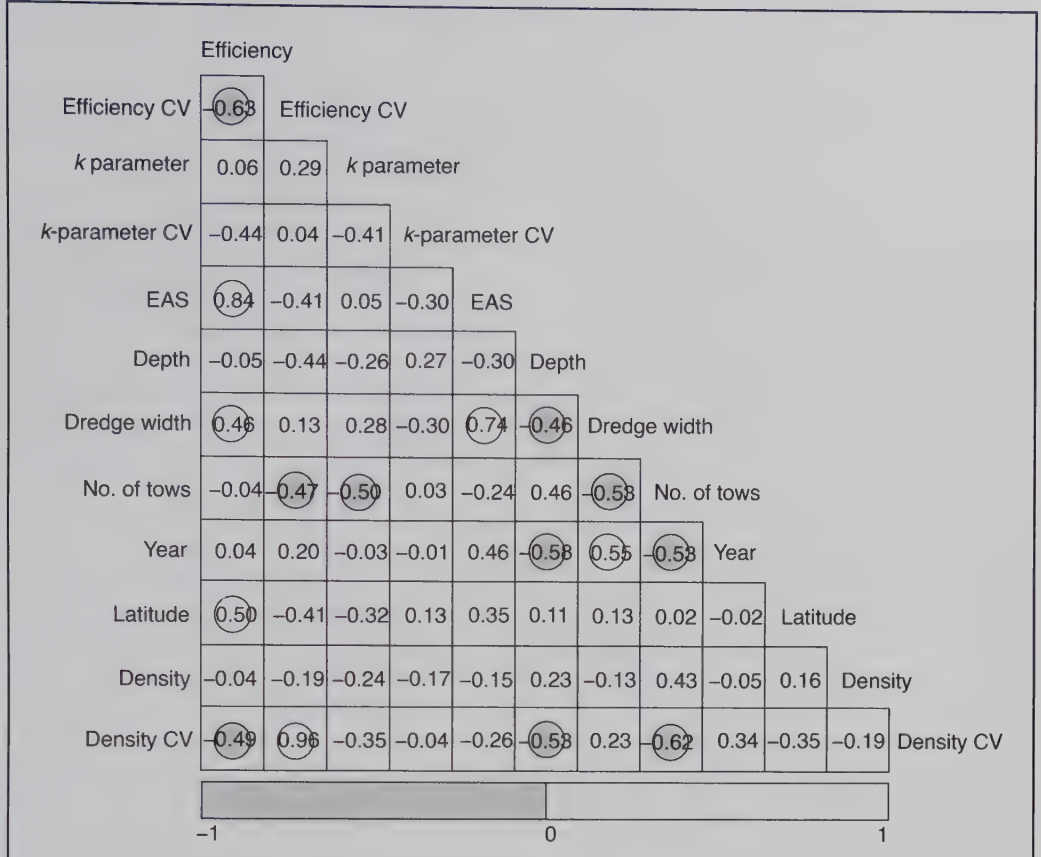

Figure 4

Correlogram for depletion experiments that targeted ocean quahogs (*Arctica islandica*) off the mid-Atlantic coast of the United States between 1997 and 2011. Numerals in the squares are Pearson's correlation coefficients. Circles denote significant correlations ($P \leq 0.05$). White circles indicate positive correlations, and gray circles indicate negative correlations. Characteristics used to describe experiments include dredge efficiency and its coefficient of variation (CV); the *k* parameter, which is the negative binomial dispersion parameter; CV of the *k* parameter; effective area swept (EAS); depth; dredge width; number of tows of the dredge; year; latitude; and clam density and its CV.

The parameters describing clam distribution do not fall on any axis and are grouped in the middle of the correspondence analysis plots on all dimensions; therefore, they are not included in the figures to improve clarity. Although clam distribution clearly affects the outcome of individual experiments, as observed through simulation analysis (Poussard et al., 2021), this effect is distributed across the experimental spectrum, apportioning uncertainty in a relatively random way with respect to the field experimental data set.

Discussion

Estimation of efficiency

The 4 error terms identify field depletion experiments that engender misgivings about their quality. Because the 4 characteristics used to generate 2 of the error estimates (*Err1* and *Err2*), CV_E, CV_K, OS, and average EAS, are orthogonal to each other, identification of a subset of experiments flagged by *Err1* and *Err2* indicates that these experiments are characterized by an unusual distribution of these 4 descriptive measures. It is important to note that using a log transformation of EAS did not change which experiments were flagged by these 2 error terms. A close fit to the values of these 4 characteristics was not found among the 9000 simulations of Poussard et al. (2021) that covered a wide range of experimental protocols and field conditions of clam dispersion (Table 1). The absence of a close fit is reason to suspect that these experiments may be uninformative or may have produced inaccurate efficiency estimates.

Error terms *Err3* and *Err4* relate to inferred inaccuracies in the efficiency estimates, also gleaned from comparison with the simulation data set of Poussard et al. (2021). Experiments flagged by these error terms are most comparable to simulations with high average error

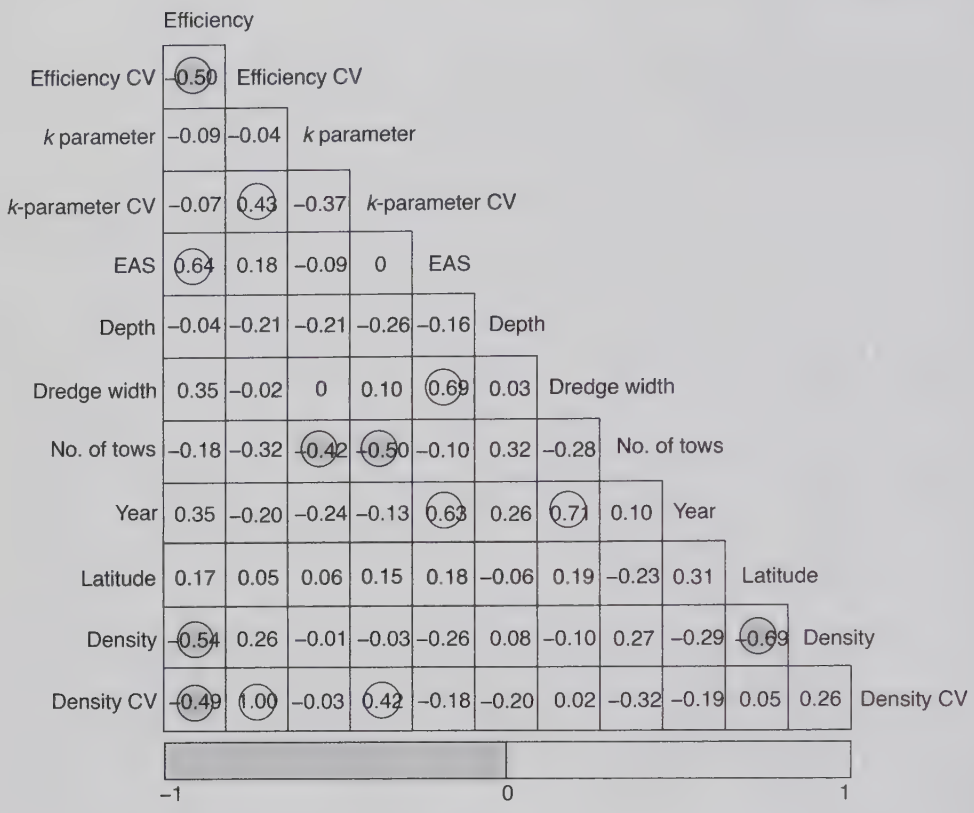

Figure 5

Correlogram for depletion experiments that targeted Atlantic surfclams (*Spisula solidissima*) off the mid-Atlantic coast of the United States between 1997 and 2011. Numerals in the squares are Pearson's correlation coefficients. Circles denote significant correlations ($P \leq 0.05$). White circles indicate positive correlations, and gray circles indicate negative correlations. Characteristics used to describe experiments include dredge efficiency and its coefficient of variation (CV); the *k* parameter, which is the negative binomial dispersion parameter; CV of the *k* parameter; effective area swept (EAS); depth; dredge width; number of tows of the dredge; year; latitude; and clam density and its CV.

Table 6

Average and median values of the following Patch model parameters for depletion experiments that were flagged because estimates were at or above the 80th percentile for each error term: dredge efficiency; clam density; the *k* parameter, which is the negative binomial dispersion parameter; effective area swept (EAS); and overlap score (OS), which describes the overlap of tows of the dredge. Standard deviations (SDs) were calculated with the maximum likelihood equation (Equation 5), and CVs were calculated with Equation 6. Data used in the model are from depletion experiments conducted during 1997–2011 for populations of ocean quahogs (*Arctica islandica*) and Atlantic surfclams (*Spisula solidissima*) off the mid-Atlantic coast of the United States.

Error term	Type of value	No. of flagged experiments	Efficiency			Density (individuals/m^2)			*k* parameter			EAS (m^2)	OS
			Value	SD	CV	Value	SD	CV	Value	SD	CV		
Err1	Average	10	0.514	0.124	26.80	2.26	0.49	214.34	5.41	2.57	88.60	99,871	0.96
	Median		0.567	0.115	24.06	0.67	0.13	193.92	4.52	1.99	32.24	14,196	0.96
Err2	Average	10	0.464	0.171	134.74	1.36	5.82	3933.21	20.94	2.91	59.22	99,251	1.00
	Median		0.551	0.109	25.30	0.88	0.23	189.55	6.68	2.24	31.95	10,666	1.10
Err3	Average	9	0.384	0.106	34.09	1.51	0.36	292.30	5.30	2.10	58.50	6584	0.92
	Median		0.381	0.103	32.08	0.97	0.36	238.35	4.45	1.58	29.87	6302	1.02
Err4	Average	10	0.419	0.104	31.92	1.15	0.33	273.36	5.34	2.07	55.78	8134	0.92
	Median		0.435	0.097	27.39	0.92	0.32	205.66	5.07	1.62	29.91	6400	0.96

Table 7

Results of Wilcoxon rank sums tests for depletion experiment variables classified by error terms. Experiments were flagged because estimates of variables were at or above the 80th percentile for one or more error terms. The tests were used to evaluate relationships between data from the field experiments flagged by one or more error terms with the rest of the data set from experiments conducted during 1997–2011 for ocean quahogs (*Arctica islandica*) and Atlantic surfclams (*Spisula solidissima*) off the mid-Atlantic coast of the United States. A dash indicates that the relationship between an error term and a variable are not significant ($P>0.05$). Variables that describe the experiments include dredge efficiency; clam density; the k parameter, which is the negative binomial dispersion parameter; effective area swept (EAS); and number of tows of the dredge. CV=coefficient of variation.

	$P>\|Z\|$			
	Error term			
Variable	*Err1*	*Err2*	*Err3*	*Err4*
Efficiency	–	0.0454	0.0004	0.0014
Efficiency CV	–	–	0.0180	–
Density	–	–	–	–
Density CV	–	–	0.0250	–
k parameter	–	–	–	–
k-parameter CV	–	–	0.0340	0.0250
EAS	–	–	0.0001	0.0009
No. of tows	–	–	–	–

in efficiency estimates and potentially have high average error in efficiency themselves. Nine out of 10 experiments flagged by *Err4* were also flagged by *Err3*, as these 2 error terms are very similar. These experiments may be uninformative or may have produced inaccurate efficiency estimates.

Ultimately, because of the nature of the error terms and the inability to evaluate all possible experimental conditions (e.g., all possible tow numbers and clam distributions, or all possible true efficiencies), the inference that the flagged experiments produced uninformative or inaccurate efficiency estimates cannot be affirmed. In aggregate, however, the analysis of the field experiments points to a subset of field experiments of lower quality than the remainder.

Interestingly, the experiments flagged by *Err1*, which might identify suspect experiments, exert less influence on the final objective of determining the efficiency of hydraulic dredges. The distribution of these experiments is unbiased relative to the remaining experiments, regardless of the characteristic used for comparison (Table 5). The same cannot be said for *Err2*, *Err3*, and *Err4*. The series of 16 depletion experiments with estimates of *Err2*, *Err3*, and *Err4* that fall at or above the 80th percentile is clearly biased relative to the remaining experiments, on the basis of the results of Wilcoxon rank sums tests (Table 7), and the existence of this bias is reinforced by correspondence analysis (Figs. 6–8). In addition, the direction of bias is noteworthy. Experiments identified by *Err2*, *Err3*, and *Err4* are characterized by lower efficiency estimates on

Table 8

Comparison of mean and median values of model parameters between depletion experiments with parameter estimates at or above the 80th percentile for error terms *Err2*, *Err3*, and *Err4* and experiments with estimates below the 80th percentile for the same error terms. The parameters are dredge efficiency and its coefficient of variation (CV); the CV of the k parameter, which is the negative binomial dispersion parameter; clam density and its CV; overlap score (OS), which describes the overlap of tows of the dredge; and effective area swept (EAS). Data used in the model are from depletion experiments conducted during 1997–2011 for populations of ocean quahogs (*Arctica islandica*) and Atlantic surfclams (*Spisula solidissima*) off the mid-Atlantic coast of the United States.

		Error term					
		Err2		*Err3*		*Err4*	
Parameter	Type of value	<80th percentile	≥80th percentile	<80th percentile	≥80th percentile	<80th percentile	≥80th percentile
Efficiency	Mean	0.654	0.464	0.667	0.384	0.666	0.419
	Median	0.645	0.551	0.652	0.381	0.652	0.435
Efficiency CV	Mean	19.496	134.744	44.402	34.089	45.202	31.920
	Median	19.232	25.299	16.789	32.075	17.325	27.392
k-parameter CV	Mean	41.785	59.215	42.368	58.497	42.644	55.783
	Median	32.924	31.953	33.139	29.869	33.257	29.913
Density (individuals/m^2)	Mean	1.389	1.356	1.345	1.507	1.367	1.421
	Median	0.743	0.887	0.743	0.969	0.743	0.915
Density CV	Mean	162.998	3933.081	1054.153	292.294	1077.931	273.350
	Median	135.765	189.542	132.375	238.345	132.924	205.655
OS	Mean	0.948	0.997	0.967	0.917	0.969	0.915
	Median	0.911	1.103	0.926	1.020	0.940	0.961
EAS (m^2)	Mean	18,048.6	99,251.5	40,370.7	6584.3	40,827.9	8134.3
	Median	15,489.3	10,666.3	16,066.2	6302.6	16,050.7	6400.2

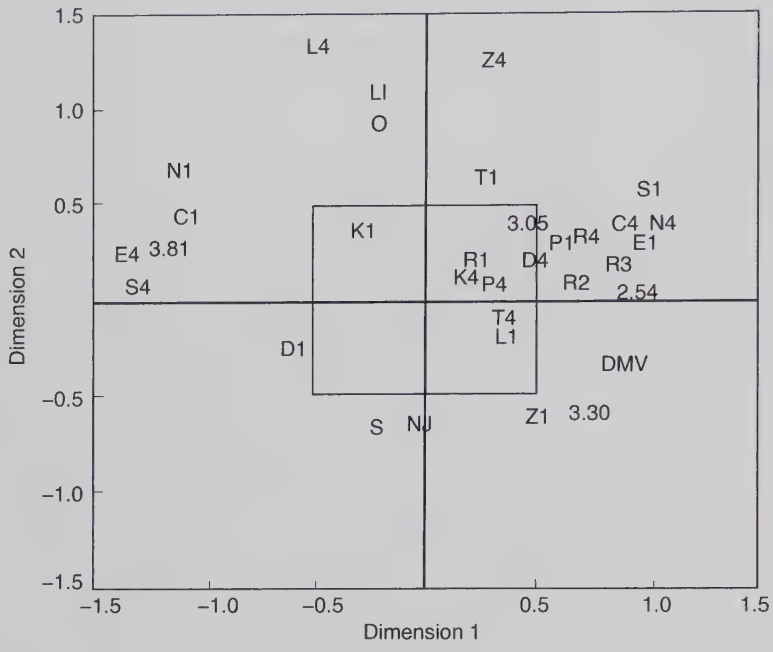

Figure 6

Correspondence analysis for dimensions 1 and 2 for the data set from depletion experiments conducted during 1997–2011 to examine efficiency of hydraulic dredges for capturing clam species and to estimate stock density for populations of ocean quahogs (*Arctica islandica*) and Atlantic surfclams (*Spisula solidissima*) off the mid-Atlantic coast of the United States. Error terms *Err1* (R1), *Err2* (R2), *Err3* (R3), and *Err4* (R4) are supplementary variables. Estimates of the following characteristics are entered as quartiles: dredge efficiency (E); clam density (D); the *k* parameter (K), which is the negative binomial dispersion parameter; coefficient of variation (CV) of efficiency (C); CV of density (N); CV of the *k* parameter (P); effective area swept (S); overlap score (T); latitude (L); and depth (Z); only quartiles 1 and 4 are shown in the plot. Other variables that describe the experiments include species, the ocean quahog (O) and Atlantic surfclam (S); region, Long Island (LI) in New York, New Jersey (NJ), and the Delmarva Peninsula (DMV) of Delaware, Maryland, and Virginia; and dredge width. Dredge widths are 2.54, 3.05, 3.30, and 3.81 m. Error estimates are entered as 1 (below the 80th percentile) or 2 (at or above the 80th percentile). The inner box demarcates the area with loading factors from −0.5 to 0.5 on both axes.

average, and their inclusion in the depletion data set may bias the overall efficiency estimates used to inform stock assessments.

In correspondence analysis, *Err2*, *Err3*, and *Err4* also fall on the same dimensional axis as a low EAS value. Low EAS and low efficiency generally occur together because the efficiency value is a variable in the equation determining EAS (Equation 3). The relationship is well-documented by Poussard et al. (2021). This expectation is confirmed by Pearson's correlation coefficients calculated by using the field depletion experiment data set (Figs. 4 and 5). The EAS is also positively correlated with year for experiments that targeted ocean quahogs and with dredge width for experiments with both ocean quahogs and Atlantic surfclams (Figs. 4 and 5). The relationship is driven by the largest dredge width (3.81 m [12.5 ft]); experiments with dredges of this size clearly had superior performance.

High OS in a depletion experiment does not always reduce uncertainty in Patch model estimates. An explanation for this may come from the pragmatic efforts of a field experiment. Depletion experiments are costly in vessel time and crew effort, often requiring more than 8 h of nearly continual dredging. Cost at sea was sufficient in that adaptive time management during the experiment was directed at limiting tow number, albeit with limited empirical guidance to determine the stopping point for the depletion experiment.

One consequence of adaptive time management during the depletion experiment was a decision to add tows if the experiment appeared not to be generating a clear and consistent reduction in catch per tow. Results of correspondence analysis indicate the danger of the use of adaptive decisions during depletion experiments without rigorous empirical determination criteria designed to optimize the cost and benefit of increasing tow number. The danger of terminating a depletion experiment early on the basis of a potentially misleading depletion curve was present as well. The OS did not fall out cleanly in any of the dimensions on the plots of correspondence analysis, the opposite of what was expected given the clear improvement afforded by higher tow numbers, and more tow overlap, in the simulation study of Poussard et al. (2021). However, the absence of OS did not diminish its effect on estimates of gear efficiency in depletion experiments. Notably, OS and the distribution of clams on the bottom (e.g., NP, P, T, or HP), which in some fashion are measures of dredge overlap with tow paths or with clams in the area, are both relatively unbiased parameters. That is, they are not associated with any depth, dredge size, species, or other characteristic of the experiment. The distribution of clams relative to the distribution of tows is a critical constraint on efficiency estimation.

Results of correspondence analysis clearly reveal the relationships earlier identified by using the Wilcoxon rank sum tests and by Pearson's correlation coefficients. The error terms *Err2*, *Err3* and *Err4*, which the results of Wilcoxon analyses indicate were highly significant, fall on the positive side of dimension 1 along with the parameters and experiment characteristics significantly influenced by them. The error term *Err1*, which did not have significant differences in the Wilcoxon rank sum tests,

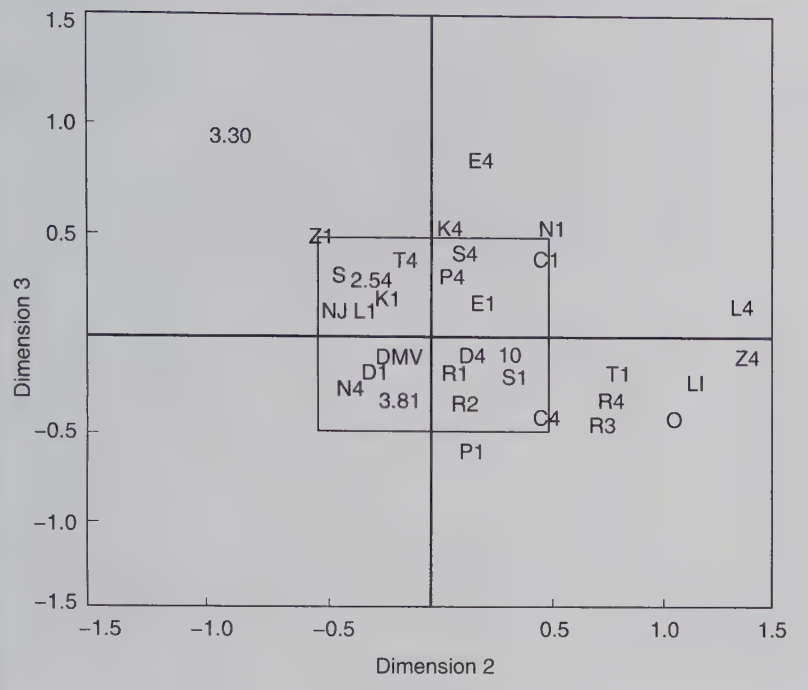

Figure 7

Correspondence analysis for dimensions 2 and 3 for the data set from depletion experiments conducted during 1997–2011 to examine efficiency of hydraulic dredges for capturing clam species and to estimate stock density for populations of ocean quahogs (*Arctica islandica*) and Atlantic surfclams (*Spisula solidissima*) off the mid-Atlantic coast of the United States. Error terms *Err1* (R1), *Err2* (R2), *Err3* (R3), and *Err4* (R4) are supplementary variables. Estimates of the following characteristics are entered as quartiles: dredge efficiency (E); clam density (D); the *k* parameter (K), which is the negative binomial dispersion parameter; coefficient of variation (CV) of efficiency (C); CV of density (N); CV of the *k* parameter (P); effective area swept (S); overlap score (T); latitude (L); and depth (Z); only quartiles 1 and 4 are shown in the plot. Other variables that describe the experiments include species, the ocean quahog (O) and Atlantic surfclam (S); region, Long Island (LI) in New York, New Jersey (NJ), and the Delmarva Peninsula (DMV) of Delaware, Maryland, and Virginia; and dredge width. Dredge widths are 2.54, 3.30, and 3.81 m. Error estimates are entered as 1 (below the 80th percentile) or 2 (at or above the 80th percentile). The inner box demarcates the area with loading factors from −0.5 to 0.5 on both axes.

falls near the origin in all 3 dimensions, indicating that the experiments identified by this error estimate are more or less randomly distributed throughout the field depletion data set. A tendency for large dredges to be associated with improved experimental performance is shown in Figure 6; however, the influence of dredge size is complex, as the various dredge sizes do not fall in order of size on dimensions 1 or 2. Dredge size to some extent is likely conflated with other variables, such as species, year, and depth, and was determined more by boat availability and increased familiarity of the crew and scientific staff with depletion experiment methods over time than by experiment performance; the clear exception is the largest dredge size. The fact that species as a variable falls near the origin on dimensions 1 and 3 indicates the similarity in efficiency estimates for the 2 species, which essentially are separated solely by depth.

In the correspondence analysis, *Err2*, *Err3*, and *Err4* are associated with experiments characterized by smaller dredges, higher CV_E values, and higher CV_D values than those of other experiments. The co-occurrence of these characteristics instills suspicion about the quality of the results obtained from a subset of the depletion experiments. Essentially, experiments with estimates of *Err2*, *Err3*, and *Err4* that fall at or above the 80th percentile produced low efficiency estimates. Experiments most similar to simulations with high average error in efficiency estimates were flagged by *Err3* and *Err4*, indicating that these experiments could have high uncertainty in efficiency estimates and that these experiments should be removed from further evaluation of the inherent efficiency of hydraulic clam dredges.

Estimation of density

Interestingly, experiments with high CV_D are grouped with the experiments with low efficiency identified by *Err2*, *Err3*, and *Err4* in the correspondence analysis, indicating that experiments with more uncertain estimates of clam density also produced low efficiency estimates and were flagged by the error terms. Poussard et al. (2021) clearly showed that the accuracy of efficiency estimates and the density of clams in the area are not correlated in simulated depletion experiments, save for instances where low clam density combines with an irregular distribution of clams in the benthos to bias efficiency to a low value. Efficiency estimates not being influenced heavily by clam density is a logical outcome on the basis of an expectation that hydraulic dredges should be equally efficient whether used in low-density or high-density regions. The apposition of high CV for the density estimate and low efficiency is likely a product of high uncertainty in the density estimate co-occurring with high uncertainty in the efficiency estimate. Uncertainties in the efficiency and density estimates could be indicative of an experimental design failing or of environmental parameters not being conducive to accurate and precise estimation of efficiency and density.

The accuracy of the density estimate from the Patch model was evaluated thoroughly in Hennen et al. (2012). The *k* parameter was not evaluated for accuracy in that study because a negative binomial distribution was not

Table 9

Variables that fall on each of the 3 dimensions of correspondence analysis with loading factors ≤–0.5 or ≥0.5. Variables describe depletion experiments conducted during 1997–2011 to examine efficiency of hydraulic dredges for capturing clam species and to estimate stock density for populations of ocean quahogs (*Arctica islandica*) and Atlantic surfclams (*Spisula solidissima*) off the mid-Atlantic coast of the United States. Variables include dredge width; dredge efficiency and its coefficient of variation (CV); effective area swept (EAS); CV of the *k* parameter, which is the negative binomial dispersion parameter; error terms *Err2*, *Err3*, and *Err4*; CV of clam density; region, Long Island (LI) in New York, New Jersey (NJ), or the Delmarva Peninsula (DMV) of Delaware, Maryland, and Virginia; overlap score (OS), which describes the overlap of tows of the dredge; species; and latitude. N/A indicates that the variable fell close to the origin and not strongly on the positive or negative side of the dimension.

Dimension 1			Dimension 2			Dimension 3		
Variable	Negative (≤–0.5)	Positive (≥0.5)	Variable	Negative (≤–0.5)	Positive (≥0.5)	Variable	Negative (≤–0.5)	Positive (≥0.5)
Dredge width (m)	3.81	2.54, 3.30	Dredge width	3.30	N/A	Dredge width	3.30	N/A
Efficiency	High	Low	OS	N/A	Low	Efficiency	N/A	High
Efficiency CV	Low	High	Species	Atlantic surfclam	Ocean quahog	EAS	N/A	High
EAS	High	Low	EAS	N/A	Low	*k*-parameter CV	High	N/A
k-parameter CV	N/A	Low	Region	NJ	LI			
Err2, *Err3*, and *Err4*	N/A	High	Depth	Low	High			
Density CV	Low	High	Latitude	N/A	High			
Region	N/A	DMV	Density CV	N/A	Low			

used to create the distribution of clams. The *k* parameter is indirectly related to clam distribution and tow distance (Hennen et al., 2012). Results from the simulations of Poussard et al. (2021) indicate that the estimates of *k* are higher with a uniform distribution of clams and lower with a more irregular distribution. This parameter is influenced by the same conditions of the experiment that influence efficiency, but correspondence analysis does not cleanly separate the *k* parameter or its CV from other variables, such as the efficiency estimate, density estimate, depth, region, dredge width, and the values of CV_E and CV_D. (Figs. 7 and 8). The results of correspondence analysis identify a tendency for low uncertainty in the *k* parameter (and in CV_K) to be associated with low efficiency and high CV_E in comparison with those of other experiments. Experiments with these characteristics also were flagged by the error terms.

Poussard et al. (2021) reported that the dispersion of clams on the bottom clearly can cause a decrease in performance in the depletion experiment. This outcome is exacerbated by low tow number and low amount of tow overlap. In practice, even an ideal experiment, with many dredge tows and a high degree of overlap in the tow paths, would appear to be susceptible to producing an unreliable efficiency estimate if the distribution of clams in the benthos is irregular. Clam dispersion is a random effect for the field experiments, despite its documented importance in determining outcomes. This notion is consistent with the fact that the locations for the experiments were chosen without any a priori knowledge of the characteristics of clam dispersion at the site. As Hennen et al. (2012) concluded, the ability to have divers determine or to use remote optical methods to determine the size, location, and approximate density of clam aggregations would be useful in choosing the site and tow pattern in a depletion experiment.

Factors affecting field outcomes

The size of the dredge is related to the efficiency estimated, with larger dredges being used with experiments with higher efficiency estimates. Small dredge sizes (2.54 m [8.33 ft] and 3.05 m [10.00 ft]) were used in many experiments, and they contributed disproportionately to the subset identified by estimates of *Err2*, *Err3*, and *Err4* (Fig. 6). It may be that smaller dredges are harder to control precisely, leading to greater uncertainty in the exact position of the dredge, uncertainty that can lead to error in the estimation of efficiency (Hennen et al., 2012; Willberg et al., 2013). The majority of flagged experiments identified by estimates of the 4 error terms were conducted in 1997, 1999, and 2005, and among these experiments are those categorized as having lower efficiency estimates with more uncertainty in the estimate, relative to those of the other experiments. Although speculative, 2 possibilities may explain this trend. A wider dredge may be inherently more efficient because loss in efficiency is likely associated with the encounter of clams near the lateral edges of the dredge knife blade, and these clams are a lower fraction of the potential catch with the larger dredge. In addition, the narrow dimension of the depletion rectangle was generally set at 10 dredge widths; therefore, the largest dredge (3.81 m [12.50 ft]) was used to deplete larger regions, possibly reducing the influence of small-scale variations in clam dispersion within the depletion rectangle. It is noteworthy that experiments with the

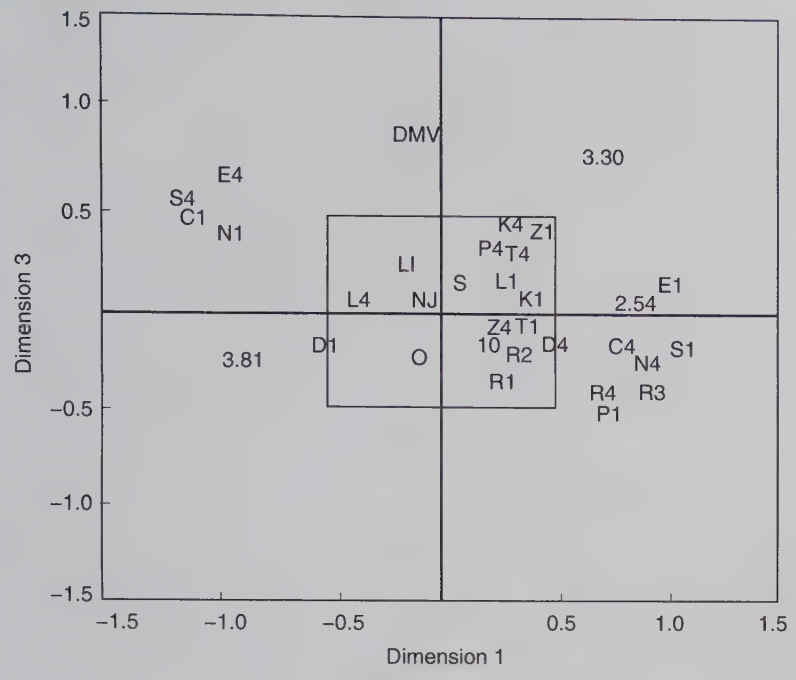

Figure 8

Correspondence analysis for dimensions 1 and 3 for the data set from depletion experiments conducted during 1997–2011 to examine efficiency of hydraulic dredges for capturing clam species and to estimate stock density for populations of ocean quahogs (*Arctica islandica*) and Atlantic surfclams (*Spisula solidissima*) off the mid-Atlantic coast of the United States. Error terms *Err1* (R1), *Err2* (R2), *Err3* (R3), and *Err4* (R4) are supplementary variables. Estimates of the following characteristics are entered as quartiles: dredge efficiency (E); clam density (D); the *k* parameter (K), which is the negative binomial dispersion parameter; coefficient of variation (CV) of efficiency (C); CV of density (N); CV of the *k* parameter (P); effective area swept (S); overlap score (T); latitude (L); and depth (Z); only quartiles 1 and 4 are shown in the plot. Other variables that describe the experiments include species, the ocean quahog (O) and Atlantic surfclam (S); region, Long Island (LI) in New York, New Jersey (NJ), and the Delmarva Peninsula (DMV) of Delaware, Maryland, and Virginia; and dredge width. Dredge widths are 2.54, 3.30, and 3.81 m. Error estimates are entered as 1 (below the 80th percentile) or 2 (at or above the 80th percentile). The inner box demarcates the area with loading factors from −0.5 to 0.5 on both axes.

largest dredge were conducted in later years, when the depletion experiment method was more consistent among experiments and produced higher efficiency estimates, yielding higher OS values. Accordingly, the improved performance cannot unequivocally be assigned to the largest size of the dredge used.

Location of the depletion experiment might also have affected the efficiency estimate. Depletion experiments that targeted ocean quahogs off Long Island have higher efficiency estimates than experiments conducted farther south. The relationship is shown objectively (Fig. 1) and in correlation (Fig. 4). Results of the correlation analysis do not indicate a significant relationship between latitude and the efficiency estimate, but this finding accrues from the inclusion of high-efficiency experiments with Atlantic surfclams that took place farther south (Fig. 1). The relationship is not associated with dredge width, although efficiency and dredge width are significantly correlated for experiments with ocean quahogs (Fig. 4). These experiments took place in deeper water, on the average, but correlation and correspondence analysis agree that depth, per se, does not influence outcomes. Edaphic factors may be examined as proxies for the influence of region, but little information is available to make a determination.

Depth might be considered to be an effective variable that determines the success of a depletion experiment for hydraulic dredges because these dredges are operated by using an onboard water pump attached to the dredge by means of a large hose. The vessel is less maneuverable in deeper water because of the increased amount of hose required to maintain an adequate scope while dredging. Surprisingly, neither correlation analysis nor correspondence analysis offer any evidence for a significant correlation between depth and experimental performance or the final efficiency estimate. Depth-related variables, in fact, fall orthogonally to experiment performance characteristics and estimates of the error terms *Err2*, *Err3*, and *Err4* in correspondence analysis.

Conclusions

When the 16 experiments (7 experiments with Atlantic surfclams and 9 experiments with ocean quahogs) that had estimates of error terms *Err2*, *Err3* and *Err4* that fall at or above the 80th percentile were removed from the field depletion data set, the mean efficiency estimate increased from 0.635 to 0.694 for experiments that targeted Atlantic surfclams (Table 10). The median likewise rose substantially from 0.590 to 0.647 and the interquartile range, although remaining relatively unchanged in dimension, shifted to higher efficiency values. The mean efficiency estimate for experiments that targeted ocean quahogs increased from 0.586 to 0.711, and the median rose from 0.629 to 0.667. The interquartile range was substantially reduced in dimension and shifted to higher efficiency values. The efficiency estimates for the data set after removal of experiments flagged by an error term indicate that experiments flagged by *Err1* do not have efficiency estimates that are biased in either direction and do not meaningfully negate the trends established with the other 3 error terms.

Table 10

Comparison of mean, standard deviation (SD), and median values and quartiles of model estimates of dredge efficiency between all depletion experiments and subsets of experiments flagged by all error terms or by error terms *Err2*, *Err3*, and *Err4*. Experiments were flagged because estimates were at or above the 80th percentile for an error term. Data used in the model are from depletion experiments conducted during 1997–2011 for populations of ocean quahogs (*Arctica islandica*) and Atlantic surfclams (*Spisula solidissima*) off the mid-Atlantic coast of the United States.

Species	Efficiency estimate	Mean	SD	1st quartile	Median	3rd quartile
Ocean quahog	All experiments	0.586	0.260	0.381	0.629	0.779
	9 experiments flagged by error terms 2, 3, and 4 removed	0.711	0.195	0.629	0.667	0.795
	10 experiments flagged by all error terms removed	0.758	0.169	0.641	0.716	0.898
Atlantic surfclam	All experiments	0.635	0.229	0.533	0.590	0.779
	7 experiments flagged by error terms 2, 3, and 4 removed	0.694	0.196	0.570	0.647	0.852
	13 experiments flagged by all error terms removed	0.738	0.172	0.584	0.733	0.889

Interestingly, the mean and median efficiency estimates for the hydraulic dredges that targeted Atlantic surfclams and ocean quahogs are nearly identical. Neither the species nor the presence of one generally in deeper water than the other significantly influences the overall efficiency that stands at approximately 70% regardless of mean or median determination.

The analyses of this study permit the evaluation of the factors involved in defining a standard operating protocol for experiments of this kind that are inherently extremely expensive to conduct. Several characteristics that define the success of the experimental design, such as the dispersion of clams on the bottom, will likely be unknown. As a consequence of the uncertainty behind these experiments, a sufficient number of replicates will always be required in order to provide a useful recommendation for catchability. Effectively the same conclusion was made in other studies of dredge calibration with a significant number of experiments (Hennen et al., 2012; Morson et al., 2018).

Estimates from the Patch model are useful in development of stock assessment models in the future; for example, capture efficiency estimates can be used to form prior distributions for catchability parameters (NEFSC, 2010a, 2010b). However, these estimates are only as useful as the data from the depletion experiments used to inform the Patch model. Three groups of experiments have significantly different efficiency estimates and CVs from the remainder, as indicated by results of the Wilcoxon rank sums tests conducted on efficiency estimates flagged by *Err2*, *Err3*, and *Err4*. Although these error estimates can be used only to infer experimental quality, they identify experiments with a range of questionable attributes that strongly implicate them as outliers biasing the efficiency estimates for the entire data set. Removing these questionable experiments from the NMFS depletion data set provided the best estimates of efficiency for these commercial hydraulic dredges, and the results of the removal indicate that these dredges are highly efficient and minimize the degree of bottom contact relative to the catch.

Acknowledgments

This research was supported by the Science Center for Marine Fisheries, an Industry–University Cooperative Research Center of the National Science Foundation (NSF), through membership fees under the direction of the Industry Advisory Board provided through NSF award no. 1266057 and no. 1841112. We thank the NOAA Northeast Fisheries Science Center for making the data sets used in this study available, and we acknowledge the scientists and crew who participated in the depletion experiments at sea.

Literature cited

Chai, A.-L., M. Homer, C.-F. Tsai, and P. Goulletquer.
1992. Evaluation of oyster sampling efficiency of patent tongs and an oyster dredge. North Am. J. Fish. Manage. 12:825–832.

Clausen, S. E.
1998. Applied correspondence analysis: an introduction, 80 p. Sage Publ. Inc., Thousand Oaks, CA.

Da Ros, L., N. Nesto, C. Nasci, V. Moschino, D. Pampanin, and M. G. Marin.
2003. Biochemical and behavioural effects of hydraulic dredging on the target species *Chamelea gallina*. Fish. Res. 64:71–78.

Gedamke, T., W. D. DuPaul, and J. M. Hoenig.
2005. Index-removal estimates of dredge efficiency for sea scallops on Georges Bank. North Am. J. Fish. Manage. 25:1122–1129.

Gilkinson, K. D., G. B. J. Fader, D. C. Gordon, R. Charron, D. McKeown, D. Roddick, and Q. Liu.
2003. Immediate and longer-term impacts of hydraulic clam dredging on an offshore sandy seabed: effects on physical habitat and processes of recovery. Cont. Shelf Res. 23:1315–1336.

Gilkinson, K. D., D. C. Gordon, K. G. MacIsaac, D. L McKEown, E. L. R. Kenchington, C. Bourbonnais, and W. P. Vass.
2005. Immediate impacts and recovery trajectories of macrofaunal communities following hydraulic clam dredging on Banquereau, eastern Canada. ICES J. Mar. Sci. 62:925–947.

Hauton, C., T. R. W. Howell, R. J. A Atkinson, and P. G. Moore.
2007. Measures of hydraulic dredge efficiency and razor clam production, two aspects governing sustainability within the Scottish commercial fishery. J. Mar. Biol. Assoc. U.K. 87:869–877.

Hennen, D. R., L. D. Jacobson, and J. Tang.
2012. Accuracy of the Patch model used to estimate density and capture efficiency in depletion experiments for sessile invertebrates and fish. ICES J. Mar. Sci. 69:240–249.

Lambert, J., and P. Goudreau.
1996. Performance of the New England hydraulic dredge for the harvest of Stimson's surf clams (*Mactomeris polynyma*). Can. Ind. Rep. Fish. Aquat. Sci. 235, 28 p. [Available from website.]

Lasta, M. L., and O. O. Iribarne.
1997. Southwestern Atlantic scallop (*Zygochlamys patagonica*) fishery: assessment of gear efficiency through a depletion experiment. J. Shellfish Res. 16:59–62.

Leslie, P. H., and D. H. S. Davis.
1939. An attempt to determine the absolute number of rats on a given area. J. Anim. Ecol. 8:94–113.

Meseck, S. L., R. Mercaldo-Allen, J. M. Rose, P. Clark, C. Kuropat, J. J. Pereira, and R. Goldberg.
2014. Effects of hydraulic dredging for *Mercenaria mercenaria*, northern quahog, on sediment biogeochemistry. J. World Aquat. Soc. 45:301–311.

Meyer, T. L., R. A. Cooper, and K. J. Pecci.
1981. The performance and environmental effects of a hydraulic clam dredge. Mar. Fish. Rev. 43(9):14–22.

Morson, J. M., D. M. Munroe, K. A. Ashton-Alcox, E. N. Powell, D. Bushek, and J. Gius.
2018. Density-dependent capture efficiency of a survey dredge and its influence on the stock assessment of eastern oysters (*Crassostrea virginica*) in Delaware Bay. Fish. Res. 205:115–121.

Moschino, V., M. Deppieri, and M. G. Marin.
2003. Evaluation of shell damage to the clam *Chamelea gallina* captured by hydraulic dredging in the Northern Adriatic Sea. ICES J. Mar. Sci. 60:393–401.

NEFSC (Northeast Fisheries Science Center).
2010a. Monkfish (goosefish) stock assessment for 2010. *In* 50th Northeast regional stock assessment workshop (50th SAW) assessment report, p. 15–392. Northeast Fish. Sci. Cent. Ref. Doc. 10-17. [Available from website.]
2010b. Atlantic sea scallop stock assessment for 2010. *In* 50th Northeast regional stock assessment workshop (50th SAW) assessment report, p. 393–708. Northeast Fish. Sci. Cent. Ref. Doc. 10-17. [Available from website.]
2017a. 61st Northeast regional stock assessment workshop (61st SAW) assessment report. Northeast Fish. Sci. Cent. Ref. Doc. 17-05, 466 p. [Available from website.]
2017b. 63rd Northeast regional stock assessment workshop (63rd SAW) assessment report. Northeast Fish. Sci. Cent. Ref. Doc. 17-10, 409 p. [Available from website.]

NMFS (National Marine Fisheries Service).
2011. Fisheries economics of the United States, 2009. NOAA Tech. Memo. NMFS-F/SPO-118, 172 p.

Paloheimo, J. E., and L. M. Dickie.
1964. Abundance and fishing success. Rapp. P.-v. Réun. Cons. Int. Exp. Mer 155:152–163.

Parker, P. S.
1971. History and development of surf clam harvesting gear. NOAA Tech. Rep. NMFS CIRC-364, 15 p.

Pezzuto, P. R., C. Schio, and T. C. M. Almeida.
2010. Efficiency and selectivity of the *Anomalocardia brasiliana* (Mollusca: Veneridae) hand dredge used in southern Brazil. J. Mar. Biol. Assoc. U.K. 90:1455–1464.

Poussard, L. M., E. N. Powell, and D. R. Hennen.
2021. Efficiency estimates from depletion experiments for sedentary invertebrates: evaluation of sources of uncertainty in experimental design. Fish. Res. 234:10586.

Powell, E. N., K. A. Ashton-Alcox, and J. N. Kraeuter.
2007. Reevaluation of eastern oyster dredge efficiency in survey mode: application in stock assessment. North Am. J. Fish. Manage. 27:492–511.

R Core Team.
2019. R: a language and environment for statistical computing. R Foundation for Statistical Computing, Vienna, Austria. [Available from website, accessed April 2019.]

Ragnarsson, S. A., and G. G. Thórarinsdóttir.
2002. Abundance of ocean quahog, *Arctica islandica*, assessed by underwater photography and a hydraulic dredge. J. Shellfish Res. 21:673–676.

Rago, P. J., J. R. Weinberg, and C. Weidman.
2006. A spatial model to estimate gear efficiency and animal density from depletion experiments. Can. J. Fish. Aquat. Sci. 63: 2377–2388.

Sala, A., J. Brčić, B. Herrmann, A. Lucchetti, and M. Virgili.
2017. Assessment of size selectivity in hydraulic clam dredge fisheries. Can. J. Fish. Aquat. Sci. 74:339–348.

Skalski, J. R., D. S. Robson, and C. L. Matsuzaki.
1983. Competing probabilistic models for catch-effort relationships in wildlife censuses. Ecol. Model. 19:299–307.

Sokal, R. R., and F. J. Rohlf.
1998. Biometry: the principals and practice of statistics in biological sciences, 3rd ed., 887 p. W. H. Freeman and Co., New York.

Vølstad, J., G. Davis, A. Sharov, and B. Davis.
2000. A method for estimating dredge catching efficiency for blue crabs, *Callinectes sapidus*, in Chesapeake Bay. Fish. Bull. 98:410–420.

Wilberg, M. J., J. M. Robinson, S. A. M. Rains, J. L. Humphrey, and R. N. Lipcius.
2013. Effects of location errors on estimates of dredge catchability from depletion based methods. Fish. Res. 148:1–8.

Acknowledgment of reviewers

The editorial staff of *Fishery Bulletin* would like to acknowledge the scientists who reviewed manuscripts in 2020–2021. Their contributions have helped ensure the publication of quality science.

Michael Andres
Chevonne Angus

Cheryl Barnes
Henry L. Bart Jr.
Brian Beckman
Bryan Black
Brian Burke

Matthew Campbell
Shannon Cass-Calay
Liese Carleton
Peter Coulson
Daniel Cullen

John Denton
William Driggers III

Scott Eckert

Brian Fadely
Anthony Fowler
James Franks

John Galbraith
Gretchen Grammer

Ryan Heise
Allison Henry
Julian Hughes

P. Alexander Hulley
Peter Hulson

James Kennedy
Amy Knowlton
Kyne Krusic-Golub

Richard Langton

Mary Matta
Mark Maunder
Richard McBride
Chris McGonigle
John McGovern
Marissa McMahan
Richard Merrick
Richard Methot
Nina Mikkelsen
Ryo Misawa
Jason Morson

Lisa Natanson
Gavin Naylor

Andrew Ostrowski

William Patterson III
Mark Peterson
Bill Pine
Gregg Poulakis

André Punt

Joseph Quattro

Eric Robillard
Nathan Robinson
Christopher Rooper
Stephen Ross
Rodney Rountree

Chiyuki Sassa
George Sedberry
Kevin Siwicke
Szymon Smolinski
Mridula Srinivasan
Jan Straley

Wendy Teas
Todd Tenbrink
Jared Towers
Sara Turner

Francisco Velasco

John Walter III
Michael Weiss
Bruce Wright

Hong Yan

Fishery Bulletin

Guidelines for authors

Contributions published in *Fishery Bulletin* describe original research in marine fishery science, fishery engineering and economics, and marine environmental and ecological sciences (including modeling). Preference will be given to manuscripts that examine processes and underlying patterns. Descriptive reports, surveys, and observational papers may occasionally be published but should appeal to an audience outside the locale in which the study was conducted.

Although all contributions are subject to peer review, responsibility for the contents of papers rests upon the authors and not on the editor or publisher. *Submission of an article implies that the article is original and is not being considered for publication elsewhere.*

All submissions are subject to a double-blind review to remove the identity of author and reviewer during the review process.

Plagiarism and double publication are considered serious breaches of publication ethics. To verify the originality of the research in papers and to identify possible previous publication, manuscripts may be screened with plagiarism-detection software.

Manuscripts must be written in English; authors whose native language is not English are strongly advised to have their manuscripts checked by English-speaking colleagues before submission.

Once a paper has been accepted for publication, online publication takes approximately 2 weeks.

There is no cost for publication in *Fishery Bulletin*.

Types of manuscripts accepted by the journal

Articles generally range from 20 to 30 double-spaced typed pages (12-point font) and describe an original contribution to fisheries science, engineering, or economics. Tables and figures are not included in this page count, but the number of figures should not exceed 1 figure for every 4 pages of text. Articles contain the following divisions: abstract, introduction, methods, results, discussion, and conclusions.

Notes are generally less than 10 double-spaced typed pages (12-point font), including the Literature cited section. Like articles, notes describe an original contribution to fisheries science. They follow a format similar to that for articles: abstract, introduction, methods, results, and discussion, but the results and discussion sections may be combined and a conclusions section should not be included. They should include no more than 2 figures or tables (2 of each would be too many). They are distinguished from full articles in that they report a noteworthy new observation or discovery—such as the first report of a new species, a unique finding, condition, or event that expands our knowledge of fisheries science, engineering, or economics—and do not require a lengthy discussion. Manuscripts on range extensions will not be considered.

Companion articles should be submitted together and are published together as a scientific contribution. Both articles should address a closely related topic and may be articles that result from a workshop or conference.

Review articles of exceptional quality may be considered occasionally for publication on a case-by-case basis. They address a timely topic that is relevant to aspects of fisheries science. They should include an abstract, but the format of the article, per se, will be up to the author. Please contact the scientific editor to discuss your ideas regarding a potential review article before embarking on such a project.

Perspective essays generally are less than 5 double-spaced typed pages (12-point font) and provide clarification of misused terms or misunderstood topics in fisheries science. Essays are accepted at the discretion of the scientific editor. Opinion pieces on policy will not be considered. They should include an abstract and a list of the literature cited, but no other sections should divide the article. Please contact the scientific editor to discuss your idea before making a submission.

Preparation of manuscript

Title page should include authors' full names, affiliations, mailing addresses, and the senior author's email address.

Abstract should be limited to 200 words (one-half typed page), state the main scope of the research, and emphasize the authors' conclusions and relevant findings. Do not review the methods of the study or list the contents of the paper. Because abstracts are circulated by abstracting agencies, it is important that they represent the research clearly and concisely.

General text must be typed in 12-point Times New Roman font throughout. A brief introduction should convey the broad significance of the paper; the remainder of the paper should be divided into the following sections: Materials and methods, Results, Discussion, Conclusions, and Acknowledgments. Headings within each section must be short, reflect a logical sequence, and follow the rules of subdivision (i.e., there can be no subdivision without at least 2 subheadings). The entire text should be intelligible to interdisciplinary readers; therefore, all acronyms, abbreviations, and technical terms should be written out in full and defined the first time they are mentioned. Abbreviations should be used sparingly because they are not carried over to indexing databases and slow readability for those readers

outside a discipline. They should never be used for the main subject (e.g., species or method) of a paper.

For general style, follow the U.S. Government Publishing Office *Style Manual* (2016, available at website) and *Scientific Style and Format: the CSE Manual for Authors, Editors, and Publishers* (2014, 8th ed.) published by the Council of Science Editors. For scientific nomenclature, use the current edition of the American Fisheries Society's (AFS) *Common and Scientific Names of Fishes from the United States, Canada, and Mexico* and its companion volumes (*Crustaceans, Mollusks, Cnidaria and Ctenophora*, and *World Fishes Important to North Americans*). For species not found in the previously mentioned AFS publications and for more recent changes in nomenclature, use the Integrated Taxonomic Information System (ITIS, available at website), or, secondarily, the California Academy of Sciences *Catalog of Fishes* (available at website) for species names not included in ITIS. Common (vernacular) names of species should be lowercase. Citations must be given for the identification of specimens. For example, "Fish species were identified according to Collette and Klein-MacPhee (2002); sponges were identified according to Stone et al. (2011)."

Dates should be written as follows: 11 November 2018. Measurements should be expressed in metric units, for example, "58 metric tons (t);" if other units of measurement are used, please make this fact explicit to the reader. Use numerals, not words, to express whole and decimal numbers in the general text, tables, and figure captions (except at the beginning of a sentence). For example, "We considered 3 hypotheses. We collected 7 samples in this location." Use American spelling. Refrain from using the shorthand slash (/), an ambiguous symbol, in the general text.

Cite all software, special equipment, and chemical solutions used in the study within parentheses in the general text, including the version number, company name, and the city and state (or nation) of the company headquarters, for example, "SAS, vers. 9.4 (SAS Institute Inc., Cary, NC)."

Word usage and grammar that may be useful are the following:

- *Aging*
  For our journal, the word *aging* is used to mean both age determination and the aging process (senescence). Authors should make clear which meaning is intended where ambiguity may arise.

- *Fish and fishes*
  The plural of the word fish (a collective noun that implies individuals without regard to species) is *fish*.
  Example: The *fish* were collected by trawl net.
  Example: The numbers of *fish* collected that season were less than the numbers from previous years.

  The plural for *fish species* is *fishes* (a contrived plural used by taxonomists to mean several or more *fish species*) or one can use *fish species* (which is preferred in this journal for clarity across disciplines).
  Example: The *fishes* of Puget Sound [biodiversity is implied] or
  Example: The *fish species* of Puget Sound [preferred plural for clarity across disciplines].

- *Crab and crabs, squid and squids, etc.*
  The plural of the word *crab* (i.e., many individuals without regard to species) is *crab*.
  Example: The crab were sorted by weight.
  Example: Many red king *crab* were dying [Many individuals of one species of crab.]

  The plural of *crab species* is *crabs* (a word used by taxonomists) or *crab species* (the latter is preferred in this journal for clarity).
  Example: These *crabs* were selected for treatment. [Different crab species are implied.]
  Example: These *crab species* were selected for treatment. [Preferred word choice for clarity.]
  Example: Snow *crabs* are found throughout the North Pacific Ocean and Bering Sea. [There are 2 species of snow crab; therefore the word *crabs* can be used here.]
  Example: *Two species* of snow *crab* are found throughout the North Pacific Ocean and Bering Sea. [Preferred usage for clarity.]
  Example: Three crabs were selected for treatment. [3 species of crab are implied.]
  Example: Three crab species were selected for treatment. [Preferred word choice for clarity.]

- We use *fisherman* and *fishermen*, not *fisher* and *fishers*, in this journal. One can always use crew member, vessel operator, and angler (the latter for recreational fishing).

- *The definite article with common names of species*
  When the singular common name of a species represents the entire class or group to which it belongs, use the definite article.
  Example: Only one species of the genus *Salmo* is found in the Atlantic Ocean—*the* Atlantic salmon (*Salmo salar*).
  Example: The sonic emissions of *the* bottlenose dolphin are complex.

  For plural common names, this rule does not apply.
  Example: Chinook salmon are found throughout the Pacific Ocean.
  Example: Bottlenose dolphins are found in temperate and tropical waters.

- *Sex*
  For the meaning of male and female, use the word *sex*, not *gender*. Do not write, "fish were sexed." Write, "sex was determined."

- *Participles*
  As adjectives, participles must modify a specific noun or pronoun.
  Example: Using mark-recapture methods, these scientists determined the size of the population. [Correct. The participle *using* modifies the word *scientists*.]

Example: These scientists, based on the collected data, concluded that the mortality rate of these fish had increased. [Incorrect. The scientists were not based on the collected data.]

Example: These scientists concluded, on the basis of collected data, that the mortality rate of these fish had increased. [Correct. The offending participle has been eliminated and an adverbial phrase modifies the verb *concluded*.]

Equations and mathematical symbols should be set from a standard mathematical program (MathType or Equation Editor). Equations formatted in LaTex are not acceptable. For mathematical symbols in the general text (α, χ^2, π, $\pm$, etc.), use the symbols provided by the MS Word program and italicize all variables, except those variables represented by Greek letters and the superscript and subscript parts of variables and expressions. Do not use photo mode when creating these symbols in the general text, and do not cut and paste equations, letters, or symbols from a different software program.

Number equations (if there are more than one) for future reference by scientists; place the number within parentheses at the end of the first line of the equation.

Literature cited section comprises published works and those accepted for publication (in press) in peer-reviewed journals. Follow the name and year system for citation format in this section (i.e., citations should be listed alphabetically by the authors' last names, and then by year if there is more than one citation by the same author. A list of abbreviations for citing journal titles can be found on our website.

Authors are responsible for the accuracy and completeness of all citations. Avoid the use of multiple citations when a single citation sufficiently supports a statement; cite the work that first reported the information that supports a statement, not all of the subsequent works. Literature citation format: Authors (last name, followed by initials for first name and, if given, middle name of first author; then list names of additional authors with initials before last names). Year. Title of article. Abbreviated title of the journal in which it was published. Always include either the range of page numbers (for a journal article) or a total number of pages (for a book or other type of publication). List a sequence of citations in the general text chronologically, for example, "(Smith, 1932; Green, 1998; Smith and Jones, 2015)."

Acknowledgments should be no more than 6 lines of text. Only those who have contributed in an outstanding way should be acknowledged by name. For recognition of other persons or groups, use a general term, such as *crew*, *observers*, or *research coordinators*, and do not include names with these terms.

Digital object identifier (doi) code ensures that a publication has a permanent location online. A doi link (which may include a doi code) should be included at the end of citations of published literature. Authors are responsible for submitting accurate doi links. Faulty links will be deleted at the page-proof stage.

Footnotes are used for all documents that have not been formally peer reviewed and for observations and personal communications, but these types of references should be cited sparingly in manuscripts submitted to the journal.

All reference documents, administrative reports, internal reports, progress reports, project reports, contract reports, personal observations, personal communications, unpublished data, manuscripts in review, and council meeting notes are footnoted in 10-point font and placed at the bottom of the page on which they are first cited. Footnote format is the same as that for formal literature citations. A link to the online source (e.g., [Available from http://www..., accessed July 2017.]), or the mailing address of the agency or department holding the document, should be provided so that readers may obtain a copy of the document.

Tables are often overused in scientific papers; it is seldom necessary to present all the data associated with a study. Tables should not be excessive in size and must be cited in numerical order in the text. Headings should be short but ample enough to allow the table to be intelligible on its own.

All abbreviations and unusual symbols must be explained in the table legend. Other incidental comments may be footnoted with numeral footnote markers. Use asterisks only to indicate significance in statistical data. Do not put a table legend on a page separate from the table; place the legend above the table. *Do not submit tables in photo mode.*

- Note probability with a capital, italic *P*.
- Provide a zero before all decimal points for values less than one (e.g., 0.07).
- Round all values to 2 decimal points.
- Use a comma in numbers of 5 digits or more (e.g., 13,000 but 3000).

Figures must be cited in numerical order in the text. Graphics should aid in the comprehension of the text, but they should be limited to presenting patterns rather than raw data. The number of figures should not exceed 1 figure for every 4 pages of text.

Figure legends should explain all symbols and abbreviations seen in the figure and should be double spaced on a separate page at the end of the manuscript.

Line art and halftone figures should be saved at resolutions >600 dots per inch (dpi) and >300 dpi, respectively. Color is allowed in figures to show morphological differences among species (for species identification), to show stain reactions, to show gradations (such as those of temperature and salinity within maps), and to distinguish

between numerous lines and symbols in graphs. Figures approved for color should be saved in CMYK format.

All figures must be submitted as PDF, TIFF, or EPS files.

- Capitalize only the first letter of the first word and proper nouns in all labels within figures.
- Do not use overly large font sizes for labels in maps and for axis labels in graphs.
- Use the same point size for all labels, except for panel labels (e.g., **A**), which should be slightly larger than other labels (e.g., 11 point versus 8 point).
- Use a sans serif font for all labels. Panel labels (e.g., **A**), however, should be in Times New Roman font.
- Do not use bold fonts or bold lines in figures. Do not use italic fonts. Exceptions include use of italic fonts for labels of bodies of water in maps and a bold font for panel labels (e.g., **A**).
- Do not place outline rules around graphs.
- Do not include vertical and horizontal lines in the background of graphs. Ticks for values on the x-axis and y-axis will suffice.
- Place a north arrow and label degrees latitude and longitude (e.g., 170°E) in all maps. If scale of map requires more than degrees, use degrees minutes, not decimal degrees.
- Place panel labels (e.g., **A**, **B**, **C**) within the upper-left area of each graph or photo in a multi-panel figure, from left to right, then top to bottom. If the letter is not visible against a dark background, put a white box behind it. Do not use white labels.
- Avoid placing labels vertically or diagonally. Y-axis labels can be vertical. Words in horizontal labels can be stacked vertically to fit.
- Use symbols, shading, or patterns (not clip art) in maps and graphs.
- For scale bars in maps, use kilometers. Use the label *km* or *kilometers* (lowercased).

Supplementary materials that are considered essential, but are too large or impractical for inclusion in a paper (e.g., metadata, figures, tables, videos, and websites), may be provided at the end of an article. These materials are subject to the editorial standards of the journal. A URL to the supplementary material and a brief explanation for including such material should be sent at the time of initial submission of the paper to the journal.

- **Metadata, figures, and tables** should be submitted in standard digital format (MS Word or PDF file) and should be cited in the general text, for example, as ". . . was determined (Suppl. Table 3, Suppl. Fig. 1)."
- **Websites** should be cited with a URL in the general text.
- **Videos** must not be larger than 30 MB to allow a swift technical response for viewing the video. Authors should consider whether a short video uniquely captures what text alone cannot capture for the understanding of a process or behavior under examination in the article. Supply an online link to the location of the video.

Copyright law does not apply to *Fishery Bulletin*, which falls within the public domain. However, if an author reproduces any part of an article from *Fishery Bulletin*, reference to source is considered correct form (e.g., Source: Fish. Bull. 117:105).

Failure to follow these guidelines and failure to correspond with editors in a timely manner will delay publication of a manuscript.

Submission of manuscript

Submit a manuscript online at the ScholarOne Manuscripts website for *Fishery Bulletin*. Commerce Department authors must provide proof of internal clearance of their manuscripts with either a completed and signed NOAA Form 25-700 or a copy of the clearance email from the Research Publication Tracking System. For further details on electronic submission, please contact the associate editor, Cara Mayo, at

cara.mayo@noaa.gov.

When requested, the text and tables should be submitted in MS Word format. Each figure should be sent as a separate PDF, TIFF, or EPS file. Send a copy of a figure in the original software if conversion to any of these formats yields a degraded version of the figure.

Questions? If you have questions regarding these guidelines, please contact the managing editor, Kathryn Dennis, at

kathryn.dennis@noaa.gov.

Questions regarding manuscripts under review should be addressed to Associate Editor Cara Mayo.

Fishery Bulletin

Subscription form

Superintendent of Documents **Publications** Order Form

*5178

☐ YES, please send me the following publications:

____ Subscriptions to *Fishery Bulletin*
for $32.00 per year ($44.80 foreign)

The total cost of my order is $ _____ . Prices include regular domestic postage and handling and are subject to change.

_____
(Company or Personal Name) (Please type or print)

_____
(Additional address/attention line)

_____
(Street address)

_____
(City, State, ZIP Code)

_____
(Daytime phone including area code)

_____
(Purchase Order No.)

Charge your order. IT'S EASY!

VISA

MasterCard

Please Choose Method of Payment:

☐ Check payable to the Superintendent of Documents
☐ GPO Deposit Account ☐☐☐☐☐☐–☐
☐ VISA or MasterCard Account
☐☐☐☐☐☐☐☐☐☐☐☐☐☐☐☐
☐☐☐☐ (Credit card expiration date)

To fax your orders (202) 512-2104

_____
(Authorizing Signature)

Mail to: Superintendent of Documents
P.O. Box 979050, St. Louis, Missouri 63197
Tel. no. (U.S. callers): 866-512-1800
Tel. no. (International callers): 1-202-512-1800

Thank you for your order!

Also available online at
https://bookstore.gpo.gov/products/fishery-bulletin
email: ContactCenter@gpo.gov